Identification of MAMP-triggered immunity (MTI)-suppressing RXLR effectors from *Phytophthora infestans* and functional characterization of the calmodulin-binding effector SFI5

Dissertation

der Mathematisch-Naturwissenschaftlichen Fakultät

der Eberhard Karls Universität Tübingen

zur Erlangung des Grades eines

Doktors der Naturwissenschaften

(Dr. rer. nat.)

Vorgelegt von

Xiangzi Zheng

aus

Fuzhou, China

Tag der mündlichen Qualifikation:	21.06.2016
Dekan:	Prof. Dr. Wolfgang Rosenstiel
1. Berichterstatter:	Dr. Frédéric Brunner
2. Berichterstatter:	Prof. Dr. Georg Felix

Summary

An important branch of the plant immune system is based on the sensing of potential pathogens by the recognition of highly conserved microbe-associated molecular patterns (MAMPs), such as the peptide epitope flg22 from bacterial flagellin, and the activation of complex defense signaling events yielding a generic anti-microbial response, which is called MAMP-triggered immunity (MTI). The successful establishment of infection relies on the pathogen's capability to deliver effectors that subvert plant immunity. Although some effectors from eukaryotic filamentous pathogens have been identified as MTI-compromising factors, our general understanding of the effector-target biology and the molecular mechanisms underlying the mode of action of these effectors is still in its infancy. A large repertoire of candidate effector genes, including hundreds of putative host-targeting RXLR effectors, is present in the genome of *Phytophthora infestans*, the causal agent of potato and tomato late blight. In this thesis, we used protoplast-based high-throughput assays to identify and characterize RXLR effectors interfering with the early stages of MAMP-induced immune signaling responses e.g. calcium and oxidative burst, post-translational MAP kinase activation and transcriptional up-regulation of MAMP-inducible genes. Among 33 RXLR effectors tested, eight were identified as Suppressor of early Flg22-induced Immune responses (SFI effectors) in tomato protoplasts. Epistatic analysis showed that three RXLR effectors (SFI5-SFI7) disturb flg22-mediated signaling at- or upstream of the MAP kinase cascade, concomitant with their localization at the host plasma membrane. The remaining five RXLR effectors (SFI1-4 and SFI8) act downstream of the MAP kinase cascade, four of them are localized in the host nucleus. Furthermore, we provide evidence that all but one SFI effectors enhance host susceptibility to *P. infestans* infection.

We have identified the calcium sensor calmodulin (CaM) as an interacting plant protein of SFI5 using bioinformatics, proteomics and biochemical approaches. Structure-function analyses with SFI deletion and point mutants showed that the CaM-binding motif in the C-terminal part of SFI5 is crucial for the plasma membrane (PM) localization, MTI-suppressing activity and virulence function of SFI5. In addition, a predicted ATP/GTP-binding site motif (P-loop) at the N-terminus of SFI5 was demonstrated to be necessary for the effector activity but has no influence on CaM binding and PM localization. Our current model predicts a two-step activation mechanism of SFI5 with CaM serving as a co-factor and regulating SFI5 to target potential MTI components at the PM.

Altogether, we have shown that *P. infestans* contains functionally redundant effectors to inhibit MAMP-dependent early signal transduction during host infection. Our results present a conceptual advance in the understanding of the biology of effectors originated from eukaryotic plant pathogens and show parallels with the strategies developed by prokaryotic pathogens.

Zusammenfassung

Ein wichtiger Zweig des Immunsystems der Pflanzen beruht auf der Erkennung von potenziellen Krankheitserregern über konservierte, Mikroben-assoziierte molekulare Muster (MAMPs), wie beispielsweise das flg22-Peptid aus der Bakteriengeißel (Flagellen). MAMP-Erkennung aktiviert eine komplexe, intrazelluläre Signalkaskade, die zu einer generischen, antimikrobiellen Antwort führt, die allgemein MAMP-induzierte Immunität (MTI) genannt wird. Viele erfolgreiche Pathogene haben aber die Fähigkeit, Effektoren zu produzieren, welche die Immunität der Pflanzen unterdrücken. Obwohl bereits einige dieser Effektoren als MTI-suprimierende Faktoren identifiziert wurden, ist unseres Verständnis über die molekularen Wirkungsweisen der meisten Effektoren noch sehr beschränkt. *Phytophthora infestans*, der Erreger der Kraut- und Knollenfäule in Tomaten und Kartoffeln, verfügt über ein großes Repertoire von Effektorkandidaten, darunter hunderte von so-gennanten RXLR Effektoren. In der hier vorgelegten Arbeit wurde ein Zell-basiertes System verwendet, um diejenigen RXLR Effektoren zu identifizieren und charakterisieren, welche bereits fühe Schritte der MAMP-induzierten Immunantworten, wie etwa den Einstrom von Calcium, die Induktion eines ´oxidativen Burst´, die posttranslationale MAP-Kinase-Aktivierung oder die transkriptionale Hochregulierung von MAMP-induzierbaren Genen, inhibieren. Insgesamt konnte für 8 von 33 geprüften RXLR Effektoren eine supprimierende Funktion frühen flg22-induzierten Immunantworten (SFI Effektoren) in Tomatenprotoplasten nachgewisen werden. Für drei dieser RXLR Effektoren (SFI5-SFI7) konnte gezeigt werden, dass sie die flg22-abhängige Signaltransduktion auf- oder oberhalb der MAP-Kinase Aktivierungsebene stören, was mit ihrer Lokalisierung in der Wirtszell-Plasmamembran (PM) verbunden ist. Die restliche fünf RXLR Effektoren (SFI1-4 und SFI8) wirken unterhalb der MAP Kinase Kaskade, vier davon sind im Wirtszellkern lokalisiert. Durch transiente Expression in Wirtszellen konnte für sieben der SFI Effektoren eine Virulenzfunktion gezeigt werden, die sich durch eine erhöhte Susceptibilität gegenüber *P. infestans* äussert.

Durch Bioinformatik, Proteomik und biochemische Ansätze konnten wir für SFI 5 den Kalziumsensor Calmodulin (CaM) als pflanzliches Zielprotein (target) identifizieren. Die Struktur-Funktions Analysen mit Deletions- und Punktmutanten zeigen, dass das CaM-bindende Motiv im C-terminalen Teil von SFI5 entscheidend für die subzelluläre Lokalisierung, die MTI-supprimierende Aktivität und die Virulenzfunktion von SFI5 ist. Darüber hinaus wurde ein mutmaßliches ATP / GTP-Bindungsstelle Motiv (P-Schleife) am N-Terminus von SFI5 identifiziert, das für die Effektoraktivität notwendig ist aber keinen

Einfluss auf die CaM Bindung und PM Lokalisierung hat. Unser aktuelles Modell sagt voraus, dass SFI 5 über einen zweischrittigen Aktivierungsmechanismus das CaM Protein zur MTI-supprimierenden Aktivität an der Plasmamembran nutzt.

Zusammenfassend haben wir gezeigt, dass *P. infestans* funktionell redundante Effektoren produziert, um während der Infektion frühe Antworten der MAMP-induzierten Abwehrantwort zu verhindern. Unsere Ergebnisse stellen einen konzeptionellen Fortschritt für das Verständnis der Biologie von Effektoren aus eukaryotischen Phytopathogenen.

Contents

1. Introduction 1

1.1. The plant innate immune system: MTI and ETI 1

1.2. MAMPs perception through transmembrane receptor-like kinases and receptor-like proteins 5

1.3. Early MTI responses 7

1.3.1. Ca^{2+} influx 9

1.3.2. ROS burst 10

1.3.3. MAPK activation 11

1.3.4. Transcriptional reprogramming 12

1.4. Late MTI responses 13

1.5. Suppression of MTI by pathogen effectors 14

1.5.1. Bacterial effectors 14

1.5.2. Fungal effectors 16

1.5.3. Oomycete effectors 17

1.6. Objective of this thesis 21

2. Materials and Methods 22

2.1. Materials 22

2.1.1. Microbial organisms 22

2.1.2. Plant organisms 22

2.1.3. Vectors 23

2.1.4. Primers 23

2.1.5. Elicitor and Peptides 24

2.1.6. Chemicals, enzymes and antibodies 24

2.1.7. Media and Antibiotics 24

2.1.8. Buffers and solutions 26

2.2. Methods 26

2.2.1. Cultivation of microorganisms 26

2.2.1.1. Cultivation of *Escherichia coli* 26

2.2.1.2. Cultivation of *Agrobacterium tumefaciens* 26

2.2.1.3. Cultivation of *Phytophthora infestans* 26

2.2.2. Plant growth conditions 26

2.2.2.1. Growth of *Arabidopsis thaliana* 26

2.2.2.2. Growth of *Solanum lycopersicum* 26

2.2.2.3. Growth of *Nicotiana benthamiana* 27
2.2.3. Plant methods 27
2.2.3.1. Isolation and transfection of mesophyll protoplasts from *Arabidopsis thaliana* and *Solanum lycopersicum* 27
2.2.3.2. *Agrobacterium*-mediated transient transformation of *Nicotiana benthamiana* 29
2.2.4. Molecular biological analysis 29
2.2.4.1. Bacterial plasmid DNA extraction 29
2.2.4.2. Standard PCR 30
2.2.4.3. Gateway reactions 30
2.2.4.4. DNA Sequencing 30
2.2.4.5. RNA isolation from protoplasts 30
2.2.4.6. cDNA synthesis 31
2.2.4.7. Quantitative real time-PCR (qRT-PCR) 31
2.2.4.8. Preparation and transformation of chemically competent *E. coli* DH5α cells 31
2.2.4.9. Transformation of competent *A. tumefaciens* cells 32
2.2.4.10. Construction of deletion mutants of SFI5 and site-directed mutagenesis 32
2.2.5. Protein analysis 32
2.2.5.1. Protein extraction from plant tissue 33
2.2.5.2. Expression and purification of recombinant proteins in *E. coli* 33
2.2.5.3. Immunoprecipitation from protoplasts 34
2.2.5.4. *In vitro* kinase activity assay 34
2.2.5.5. Mass Spectrometry Analysis 35
2.2.5.6. SDS-PAGE 35
2.2.5.7. Western blot 36
2.2.5.8. Native-PAGE analysis 36
2.2.5.9. Immunoblot of native gels 37
2.2.5.10. Coomassie Brillant Blue staining 37
2.2.5.11. 1-Anilinonaphthalene-8-sulfonate (ANS) fluorescence measurement 38
2.2.6. Bioassay methods 38
2.2.6.1. Luciferase activity measurement 38
2.2.6.2. GUS activity measurement 38
2.2.6.3. Cell death rate measurement 39
2.2.6.4. Post-translational MAP Kinase activation assay 39

2.2.6.5. Oxidative burst assay 39
2.2.6.6. Calcium influx assay 39
2.2.6.7. Programmed Cell death suppression assay 40
2.2.6.8. *Phytophthora infestans* infection assay 40
2.2.7. Confocal fluorescence microscopy 41

3. Results 42

3.1. Identification of RXLR effectors from *P. infestans* suppressing early MTI signaling 42

3.1.1. Establishment of plant protoplast systems for monitoring flg22-induced immune responses 42
3.1.2. Comparative analysis of flg22-inducible gene activation in tomato and Arabidopsis protoplasts expressing RXLR effectors from *P. infestans* 45
3.1.2.1. Identification of RXLR effectors from *P. infestans* suppressing *pFRK1-Luc* activity upon flg22 treatment in tomato protoplasts 45
3.1.2.2. Identification of RXLR effectors from *P. infestans* suppressing *pFRK1-Luc* activity upon flg22 treatment in Arabidopsis protoplasts 47
3.1.2.3. SFI1, SFI2 and SFI8 attenuate flg22-induced endogenous MAMP-marker gene expression in Arabidopsis protoplasts 49
3.1.3. SFI 5-7 suppress post-translational MAP kinase activation by flg22 in tomato but not in Arabidopsis protoplasts 50
3.1.4. SFI5-SFI7 interfere upstream of the flg22-mediated MAP kinase activation in tomato protoplasts 52
3.1.5. SFI7 interferes with PCD triggered by INF1 but not by Cf-4/Avr4 55
3.1.6. SFI1-8 effectors display different sub-cellular localization patterns 56
3.1.7. SFI effectors contribute to *P. infestans* virulence 59
3.1.8. The nuclear localization is important for the function of SFI1 60

3.2. Functional characterization of SFI5 62

3.2.1. *In silico* prediction of CaM interaction with SFI5 63
3.2.2. SFI5 interacts *in vitro* with CaM in a Ca^{2+} -dependent manner 64
3.2.3. SFI5 interacts *in vivo* with both Arabidopsis and tomato CaMs 65
3.2.4. The C-terminal amphipathic helix of SFI5 is critical for CaM-binding 67
3.2.5. The CaM-binding motif is necessary for the plasma membrane localization of SFI5 71

3.2.6. Both C-terminal CaM-binding motif and N-terminal region are required for the full function of SFI5 72
3.2.7. A predicted ATP/GTP-binding motif at the N-terminal of SFI5 is also important for suppression of MTI signaling 77
3.2.8. Does SFI5 inhibit CaM function? 80

4. Discussion 82
4.1. Advantages/disadvantages in using the protoplast system to study flg22-induced early immune responses 83
4.2. Defining the repertoire and function of MTI-suppressing PiRXLR effectors in host adaptation (and specificity) 85
4.3. MTI-suppressing PiRXLR effectors in non-adapted plant species 88
4.4. SFI5 is a member of a larger family of RXLR effectors 92
4.5. The molecular basis of SFI5-CaM interaction 94
4.6. CaMs regulate multiple biological functions in plants 95
4.7. Site of action of SFI5 in the host cell 97
4.8. Molecular mechanisms underlying SFI5 MTI-suppressing activity 98
4.9. Conclusion 103

5. Reference 104

6. Appendix 124

7. Acknowledgements 137

8. Curriculum vitae 138

Abbreviations

4CL	4-Coumarate coenzyme A ligase
ANS	1-Anilinonaphthalene-8-sulfonate
Avr gene	Avirulence gene
BAK1	BRI1-associated kinase 1
BN-PAGE	Blue native-polyacrylamide gel electrophoresis
CaM	Calmodulin
CaMBD	CaM-binding domain
CaMBP	CaM-binding protein
CAMTA	CaM-binding transcription activator
CBD	Ca^{2+}-binding domain
CBL	Calcineurin B-like
CCaMK	Ca^{2+}/CaM-dependent protein kinase
cDNA	Complementary DNA
CDPK/CPK	Calcium-dependent protein kinase
CML	CaM-like protein
CNGC	Cyclic nucleotide gated channel
CRISPR/Cas	Clustered regularly interspaced short palindromic repeats/CRISPR-associated proteins
DAMP	Damage-associated molecular pattern
ED	Effector domain
EDV	Effector-detector vector
EF1α	Elongation factor 1 a
EFR	EF-Tu receptor
EIX	Xylanase
Elf18	The 18 amino acid fragment of EF-Tu
ER	Endoplasmic reticulum
ET	Ethylene
ETI	Effector-triggered immunity
ETS	Effector-triggered susceptibility
Flg22	The 22 amino acid fragment of flagellin

FLS2	Flagellin-Sensing 2
FRK1	Flagellin-induced Receptor Kinase 1
GFP	Green fluorescent protein
GO	Gene ontology
GSH	Glutathione
GST	Glutathione S-transferase
GUS	β-glucuronidase
HA	Hemagglutinin
HR	Hypersensitive response
HRP	Horseradish peroxidase
HTS	Host targeting signal
IB	Immunoblotting
IP	Immunoprecipitation
IPTG	Isopropyl β-D-thiogalactopyranoside
JA	Jasmonic acid
kDa	Kilo Dalton
LRR	Leucine-rich repeat
Luc	Firefly luciferase gene
LysM	Lysine motifs
MAMP	Microbe-associated molecular pattern
MAPK/MPK	Mitogen-activated protein kinase
MBP	Maltose-binding protein / Myelic basic protein
MTI	MAMP-triggered immunity
MLO	Barley Mildew resistance Locus O
MTS	MAMP-triggered susceptibility
NADPH	Nicotinamide adenine dinucleotide phosphate
NB-LRR	Nucleotide-binding and leucine-rich repeat domain
NLP	Necrosis- and ethylene-inducing-Like Protein
OG	Oligogalacturonide
PAMP	Pathogen-associated molecular pattern
PCD	Programmed cell death

PG	Polygalacturonase
PGN	Peptidoglycan
PI	Propidium iodide
PM	Plasma membrane
PR gene	Pathogenesis-related gene
PRR	Pattern recognition receptor
PSK	Phytosulfokine
PSKR1	PSK receptor 1
PTI	Pattern-triggered immunity
qRT-PCR	Quantitative real time-PCR
R protein	Resistance protein
RBOHD	Respiratory burst oxidase homolog D
RFP	Red fluorescent protein
RLK	Receptor-like kinase
RLP	Receptor-like protein
RNAi	RNA interference
ROS	Reactive oxygen species
RSS	RNA silencing suppressor
RXLR	Arginine-any amino acid-leucine-arginine
SA	Salicylic acid
SDS-PAGE	SDS polyacrylamide gel electrophoresis
SEM	Standard error of the mean
SOBIR1	Suppressor of bir1-1
SFI	Suppressor of early flg22-induced immune response
SP	Secretion peptide
T3E	Type III effector
TALE	Transcription activator-like effector
TF	Transcription factors
TTSS	Type III secretion system
WRKY	WRKY DNA-binding protein
WT	Wild type

List of Figures

Figure 1-1. Zigzag models representing the plant immune system. 4

Figure 1-2. MAMP (flg22)- induced immune responses in Arabidopsis. 8

Figure 1-3. Plant immunity-suppressing function of effectors from phytopathogenic oomycetes. 20

Figure 3-1. *S. lycopersicum* and *A. thaliana* protoplast-based transient expression system for monitoring reporter gene expression and MAPK activation. 43

Figure 3-2. Identification of PiRXLR effectors inhibiting flg22-induced reporter gene activation in *S. lycopersicum* protoplasts. 46

Figure 3-3. Identification of PiRXLR effectors inhibiting flg22-induced reporter gene activation in *A. thaliana* protoplasts. 48

Figure 3-4. Real time PCR-analysis of MAMP-responsive genes in *A. thaliana* protoplasts expressing the SFI effectors. 50

Figure 3-5. Flg22-mediated activation of MAPKs in protoplasts producing SFI effectors. 51

Figure 3-6. SlMEK2 and SlMAP3Kα activate SlMPK1 and SlMPK3 in *S. lycopersicum* protoplasts. 53

Figure 3-7. SFI5, SFI6 and SFI7 do not inhibit SlMEK2 or SlMAP3Kα activation of endogenous MAPKs in *S. lycopersicum* protoplasts. 54

Figure 3-8. Effect of GFP-fused SFI5, SFI6 and SFI7 on INF1-mediated PCD as well as Avr4/Cf4-triggered HR responses in *N.benthamiana*. 55

Figure 3-9. Expression profile and *pFRK1-Luc* reporter gene assay for GFP-tagged SFI effectors in protoplasts. 56

Figure 3-10. Subcellular distribution of GFP-SFI effectors in *S. lycopersicum* protoplasts and in *N. benthamiana* leaves. 58

Figure 3-11. Expression of SFI effectors in *N.benthamiana* promote the growth of *P. infestans*. 59

Figure 3-12. The nuclear accumulation of SFI1 is critical for inhibiting flg22-triggered *pFRK1-Luc* expression and promoting growth of *P. infestans*. 60

Figure 3-13. Schematic illustration of SFI5. 63

Figure 3-14. *In vitro* Ca^{2+}-dependent interaction between SFI5 and AtCaM1/4. 64

Figure 3-15. SFI5 interacts with Arabidopsis and tomato CaMs *in vivo*. 66

Figure 3-16. The C-terminal α-helix of SFI5 binds to CaM *in vitro*. 68

Figure 3-17. The C-terminal amphipathic helix is necessary and sufficient for SFI5/CaM interaction *in vivo*. 70

Figure 3-18. The CaM binding motif of SFI5 is required for plasma membrane localization. 72

Figure 3-19. Suppression of flg22-triggered *FRK1* promoter activity by HA-SFI5 deletion and point mutants. 73

Figure 3-20. Suppression of flg22-triggered MAP kinase, ROS and Ca^{2+} burst by HA-SFI5 deletion and point mutants. 75

Figure 3-21. N-terminal and CaM-binding domain deletion in SFI5 abolish growth of *P. infestans* in *N. benthamiana*. 76

Figure 3-22. The predicted N-terminal ATP/GTP-binding motif of SFI5 is not critical for CaM binding and PM localization. 78

Figure 3-23. The predicted N-terminal ATP/GTP-binding motif of SFI5 is required for the inhibition of early flg22-induced immune responses *in S. lycopersicum* protoplasts. 79

Figure 3-24. Overexpression of SlCaM3/4/5 did not alter SFI5 activities on suppressing flg22-triggered immune responses in *S.lycopersicum.* 81

Figure 4-1. SFI1-8 effectors act at different steps to suppress early MTI signaling in tomato cells. 88

Figure 4-2. Relative contribution of MTI to non-host resistance. 92

Figure 4-3. A neighbor-joining tree of RXLRfam6 members from *P. infestans*. 93

Figure 4-4. Schematic mode of action of *P. infestans* RXLR effector SFI5 in tomato. 102

List of Tables

Table 1-1. Several identified MAMPs and plant DAMPs eliciting plant immunity 7

Table 2-1. Microbial strains used in this study 22

Table 2-2. Vectors applied in this work 23

Table 2-3. Antibodies used in this work 25

Table 2-4. Media used in this study 25

Table 2.5. Antibiotics used in this study 25

Table 2-6. Solutions for protoplast preparation and transformation 28

Table 3-1. Summary of PiRXLR effectors with MTI-suppressing activity 62

Table 6-1. List of Primers mentioned in this study 124

Table 6-2. List of the PiRXLR effector genes tested in the MTI-suppressor screen in *S. lycopersicum* and *A. thaliana* protoplasts. 126

Table 6-3. Potential SFI5-interacting proteins identified by LC-MS/MS analysis. 136

1. Introduction

Unlike animal and humans, plants are sessile organisms, which under natural growing conditions are continuously exposed to various threats in their environment. Besides numerous harmless microbes present in the rhizosphere and phylosphere and sharing a commensal or symbiotic relationship with plants, phytopathogenic microorganisms have evolved to become specialized in attacking and feeding on host plants for replication and propagation. Depending on their life style, ranging from feeding on living host cell to dead plant tissue or both, they are classified into biotrophic, necrotropic and hemibiotrophic pathogens, respectively (Glazebrook, 2005; Kemen and Jones, 2012). To protect against the majority of pathogens, plants first deploy physical barriers such as the cuticle and the cell wall, which constitute obstacles to tissue penetration by microorganisms (Hamann, 2012; Yeats and Rose, 2013). Some microbes can overcome these obstacles either by entering into plants through natural openings (e.g. stomata, hydathode) or wounds (Melotto et al., 2008) or with help of specialized structures (e.g. fungal appressorium) (O'Connell and Panstruga, 2006). When pathogens have successfully penetrated into the apoplast, they have to face the plant immune system, which detects both adapted and non- adapted microbes. Only in the case of non-adapted pathogens there is a robust and strong induction of defense responses while adapted pathogens are capable to turn down the plant immune system by producing effectors (Boller and He, 2009; Thomma et al., 2011).

1.1. The plant innate immune system: MTI and ETI

Plants rely on a double-layered innate immune system to combat most potential pathogens (Figure 1-1). The first layer of active plant immune responses is established by cell surface-resident pattern recognition receptors (PRRs). These PRRs can recognize a range of pathogen-associated molecular patterns (PAMPs), which are generally highly conserved molecules or structural components derived from microbes and indispensable for microbial fitness or life style (Medzhitov and Janeway, 1997; Nurnberger and Brunner, 2002). Since non-pathogenic microbes can also produce effective PAMPs detected by plants, the term microbe-associated molecular patterns (MAMPs) is used preferentially (Ausubel, 2005; Boller and Felix, 2009). The defense responses induced by PRR-mediated perception of MAMPs is called pattern-triggered immunity (PTI) or MAMP-triggered immunity (MTI), and is accompanied by rapid changes in cytosolic ion levels, the production of reactive oxygen species (ROS), the activation of mitogen-activated protein kinases (MAPKs) and calcium-dependent protein

kinases (CDPKs), the activation of the expression of immunity-associated genes as well as the induction of callose deposition at the cell wall and stomatal closure (Boudsocq and Sheen, 2013; Bigeard et al., 2015; Lee et al., 2015).

However, successful pathogens have learned to suppress MTI by delivering virulence proteins (effectors) into host cells that interfere with MAMP-induced signal transduction, leading to effector-triggered susceptibility (ETS) (Figure 1-1 A). For example, many bacterial pathogens directly inject diverse effectors into the host cytoplasm through the type III secretion apparatus to modulate plant innate immunity (Xin and He, 2013; Liu et al., 2014). As a consequence of co-evolution, plants have developed additional intracellular immune receptors (R proteins) to specifically recognize some of these effectors either directly or indirectly, resulting in a second layer of plant immunity, which is called effector-triggered immunity (ETI) (Figure 1-1 A) (Chisholm et al., 2006; Ingle et al., 2006; Jones and Dangl, 2006). Most R proteins contain conserved nucleotide-binding and leucine-rich repeat (NB-LRR) domains that allow for pathogen sensing and defense signaling (Meyers et al., 2003; Collier and Moffett, 2009). Detection of the effectors (so-called AVR proteins) by the corresponding NB-LRR proteins determines the occurrence of ETI in a race-specific manner. One typical reaction associated with ETI is the hypersensitive response (HR), a form of programmed cell death (PCD) that may restrict disease spread (Jones and Dangl, 2006). Due to selection pressure, pathogen isolates have developed strategies to avoid ETI, either by losing or modifying the effectors recognized by R proteins, or gaining new effectors suppressing ETI. In parallel, plants have evolved novel receptor proteins to perceive newly acquired effectors, reflecting the continuous coevolutionary arms race of plant-pathogen interactions and illustrated by the Zigzag model (Jones and Dangl, 2006) (Figure 1-1 A).

Although the signaling network shared by ETI and MTI is highly overlapping, the immune responses activated in ETI are thought to be more prolonged and robust compared to MTI (Tao et al., 2003; Jones and Dangl, 2006; Tsuda and Katagiri, 2010). The dynamic interplay and evolutionary arms race between plants and pathogens put forward the notion that MTI evolved before ETI and might be the basic driving force for evolution of ETI (Jones and Dangl, 2006). However, several lines of evidence indicate that the dichotomy between MTI and ETI is ambiguous and eventually obsolete (Thomma et al., 2011).

It has been reported that flagellin, a *bona fide* bacterial MAMP, purified from incompatible *Pseudomonas syringae* pathovars can cause a HR-like response in the non-host plants tobacco and tomato (Taguchi et al., 2003; Hann and Rathjen, 2007) and the flg22 peptide, derived

from flagellin of *P. syringae pv. tabaci* and *P. aeruginosa,* can induce cell death in Arabidopsis (Naito et al., 2008). This suggests that the induction of cell death is not only associated with ETI, but can also occur in MTI. Moreover, some MAMPs are sparely distributed among microorganisms or they are only recognized by a narrow range of plant species, which are typical criteria of ETI. For example, the MAMP Pep-13 is only conserved among *Phytophthora* species (Brunner et al., 2002) and the perception of bacterial MAMP EF-Tu is limited to the *Brassicaceae* (Zipfel et al., 2006). On the other side, several effectors display characteristics of MAMPs, based on their wide taxonomic distribution. For instance, Ecp6, an effector from the fungal pathogen *Cladosporium fulvum* interferes with chitin-triggered immune signaling in tomato (de Jonge et al., 2010). Ecp6 orthologs are widely conserved in the fungal kingdom, a feature that is reminiscent of a MAMP (Bolton et al., 2008; de Jonge and Thomma, 2009). In this respect, Ecp6-mediated suppression of MTI is designated as MAMP-triggered susceptibility (MTS) in a modified Zigzag model (Thomma et al., 2011) (Figure 1-1 B). Another example is provided by the Necrosis- and ethylene-inducing-Like Proteins (NLPs), which are broadly distributed across bacteria, fungi and oomycetes and act, on one hand, as toxin-like virulence factors and, on the other hand, as activators of the plant immune system through the recognition of an immunogenic peptide motif (nlp20) derived from the protein (Qutob et al., 2006; Oome et al., 2014). The occurence of a MAMP motif within a microbial virulence factor further blurs the boundary line between MAMP and effector terminology and implies in fact a continuum between MTI and ETI.

In addition to MAMPs and effectors, plants can detect a variety of damage-associated molecular patterns (DAMPs), which are endogenous danger signals released during cell or tissue damage. For example, solanaceous plants produce in response to wounding and insect attacks the peptide systemin that acts as an activator of the immune signaling pathway (Ryan and Pearce, 2003). Recently, it was discovered that extracellular ATP also serves as a DAMP signal to evoke plant defense responses during attack by herbivores or pathogens (Choi et al., 2014; Tanaka et al., 2014). Oligogalacturonides (OGs), which are fragments of pectin in the plant cell wall, are processed to a certain size through the combined action of pathogenic polygalacturonases (PGs) and plant polygalacturonases-inhibiting proteins (PGIPs) and function as plant immunity-activating DAMPs (Benedetti et al., 2015).

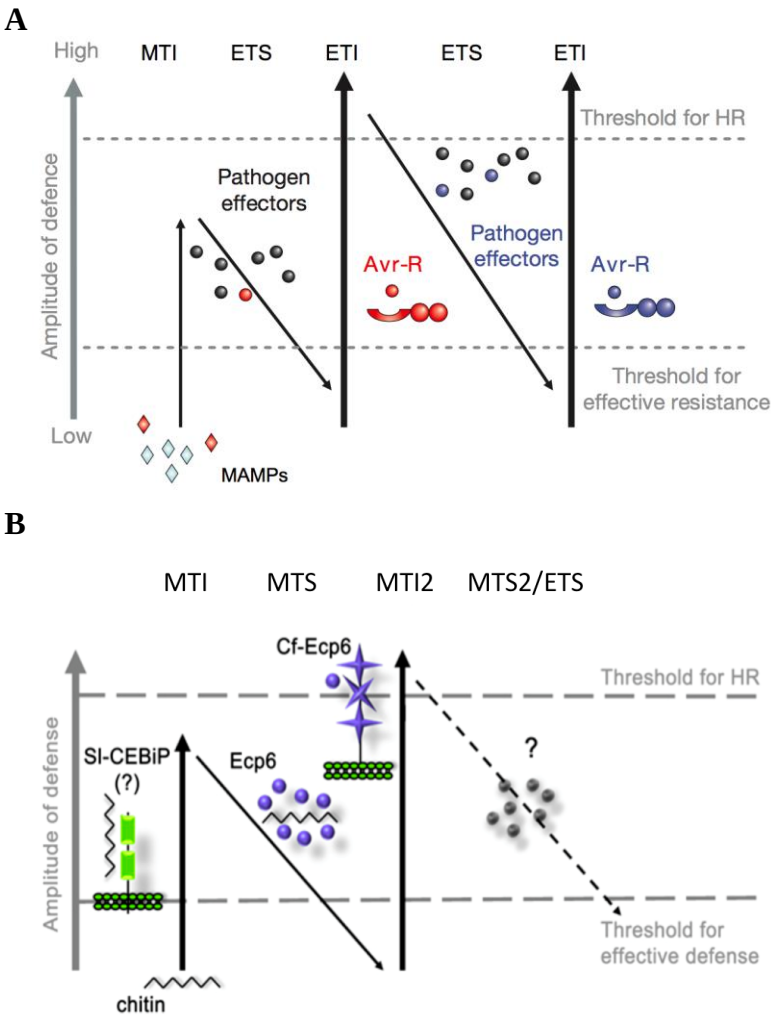

Figure 1- 1. Zigzag models representing the plant immune system.

(A) Upon pathogen infection, plants perceive at first microbe-associated molecular patterns (MAMPs, red diamonds) and activate MAMP-triggered immunity (MTI), while successful pathogens produce virulent effetors (round) to interfere with MTI, leading to effector-triggered susceptibility (ETS). In turn, plants have evolved NB-LRR protein (R) to recognize some effectors (Avr) (indicated in red, round), resulting in effector-triggered immunity (ETI), which often passes the threshold for induction of the hypersensitive response (HR). In an ongoing arms race, pathogen isolates have evolved to lose or modify the Avr effector and perhaps acquire novel effectors (indicated in blue, round) suppressing ETI. In parallel, plants are selected to gain new NB-LRR protein to recognize modifies or newly acquired effectors, leading to ETI again. (Adapted from Jones and Dangl, 2006) **(B)** Chitin, a fungal MAMP from *Cladosporium fulvum*, is presumably perceived by Sl-CEBiP, the tomato homolog of the rice chitin receptor CEBiP, and triggers MTI. To disturb MTI signaling, *C. fulvum* secrets the LysM effector Ecp6 that binds chitin, leading to prevention of Sl-CEBiP-mediated immune signaling. Since LysM effectors are widely conserved in the fungal kindom, they qualify as MAMPs, and therefore the MTI suppression by Ecp6 should be referred to as MAMP-triggered susceptibility (MTS). Some tomato genotypes may have evolved specifiec cell surface receptor for recognizing Ecp6 by inducing an HR. This cell surface receptor is temporarily named *C. fulvum* resistance to Ecp6 (Cf-Ecp6) and again mediates MTI (MTI2). The question mark indicates that subsequent susceptibility can again be provoked by *C. fulvum*, either through mutation of the Ecp6 protein, such that it still sequesters chitin fragments but is no longer recognized by Cf-

Ecp6, or by producing an effector that suppresses Sl-CEBiP signaling in an alternative manner. (Adapted from Thomma et al., 2011).

1.2. MAMPs perception through transmembrane receptor-like kinases and receptor-like proteins

In Arabidopsis, several hundreds of putative PRRs have been identified (Shiu and Bleecker, 2003; Fritz-Laylin et al., 2005) and many genes encoding PRR candidates are induced upon MAMP treatment (Zipfel et al., 2004; Zipfel et al., 2006), implying that they are involved in immune signaling. A few PRRs have been characterized to date (Table 1-1) and most of them are single transmembrane proteins containing an extracellular leucine-rich repeat (LRR) or lysine motif-containing (LysM) domain, which is responsible for ligand-binding and/or signal transduction. They are classified into receptor-like kinases (RLKs) and receptor-like proteins (RLPs), depending on whether or not they harbor a cytoplasmic kinase domain for intracellular signal transduction (Bi et al., 2010; Wang et al., 2010a). Thus, RLK proteins combine a "receptor" and a "signaling" domain in one molecule, whereas RLP proteins lacking the intracellular "signaling" domain are supposed to require the association with adapter molecules for proper function (Shiu and Bleecker, 2003; Altenbach and Robatzek, 2007; Sun et al., 2012; Gust and Felix, 2014).

The best-studied plant LRR-RLKs are the flagellin receptor, Flagellin Sensing 2 (FLS2), and bacterial elongation factor thermo unstable (EF-Tu) receptor, EFR, in Arabidopsis (Gomez-Gomez and Boller, 2000; Zipfel et al., 2006). FLS2 and EFR with 28 and 21 LRR motifs, respectively, are highly structurally similar and belong to the same subfamily XII of LRR-RLK (Shiu et al., 2004). Both receptors can physically interact with their corresponding epitope, flg22, a 22-amino acid peptide in the N-terminus of flagellin in the case of FLS2, and elf-18, the first 18 amino acids of EF-Tu, in the case of EFR (Chinchilla et al., 2006; Zipfel et al., 2006). The homologs of Arabidopsis FLS2 have been detected in tomato, tobacco, barley and rice, suggesting an evolutionary conservation of flagellin perception in both dicotyledonous and monocotyledonous plants (Dunning et al., 2007; Hann and Rathjen, 2007; Robatzek et al., 2007; Takai et al., 2008; Shinya et al., 2010). By contrast, EFR/elf-18 responsiveness was found only in *Brassicaceae* species (Kunze et al., 2004). Strikingly, ectopic expression of Arabidopsis EFR in *N. benthamiana*, which is unable to perceive EF-Tu, rescued the ability to recognize elf-18, implying that the downstream signaling components are conserved between *Brassicaceae* and *Solanaceae* (Zipfel et al., 2006; Nicaise et al., 2009).

Furthermore, a LysM-RLK receptor, designated Chitin Elicitor Receptor Kinase 1 (CERK1)/RLK1/LYK1, was identified in Arabidopsis as a PRR for oligosaccharidic fragments of chitin (Miya et al., 2007; Wan et al., 2008). Unlike FLS2 and EFR, CERK1 possesses 3 lysM motifs instead of LRR motifs in the extracellular domain, which can bind chitin oligomers (seven to eight GlcNAc residues) and results in homodimerization of CERK1 and initiation of chitin-dependent immune signaling (Miya et al., 2007; Petutschnig et al., 2010; Liu et al., 2012). It was recently discovered that another LysM-RLK, LYK5, shows much higher chitin binding affinity than CERK1 and interacts with CERK1 upon chitin treatment, suggesting that LYK5 is the primary chitin binding site in Arabidopsis and essential for subsequent CERK1 phosphorylation and proper activation of the immune signaling cascade (Cao et al., 2014). In rice, the major receptor for chitin binding is a LysM-RLP, named CEBiP, which also contains three extracellular LysM domains but not the intracellular kinase domain (Kaku et al., 2006; Kouzai et al., 2014). Given that it lacks the "signaling" domain in the C-terminal region, Shimizu et al., have demonstrated that CEBiP cooperates with the rice ortholog of the Arabidopsis CERK1 to bind biologically active chitin fragments by forming a heteromeric receptor complex, while the rice CERK1 alone can not bind chitin (Shimizu et al., 2010). These observations reveal a difference in the chitin perception system between rice and Arabidopsis (Shinya et al., 2012).

By means of genetic mapping, two tomato LRR-RLP proteins, LeEix1 and LeEix2, were found to recognize fungal ethylene-inducing xylanase (EIX), which activates immune responses in specific cultivars of tobacco and tomato (Furman-Matarasso et al., 1999; Ron and Avni, 2004). Although both receptors are able to bind EIX, only LeEix2 plays a function in triggering defense responses, which requires the action of the co-receptor BAK1 (BRI1-ASSOCIATED RECEPTOR KINASE 1) (Bar et al., 2011). In the past years, more and more RLP-type proteins have been documented to play key roles in MAMP perception and plant immunity, like the Arabidopsis LYM1/LYM3 sensing the bacterial peptidoglycan (PGN) (Willmann et al., 2011), ReMAX/RLP1 for eMAX of *Xanthomonas* (Jehle et al., 2013), RLP30 for SCFE1 of the necrotrophic fungus *Sclerotinia sclerotiorum* (Zhang et al., 2013), RBPG1 for the polygalacturonase of *Botrytis cinerea* (Zhang et al., 2014) and RLP23 for the NLP-derived peptide nlp20 (Albert et al., 2015). As all these RLPs lack a cytoplasmic kinase domain, accumulating evidence indicate that the LRR-RLK SOBIR1 (SUPPRESSOR OF BIR1-1) acts as a scaffold or co-receptor in a constitutive, ligand-independent manner and engages next BAK1 upon ligand binding to form a functional tripartite receptor complex (Gust and Felix, 2014; Liebrand et al., 2014; Albert et al., 2015).

Table 1-1. Several identified MAMPs and plant DAMPs eliciting plant immunity

MAMPs (minimal elicitor motif)	PRR	Receptor type	Reference
Flagellin (flg22)	FLS2	LRR-RLK	(Chinchilla et al., 2006)
Elongation factor (elf18)	EFR	LRR-RLK	(Zipfel et al., 2006)
Cold shock protein (CSP22)	undefined	undefined	(Felix and Boller, 2003)
Peptidoglycan (undefined)	LYM1/LYM3/CERK1	LysM-RLK	(Willmann et al., 2011)
Lipopolysaccharides (lipid A and O-antigen oligosaccharides)	LORE	Lectin-like RLK	(Newman et al., 1995; Ranf et al., 2015)
Xanthomonas eMax (undefined)	ReMAX	LRR-RLP	(Jehle et al., 2013)
Chitin (oligosaccharides DP>3)	AtLYK5/AtCERK1 OsCEBiP1/OsCERK1	LysM-RLK LysM-RLP	(Kaku et al., 2006; Shimizu et al., 2010; Cao et al., 2014)
Xylanase (TKLGE peptide)	Eix2	LRR-RLP	(Ron and Avni, 2004)
Sclerotinia sclerotiorum effector-SCFE1 (undefined)	RLP30	LRR-RLP	(Zhang et al., 2013)
OPEL (undefined)	undefined	undefined	(Chang et al., 2015)
Transglutaminase (Pep-13)	undefined	undefined	(Brunner et al., 2002)11
Cellulose-binding elicitor lectin (CBEL) (undefined)	undefined	undefined	(Gaulin et al., 2006)
INF1 (undefined)	StELR	LRR-RLP	(Du et al., 2015)
XEG1 (undefined)	undefined	undefined	(Ma et al., 2015)
Beta-glucans (linear or branched oligosaccharides)	undefined	undefined	(Cheong et al., 1991; Klarzynski et al., 2000)
Necrosis-and ethylene-inducing like protein (nlp20)	RLP23	LRR-RLP	(Bohm et al., 2014; Oome et al., 2014; Albert et al., 2015)
DAMPs (minimal elicitor motif)			
PROPEP1-7 (Pep1-7)	AtPEPR1/2	LRR-RLK	(Yamaguchi et al., 2006; Krol et al., 2010)
Prosystemin (Systemin)	undefined	undefined	(Narvaez-Vasquez and Ryan, 2004)
Oligogalacturonides (DP>6)	WAK1	LRR-RLK	(Brutus et al., 2010)
Extracellular ATP	DORN1	Lectin-like RLK	(Choi et al., 2014)

1.3. Early MTI responses

Upon perception of MAMPs by their cognate PRRs at the cell surface, there is an activation of an intracellular signaling pathway implying several second messengers, such as Ca^{2+} or

ROS, and post-translational modifications that deliver the information to the nucleus, where the initiation of defense gene expression takes place (Boller and Felix, 2009; Bigeard et al., 2015) (Figure 1-2). Despite the high complexity of the signaling network and fragmentary knowledge about the molecular mechanisms underlying the integration and transmission of the input signal, diverse PRRs activate a conserved signaling pathway, recruiting key immune components and leading to the induction of generic defense responses (Zipfel et al., 2006; Gust et al., 2007; Denoux et al., 2008; Wan et al., 2008; Boller and Felix, 2009). In the following section, I will focus on the description of typical responses elicited during early i.e within minutes of MAMP-induced signaling.

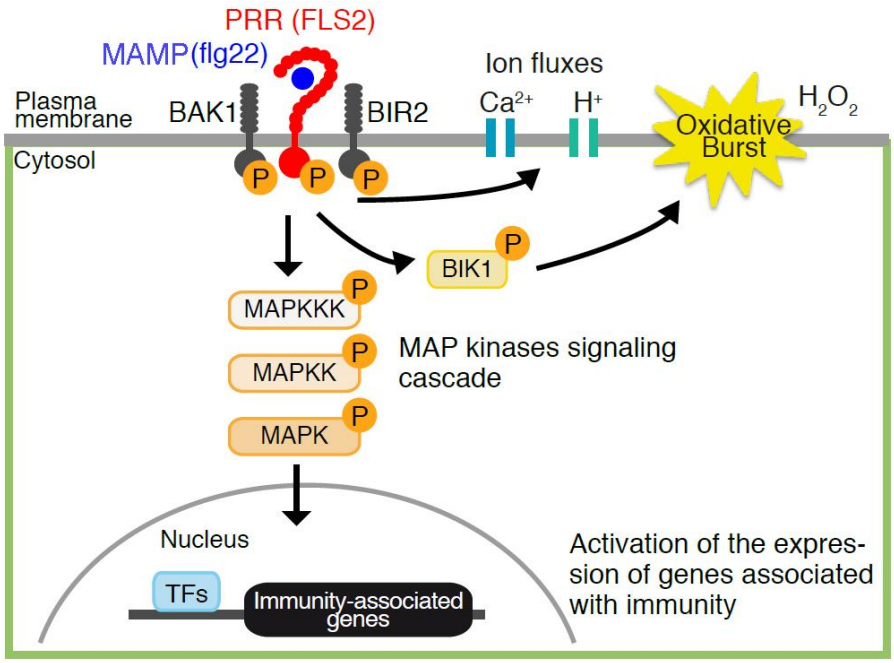

Figure 1- 2. MAMP (flg22)- induced immune responses in Arabidopsis.

Flg22 perception by the PRR FLS2 induces the association of BAK1 with FLS2 and the release of BIR2, a negative regulator of BAK1 interaction with FLS2, from BAK1 as well as the release of BIK1 from FLS2, which are accompanied by different auto- and trans-phosphorylation events of these actors. Tansmembrane ion fluxes e.g. Ca^{2+}, H^{+} influx occur at the very early stage through yet unidentified membrane channels. BIK1 released from the receptor complex acts as as positive regulator of the flg22-induced oxidative burst. In parallel, there is an activation of a MAP kinase signaling cascade regulating the activity of immunity-related transcription factors (TFs) and subsequent activation of defense-associated gene expression. MAMP, microbe-associated molecular pattern; PRR, pattern recognition receptor; MAPK, mitogen-activated protein kinases; MAPKK, mitogen-activated protein kinase kinase; MAPKKK, mitogen-activated protein kinase kinase kinase; FLS2, Flagellin-Sensing 2; flg22, the 22 amino acid fragment of flagellin; BAK1, BRI1-associated receptor kinase 1; BIR2, BAK1-interacting RLK 2; BIK1, *Botrytis*-induced kinase 1; TFs, transcription factors. Adapted from (Macho and Zipfel, 2014).

1.3.1. Ca^{2+} influx

One of the earliest physiological response induced by MAMP perception is the opening of ion channels at the plasma membrane (PM), which enables influx of H^+, Ca^{2+} and concomitant efflux of K^+, Cl^- and NO_3^-, causing transient membrane depolarization and extracellular alkalinisation (Felix et al., 1999; Sakano, 2001; Felle et al., 2004; Jeworutzki et al., 2010). Most experiments to reflect this phenomenon were conducted by using a pharmacological approach with both activators and inhibitors of ion channels or pumps (Ma et al., 2008; Nomura et al., 2012)

MAMP treatment triggers an increase in cytosolic Ca^{2+} level within 5-30 min but it has been noted that the Ca^{2+} signatures between MAMPs differ in amplitude or duration (Aslam et al., 2009; Ranf et al., 2011). This finding supports the notion that the specificity of signal transduction in response to different MAMPs occurs very early at the level of the receptor complex (Seybold et al., 2014).

So far, genetic screens aiming at identifying components that control Ca^{2+} influx upon flg22 treatment did not reveal Ca^{2+} channels or pumps but novel *fls2* and *bak1* alleles with altered Ca^{2+} elevation (Ranf et al., 2012). This approach was also successful in identifing the DAMP ATP receptor DORN1 and the bacterial MAMP lipopolysaccharide (LPS) receptor LORE but not the Ca^{2+} channels/pumps involved in the process (Choi et al., 2014; Ranf et al., 2015). A possible explanation for the failure to identify Ca^{2+} channel/pump associated with MAMP signaling would be their functional redundancy or the lethality of knock out mutant(s).

Nevertheless, a few studies have identified putative candidate PM-localized proteins that could be Ca^{2+} channels or pumps although, their identity and function has not been unambiguously demonstrated. Recently, in a proteomics approach, the PM-associated autoinhibited Ca^{2+}-ATPases, ACA8 and ACA10, were found to complex with FLS2 and to be involved in the Ca^{2+} burst (Frei dit Frey et al., 2012). It is assumable that Ca^{2+} channels/pumps and receptor complexes are in close proximity to mediate the rapid Ca^{2+} response. Thus, glutamate receptor-like channels (GLRs) and cyclic nucleotide-gated channels (CNGCs), which are implicated in DAMP-induced Ca^{2+} influx (Qi et al., 2010; Manzoor et al., 2013) might also participate in MAMP-induced Ca^{2+} burst.

The transient elevation of $[Ca^{2+}]_{cyt}$ serves as second messenger sensed by intracellular Ca^{2+}-binding proteins, which transmit the signal to downstream components leading to appropriate

cellular responses (DeFalco et al., 2010; Kudla et al., 2010). The mechanism how differential Ca^{2+} signatures are decoded remains to be uncovered (Spalding and Harper, 2011). Free Ca^{2+} can be sensed by a large group of Ca^{2+}-binding domain (CBD)-containing proteins, such as calmodulins (CaMs), CaM-like proteins (CMLs), calcineurin B-like (CBL) proteins and Ca^{2+}-dependent protein kinases (CDPKs) (DeFalco et al., 2010). CaMs, CMLs and CBLs have no intrinsic catalytic activity but they act as mediator of Ca^{2+} signaling since, upon Ca^{2+} binding, they interact and regulate the activity of a large subset of target proteins or kinases (Reddy et al., 2011; Yu et al., 2014).

CDPKs have been more intensively studied in the context of plant immunity and they are proposed to be eligible for rapid response to elicitors, as these proteins possess both Ca^{2+}-binding EF hand motifs and a catalytic kinase domain that regulates the activity of target proteins. A couple of reports indicated that several closely related CDPKs (CPK4, 5, 6 and 11) fulfill crucial functions in MTI-mediated transcriptional reprogramming by regulating the activity of specific WRKY transcription factors (WRKY8, 28, 48) (Boudsocq et al., 2010; Gao et al., 2013). Furthermore, it has been confirmed that NADPH oxidases, responsible for ROS production upon MAMP treatment, can be phosphorylated by Ca^{2+}-activated CPK1, 2, 4, 5 and 11 (Dubiella et al., 2013; Gao et al., 2013).

1.3.2. ROS burst

Another very early-induced response, occurring within few minutes upon MAMP treatment, is the production of reactive oxygen species (ROS), also known as oxidative burst, which can be easily detected using luminescence-based techniques (Chinchilla et al., 2007; Nuhse et al., 2007; Ranf et al., 2011). ROS include many forms like superoxide (O^{2-}), singlet oxygen ($^1O_2$), hydrogen peroxide (H_2O_2), and hydroxyl radical ($OH^{\cdot}$). The membrane-impermeable O^{2-} is produced at the outer membrane surface by PM-localized NADPH oxidase homologs of the catalytic subunit of mammalian phagocyte $gp91^{phox}$ and rapidly dismutated via superoxide dismutase (SOD) to relatively stable and membrane-permeable H_2O_2 (Grant and Loake, 2000; Sagi and Fluhr, 2006). A NADPH oxidase homolog, termed respiratory burst oxidase homolog D (RBOHD), is responsible for the MAMP-triggered ROS production in Arabidopsis (Simon-Plas et al., 2002; Wong et al., 2007; Asai et al., 2008; Pogany et al., 2009; Noirot et al., 2014). RBOHD activity can be regulated both in a Ca^{2+}-dependent and –independent manner (Kadota et al., 2015). There is biochemical evidence for the association of RBOHD with the PRR complex and its phosphorylation upon MAMP perception on

specific serine residues within the N-terminal part through the receptor-like cytoplasmic kinase BIK1 (Dubiella et al., 2013; Kadota et al., 2014; Li et al., 2014b; Kadota et al., 2015). BIK1 –mediated phosphorylation of RBOHD occurs in the absence of Ca^{2+} or in Ca^{2+} signaling mutants (Kadota et al., 2014; Li et al., 2014b). In addition, the presence of Ca^{2+}-binding EF hands motif in the N-terminal part of RBOHD indicates that Ca^{2+} also plays a role in the regulation of ROS activity in response to MAMP (Ranf et al., 2011; Segonzac et al., 2011; Kadota et al., 2014). Moreover, it was shown that Ca^{2+}-dependent protein kinase 5 (CPK5) also regulates the activity of RBOHD through serine residues phosphorylation (Dubiella et al., 2013). In addition to the NADPH oxidases, cell wall peroxidases have been shown to take part in ROS production in MAMP-elicited defense (Daudi et al., 2012; Lehtonen et al., 2012; O'Brien et al., 2012). ROS may directly contribute to plant defense by acting as antimicrobial agents and by strengthening the cell wall (Grant and Loake, 2000; Apel and Hirt, 2004) and/or act as second messengers to trigger defense signaling (Gupta and Luan, 2003; Vandenabeele et al., 2003; Desikan et al., 2005; Torres et al., 2006; Sang et al., 2012).

1.3.3. MAPK activation

Mitogen-activated protein kinase (MAPK) cascades play a central role in immunity signaling and appear to be convergent nodes for different MAMP-induced pathways (Meng and Zhang, 2013). The Arabidopsis genome encodes 60 MAPKKKs, 10 MAPKKs and 20 MAPKs (Ichimura at al., 2002). Stimulated with flg22 or other MAMPs, an increased activity of 4 MAPKs (AtMPK3, AtMPK4, AtMPK6 and AtMPK11) was observed, starting within 1-2 min and peaking around 10-15 min (Nuhse et al., 2000; Asai et al., 2002; Zipfel et al., 2006; Bethke et al., 2012). In Arabidopsis, two distinct MAPK signaling modules were shown to regulate flg22-dependent immune responses. The module MEKK1/MEKKs-MKK4/MKK5-MPK3/MPK6 positively regulates immune responses (Ren et al., 2002; Pitzschke et al., 2009a; Rasmussen et al., 2012; Zhao et al., 2014), while the cascade of MEKK1-MKK1/MKK2-MPK4 negatively control defense responses (Suarez-Rodriguez et al., 2007; Gao et al., 2008; Qiu et al., 2008a; Pitzschke et al., 2009b). The substrates of the MAMP-induced MAPKs remain largely elusive but transcription factors that are involved in the regulation of immunity-associated genes seem to be preferentially targeted. For example, the bZIP transcription factor, VIP1, binds to and is phosphorylated by MPK3 (Djamei et al., 2007). The ethylene response factors, EFR104 and ERF6, are targeted by MPK3/MPK6 to initiate defense gene expression (Bethke et al., 2009; Meng and Zhang, 2013). In addition, WRKY

transcription factors are extensively studied for their function to promote, in response to MAMP treatment, the expression of many Pathogenesis-Related (PR) genes and genes of the biosynthetic pathway of anti-microbial metabolites (Ulker and Somssich, 2004).

For instance, WRKY33 was reported to form a complex with MPK4 and MKS1, a substrate of MPK4, in the nucleus in Arabidopsis. Upon pathogen or flagellin treatment, activated MPK4 phosphorylates MKS1 and the MKS1-WRKY33 complex activates the expression of *PAD3*, which encodes a key biosynthetic enzyme of camalexin, an anti-microbial phytoalexin (Qiu et al., 2008b). Another report showed that WRKY33 is directly phosphorylated by MPK3/MPK6 in response to *Botrytis cinerea* infection (Mao et al., 2011). Similarly, WRKY22/29 have been confirmed to function downstream of MPK3/MPK6 in FLS2-mediated immune response (Asai et al., 2002). The fact that a subgroup of WRKYs including WRKY8/28/48 is phosphorylated and activated by CPK4/5/6/11 (Gao et al., 2013), suggests the existence of a synergistic effect between MAPKs and CDPKs to regulate the function of WRKY transcription factors involved in MAMP-induced immunity.

1.3.4. Transcriptional reprogramming

To efficiently activate plant immunity, genome-wide transcriptional reprogramming is believed to be the main link between MAMP signal transduction and induction of defense phenomenons (e.g. production of antimicrobial proteins and metabolites, programmed cell death). This is a highly sensitive and dynamic process which includes numerous transcription factors (e.g WRKYs) (Buscaill and Rivas, 2014).

Upon treatment with flg22 or elf26 (peptide containing the elf18 sequence) for 60 min, a similar set of nearly 1000 genes was up-regulated in Arabidopsis (Zipfel et al., 2004; Zipfel et al., 2006). Another studies have shown that the changes in gene expression caused by 1 h treatment of peptidoglycan (PGN) or oligogalacturonides (OGs) are highly overlapping with flg22-dependent transcriptional reprogramming, suggesting that a common transcription program is deployed by plants in response to multiple MAMPs at the earliest stages of MTI signaling (Gust et al., 2007; Denoux et al., 2008). However, transcriptome changes appeared to be more transient and weaker in response to OGs by comparison to flg22 with much less genes that were down- or up-regulated after 3 h treatment (Denoux et al., 2008). DNA microarray analysis with chitin has shown that only 4 among 118 chitin-regulated TF genes in Arabidopsis are also differentially regulated by flg22 (Libault et al., 2007). Altogether, these results suggest the existence of qualitative and quantitative differences in the gene expression

patterns in response to different MAMPs, a phenomenon that reflects perhaps qualitative and quantitative differences in the expression and execution of the immune program between different types of cell surface receptors.

According to gene ontology (GO) annotations, a tremendous number of upregulated genes are involved in signal perception (genes encoding RLKs), signal transduction (genes encoding protein kinases) and transcriptional regulation (genes encoding TFs) (Navarro et al., 2004; Zipfel et al., 2006; Gust et al., 2007). Exposure to OGs or flg22, many genes encoding components associated with plant resistance and salicylic acid (SA), jasmonic acid (JA), ethylene (ET)-signaling networks are strongly activated at 1 h, while genes encoding enzymes for the biosynthesis of antimicrobial secondary metabolites are most highly upregulated at 3 h. Interestingly, the transcription of genes implicated in Nonexpressor of PR genes (NPR1)-dependent secretory pathways and activation of the senescence program is substantially induced only by flg22 but not by OGs (Denoux et al., 2008). Recently, a high-temporal resolution microarray analysis revealed the transcriptional dynamics in Arabidopsis leaves challenged by the nonpathogenic bacterial mutant strain DC3000 *hrpA*-, which fails to deliver effectors into host cells and triggers essentially an MTI (Lewis et al., 2015). The early MAMP-triggered biological responses, illustrated by selected GO terms, were refined into respiratory burst, phosphorylation, posttranslational modification, and salicylic acid synthesis followed by jasmonic acid biosynthesis and responses to oxidative stress. 7 h post-inoculation, the dominant ontology was ubiquitin-dependent protein metabolism. Biological processes that are suppressed during MTI are related to photosynthesis and plastid organization at the early stage and to fatty acid metabolism and cuticle development at the later stage (Lewis et al., 2015).

1.4. Late MTI responses

MAMP-induced transcriptional reprogramming leads to a series of molecular, biochemical and physiological changes to defend against pathogen infection. Typical late-induced immune responses i.e. several hours up to days after MAMP recognition, include the accumulation of pathogenesis-related (PR) proteins, production of antimicrobial compounds as well as physical strengthing of the plant cell wall through lignification and callose deposition (Newman et al., 2013). PR proteins comprise a number of hydrolytic enzymes, such as chitinases, lysozymes and β-1, 3-glucanases, which can degrade the bacterial, fungal or oomycete cell wall (Ebrahim et al., 2011). Phytoalexins are a heterogeneous group of secondary metabolites with antimicrobial activity towards a broad range of pathogens (Ahuja

et al., 2012). The synthesis of camalexin, the major phytoalexin in Arabidopsis, is induced by several MAMPs, such as oomycete NLPs and bacterial PGN (Qutob et al., 2006; Gust et al., 2007). Many phytohormones, especially SA, JA and ET, have been demonstrated to contribute to plant immunity (Robert-Seilaniantz et al., 2011; Kazan and Lyons, 2014). It has been proposed that induction of the SA pathway is correlated with resistance against biotrophic or hemibiotrophic pathogens, while the JA and ET pathways are induced in response to herbivores or necrothophic pathogens (Pieterse et al., 2009; Thaler et al., 2012). However, increasing evidence revealed that plants engage complex signaling crosstalk between SA, JA and ET to antagonistically or synergistically fine tune innate immune system (Pieterse et al., 2009; Thaler et al., 2012). When exposed to pathogens or MAMPs, the plant cell wall is actively reinforced by the formation of callose (β-1, 3-glucan)-rich papillae (Voigt, 2014). Another well-studied physiological response to MAMP treatment is the closure of stomata that restricts bacterial entry into plant tissues (Melotto et al., 2006).

1.5. Suppression of MTI by pathogen effectors

Although plants can detect diverse pathogens by activating corresponding PRRs and mount a general defense response, adapted pathogens have evolved multiple effectors, which interfere with MTI signaling pathways in order to invade plant tissues (Boller and He, 2009). Pathogenic bacteria possess several secretory systems and among them, the type III secretion system (TTSS) is used for direct translocation of effectors into cytoplasm of plant cells (Alfano and Collmer, 2004; Abramovitch et al., 2006; Cunnac et al., 2009). Eukaryotic plant pathogens, such as fungi and oomycetes, secrete during infection a large amount of effectors, which act outside or inside the host cells (Giraldo and Valent, 2013; Lo Presti et al., 2015). Bioinformatic analysis of the genome of several fungi and oomycetes identified hundreds of predicted effectors, many of which contain, next to the N-terminal secretion peptide (SP), a putative host targeting signal (HTS), such as the RXLR or LXLFLAX motif in the case of oomycete effectors (Tyler et al., 2006; Whisson et al., 2007; Jiang et al., 2008; Haas et al., 2009) or an RXLR-like motif in some fungal effectors (Kamper et al., 2006; Schirawski et al., 2010).

1.5.1. Bacterial effectors

So far, the best characterized effectors from bacterial pathogens e.g. *Pseudomonas syringae* and *Xanthomonas spp*, are the type III effectors (T3Es) which are injected into the plant cells via the TTSS needle-like structure (White et al., 2009; Block and Alfano, 2011). By

interacting with diverse host targets including proteins or DNA inside the plant cell, these effectors manipulate different steps of MTI signaling pathways in order to promote pathogen propagation and disease development (Gohre and Robatzek, 2008; Boller and He, 2009; Deslandes and Rivas, 2012; Feng and Zhou, 2012).

It has been shown that several effectors directly target the PRR complex and disturb very early steps of MAMP signal transduction. For example, two *P. syringae* T3Es, AvrPto and AvrPtoB, bind to the cytoplasmic kinase domains of multiple RLK proteins, such as FLS2, EFR, BAK1 and CERK1 in Arabidopsis and tomato (Gohre et al., 2008; Shan et al., 2008; Xiang et al., 2008; Gimenez-Ibanez et al., 2009; Cheng et al., 2011; Zeng et al., 2012). The mechanism of AvrPto-triggered suppression of PRR complex function is still not fully elucidated and the inhibition of the kinase activity of the aforementioned RLKs and/or interference with the association between the partners of the complex (for instance interference with the flg22-mediated FLS2/BAK1 interaction) are possible mode of actions (Shan et al., 2008; Xiang et al., 2008; Xiang et al., 2011). AvrPtoB carries an ubiquitin E3-ligase activity, which mediates degradation of FLS2, EFR and CERK1 (Gohre and Robatzek, 2008; Gimenez-Ibanez et al., 2009). These results provide a logical explanation to previous observations showing that AvrPto and AvrPtoB suppress a series of early MTI responses including MAP kinases activation, the induction of MAMP responsive genes and callose deposition (Hauck et al., 2003; He et al., 2006). More recently, AvrPphB from *P. syringae* was demonstrated to impair MTI signaling by cleaving several PBS1-like (PBL) kinases, like the FLS2/BAK1 interacting BIK1 (Zhang et al., 2010a). A *Xanthomonas campestris* effector, AvrAC, also targets and prevents kinase activity of BIK1 and the closely related RIPK (Feng et al., 2012).

MAPK pathways act downstream of MAMP recognition by PRRs and play a central role in initiating immune signaling. Therefore, MAPK cascades are one of the main battlefields in plant-bacteria interactions. The *P. syringae* T3E, HopF2, in addition of targeting BAK1 (Zhou et al., 2014), interrupts flg22-dependent MAPK activation by ADP-ribosylation of MKK5, a key component in the MEKK1/MEKKs-MKK4/MKK5-MPK3/MPK6 cascade (Wang et al., 2010b). Another T3E from *P. syringae*, named HopAI1, possesses phosphothreonine lyase activity and inactivates MPK3, MPK6 and MPK4 by irreversible threonine residues dephosphorylation (Zhang et al., 2007; Zhang et al., 2012). By contrast, upon the association with RAR1 (Required for Mla12 Resistance), which is a cochaperone of HSP90 (heat shock protein 90), the *P. syringae* effector AvrB is able to interact with MPK4 and specifically

promotes the phosphorylation of MPK4 in a HSP90-dependent manner, leading to enhancement of JA responses and plant susceptibility (Cui et al., 2010).

Besides targeting PRR complex or MAPK cascades, other type III effectors appear to function downstream of the MAPK cascades by modifying the transcription of defense-related genes or chromatin configuration in plant cell nucleus. The effector XopD from *X. campestris* acts as a transcriptional regulator to target and inactivate AtMYB30, a transcription factor positively regulating plant defense and cell death-associated response to bacteria (Kim et al., 2008; Canonne et al., 2011). The presence of XopD results in non-specific relocalization of nuclear proteins from nucleoplasm into nuclear foci, suggesting that XopD may be able to modulate chromatin structure (Canonne et al., 2011). Recently, it was documented that several defense-related WRKY TFs are attached to PopP2 from *R. solanacearum* and AvrRps4 from *P. syringae* (Sarris et al., 2015). Acetylation of the WRKY domain by PopP2 likely interferes with the capability of W-box DNA binding, leading to dysfunction of these TFs and attenuation of basal immune responses (Le Roux et al., 2015; Sarris et al., 2015). The AvrBs3 family effectors found in many *Xanthomonas* and *Ralstonia* species forms an interesting group of nuclear localized T3Es, which can mimic eukaryotic TFs to activate host promoters by DNA binding and are thus designated transcription activator-like effectors (TALEs) (Bogdanove et al., 2010; Boch et al., 2014). Several TALEs are reported to aid bacterial infection *in planta* by promoting the expression of disease susceptibility genes, such as the *SWEET* sucrose transporter family members, helping the pathogen to acquire nutrients from the host (Yang et al., 2006; Chen et al., 2010).

1.5.2. Fungal effectors

Like bacteria, pathogenic fungi are thought to secrete numerous virulence effectors during the time course of the infection. Many fungi have evolved specialized structures named haustoria, which are the major sites for the acquisition of nutrients and the secretion of effectors (Koeck et al., 2011; Giraldo and Valent, 2013). Repression or downregulation of MTI signaling has been shown to be performed by effectors acting in the apoplast or inside the host cells, although the translocation mechanisms underlying the delivery of effectors are still superficially understood (Ellis et al., 2009; Panstruga and Dodds, 2009; Petre and Kamoun, 2014).

Chitin is a major structural component in fungal cell walls and can be hydrolysed by plant chitinases into oligomers of different length, which are recognized by lysM-containing plant

receptors to activate defense responses (Kaku et al., 2006). Fungal pathogens have evolved different mechanisms to evade or dampen plant immunity induced by chitin. The apoplastic effector Avr4 from the leaf mold fungus *Cladosporium fulvum* is capable to bind chitin in order to prevent hydrolysis by plant chitinases (van den Burg et al., 2004; van den Burg et al., 2006; van Esse et al., 2007). Another effector of *C. fulvum*, Ecp6 (already mentioned in 1.1), and Slp1 of *Magnaporthe oryzae* are extracellular lysM-containing proteins that subvert chitin-elicited immunity by scavenging chitin oligosaccharides released from cell walls of fungal hyphae, thus preventing their perception by cognate PRRs (de Jonge et al., 2010; Mentlak et al., 2012; Sanchez-Vallet et al., 2013).

Upon infection, plants produce a large number of pathogenesis-related proteases in the apoplast to hinder disease development and therefore, represent prime choice targets of various effectors from filamentous pathogens (Ferreira et al., 2007; van der Hoorn, 2008). For instance, secretion of Avr2 by *C. fulvum* and Pti2 by *Ustilago maydis* selectively inhibit the activity of a set of apoplastic host cysteine proteases, including tomato's PIP1, Rcr3 and maize's CP1, CP2 (Shabab et al., 2008; van Esse et al., 2008; Mueller et al., 2013). The secreted effector, Pep1, conserved in the smut fungi *U. maydis* and *U. hordei* is essential for penetration and accumulates in the apoplastic space, where it blocks early immune responses by inhibiting POX12, a plant peroxidase important for the generation of extracellular ROS generation at the infection site (Doehlemann et al., 2009; Hemetsberger et al., 2012).

In addition to extracellular targets of plant resistance, fungal effectors also interfere with intracellular components involved in MTI signaling pathways. However, only a few of them have been identified and characterized so far. An example is the avirulence protein of *M. oryzae*, AvrPiz-t, which is translocated into rice cells during infection and performs virulence activity in rice lacking the resistance protein Piz-t by suppressing MAMP-triggered immune responses through the interaction and degradation of the rice RING E3 ubiquitin ligase APIP6 (Park et al., 2012).

1.5.3. Oomycete effectors

Oomycete pathogens, including downy mildews and *Phytophthora* species, cause many economically disastrous diseases on different crop species, such as tomato and potato late blight caused by *Phytophthora infestans.* Although phylogenetically very distant from fungi, oomycetes possess a range of fungus-like morphological features for tissue colonization (Judelson and Blanco, 2005; Fawke et al., 2015). For many biotrophic and hemibiotrophic

species, haustoria are formed following penetration and enter into host cells for nutrient uptake and effector secretion (Bozkurt et al., 2012; Kemen and Jones, 2012).

The knowledge about the biochemical properties and virulence functions of oomycete effectors has increased in the past decade. A few apoplastic effectors have been shown to affect the activity of defense-related proteases secreted by plants upon infection. Two Kazal-like protease inhibitors, EPI1 and EPI10, from *P. infestans*, interact with and disturb the activity of P69B, a subtilisin-like serine protease of tomato (Tian et al., 2004; Tian et al., 2005). Another two effectors, EPIC1 and EPIC2B, bind and inhibit the tomato cysteine proteases $Rcr3^{pim}$ and C14, respectively (Song et al., 2009; Kaschani et al., 2010). GIP1, a glucanase inhibitor delivered by *P. sojae*, selectively associates with and inhibits soybean endoglucanase EgaseA activity in apoplast, thereby reducing the release of glucan elicitors from *P. sojae* cell wall and probably protecting the mycelium against EgaseA-mediated cellular lysis (Rose et al., 2002).

Besides apoplastic effectors, cytoplasmic effectors suppressing plant immunity have been identified and characterized (Anderson et al., 2015). A large group of these cytoplasmic effectors is called RXLR effectors, since they carry an N-terminal secretion peptide followed by a conserved RXLR (arginine-any amino acid-leucine-arginine) motif, which has been shown to enable translocation of effector proteins inside plant cells (Whisson et al., 2007; Dou et al., 2008; Grouffaud et al., 2008). It is supposed that RXLR effectors may be adapted to facilitate biotrophy, because their expression is usually upregulated during the biotrophic stage of the infection (Whisson et al., 2007; Oh et al., 2009). The elucidation of the function and mode of action of many RXLR effectors has become an important objective and is documented by an abundant literature in the past 5-6 years. These studies have shown that RXLR effectors interfere with MAMP-induced immunity at different levels, through different mechanisms and with different sub-cellular localizations, from the cell periphery to the nucleus (Figure 1-3). The intensively studied RXLR effector AVR3a from *P. infestans* represses INF1-induced cell death by targeting and stabilizing the plant E3 ligase CMPG1 (Bos et al., 2006; Bos et al., 2010; Gilroy et al., 2011). Recently, it was found that Avr3a compromises flg22-induced responses in *N. benthamiana* by associating with NtDRP2, a GTPase involved in receptor-mediated endocytosis (Chaparro-Garcia et al., 2014). Avr3b from *P. sojae* contains a Nudix hydrolase motif in the C-terminal part of the effector domain and displays ADP-ribose/NADH pyrophosphorylase enzymatic activity, which impairs host immunity by reducing ROS accumulation (Dong et al., 2011). The hydrolase activity of

Avr3b is dependent on the interaction with the plant cyclophilin CYP1 through a putative Glycine-Proline (GP) motif (Kong et al., 2015). Suppression of MAMP-activated callose deposition and ROS production has also been reported for the ATR1 and ATR13 RXLR effectors from *Hyaloperonospora arabidopsidis*, an oomycete pathogen of Arabidopsis (Sohn et al., 2007). The overexpression of the *P. infestans* RXLR effector IPI-O in transgenic Arabidopsis lines disrupted MAMP-triggered callose deposition and increased susceptibility towards *Phytophthora brassicae*, which was proposed to be due to the binding of its RGD motif to the membrane-associated receptor LecRK-1.9 and following alteration of the cell wall – plasma membrane continuum (Bouwmeester et al., 2011). Interestingly, LecRK-1.9 is DORN1, recently reported as the receptor for extracellular ATP (Choi et al., 2014), raising the possibility that IPI-O effector might be involved in disruption of DAMP signal transduction. Members of the AVRblb2 RXLR effector family are highly variable and under diversifying selection in different *P. infestans* isolates (Oh et al., 2009). When expressed in plant cells, AVRblb2 localizes to the cell periphery and blocks the secretion of the defense-associated protease C14 into the apoplast resulting in a decreased resistance against *P. infestans* (Bozkurt et al., 2011). MAPK signaling, as an important node in the plant immune network, is a prime target of the attack by different pathogens. One RXLR effector of *P. infestans*, PexRD2, has been found to interact with the kinase domain of MAPKKKε and perturb MAPKKKε-dependent signaling pathway that is apparently regulating ETI but not MTI (Oh et al., 2009; King et al., 2014). One example of an RXLR effector manipulating host transcription is given by PITG_03192, which targets two predicted potato NAC transcription factors, NTP1 and NTP2, at the membrane of the endoplasmic reticulum (ER) and prevents their re-localization to the nucleus upon MAMP application (McLellan et al., 2013). The role of autophagy in plant protection toward pathogen infection is unclear and controversial but one effector of *P. infestans*, PexRD54, binds ATG8CL, a key component in autophagosome formation, and prevents its interaction with the cargo receptor Joka2, which resulted in increased *P. infestans* growth on *N. benthamiana* leaves (Dagdas et al., 2016).

Several RXLR effectors have been show to localize in the nucleus where they are thought to interfere with the transcriptional, post-transcriptional or translational machinery of the host cell. The *H. arabidopsidis* nuclear-localized effector, HaRxL44, was shown to associate with Mediator subunit 19a (MED19a), leading to proteasome-dependent degradation of MED19a and the activation of JA/ET-signaling which antagonizes SA-signaling and the activation of SA-responsive genes that are thought to be more important in immunity to biotrophic pathogens like *H. arabidopsidis* (Caillaud et al., 2013). In another study, the *P. infestans*

effector Pi04314 associated with different isoforms of host protein phosphatase type 1c (PP1c) and caused their re-localization within the nucleus without affecting their biochemical activity. The PP1c isoforms were proposed to be susceptibility factors, manipulated by Pi04314 to promote disease development by attenuating SA and JA signaling (Boevink et al., 2016).

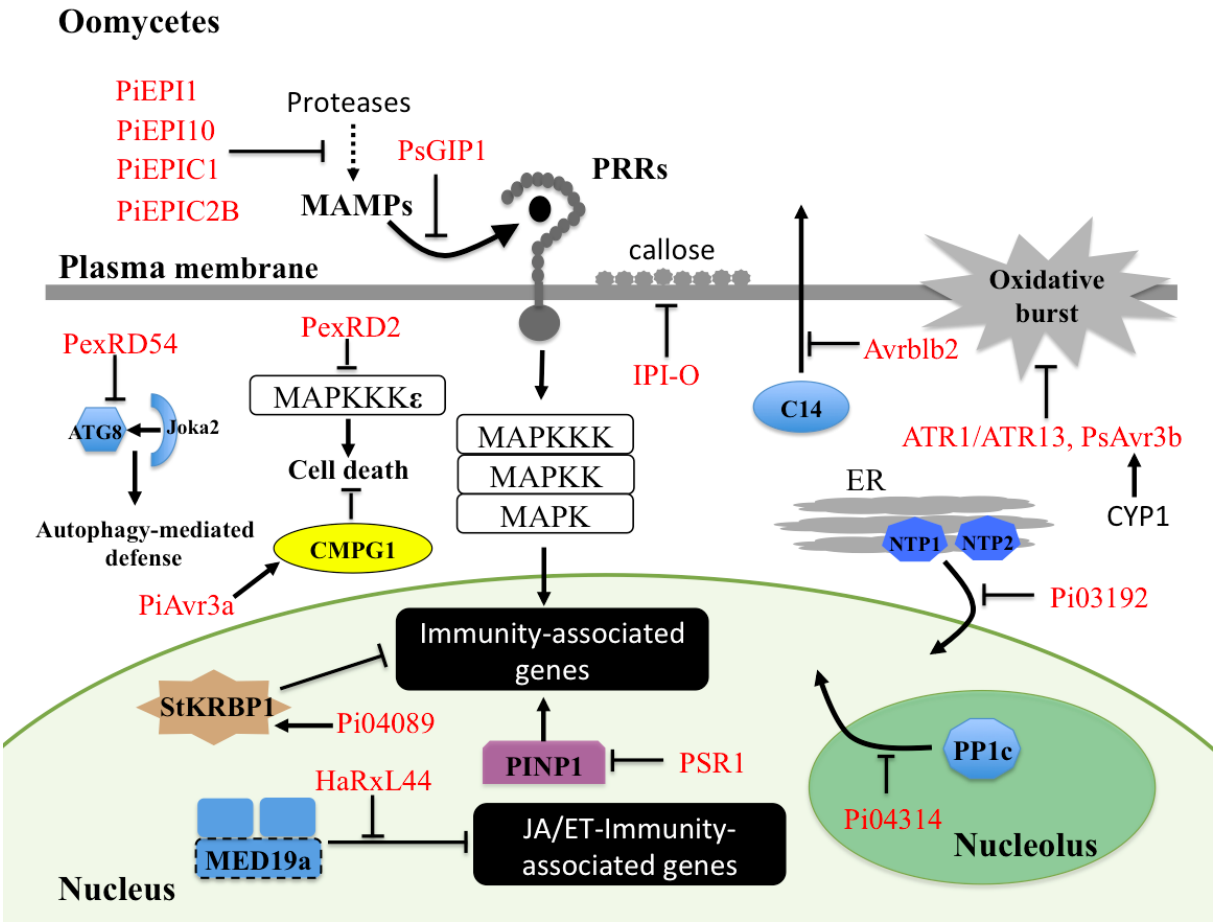

Figure 1- 3. Plant immunity-suppressing function of effectors from phytopathogenic oomycetes.

Apoplastic and cytoplasmic effectors secreted by pathogenic oomycetes disturb plant immunity at different levels. Components involved in plant immune system and defense-interfering effectors (in red) are delineated. Plain line: demonstrated function, dashed line: hypothetical function. See main text for additional details. Abbreviations appeared in the figure: MAMP, microbe-associated molecular patterns; PRR, pattern recognition receptor; MAPK, mitogen-activated protein kinases; MAPKK, mitogen-activated protein kinase kinases; MAPKKK, mitogen-activated protein kinase kinase kinases; MAPKKKε, mitogen-activated protein kinase kinase kinase ε; CMPG1, ubiquitin-protein ligase CMPG1; ATG8, autophagy-related proteins ATG8; Joka2, the autophagy cargo receptor Joka2; C14, papain-like cysteine protease C14; ER, endoplasmic reticulum; NTP1 and NTP2, NAC transcription factor Targeted by *Phytophthora* 1 and 2; StKRBP1, putative potato K-homology (KH) RNA-binding protein 1, MED19a, Mediator subunit 19a; PINP1, PSR1-Interacting Protein 1; PP1c, protein phosphatase type 1c; SA, salicylic acid. The Figure is modified from (Doehlemann et al., 2014).

The *P. infestans* effector Pi04089 could represent a possible case of interference of host post-transcriptional processes through its interaction and stabilization of a putative potato KH RNA-binding protein (StKRBP1) in the nucleus (Wang et al., 2015). The function of StKRBP1 and the consequence of its interaction with Pi04089 on cellular homeostasis are unknown but, StKRBP1 is also a susceptibility factor and its absence confers enhanced resistance to infection by *P. infestans* (Wang et al., 2015). In addition, oomycete RXLR effectors interfering with siRNA-mediated host defenses have also been identified, illustrating further the huge functional diversity acquired by this class of effectors. Two *P. sojae* RXLR effectors were identified as Phytophthora Suppressors of RNA silencing (PSRs) because of their negative impact on small RNA biogenesis (Qiao et al., 2013). One of them, PSR1, appears to target the plant nuclear protein PINP1 with a DEAH-box RNA helicase domain, which regulates small RNA accumulation, probably by affecting correct assembly of the Dicer complex (Qiao et al., 2015). Importantly, both PINP1 and StKRBP1 have not been reported to be components involved in plant immunity prior to their identification as effector target proteins, which is a strong argument to use effectors as probes to dissect the plant immune network.

1.6. Objective of this thesis

With the beginning of my thesis work, complete genome sequencing of several oomycete species has been performed or was in progress. Bioinformatics analysis identified RXLR motif-containing proteins as the major group of effectors with a proven virulence function. RXLR effector genes are under strong diversification pressure and exhibit high rates of presence/absence polymorphism, high copy number variation and strong positive selection, suggesting that they play a major role in host adaptation. However, the function and mode of action of RXLR effectors was largely unknown and notably, the importance of MTI suppression in the process of host colonization by oomycetes has ben poorly studied.

The objective of this thesis was to demonstrate whether and how RXLR effectors from *P. infestans* subvert early-induced MTI signaling. In the first chapter, I used a medium/high throughput cell-based system to identify and characterize putative MTI-suppressing RXLR effector candidates. In the second chapter, I have performed a deeper analysis of the association of host calmodulin with SFI5, one of the effector identified in the primary functional screen, to improve the understanding of the mechanistic basis of MTI-suppression and host adaptation driven by this individual effector.

2. Materials and Methods

2.1. Materials

2.1.1 Microbial organisms

All microbial strains that are used in this study are listed in Table 2-1.

Table 2-1. Microbial strains used in this study

Species	Strain/Isolate	Genotype
Escherichia coli	DH5α	F– *endA1 glnV44 thi-1 recA1 relA1 gyrA96 deoR nupG purB20* φ80d*lacZ*ΔM15 Δ(*lacZYA-argF*)U169, hsdR17(rK–mK+), λ–
	DB3.1	F- gyrA462 endA1 glnV44 Δ(sr1-recA) mcrB mrr hsdS20(rB-, mB-) ara14 galK2 lacY1 proA2 rpsL20(Smr) xyl5 Δleu mtl1
	Rosetta™(DE3)	F- ompT hsdSB(RB- mB-) gal dcm λ(DE3 [lacI lacUV5-T7 gene 1 ind1 sam7 nin5]) pLysSRARE (Cam^R)
Agrobacterium tumefaciens	C58C1	T-DNA^- vir^+ rif^r, $carb^r$
Phytophthora infestans	88069	virulent on R3a

2.1.2. Plant organisms

Arabidopsis thaliana ecotype Col-0 and *Solanum lycopersicum* cultivar Moneymaker were used for protoplast preparation. *Nicotiana benthamiana* was used to transiently express proteins of interest *in planta* by Agro-infiltration.

2.1.3. Vectors

Table 2-2. Vectors applied in this work

Vector	Description	Reference
pDONR201	Entry vector for the Gateway system	Invitrogen
p2GW7	Gateway destination vector to express proteins in protoplasts, driven by CaMV 35S promoter	Invitrogen
p2FGW7	Gateway destination vector to express N-terminal GFP fusion proteins in protoplasts, driven by CaMV 35S promoter	VIB, University of Gent
p2GWF7	Gateway destination vector to express C-terminal GFP fusion proteins in protoplasts, driven by CaMV 35S promoter	VIB, University of Gent
p2HAGW7	Gateway destination vector to express N-terminal HA-tagged proteins in protoplasts, driven by CaMV 35S promoter	VIB, University of Gent
pB7WG2	Binary Gateway destination vectors to express proteins *in planta*, driven by CaMV 35S promoter	Invitrogen
pB7WGF2	Binary Gateway destination vectors to express N-terminal GFP fusion proteins *in planta*, driven by CaMV 35S promoter	(Karimi et al., 2002)
pDEST15	*E. Coli* expression vector with a N-terminal GST tag (Gateway destination vector)	Invitrogen
pMAL-p5x	*E. Coli* expression vector with a N-terminal MBP tag	NEB
pFRK1-Luc	Luciferase reporter gene assay in protoplasts	(He et al., 2006)
pUBQ-GUS	GUS activity assay in protoplasts	(He et al., 2006)

2.1.4. Primers

The primers used in this study were ordered from Eurofins MWG Operon (Ebersberg). Lyophilized oligonucleotides were resuspended in nuclease-free water to a stock

concentration of 100 µM and diluted to 10 µM for the working concentration. The sequences of these primers are listed in the Appendix Table 6-1.

2.1.5. Elicitor and Peptides

The elicitor flg22 was used as a MAMP-active surrogate in our study. Flg22 peptide (QRLSTGSTINSAKDDAAGLQIA) was kindly provided by Prof. Georg Felix and dissolved in milli-Q water with 1mg/ml BSA and 0.1 M NaCl to a stock concentration of 10 mM and stored at -20 °C.

The peptides derived from identified effector SFI5 were synthetized by Genscript Inc. (USA) and prepared as 20 mg/ml stock solutions in Milli-Q water containing 0.1 % DMSO (stored at -20 °C), and diluted in water to obtain the desired concentration prior to use.

2.1.6. Chemicals, enzymes and antibodies

All used chemicals and reagents were of standard purity and ordered from Carl Roth (Karlsruhe), Merck (Darmstadt), Sigma-Aldrich (Taufkirchen), Qiagen (Hilden), Invitrogen (Karlsruhe), Duchefa (Haarlem, Niederlande), Fluka (Buchs, Schweiz), Promega (Mannheim), Serva (Heidelberg), Roche (Mannhein), Molecular Probes (Leiden, Niederlande) and BD (Sparks, USA), unless stated otherwise in the text. Membranes for blotting were ordered from GE Healthcare (Freiburg).

For nucleic acids studies and gene cloning, *Pfu* DNA polymerase, restriction enzymes, T4 DNA ligase were used and ordered from Fermentas (St. Leon- Rot). SYBR Green Master Mix for quantitative RT-PCR was purchased from Fermentas (St. Leon- Rot). Gateway® BP clonase and LR clonase enzyme mix were ordered form Invitrogen (Karlsruhe).

Antibodies were received from the companies New England Biolabs (Beverly, USA), Sigma-Aldrich (Taufkirchen) or Acris Antibody GmbH (Herford) and are listed in Table 2-3.

2.1.7. Media and Antibiotics

All media were prepared using deionized water and sterilized by autoclaving for 20 minutes at 121 °C. For solid media, 15 g/L Bacto-agar (BD) was added to the medium prior to autoclaving. Table 2-4 summarizes the media used in this work. Media, if necessary, were supplemented with antibiotics at appropriate final concentrations, as listed in Table 2-5.

Table 2-3. Antibodies used in this work

	Antibody	**Host**	**Dilution**	**Reference**
Primary antibodies	@phospho-p44/p42 MAPK	rabbit	1:1000	New England Biolabs
	@GFP	goat	1:5000	Acris
	@HA	mouse	1:3000	Sigma-Aldrich
	@GST	mouse	1:7000	Sigma-Aldrich
	@MBP	mouse	1:10000	New England Biolabs
Secondary antibodies	@goat IgG HRP conjugated	rabbit	1:10000	Sigma-Aldrich
	@mouse IgG HRP conjugated	rabbit	1:10000	Sigma-Aldrich
	@rabbit IgG-Alkaline Phosphatase	goat	1:3000	Sigma-Aldrich
	@mouse IgG-Alkaline Phosphatase	rabbit	1:3000	Sigma-Aldrich
	@goat IgG-Alkaline Phosphatase	rabbit	1:3000	Sigma-Aldrich

Table 2-4. Media used in this study

Medium	Ingredients per 1 liter	Species
LB	10 g Bacto-Tryptone, 5 g NaCl, 5 g Yeast extract (YE)	*E. coli*
Rye-sucrose (Caten and Jinks, 1968)	60 g rye, 20 g Sucrose, pH 7.0 (NaOH)	*P. infestans*

Table 2.5. Antibiotics used in this study

Antibiotics	Final concentration (μg/ml)	Solvent
Ampicillin	50-100	H_2O
Kanamycin	50	H_2O
Rifampicin	50	DMSO
Gentamycin	25	H_2O
Carbenicillin	50-100	H_2O

2.1.8. Buffers and solutions

All buffers and solutions used in this study were prepared, if not noted otherwise, in Milli-Q water. Aqueous solutions were sterilized by autoclaving at 121 °C for 20 minutes or filtered.

2.2. Methods

2.2.1. Cultivation of microorganisms

2.2.1.1. Cultivation of *Escherichia coli*

E. coli strains were grown either on LB-agar plates or in liquid LB medium while shaking at 200 rpm overnight in a 37 °C incubator. The plates and the medium were supplemented with appropriate antibiotics based on the resistance gene carried by the plasmid used for transformation.

2.2.1.2 Cultivation of *Agrobacterium tumefaciens*

A. tumefaciens was grown on LB-agar plates or in liquid LB medium while shaking at 230 rpm for 36 hours in a 28 °C incubator. The plates and the medium were supplemented with appropriate antibiotics based on the resistance gene carried by the plasmid used for transformation.

2.2.1.3. Cultivation of *Phytophthora infestans*

P. infestans was maintained at 18 °C on rye-sucrose agar plates in the dark as described previously (Whisson et al., 2007).

2.2.2. Plant growth conditions

2.2.2.1. Growth of *Arabidopsis thaliana*

A. thaliana plants were cultivated in a phytochamber with a photoperiod of 8 h light at 22– 24 °C /16 h dark at 20 °C, 40 %–60 % humidity, ~120 µE m^{-2} s^{-1} light intensity. They were grown on steam-sterilized soil composed of a 3.5:1 mixture of GS/90 (Patzer, Germany) and vermiculite. Leaves from 4 to 5 week-old plants were used for protoplast preparation.

2.2.2.2. Growth of *Solanum lycopersicum*

S. lycopersicum plants were cultivated in a greenhouse under stable climate conditions: 16 hours light at 24 °C /8 hours dark at 22 °C, 40 %–45 % humidity, ~200 µE m^{-2} s^{-1} light intensity. They were grown on steam-sterilized soil containing a 4.6:4.6:1 mixture of type P

soil, type T soil (Patzer, Germany) and sand. Leaves from 3 to 4 week-old plants were used for protoplast preparation.

2.2.2.3. Growth of *Nicotiana benthamiana*

N. benthamiana plants were grown on a mixture of steam-sterilized T soil and fertilizer (50:1) containing 0.1 % (v/v) Confidor and kept under the same growing conditions as *S. lycopersicum.* Leaves from 4 to 5 week-old plants were used for patho-assays.

2.2.3. Plant methods

2.2.3.1. Isolation and transfection of mesophyll protoplasts from *Arabidopsis thaliana* and *Solanum lycopersicum*

The preparation of Arabidopsis mesophyll protoplasts was conducted based on a previously described protocol (Yoo et al., 2007) with slight modifications. In brief, well-extended leaves from 4 to 5 week-old plants were cut into 0.5 mm thin strips and dipped into the enzyme solution (Enzy-A solution) with 1.5 % cellulase 'Onozuka' R10 and 0.4 % macerozyme R10 (Yakult Pharmaceutical Industry). After vacuum-infiltration and enzymatic digestion, the released protoplasts were collected by filtration through 75 µm nylon meshes and recovered by two subsequent washing with W5-A buffer. The final concentration of protoplasts was adjusted to 2×10^5 cells/ml in MMG buffer prior polyethylene glycol (PEG)-mediated transfection. For each sample, every 100 µl protoplasts were mixed with 10 µg plasmid DNA and 110 µl freshly prepared PEG buffer during transfection. Protoplasts samples were then incubated in W1 buffer at 20 °C in the dark for 9 to 12 hours allowing plasmid gene expression.

S. lycopersicum mesophyll protoplast preparation was performed as described by (Nguyen et al., 2010) with minor changes. The lower epidermis of fully expended leaflets was gently rubbed with grated quartz, rinsed with sterile water and leaf strips were floated on the enzyme solution (Enzy-T solution) containing 2 % cellulase 'Onozuka' R10 (Yakult Pharmaceutical Industry), 0.4 % pectinase (Sigma) and 0.4 M sucrose in K3 solution. After a 3 h incubation at 30°C in the dark, the enzyme-protoplast mixture was filtered through a 100 µm nylon mesh. Viable protoplasts were collected by sucrose gradient centrifugation and washed once in W5-T buffer. After recovery on ice for 1.5-2 hours, protoplasts were harvested by centrifugation and resuspended at a density of 6×10^5 cells/ml in MMG buffer prior PEG-mediated transfection, which was carried out as for Arabidopsis. The transfected protoplasts were

incubated in W1 buffer at 20 °C in the dark for 6-8 hours before further measurements.

Table 2-6. Solutions for protoplast preparation and transformation

solution/buffer	Ingredients
Enzy-A solution	20 mM KCl, 0.4 M mannitol, 20 mM MES pH 5.7, 1.5 % (w/v) cellulase "Onozuka" R10, 0.4 % (w/v) macerozyme R10, 10 mM $CaCl_2$, 0.1 % (w/v) bovine serum albumin (BSA).
W5-A buffer	125 mM $CaCl_2$, 5 mM KCl, 2 mM MES pH 5.7, 154 mM NaCl
MMG buffer	0.4 M mannitol, 4 mM MES pH 5.7, 15 mM $MgCl_2$
W1 buffer	20 mM KCl, 0.5 M mannitol, 4 mM MES pH 5.7
K3 solution	10 ml Macro-stock, 0.1 ml Micro-stock, 0.1 ml Vitamin-stock, 0.5 ml FeNa-EDTA stock, 10 mg myo-inositol, 25 mg D-xylose, 13.7 g sucrose for 100 ml; adjust pH to 5.7 (KOH), filter sterilize and store at −20 °C
Enzy-T solution	2 % (w/v) cellulase "Onozuka" R10, 0.4 % (v/v) pectinase and 0.4 M sucrose in K3 solution
W5-T buffer	18.4 g $CaCl_2$•2 H_2O, 1 g glucose, 0.4 g KCl, 9 g NaCl for 1 liter; adjust pH to 5.7 (HCl)
PEG solution	0.1 M $CaCl_2$ (for Arabidopsis) or 0.1 M $Ca(NO_3)_2$ (for tomato), 0.2 M mannitol, 40 % (w/v) PEG4000 (Sigma)

Stock solution	Ingredients
Macro-stock (10 x)	1.5 g NaH_2PO_4•H_2O, 9.0 g $CaCl_2$•2H_2O, 25 g KNO_3, 2.5 g NH_4NO_3, 1.34 g $(NH_4)_2SO_4$, 2.5 g $MgSO_4$•7H_2O for 1 liter; autoclave for storage.
Micro-stock (1000 x)	75 mg KI, 300 mg H_3BO_3, 1 g MnSO4•7H_2O, 200 mg $ZnSO_4$•7H_2O, 25 mg Na_2MoO_4•2H_2O, 2.5 mg $CuSO_4$•5H_2O, 2.5 mg $CoCl_2$•6H_2O for 100 ml; filter sterilize and freeze at −20 °C.
Vitamin-stock (1000 x)	100 mg nicotinic acid, 100 mg pyridoxine-HCl, 1 g thiamine-HCl for 100 ml; filter sterilize and freeze at −20 °C.
FeNa-EDTA stock (200 x)	1 % (w/v) ethylenediaminetetraacetic acid (EDTA) ferric sodium salt (stored at 4 °C).

2.2.3.2. *Agrobacterium*-mediated transient transformation of *Nicotiana benthamiana*

A. tumefaciens C58C1 carrying the appropriate vector constructs were grown as described in 2.2.1.2. Cultures were harvested at 4 °C for 10 minutes at 2000 g and subsequently washed twice with 10 mM $MgCl_2$. Pellets were then re-suspended in infiltration buffer (10 mM MES pH 5.6, 10 mM $MgCl_2$ and 200 mM acetosyringone) and adjusted to the desired concentration. After incubation at room temperature for 2-3 hours, the mixture was infiltrated into 4 to 6-week-old *N. benthamiana* leaves using 1 ml needleless syringe. The leaf tissue was analyzed 24-36 hours post-infiltration. For co-expression, *A. tumefaciens* strains were mixed in a 1:1 ratio.

2.2.4. Molecular biological analysis

2.2.4.1. Bacterial plasmid DNA extraction

For mini-preparation of plasmid DNA, a bacterial pellet from 2-4ml overnight LB culture of *E. coli* was resuspended in 200 µl Solution I (25 mM Tris-HCl pH 8.0, 10 mM EDTA pH 8.0, 50 mM Glucose and 0.1 mg/ml RNase A) by vortexing and then subsequently mixed with 400 µl of Solution II (0.2 M NaOH, 1 % (w/v) SDS) and 300 µl of Solution III (3 M KAc, 11.5 % HAc). The mixture was centrifuged and the aqueous phase containing plasmid DNA was precipitated with 0.7 volume isopropanol. The DNA pellet was washed with 70 % (v/v) ethanol and dissolved in TE-buffer (10 mM Tris-HCl pH 8.0, 1 mM EDTA pH 8.0) or deionized water.

For midi scale preparation, plasmid DNA was extracted from 150 ml (high copy plasmid) overnight liquid cultures by column purification using the PureYield Plasmid Midi-prep system (Promega) following the manufacturer's instructions.

For maxi scale isolation of plasmids, a manual protocol form (http://oxfordgenetics.com/cloning-resources/cloning-guides/maxiprep-protocol) was followed with slight modifications. Briefly, a 2.5 ml pre-culture from a single colony was inoculated into 500 ml pre-warmed LB medium for 20-24 hours growing at 37 °C. The cell pellets were harvested by centrifugation for 30 minutes at 5500 g and completely re-suspended in 8 ml ice cold TE50/1 (50 mM Tris-HCL pH 8.0, 1 mM EDTA pH 8.0) by shaking at 200 rpm. After subsequently mixing with 2.5 ml of freshly prepared lysozyme solution (10 mg/ml lysozyme in deionized water), 2 ml of 0.5 M EDTA pH 8.0 as well as 1 ml of mixture solution (50 µl Ribonuclease A (20 mg/ml in distilled water), 150 µl 10 % Triton x-100, 800 µl TE50/1), the suspension was incubated on ice for 60 minutes. The

supernatant was separated by centrifugation at 20000 g for 60 minutes and transferred to a clean Falcon tube. Followed by equilibrated phenol (pH 8.0 with 0.1 % 8-hydroxyquinoline) and chloroform purification, the upper aqueous phase containing plasmid DNA was collected and precipitated by adding 0.1 volume of 5 M $NaClO_4$ and 0.8 volume of isopropanol. The DNA pellets were harvested by centrifugation at 4500 g for 20 minutes and washed with 70 % (v/v) ethanol and then air-dried and re-suspended in sterile ddH_2O to a concentration of 1 µg/µl.

2.2.4.2. Standard PCR

For gene cloning, standard PCR reactions were performed with the high-fidelity *Pfu* DNA polymerase (Fermentas) following the supplier's recommendations. All PCRs were carried out in a PTC 200 Peltier thermal cycler (MJ Research).

2.2.4.3. Gateway reactions

All of the constructs used in this study for transient gene expression in protoplasts or in *N. benthamiana* leaves were generated using the Gateway recombination cloning technology (Invitrogen). In order to obtain Gateway-compatible inserts, genes of interest were amplified in a two-step nested PCR reaction with one pair of the gene-specific adapter primers and one pair of attB-adapter primers (see Appendix Table 6.2.). The PCR products were purified through gel extraction using the GeneJet Gel Extraction Kit (Fermentas) and recombined into pDONR201 or pDONR221 (Invitrogen) by the BP clonase reaction. The generated entry clones were then sub-cloned into the expression vectors p2GW7, p2FGW7, p2HAGW7, p2GWF7 or pB2GW7 by using the LR clonase reaction according to the manufacturer's specifications (Invitrogen).

2.2.4.4. DNA Sequencing

The constructs and PCR products were sequenced by GATC Biotech AG (Konstanz). 5µl DNA template with either 80-100 ng/µl plasmid or 20-80 ng/µl PCR product was added to 5µl 5 µM sequencing primer. The sequence analysis was performed using DNAstar or CLC main workbench software.

2.2.4.5. RNA isolation from protoplasts

Total RNA was extracted from *A. thaliana* protoplasts by using TRI reagent (Ambion) and treated with DNAase I (Machery-Nagel) to remove DNA contamination. 400 µl TRI reagent was added to the frozen cell pellet from 800 µl of protoplast sample, followed by immediate

vortex and incubation at room temperature for 10 minutes. After addition of 80 µl of chloroform and vortex-mixing, sample was incubated for another 10 minutes at room temperature and then centrifuged for 10 minutes at 21000 g, room temperature. The upper phase was carefully transferred into a new 1.5 ml tube and mixed with equal volume of isopropanol. RNA was precipitated by incubating the mixture at room temperature for 1 hour and harvested by centrifugation for 10 minutes at 4 °C, 21000 g. The RNA pellet was washed twice with 75 % (v/v) ethanol and air-dried and dissolved in 15 µl nuclease-free water (Fermentas). Following the DNase I treatment (according to manufacturer's protocols), RNA concentration was quantified using a Nanodrop 2000 (Peqlab Biotechnologie GmbH).

2.2.4.6. cDNA synthesis

Poly A-tailed RNA was converted to cDNA by using the RevertAid reverse transcriptase (Fermentas) and oligo-dT primers. For reverse transcription, 1-2 µg of total RNA in 10 µl nuclease-free water was denatured at 70 °C for 10 minutes and cooled down on ice. Next, 10 µl of freshly prepared RT-mix solution (4 µl 5×RT buffer, 2 µl oligo-dT (30 µM)), 2 µl dNTP-Mix (2.5 mM), 1 µl M-MuLV RT RevertAid (200 U/µl), 0.5 µl RNase inhibitor (RiboLock, 40 U/µl), 0.5 µl ddH_2O) was added and the mixture was incubated at 42 °C for 90 minutes, followed by enzyme deactivation at 70 °C for 10 minutes.

2.2.4.7. Quantitative real time-PCR (qRT-PCR)

For qRT-PCR, cDNA from the reverse transcription reaction was diluted 3 to 5 fold with nuclease-free water, and 1 µl of diluted cDNA was applied in a 20 µl reaction mix (10 µl 2 × SYBR Green Supermix, 0.5 µl Forward primer (10 µM), 0.5µl Reverse primer (10 µM), 8 µl ddH_2O). The SYBR Green Supermix is from Maxima™ SYBR Green qPCR Master Mix (Fermentas). In order to minimize the operating errors, each sample was performed in triplicates. The amplification was run on iQ5 Multicolour Real Time PCR detection system (Bio-Rad) according to the manufacturer's instructions. Relative gene expression was determined with a serial cDNA dilution standard curve. The *Actin* transcript was used as an internal control in all experiments. Data was processed with the iQ software (Biorad). Primers used in qRT-PCR reactions are listed in Appendix Table 6-1.

2.2.4.8. Preparation and transformation of chemically competent *E. coli* DH5α cells

Stocks of competent cells of *E. coli* DH5α were produced by the classical $CaCl_2$ method. One colony was grown in 3 ml LB medium by shaking at 37 °C overnight. 150 µl of the overnight culture was inoculated into 100 ml LB medium and shaken at 37 °C until OD_{600} = 0.2 ~ 0.25.

The culture was chilled on ice for 30 minutes and the cells were harvested by centrifugation at 4 °C, 1600 g for 10 minutes. The pellets were re-suspended in 30 ml ice cold 0.1 M $CaCl_2$ and then kept on ice for 30 minutes. After centrifugation, the cell pellet was re-suspended in 2.5 ml ice-cold $CaCl_2$ solution (0.1 M $CaCl_2$, 15 % glycerol), followed by freezing in liquid nitrogen and stored at -80 °C.

80 µl aliquot competent cells were thawed on ice and then added with plasmid or recombination products. After incubation on ice for 30 minutes, the mixture was heat-shocked at 42 °C for 45 seconds and immediately cooled down on ice for 2-3 minutes. Next, 500 µl LB medium was added and the cells were incubated at 37 °C with shaking (200 rpm) for 1 hour. Finally, 200 µl of transformed cell culture was spread onto solid LB plate containing appropriate antibiotics and incubated at 37 °C overnight.

2.2.4.9. Transformation of competent *A. tumefaciens* cells

50 µl electrically competent cells (stored previously at -80 °C) were thawed on ice and mixed with 100 ng plasmid DNA. The mixture was transferred to a pre-chilled electroporation cuvette. After incubation on ice for 10 minutes, the cuvette containing competent cells was pulsed once with 1500 V for 5 milliseconds (Eppendorf, Hamburg) and then put back on ice, followed by immediate addition of 500 µl LB medium. The cells were then transferred to a clean 1.5 ml Eppendorf tube and incubated at 28°C while shaking (200 rpm) for 2-3 hours. Afterwards, 200 µl of aliquot from the transformed cells was plated on selective LB agar plate and incubated at 28°C for 48 hours.

2.2.4.10. Construction of deletion mutants of SFI5 and site-directed mutagenesis

cDNA fragments encoding SFI5 variants with N- or C-terminal deletions were amplified by PCR using specific primers (described in Appendix Table 6-1.) and inserted into the entry vector pDONR201 through the BP reaction (Invitrogen), and subsequently recombined into the expression vectors p2HAGW7, p2FGW7 or pB7WG2 by the LR reaction (Invitrogen). Site-directed mutagenesis were performed following the instruction manual of the QuikChange® II XL Site-Directed Mutagenesis Kit (Stratagene). Primers used for mutagenesis are listed in Appendix Table 6-1. All the constructs were verified by sequencing.

2.2.5. Protein analysis

2.2.5.1. Protein extraction from plant tissue

Total protein from plant tissue was extracted using an extraction buffer containing detergents enabling solubilization of membrane-bound proteins (50 mM Tris-HCl pH 7.5, 150 mM NaCl, 1 % (v/v) Nonidet P40 and 1 tablet of protease inhibitor cocktail / 10 mL from Roche). 50-100 mg *N. benthamiana* leaves was collected in a 1.5 ml Eppendorf tube and grounded to fine powder by pre-cooling in liquid nitrogen. After the addition of 100 µl of ice-cold extraction buffer and incubation on ice for 30 minutes, the plant tissue was further homogenized by vortex mixing. The soluble proteins were purified from the mixture by centrifugation at 4 °C, 15000 g for 20 minutes. The protein concentration was measured by the Bradford method. 10 µl protein sample was mixed with 990 µl Roti-Quant solution (Carl Roth) and the OD_{595} of the mixture was monitored. Based on a BSA-standard curve, the protein concentration was estimated using the following formula:

Protein concentration [mg/ml] = OD_{595}/(0.0283 × used volume).

To extract protein from the protoplast samples, the cell pellet from 100 to 200µl protoplasts was harvested by short centrifugation at 6100 g for 10 seconds. Total protein was extracted by adding 40 µl 1× SDS loading buffer (50 mM Tris-HCl pH 6.8, 2 % SDS, 0.1 M DTT, 10 % Glycerol, 0.05 % Bromophenol Blue) and then incubating at 95 °C for 5 minutes.

2.2.5.2. Expression and purification of recombinant proteins in *E. coli*

The pDEST15 construct for expression of GST-AtCaM4 and the pMAL-p5x construct for expression of MBP-SFI5 were introduced into *E. coli* Rosetta™ (DE3). Positive colonies were grown in 3 ml LB medium containing ampicillin at 37°C overnight and served as pre-culture to inoculate the main culture at 1000 x dilution. When the bacteria reached an OD_{600} of 0.6 at 37 °C, the culture was transferred to 28 °C to induce expression of recombinant proteins. The expression of GST-AtCaM4 was induced by adding 0.2 % (w/v) L- Arabinose and the expression of MBP-SFI5 was induced by treatment with 0.5 mM isopropyl β-D-thiogalactopyranoside (IPTG). After 2-3 hours, the bacteria were harvested by centrifugation and the pellet was stored at -20 °C until use.

For purification of the fusion protein, 2.5 g frozen bacteria expressing GST-AtCaM4 or 5 g frozen bacteria expressing MBP-SFI5 were re-suspended in 20 ml lysis buffer containing 50 mM Tris-HCl pH 7.0, 150 mM NaCl, 5 mM $CaCl_2$ and 1 x protease inhibitor cocktail (Complete EDTA-free, Roche). The bacterial mixture was lysed on ice by sonication 3 times 10 seconds at least. After centrifugation at 34000 g for 20 minutes at 4 °C, the supernatants

were filtered and loaded to a 5 mL GST-Trap© or MBP-Trap™ (GE Healthcare Life Sciences) according to the manufacturer's protocol. The column was washed several times with washing buffer (20 mM Tris-HCl pH 7.0, 100 mM NaCl) and bound proteins were eluted with elution buffer (20 mM Tris-HCl pH 7.0, 100 mM NaCl, with 25 mM glutathione (GSH) or 10 mM maltose). Protein-containing fractions were loaded onto a Superdex 200© gel filtration (GE Healthcare Life Sciences) following the manufacturer's instructions and eluted protein fractions were analyzed by native-PAGE (2.2.5.8) followed by Coomassie blue staining (2.2.5.9) or immunoblotting (2.2.5.7).

2.2.5.3. Immunoprecipitation from protoplasts

1.5 to 2 ml transfected protoplasts were harvested by centrifugation at 100 g for 1 minute and the pellet was then re-suspended in 1 ml of immunoprecipitation (IP) buffer containing 50 mM HEPES pH 7.4, 150 mM NaCl, 0.1 % Trition X-100, 1 mM EDTA, 1 mM DTT, 1 x phosphatase inhibitor cocktail (PhosphoSTOP, Roche) and 1 x protease inhibitor cocktail (Complete EDTA-free, Roche). Total protein was released by sonication and the cell debris was removed through centrifugation. The HA-tagged proteins were immunoprecipitated from lysates by incubation with 20 µl of anti-HA antibody-coupled beads (anti-HA affinity matrix, Roche) for 3 to 6 hours while gently shaking at 4 °C. Afterwards, the beads were washed three times with 1 ml of washing buffer (50 mM HEPES pH 7.4, 150 mM NaCl, 0.2 % Triton X-100, 1 × phosphatase inhibitor cocktail (PhosphoSTOP, Roche) and 1 × protease inhibitor cocktail (Complete EDTA-free, Roche)). For elution, 50 µl 1 × SDS loading buffer without DTT was added to the beads, followed by boiling at 95 °C for 10 minutes. The immunoprecipitated proteins were then further analyzed for immunoblotting or Mass Spectrometry analysis.

2.2.5.4. *In vitro* kinase activity assay

The *in vitro* kinase assay was performed as described previously (He et al., 2006). Protoplasts expressing HA-SlMPK1 or HA-SlMPK3 fusion protein were lysed with IP buffer and immunoprecipitated with anti-HA antibody-coupled beads (anti-HA affinity matrix, Roche) (chapter 2.2.5.3). After centrifugation at 500 g for 1 minute, the harvested beads were washed once with IP buffer followed by a wash with kinase buffer (20 mM Tris-HCl pH 7.5, 20 mM $MgCl_2$, 5 mM EDTA and 1 mM DTT). The kinase reaction was carried out in 25 µl of kinase buffer complemented with 0.25 mg/ml myelin basic protein (MBP), 100 µM ATP and 5 µCi [γ-^{32}P] ATP for 30 minutes at room temperature. The reaction was terminated by adding SDS loading buffer and then incubating at 95 °C for 5 minutes. The samples were separated on a

SDS-PAGE (15 %) gel, which was then stained with Coomassie Brilliant Blue (chapter 2.2.5.10). After drying on thick filter paper for 3 hours at 80 °C, the gel was exposed to an imaging plate (2025, 18 × 24 cm) in BAS cassettes (FUJI FILM) for 24-48 hours at room temperature. The ^{32}P-labeled MBP on the gel was visualized and analyzed using a phosphorimager (FMBIO III, HITACHI).

2.2.5.5. Mass Spectrometry Analysis

5 ml *S. lycopersicum* protoplasts expressing HA-SFI1 or HA-SFI5 were harvested by centrifugation at 100 g for 1 minute and total proteins were extracted in 1ml IP buffer, followed by immunoprecipitation using 30 µl anti-HA antibody-coupled beads (anti-HA affinity matrix, Roche) (chapter 2.2.5.3). The pull-down material was incubated in 30 µl of 1 × SDS loading buffer without DTT at 95 °C for 10 minutes. After short centrifugation, the supernatant was collected and subjected to LC/MS-MS analysis, which was performed at the Quantitative Proteomics & Proteome Center, Tübingen.

2.2.5.6. SDS-PAGE

Denaturing SDS polyacrylamide gel electrophoresis (SDS-PAGE) was performed by using the gel chamber system of Mini-PROTEAN Tetra Cell (BioRad) and discontinuous polyacrylamide gels (Laemmli, 1970). In this study, a 13.5 % resolving gel overlaid with a 4.5 % stacking gel was used for separating proteins, if not mentioned otherwise. After incubating at 95 °C for 5 minutes, 20 µl protein samples mixed 1 × SDS loading buffer were loaded on SDS-PAGE gel and electrophoresis was conducted in 1 × SDS running buffer (25mM Tris base, 192 mM Glycine, 0.1 % (w/v) SDS) at 33 mA for 50 to 70 minutes depending on the protein size. The Pre-stained Protein Ladder Mix (Fermentas) was used as a protein marker.

	Resolving gel (13.5 %) 5ml/gel	Stacking gel (4.5 %) 3ml/gel
Milli-Q water	1.5 ml	1.8 ml
Acrylamide/bisacrylamide (37.5:1)	2.25 ml	0.45 ml
1.5M Tris-HCl pH 8.8	1.25 ml	--
1.0M Tris-Hcl pH 6.8	--	0.75 ml
* 10% APS	50 µl	30 µl
10% SDS	50 µl	5 µl
* TEMED	5 µl	3 µl

Note. 10 % APS: Ammonium persulfate solution, 1 g ammonium persulfate dissolved in 10 ml of ddH_2O, stored at -20 °C. *. Added right before each use

2.2.5.7. Western blot

For the Western blot analysis, the separated proteins were transferred from SDS-PAGE gel onto a Hybond nitrocellulose membrane (GE Healthcare) in 1 × transfer buffer (25 mM Tris base, 192 mM Glycine, 20 % (v/v) methanol) using a Mini Trans-Blot Electrophoretic Transfer Cell system (Biorad) for approximately one hour at 350 mA. After transfer, the protein on the membrane was investigated by Ponceau S red stain (0.1 % (w/v) Ponceau S red and 5 % (v/v) acetic acid) and scanned for a loading control. For blocking of nonspecific binding sites, the membrane was then incubated in 1 × milk-TBST (20mM Tris-HCl pH 7.5, 150 mM NaCl, 0.1 % (v/v) Tween 20, 5% (w/v) milk) for 1 hour at room temperature with gentle shaking. After washing three times with 1 × TBST buffer (20 mM Tris-HCl pH 7.5, 150 mM NaCl, 0.1 % (v/v) Tween 20), the membrane was incubated in 1 × TBST buffer containing 5 % (w/v) BSA and desired primary antibody with gentle shaking overnight at 4 °C. Following additional washings with 1 × TBST buffer for three times, the membrane was incubated with the respective secondary antibody diluted in 1× TBST for 1 to 2 hours at room temperature. Afterwards, the membrane was washed with 1 × TBST three times.

The alkaline phosphatase-coupled secondary antibody was visualized by staining in BCIP/NBT buffer (150 mM Tris-HCl pH 9.5, 50 mM $MgCl_2$, 100 mM NaCl) containing diluted BCIP and NBT. The 200 × stock solution of BCIP is 50 mg/ml 5-bromo-4-chloro-3-indolylphosphat dissolved in 70 % (v/v) dimethylformamide (DMF) and the 200 × stock solution of NBT is 50 mg/ml nitro-blue tetrazolium chloride dissolved in 100 % (v/v) dimethylformamide (DMF). For detection of a horseradish peroxidase-coupled secondary antibody, the enhanced Chemiluminescence Kit (ECL, GE Healthcare) was applied following the manufacturer's instructions.

2.2.5.8. Native-PAGE analysis

Native polyacrylamide gel electrophoresis (Native-PAGE) was carried out as previously described with minor modifications (Niepmann and Zheng, 2006; Arndt et al., 2012). 5 µl of the purified protein (1 mg/ml) in chapter 2.2.5.2 was mixed with 5 µl complex buffer (50 mM Tris pH7.0, 150 mM NaCl, 0.5 mM $CaCl_2$) and 10 µl 2 × sample loading buffer (100 mM Tris-HCl pH 6.8, 20 % Glycerol, 0.1 % Bromophenol Blue). The sample mixture was incubated at 4 °C for 10 minutes before loading to the native gels. By using Mini-PROTEAN Tetra Cell (BioRad), the vertical electrophoresis was performed in 1 × native running buffer (25 mM Tris base, 192 mM Glycine). Protein separation was processed in discontinuous native acrylamide gels (7.0 % native resolving gel overlaid with a 4.5 % native stacking gel).

The gels were run at a low current (10 mA) in the cold room (4 °C). The proteins on the gel were visualized by Coomassie Brillant Blue staining (chapter 2.2.5.10). NativeMark Unstained Protein Standard (Invitrogen) was used as a protein marker for the analysis.

To examine the Ca^{2+}-dependent *in vitro* interaction between SFI5 and CaM, 25 µg of each purified recombinant proteins were mixed in equal volumes of the complex buffer with 5 mM $CaCl_2$ or 20 mM EDTA and incubated at 4°C for 1 hour, followed by the addition of sample loading buffer.

For the CaM mobility shift assay with a synthetic peptide, 50 µM purified GST-AtCaM4 and 133 µM peptide were mixed in the complex buffer to a final volume of 10 µl and incubated at 4 °C for at least 1 hour. After adding 10 µl 2 × sample loading buffer, the CaM binding ability of these synthetic peptides were detected by Native-PAGE as the above described.

	Native Resolving gel (7.0 %) 5ml/gel	Native Stacking gel (4.5 %) 3ml/gel
Milli-Q water	2.60 ml	3.80 ml
Acrylamide/bisacrylamide (37.5:1)	1.15 ml	0.45 ml
1.5M Tris-HCl pH 8.8	1.25 ml	0.75 ml
* 10% APS	50 µl	30 µl
* TEMED	5 µl	3 µl

*. Added right before each use

2.2.5.9. Immunoblot of native gels

Native gels were blotted following a modified protocol for Western blot of SDS-PAGE gels (chapter 2.2.5.7). After electrophoresis at 4 °C, native gels were incubated in 1 × transfer buffer containing 0.1 % SDS for 10 minutes. Protein transfer on nitrocellulose membrane was performed at 350 mA for 1 hour in 1 × transfer buffer containing 0.1 % SDS. Immunodetection was performed with the adequate primary and secondary antibodies (Table 2.3) and incubation in NBT/BCIP detection solution.

2.2.5.10. Coomassie Brillant Blue staining

After SDS-PAGE or Native-PAGE, gels were incubated in Coomassie blue stain solution (0.125 % (w/v) Coomassie Brilliant Blue R-250, 50 % (v/v) MeOH, 10 % (v/v) acetic acid) and gently shacked at room temperature for 45 minutes. Afterwards, the Coomassie solution was removed and protein bands were detected by incubation in destaining solution (50 % (v/v) methanol, 10 % (v/v) acetic acid) until visualization.

2.2.5.11. 1-Anilinonaphthalene-8-sulfonate (ANS) fluorescence measurement

ANS (Sigma) was dissolved in ethanol at a stock concentration of. 10 mM. The measurements were performed using ANS at a final concentration of 100 µM incubated with 1 µM purified GST-AtCaM4 in reaction buffer (20 mM Tris-HCl pH 7.5, 100 mM NaCl and 1 mM $CaCl_2$) for 15 minutes prior addition of 0-100 µM of the synthetic peptide using for competition. Fluorescence was measured using λ_{ex} = 360 nm and λ_{em} = 460 nm.

2.2.6. Bioassay methods

2.2.6.1. Luciferase activity measurement

In order to identify MTI-suppressing effectors, transfected *A. thaliana* or *S. lycopersicum* protoplasts co-expressing the reporter constructs *pFRK1-Luc*, *pUBQ10-GUS* and an effector gene construct were prepared as described in 2.2.3.1. For the luciferase assay, D-luciferin (P.J.K.) was added to 600 µl protoplasts to a final concentration of 200 µM. Protoplasts were then aliquoted into a 96-well plate (BrandTech) at 100 µl per well and kept for at least 30 minutes at 20-22 °C in the dark. Protoplasts were treated with flg22 to a final concentration of 500 nM or left untreated. The luminescence reflecting the luciferase activity was measured at different time-points using a Berthold Mithras LB 940 luminometer. Between the measurements, the plate was covered with a lid and incubated in the dark at room temperature.

2.2.6.2. GUS activity measurement

For the GUS activity assay, 50 µl of transformed protoplasts (+/- flg22) as described in 2.2.6.1 were collected by centrifugation at 100 g for 1 minute, 3 or 6 hours after adding flg22. The cells were lysed in 100 µl 1 × CCLR solution (cell culture lysis reagent, Promega) and 10 µl of the lysate were then transferred to a 96-well plate followed by the addition of 90 µl MUG substrate solution (1 mM 4-methyl-umbelliferyl-β-D-glucuronide, 100 mM Tris-HCl pH 8.0, 2 mM $MgCl_2$). The plate was incubated at 37 °C for 30 minutes and the reaction was stopped by adding 100 µl 0.2 M Na_2CO_3 and mixing well. The fluorescence resulting from the GUS activity (production of 4-methylumbelliferone, 4-MU) was monitored using a MWG 96-well plate reader with λ_{ex} = 360 nm and λ_{em} = 460 nm. The values obtained in the GUS activity assay were used to normalize the data from the 3 hours or 6 hours time-point of the Luciferase activity as following: (value Luc +flg22/value GUS +flg22)/(value Luc −flg22/value GUS −flg22), in which value Luc and value GUS are from the same time-point.

2.2.6.3. Cell death rate measurement

To determine the cell death rate after transformation, 100µl of transformed protoplasts as described in 2.2.6.1 were incubated with 1 µl propidium iodide (100 µg/ml). Stained protoplasts reflecting dead cells were counted using a Nikon Eclipse 80i epifluorescence microscope with the following filter: TRITC EX 540/40, DM 565, BA 605/55. The cell death rate represents the percentage of dead protoplasts per total number of protoplasts.

2.2.6.4. Post-translational MAP Kinase activation assay

To determine post-translational activation of MAPK in protoplasts, 100 µl or 200 µl of transformed protoplasts as described in 2.2.6.1 were treated without or with 500 nM flg22 for 0, 15 and 30 minutes, harvested by centrifugation at 100 g for 1 minute and flash-frozen in liquid nitrogen. Total proteins were extracted in 40 µl 1 × SDS loading buffer at 95 °C for 5 minutes. 20 µl of the protein extract were loaded onto a 13.5 % SDS-PAGE gel and separated by electrophoresis as described in 2.2.5.6. Afterwards, proteins were blotted onto a Hybond nitrocellulose membrane (GE Healthcare) and stained with Ponceau S red to visualize equal sample loading (chapter 2.2.5.7). The membrane was probed with a primary antibody raised against phospho-p44/p42 MAPK and the appropriate secondary antibody (@rabbit IgG-Alkaline Phosphatase) (Table 2.3) followed by incubation in NBT/BCIP detection solution for immunodetection.

2.2.6.5. Oxidative burst assay

S. lycopersicum protoplasts transformed as described in 2.2.6.1 were used to measure ROS production using a luminol-based assay (Halter et al., 2014). Protoplasts were incubated in W2 buffer (0.5 M mannitol, 20 mM KCl) at 20-22 °C in the dark for 6-8 hours. Before measurement, the W2 buffer was replaced with W5 buffer (18.4 g/L $CaCl_2 \bullet 2H_2O$, 1.0 g/L glucose, 9.0 g/L NaCl, 0.4 g/L KCl) containing 200 µM luminol L-012 (Wako Chemicals) and 20 µg/ml horseradish peroxidase and incubated for additional 30 minutes in the dark. Upon treatment without or with 500 nM flg22, luminescence was recorded for 30 minutes by using the muliplate reader Mithras LB 940 (Berthold Technologies).

2.2.6.6. Calcium influx assay

Aequorin luminescence measurement was performed to monitor the increase of cytosolic Ca^{2+} level upon flg22 treatment. *S. lycopersicum* protoplasts were co-transformed with the *p35S-Aequorin*, *pUBQ10-GUS* and *SFI5* constructs and incubated in W2 buffer (0.5 M mannitol, 20 mM KCl) at 20-22 °C in the dark for 6-8 hours (chapter 2.2.3.1). After adding 10 µM of

coelenterazine (P.J.K., dissolved in ethanol at a stock concentration of 1mM), 100 µl transformed protoplasts were aliquoted into a 96-well plate and incubated for at least 30 minutes in the dark. Upon treatment without or with 500 nM flg22, luminescence was recorded in 45-sec intervals for 30 minutes using a Berthold Mithras LB 940 luminometer. A GUS activity assay (chapter 2.2.6.2) was performed in parallel and used to normalize the sum of photon counts between 5-15 minutes in flg22 treated or untreated protoplasts. The flg22-induced elevation of cytosolic Ca^{2+} level was presented as: (total light counts +flg22/ value GUS +flg22)/(total light counts –flg22/value GUS –flg22).

2.2.6.7. Programmed Cell death suppression assay

For the INF1-induced cell death assay, *A. tumefaciens* expressing GFP-SFI effectors, GFP-AVR3a or GFP control were first infiltrated into *N. benthamiana* leaves at an OD_{600} = 0.3 (as described in 2.2.3.2). After one day, the primary infiltration sites were re-infiltrated with *A. tumefaciens* carrying *p35S-INF1* construct at a final OD_{600} = 0.3. Cell death was scored at 7 days post-infiltration (dpi). For the AVR/R-induced cell death assay, *A. tumefaciens* expressing Avr4 or Cf-4 were adjusted to a final OD_{600} of 0.3 and 0.6, respectively, and then mixed in a 1:1 ratio prior inoculation of the primary infiltration sites expressing GFP-SFI effectors, GFP-AVR3a or GFP control. Cell death was scored at 7 days post-infiltration (dpi) and considered to be positive when more than 50 % of the inoculated area developed a clear cell death phenotype. The mean percentage of total inoculations per plant developing cell death of combined data from at least two biological replicates (3 leaves / 6 plants / replicate) was calculated. One-way ANOVA was performed to identify statistically significant differences (p-value < 0.01).

2.2.6.8. *Phytophthora infestans* infection assay

To determine the contribution of SFI effectors to *P. infestans* pathogenicity, infection assays were performed on *N. benthamiana* leaves transiently expressing SFI effectors as described previously (Bos et al., 2010). First, *A. tumefaciens* carrying GFP-SFI effectors were diluted in infiltration buffer to achieve a final OD_{600} value of 0.1. 4 to 5-week old leaves of *N. benthamiana* were infiltrated with the bacteria expressing the GFP control in one half of the leaf and the bacteria expressing a GFP-SFI effector on the other half. After one day, 10 µl of *P. infestans* sporangia-containing droplets (3×10^4 sporangia/ml) were inoculated onto the abaxial side of detached leaves and incubated for several days at high humidity at 19 °C. Lesion sizes were determined and photographed at 7 days post-infection. Three leaves per plant for 4–6 intact plants were used for each biological replicate. Statistically significant

differences in lesion size were identified by one-way ANOVA with pairwise comparisons performed using the Holm-Sidak method.

Sporangia from *P. infestans* were prepared as following: *P. infestans* isolate 88069 was grown on Rye Sucrose Agar at 19 °C for two weeks. Plates were flooded with 5 ml cold sterile water and scraped with a glass rod to release sporangia. The sporangia-containing solution was collected, counted using a haemocytometer and the sporangia concentration adjusted to 3×10^4 sporangia/ml.

2.2.7. Confocal fluorescence microscopy

Standard confocal microscopy was used for sub-cellular localization studies. Protoplast samples were observed 12 hours post-transfection and *N. benthamiana* epidermal cells 2 days after agroinfiltration. Imaging was performed using a Leica TCS SP8 AOBS confocal laser scanning microscope with HC PL APO 63 × 1.20 W water immersion objectives. Samples were excited and emitted by an argon/krypton mixed gas laser. The excitation settings for GFP, RFP and chloroplast were 488 nm, 561 nm and 633 nm, respectively. The emission filters were 505-535 nm for GFP, 575-605 nm for RFP and 647-685 nm for chloroplasts. The pinhole was set to 1.5 airy units for protoplasts and 1 airy unit for leaf cells. Single optical section images were acquired from protoplasts and z-stacks were collected from leaf cells. Image analysis was processed with the Leica LCS software, ImageJ and Adobe Photoshop CS3.

3. Results

3.1. Identification of RXLR effectors from *P. infestans* suppressing early MTI signaling

3.1.1. Establishment of plant protoplast systems for monitoring flg22-induced immune responses

The Arabidopsis protoplast-based transient expression system has been demonstrated as a fast and potent method to identify and analyze the virulence function of bacterial type III effectors subverting MAMP triggered immunity (Li et al., 2005; He et al., 2006). We have decided to use this experimental system in order to identify RXLR effectors of *P. infestans* (PiRXLR effectors) subverting early responses of MAMP signaling pathway and perform a comparative study of their activity in both a host (tomato) and non-host (Arabidopsis) plant species. Together with M. Fraiture, a postdoc in the Brunner lab, we have adapted the existing protoplast assay in Arabidopsis and developed a tomato protoplast system to measure early immune responses induced by flg22 (Fraiture et al., 2014). One major advantage of this system is that effector translocation into host cells is based on chemical transformation and does not require the help of a bacterial delivery system and therefore, it reduces the risk of interference with the read-out due to the uncontrolled presence of bacterial effectors and MAMPs. Furthermore, the assay can be used to measure very early (within minutes) MAMP-induced responses and to perform epistasis analysis without the burden of generating stable transgenic lines. We choose in our experiments the bacterial MAMP flg22 because it is ubiquitously recognized in plants and also because cell responses elicited by diverse MAMPs are largely congruent (Gomez-Gomez and Boller, 2000; Zipfel et al., 2006; Wan et al., 2008). It has been demonstrated that several elements involved in flg22-mediated signaling pathway were conserved in Arabidopsis and tomato. The functional ortholog of Arabidopsis FLS2 has been identified in tomato (Robatzek et al., 2007). The kinase activation of tomato SlMPK3 and 1, orthologs of AtMPK3 and 6, respectively, can be induced by flg22 (Nguyen et al., 2010).

Protoplasts were always freshly prepared from 4-5 week-old Arabidopsis Col-0 or 3-4 week-old tomato (*S. lycopersicum* cv moneymaker) plant leaves using a mix of cell wall-degrading enzymes containing cellulase, macerozyme and pectinase and transformed using a PEG (Polyethylene glycerol)-mediated transfection procedure (Fraiture et al., 2014). To assess cell viability and transformation efficiency, we transformed isolated protoplasts with a *p35S-GFP* (green fluorescent protein) construct (Figure 3-1 A). After 12 hours incubation, a strong GFP

signal could be observed by fluorescence microscopy and the dead protoplasts were visualized by propidium iodide (PI) staining (Figure 3-1 A). The efficiency of the transformation was routinely > 50 %. However, approximately 45 % of the tomato and 20 % of the Arabidopsis protoplasts died after transfection.

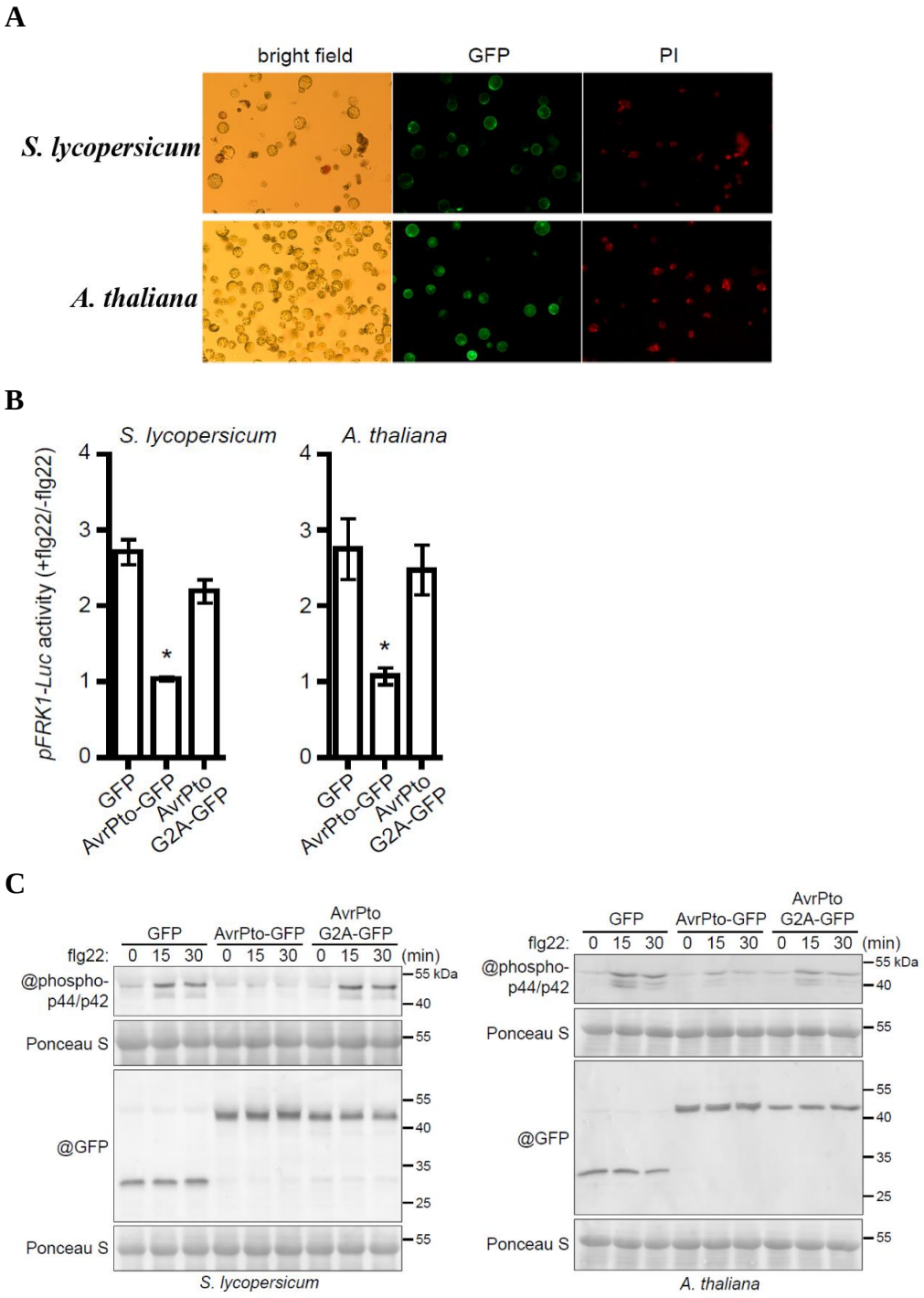

Figure 3-1. *S. lycopersicum* and *A. thaliana* protoplast-based transient expression system for monitoring reporter gene expression and MAPK activation.

(A) Transformation efficiency of *S. lycopersicum* and *A. thaliana* protoplasts transiently expressing *p35S-GFP*. After 12 hours transfection, GFP-transformed protoplasts and dead cells stained with propidium iodide (PI) were

observed with epifluorescence microscopy. **(B)** *FRK1* promoter activity assay using the reporter luc gene in *S. lycopersicum* and *A. thaliana* protoplasts. Mesophyll protoplasts were cotransfected with *pFRK1-Luc* and *pUBQ10-GUS* alone with *p35S-GFP (control) or p35S-AvrPto-GFP* (*P. syringae* effector AvrPto) or *p35S-AvrPto G2A-GFP* (non-myristoylated AvrPto). After 6 hours and 9 hours transfection for *S. lycopersicum* and *A. thaliana* respectively, protoplasts were challenged with flg22 (+flg22) or without challenge (-flg22) and the *Luc* reporter activity was measured. The promoter activity was presented by calculating the ratio of flg22-induced luciferase activity relative to the untreated sample, which was normalized to the internal GUS activities (*pFRK1-Luc* activity +flg22/−flg22). Each data point represents the mean ± SEM from seven independent replicates, for each of which three technical replicates were carried out. *, p-value < 0.05 by one-way ANOVA followed by Dunnett's multiple comparison test. **(C)** Endogenous MAPK activation upon flg22 treatment in *S. lycopersicum* and *A. thaliana* protoplasts. Transfected protoplasts expressing GFP or AvrPto-GFP or AvrPto-GFP G2A were collected 0, 15 and 30 minutes after flg22 treatment and used for immunoblotting. Phosphorylated MAP kinases were detected by antibody raised against phosphorylated mammalian MAP kinase p44/p42. GFP and GFP fusion proteins from the same samples were detected by anti-GFP antibody. Equal sample loading was assessed by Ponceau S staining. This result is representative of at least two independent experiments.

In order to test protoplast responsiveness to flg22 and effector-driven suppression efficiency of flg22-induced early MTI signaling, we compared the effect of GFP and *P. syringae* T3E AvrPto-GFP fusion protein on the induction of the expression of the reporter gene construct *pFK1-Luc* that was co-transfected into protoplasts. The reporter gene construct consists of the firefly luciferase gene (*Luc*) under control of the MAMP-inducible promoter of Arabidopsis *FRK1* (Asai et al., 2002; He et al., 2006). This reporter construct is functional in both the Arabidopsis and the tomato protoplast system. A β-glucuronidase (GUS) activity assay, reflecting the constitutive expression of concomitantly transfected *pUBQ10- GUS* (He et al., 2006) allows the normalization of +/- flg22 Luc activity and serves as an indicator for successful transfection. As shown in Figure 3-1 B, the presence of AvrPto-GFP significantly impaired flg22-induced luciferase expression in both Arabidopsis and tomato protoplasts, compared to the GFP expression control. However, the inactive AvrPto with substitution of the glycine residue in position 2 by an alanine (AvrPto G2A-GFP), whose myristoylation site and membrane localization is disrupted (Shan et al., 2000; He et al., 2006), failed to block *pFRK1-Luc* activation upon flg22 treatment. Further, AvrPto-GFP, but not AvrPto G2A-GFP, disturbed post-translational activation by flg22 of immunity-associated MAP kinases in both protoplast systems (Figure 3-1 C). These results indicated that both Arabidopsis and tomato protoplast systems are suitable to measure early immune responses triggered by flg22 and ready to be used as a screen for identification of MTI-suppressing RXLR effectors from *P. infestans*.

3.1.2. Comparative analysis of flg22-inducible gene activation in tomato and Arabidopsis protoplasts expressing RXLR effectors from *P. infestans*

3.1.2.1. Identification of RXLR effectors from *P. infestans* suppressing *pFRK1-Luc* activity upon flg22 treatment in tomato protoplasts

We first examined whether PiRXLR effectors inhibit flg22-induced p*FRK1-Luc* expression in tomato protoplasts, because it is a natural host of *P. infestans* and therefore, the pathogen must have evolved effectors capable to interfere with MTI signaling. A total of 33 effector candidates were tested in this study (Appendix table 6-2). Most of these effectors were selected because their expression was up-regulated during the biotrophic stage of infection or they were identified as avirulence proteins, which is an indication that they might also fulfill an important role in the pathogenicity of *P. infestans* (Whisson et al., 2007; Haas et al., 2009; Oh et al., 2009). In collaboration with the group of P. Birch (James Hutton Institute/University of Dundee, UK), the cDNA sequence encoding the PiRXLR effectors was cloned without the predicted signal peptide into pDONR Gateway vectors followed by introduction into the series of p2GW7 destination vectors with/without an N-terminal GFP fusion.

Among the 33 PiRXLR effector candidates, 8 (PITG_04097, PITG_04145, PITG_06087, PITG_09585, PITG_13628, PITG_13959, PITG_18215 and PITG_20303) consistently reduced the *pFRK1-Luc* activity triggered by flg22 in tomato protoplasts, in contrast to the control protoplasts expressing GFP (p-value < 0.05, Figure 3-2 A). These effectors were named Suppressor of early Flg22-induced Immune response (SFI) 1 to 8, respectively. Among them, 5 effectors (SFI1, SFI5, SFI6, SFI7 and SFI8) much strongly reduced activation of *pFRK1-Luc* by flg22, similar to the effect of the bacterial effector AvrPto (+flg22/-flg22≅1). After overnight incubation, the percentage of dead protoplasts was determined by PI staining and not significantly different between the SFI effector-expressing protoplasts and the GFP control (Figure 3-2 B), suggesting that the suppression of *FRK1* promoter activity is not caused by a toxic or a programmed cell death process in transfected protoplasts.

A

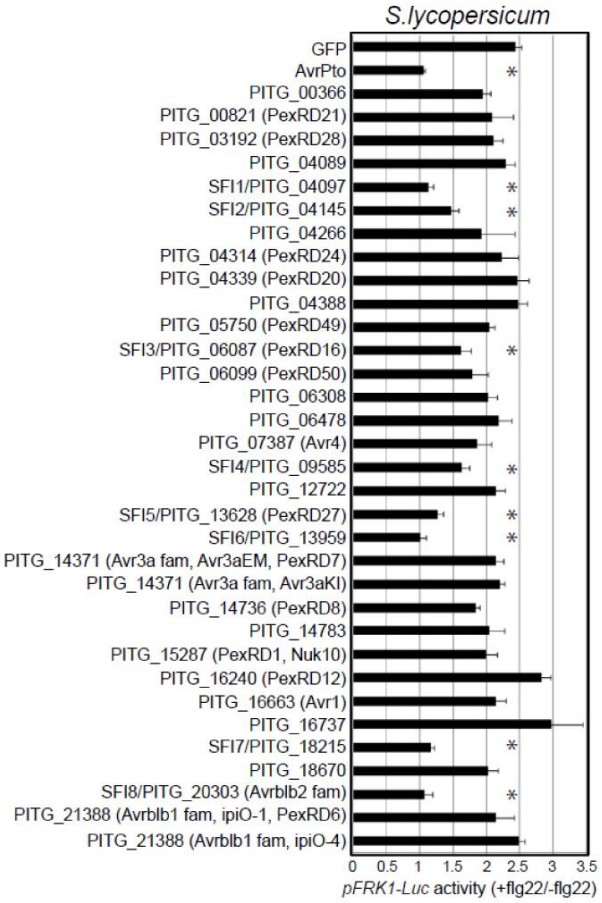

B

S. lycopersicum

Effector	Cell death (%)	SEM (+/-)	Dunnett's test
GFP	47.52	3.16	
AvrPto	58.59	2.11	ns
GFP-SFI1	44.11	5.27	ns
GFP-SFI2	43.93	0.94	ns
GFP-SFI3	44.18	2.55	ns
GFP-SFI4	41.95	2.71	ns
GFP-SFI5	56.52	3.47	ns
GFP-SFI6	62.89	5.16	ns
GFP-SFI7	48.52	2.46	ns
GFP-SFI8	41.77	7.60	ns

Figure 3-2. Identification of PiRXLR effectors inhibiting flg22-induced reporter gene activation in *S. lycopersicum* protoplasts.

(A) Suppression of flg22-triggered FRK1 promoter activity by PiRXLR effectors in *S. lycopersicum* protoplasts. After 6 hours transformation, mesophyll protoplasts co-extpressing a *p35S-effector* (or a *p35S-GFP* control) alone with the two reporter genes *pFRK1-Luc* and *pUBQ10-GUS* were challenged with flg22 (+flg22) or without challenge (-flg22) and the *Luc* reporter activity was measured. AvrPto served as a positive control for repressing *pFRK1-Luc* activation by flg22. The promoter activity was presented by calculating the ratio of flg22-induced luciferase activity relative to the untreated sample, which was normalized to the internal GUS activities (*pFRK1-Luc* activity +flg22/−flg22). Each data set represents the mean ± SEM from four independent experiments, for each of which three technical replicates were carried out. *, p-value < 0.05 by one-way ANOVA followed by Dunnett's multiple comparison test. **(B)** The rate of cell death for *S. lycopersicum* protoplasts transiently

expressing the identified effectors N-terminally tagged with GFP. By propidium iodide (PI) staining, the number of dead cells in the observed total protoplasts was assessed for determining the cell death percentage. Each data set was presented by the mean value ± SEM obtained from three independent experiments, where at least 150 protoplasts were counted. ns, no-significance between the *p35S-GFP-effector* transfected protoplasts and *p35S-GFP* control by one-way ANOVA followed by Dunnett's multiple comparison test.

3.1.2.2. Identification of RXLR effectors from *P. infestans* suppressing *pFRK1-Luc* activity upon flg22 treatment in Arabidopsis protoplasts

One of our goals is to determine whether PiRXLR effectors that suppress early MTI signaling in the host tomato are able to also suppress such responses in the non-host plant Arabidopsis. We hypothesized that only few, or even none of the 8 PiRXLR effectors identified in the tomato screen would affect flg22-dependent *pFRK1-Luc* activation in Arabidopsis protoplasts.

This experiment revealed that 4 SFI effectors (SFI1, SFI2, SFI5 and SFI8) could also disturb flg22-induced luciferase expression in Arabidopsis (p-value < 0.05, Figure 3-3 A). SFI3, SFI4, SFI5 and SFI7 did not significantly interfere with the induction of *pFRK1-Luc* activity and would rather be classified as host-specific effectors. To our surprise, another 4 effectors (PITG_00821, PITG_05750, PITG_16737 and AVRblb1/PITG_21388) were found to attenuate *pFRK1-Luc* expression only in Arabidopsis (p-value < 0.05, Figure 3-3 A). Similar to what we have observed in tomato, no significant difference in the cell death rate was observed in Arabidopsis protoplasts transiently expressing these effectors (Figure 3-3 B). In addition, we noticed that protoplasts expressing the effector PITG_18670 were hypersensitive to flg22, which was illustrated by a much stronger induction of *pFRK1-Luc* activity.

A

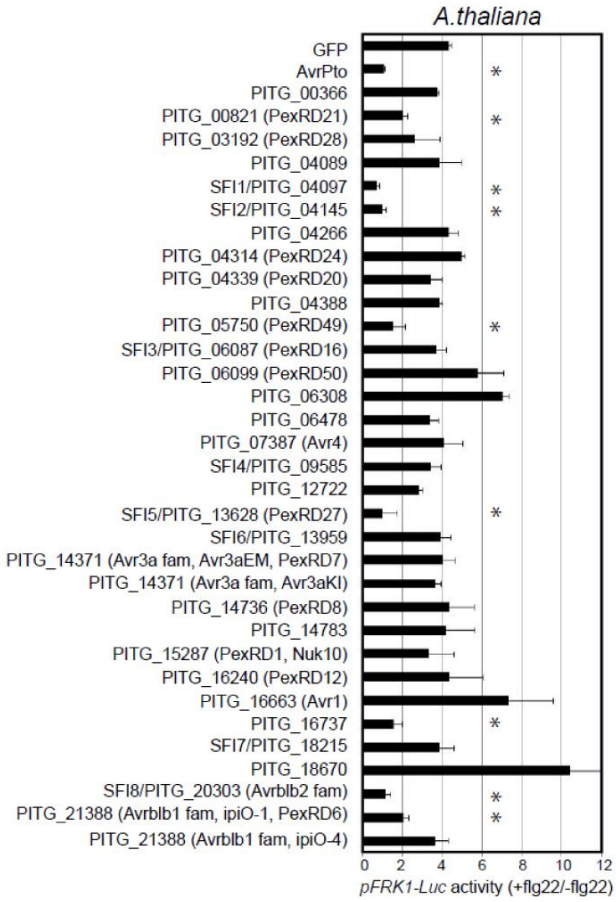

B

A. thaliana

Effector	Cell death (%)	SEM (+/-)	Dunnett's test
GFP	22.40	5.26	
AvrPto	22.26	0.71	ns
GFP-PITG_00821	26.63	5.68	ns
GFP-SFI1	26.97	1.72	ns
GFP-SFI2	27.17	3.70	ns
GFP-PITG_05750	22.80	3.92	ns
GFP-SFI5	27.67	4.62	ns
GFP-PITG_16737	22.83	3.69	ns
GFP-SFI8	21.43	1.07	ns
GFP-PITG_21388	22.00	0.57	ns

Figure 3- 3. Identification of PiRXLR effectors inhibiting flg22-induced reporter gene activation in *A. thaliana* protoplasts.

(A) Suppression of flg22-triggered *FRK1* promoter activity by PiRXLR effectors in *A. thaliana* protoplasts. After 9 hours transformation, mesophyll protoplasts co-extpressing a *p35S-effector* (or a *p35S-GFP* control) alone with the two reporter genes *pFRK1-Luc* and *pUBQ10-GUS* were challenged with flg22 (+flg22) or without challenge (-flg22) and the *Luc* reporter activity was measured. AvrPto served as a positive control for repressing *pFRK1-Luc* activation by flg22. The promoter activity was presented by calculating the ratio of flg22-induced luciferase activity relative to the untreated sample, which was normalized to the internal GUS activities (*pFRK1-Luc* activity +flg22/−flg22). Each data set represents the mean ± SEM from four independent experiments, for each of which three technical replicates were carried out. *, p-value < 0.05 by one-way ANOVA followed by Dunnett's multiple comparison test. **(B)** The rate of cell death for *A. thaliana* protoplasts transiently expressing

the identified effectors N-terminally tagged with GFP. Via propidium iodide (PI) staining, the number of dead cells in the observed total protoplasts was assessed for determining the cell death percentage. Each data set was presented by the mean value ± SEM obtained from three independent experiments, where at least 150 protoplasts were counted. ns, no-significance between the *p35S-GFP-effector* transfected protoplasts and *p35S-GFP* control by one-way ANOVA followed by Dunnett's multiple comparison test.

3.1.2.3. SFI1, SFI2 and SFI8 attenuate flg22-induced endogenous MAMP-marker gene expression in Arabidopsis protoplasts

It was unexpected that 4 PiRXLR effectors failed to affect *pFRK1-Luc* activation by flg22 in the host plant tomato but did so in the non-host plant Arabidopsis. This result prompted us to test further whether the 8 PiRXLR effectors suppressing the reporter gene activation in Arabidopsis also block the flg22-induced expression of endogenous *FRK1* and other MTI marker genes in Arabidopsis protoplasts. Consistent with the results obtained in the *pFRK1-Luc* assay, 3 effectors (SFI1, SFI2 and SFI8/AVRblb2) inhibited the flg22-induced *FRK1* expression. In contrast, the remaining 5 effectors (SFI5, PITG_00821, PITG_05750, PITG_16737 and AVRblb1/PITG_21388) failed to attenuate the up-regulation of *FRK1* expression by flg22 (Figure 3-5 A).

We extended our analysis to *WRKY DNA-BINDING PROTEIN 17* (*WRKY17*) and *4-coumarate coenzyme A ligase (4CL)*, two additional MAMP-responsive genes. As shown in Figure 3-4, SFI1, SFI2 and SFI8/AVRblb2 were also able to dramatically impair the up-regulation of *WRKY17* and *4CL* upon addition of flg22, while the other 4 PiRXLR effectors (PITG_00821, PITG_05750, PITG_16737 and AVRblb1/PITG_21388) had no effect. Notably, SFI5 disturbed flg22-elicited *4CL* expression, but had no effect on the induction of *WRKY17* gene, implying that it might specifically affect 4CL-associated phenylpropanoid metabolic pathway (Fraser and Chapple, 2011). As a control, the housekeeping gene *ELONGATION FACTOR 1A (EF1α)* was tested before and after flg22 treatment and its expression was in general not altered (Figure 3-4). Only in the case of SFI2, the transcript level of *EF1α* was decreased 2-3 fold, maybe because the overexpression of the effector affected the fitness of protoplasts.

Taken together, our initial screening with the *pFRK1-Luc* assay identified a subset of PiRXLR effectors (SFI1-SFI8) subverting early flg22-induced immune response in tomato. In addition, three of them (SFI1, SFI2 and SFI8/AVRblb2) appear to interfere with MAMP signaling in non-host Arabidopsis and suggest that they target ubiquitous components of plant immune

signaling. We have chosen to study the 8 SFI effectors in more details for a better understanding of their mode(s) of action on different processes contributing to MTI.

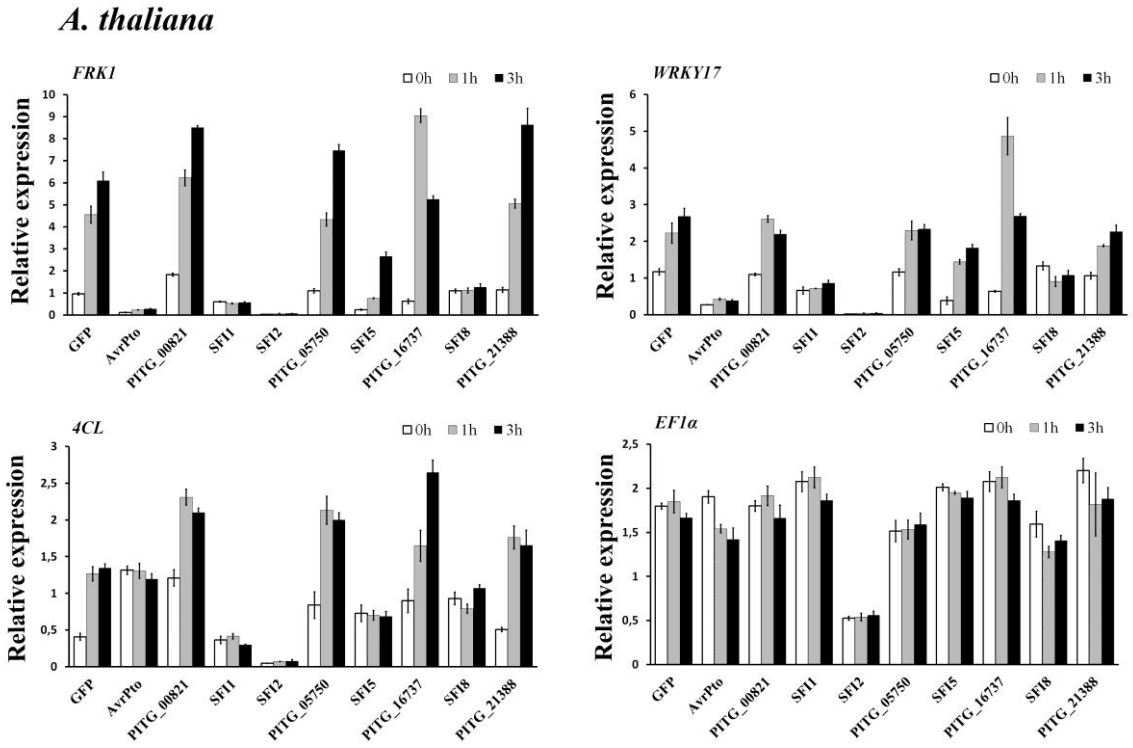

Figure 3- 4. Real time PCR-analysis of MAMP-responsive genes in *A. thaliana* protoplasts expressing the SFI effectors.

Relative expression of the flg22-induced marker genes *FRK1*, *WRKY17*, *4CL* and the housekeeping gene *EF1α* was determined in transfected protoplasts treated by flg22 for 0 hour, 1 hour and 3 hours. GFP and AvrPto were employed as a negative and a positive control, respectively, for suppression of the marker genes induction. Mean values ± SEM of technical triplicates were obtained and the data are representative of four independent experiments.

3.1.3. SFI 5-7 suppress post-translational MAP kinase activation by flg22 in tomato but not in Arabidopsis protoplasts

In order to unravel whether the SFI1-8 effectors function at- or upstream of the transcriptional or translational changes in elicited tomato protoplasts, we conducted an epistasis analysis. MAPK cascades are thought to be key components that regulate MAMP-responsive genes in MTI signaling. To investigate if our effectors affect defense-associated MAPK activation by flg22, we performed immunodetection assays by using a phospho-p44/42 antibody, which was raised against phosphorylated (activated) MAP kinases. AvrPto served as a positive control for suppression of post-translational MAP kinase activation because it is known to

suppress MAMP signaling by targeting the FLS2/BAK1 receptor complex (He et al., 2006; Shan et al., 2008; Xiang et al., 2008).

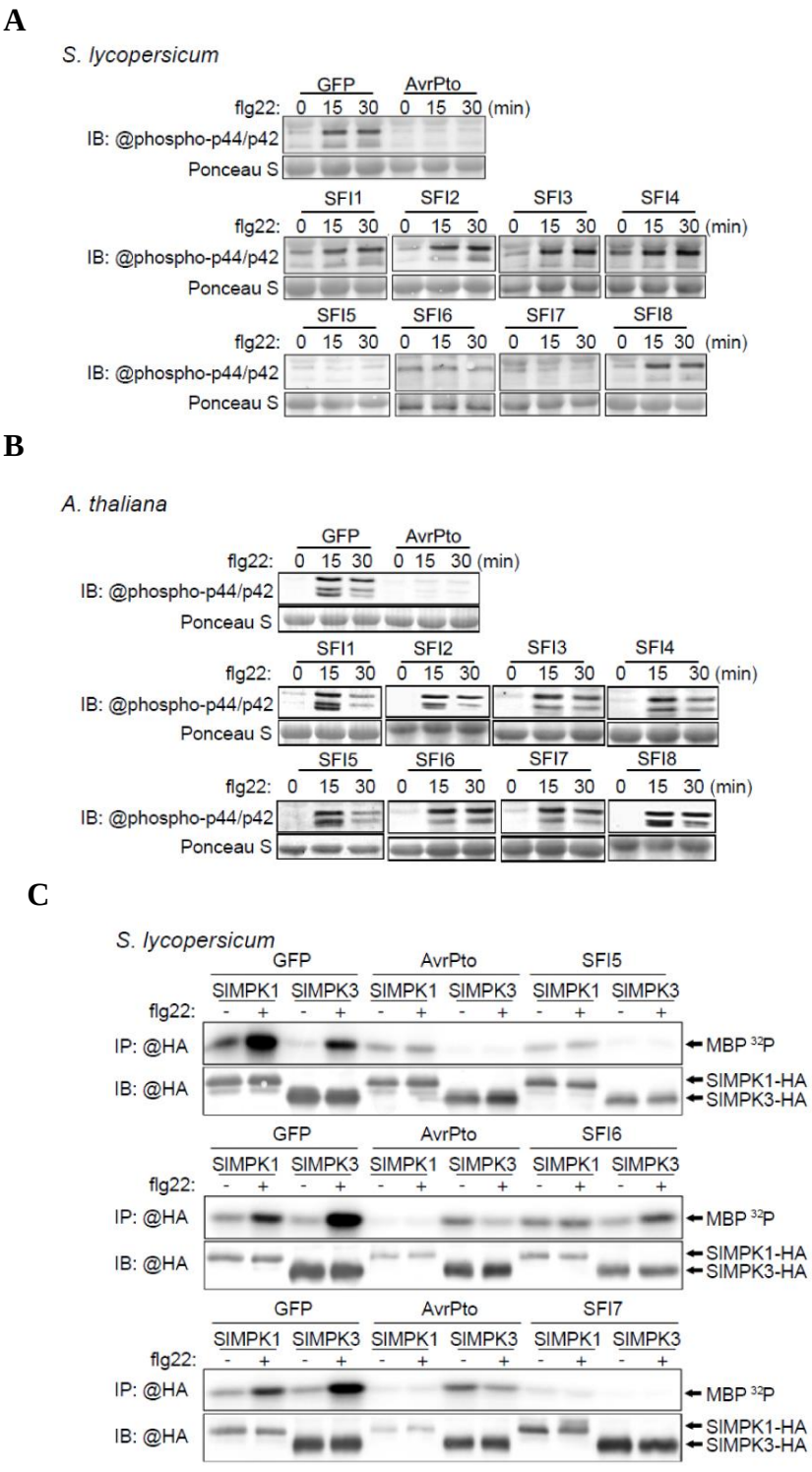

Figure 3-5. flg22-mediated activation of MAPKs in protoplasts producing SFI effectors.

(A, B) *p35S-effector*-transfected protoplasts of *S. lycopersicum* **(A)** and *A. thaliana* **(B)** were collected at 0, 15 and 30 minutes after flg22 treatment, and the activated MAPKs were detected by immunobloting with the antibody raised against phosphorylated MAP kinase p44/p42. Ponceau S staining is shown as a loading control. These result are representative of at least two independent experiments. **(C)** SFI5, SFI6 and SFI7 inhibit flg22-

induced activation of SlMPK1 and SlMPK3 in *S. lycopersicum* protoplasts. C-terminally HA-tagged tomato MAP kinase SlMPK1 or SlMPK3 were coexpressed with SFI5, SFI6 or SFI7 in protoplasts, which were collected before (-) and after (+) flg22 treatment. Following by immmunoprecipitation with anti-HA antibody, kinase activity of HA-SlMPK1 or SlMPK3 was detected by *in vitro* kinase assay and is shown in the upper panel. [γ-^{32}P] ATP and myelin basic protein (MBP) were used as phosphorylation substrates. Protein expression of SlMPK1 or SlMPK3 is presented in the lower panel. GFP and AvrPto served as a negative control and a positive control, respectively, for suppression of MAPK activation by flg22. These results are representative of at least two independent experiments.

3 effectors (SFI5, SFI6 and SFI7) were shown to consistently repress the flg22-dependent activation of MAP kinases in tomato protoplasts (Figure 3-5 A). This result was further confirmed by doing an *in vitro* MAP kinase assay following the expression and immunoprecipitation of hemagglutinin (HA)-tagged SlMPK1 and SlMPK3 in the presence of SFI5, SFI6 or SFI7, respectively (Figure 3-5 C). These data suggest that SFI5-SFI7 might play effector activity upstream of MAP kinase activation in tomato, while the other 5 effectors are likely doing so downstream of MAPK signaling. Like in tomato, SFI1, SFI2 and SFI8/AVRblb2 did not interfere with MAP kinase activation in Arabidopsis (Figure 3-5 B), reinforcing the hypothesis of a conservation of the effectors' function in both non-host and host plant species. We also verified and confirmed that SFI5-SFI7 are most likely acting in a host-specific manner as shown by the absence of effect on MAP kinase activation upon flg22 treatment in Arabidopsis (Figure 3-5 B).

3.1.4. SFI5-SFI7 interfere upstream of the flg22-mediated MAP kinase activation in tomato protoplasts

To better understand the molecular mechanisms underlying SFI5-SFI7 action in the inhibition of flg22-induced early MAPK activation in tomato, we carried out gain-of-function experiments using components located upstream of the signaling cascade that constitutively activate the MAP kinases SlMPK1 and SlMPK3 without flg22 treatment. Components that have been identified to act upstream of AtMPK3/4/6 are AtMKK4/5 or AtMEKK1 (Asai et al., 2002; He et al., 2006). Previous assays have demonstrated that the overexpression of dominant active forms of AtMKK4/5 or AtMEKK1 helped to elucidate which steps in MTI signaling are blocked by the bacterial effectors AvrPto and AvrPtoB (He et al., 2006). In tomato and other solanaceous plants, most studies about cascades of MAPK pathway are related to programmed cell death (PCD) induced by effector-triggered immunity (del Pozo et al., 2004; Pedley and Martin, 2004; Melech-Bonfil and Sessa, 2010).

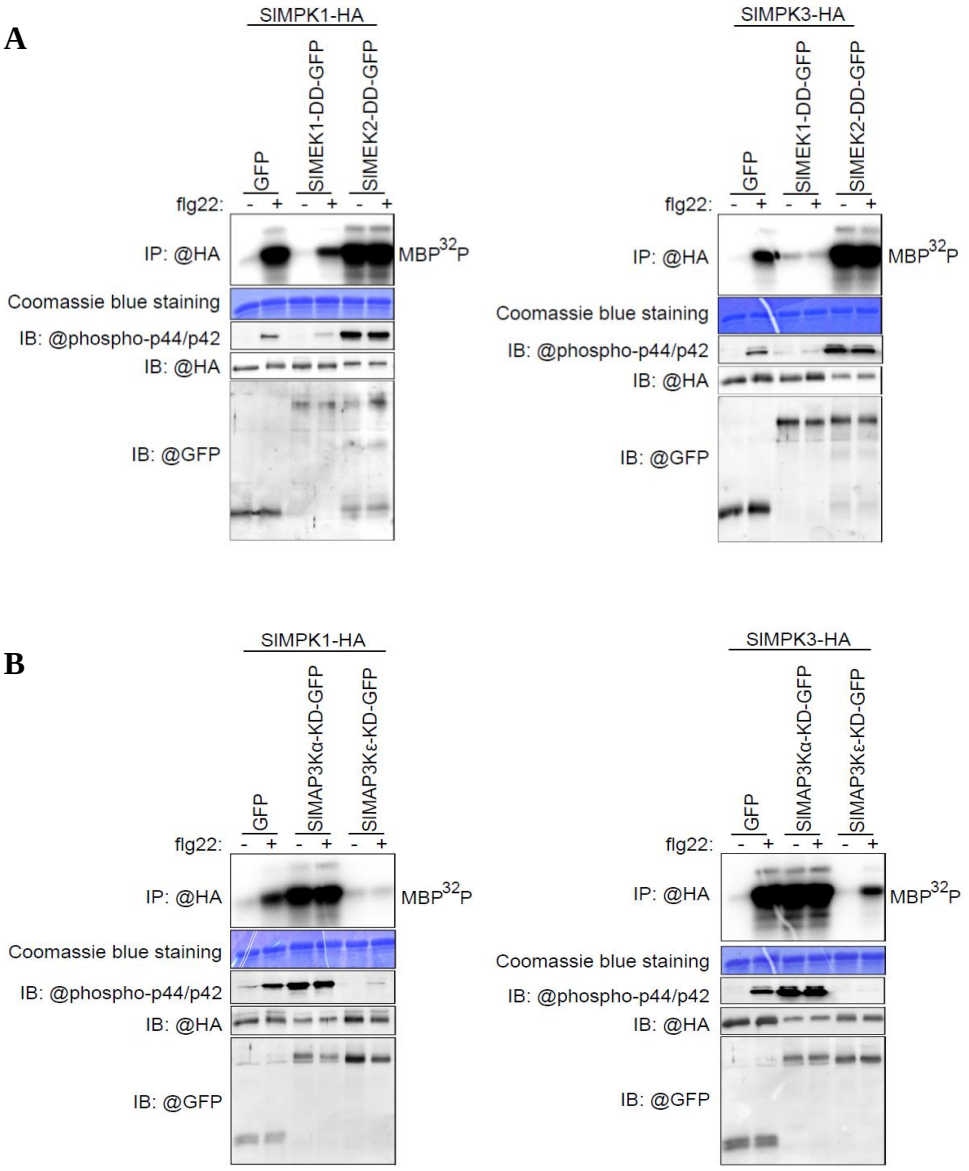

Figure 3-6. SlMEK2 and SlMAP3Kα activate SlMPK1 and SlMPK3 in *S. lycopersicum* protoplasts.

(A) Protoplasts were co-transformed with GFP or GFP-tagged constitutively active MAPK kinase mutant (SlMEK1-DD-GFP and SlMEK2-DD-GFP) and HA-tagged SlMPK1 or SlMPK3. **(B)** Protoplasts were co-transformed with GFP or GFP-tagged constitutively active MAPKK kinase mutant (SlMAP3Kα-KD-GFP and SlMAP3Kε-KD-GFP) and HA-tagged SlMPK1 or SlMPK3. After 10 hours incubation, transfected protoplasts were collected before (-) and after (+) flg22 treatment. **(A, B)** Following immmunoprecipitation with anti-HA antibody, kinase activity of HA-SlMPK1 or SlMPK3 was detected by *in vitro* kinase assay and is shown in the upper panel. [γ-^{32}P] ATP and myelin basic protein (MBP) were used as phosphorylation substrates (MBP^{32}P). Equal sample loading is presented by coomassie blue staining in the second panel. Endogenous MAPK activation was determined by antibody raised against phosphorylated MAP kinase p44/p42 (the third panel). The lower panels show the expression of GFP-fused or HA-fused proteins detected by anti-GFP or anti-HA antibodies, respectively. These results are representative of at least two independent experiments.

In *N. benthamiana*, NbMKK1 is required for *P. infestans* INF1-triggered hypersensitive response (HR)-like cell death and interacts with the downstream NbSIPK (salicylic acid-induced protein kinase; an ortholog of SlMPK1) (Takahashi et al., 2007). In tomato, two MAPKK kinases, SlMAP3Kα and SlMAP3Kε, and two MAPK kinases, SlMEK1 and SlMEK2, are demonstrated to be positive regulators involved in PCD associated with plant immunity (del Pozo et al., 2004; Melech-Bonfil and Sessa, 2010, 2011). Nevertheless, little is known about their roles in flg22-mediated signaling pathway.

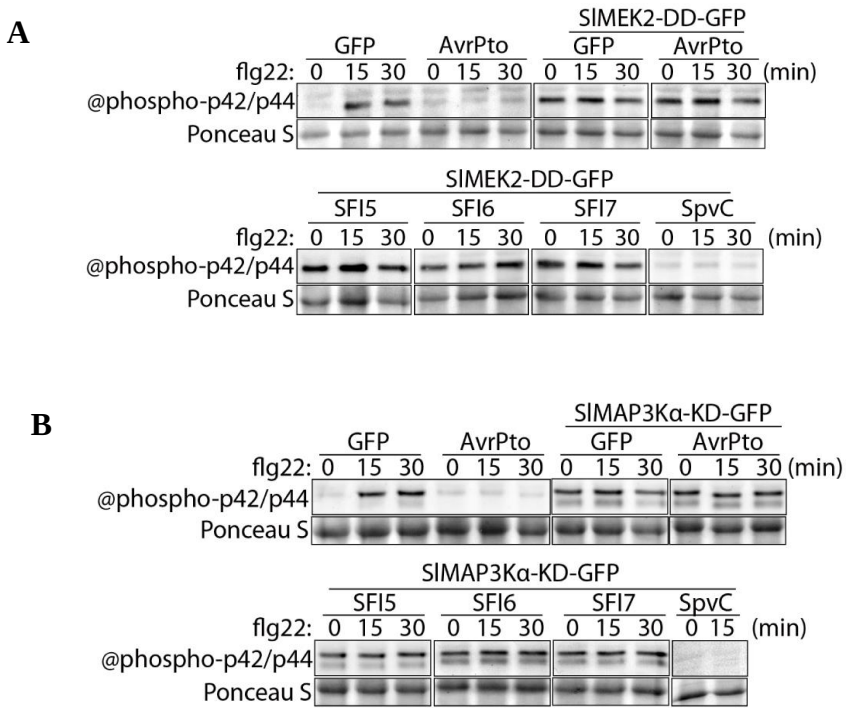

Figure 3-7. SFI5, SFI6 and SFI7 do not inhibit SlMEK2 or SlMAP3Kα activation of endogenous MAPKs in *S. lycopersicum* protoplasts.

(A) SFI5, SFI6 or SFI7 were co-expressed with the constitutively active mutant of SlMEK2 (SlMEK2-DD-GFP) or **(B)** SlMAP3Kα (SlMAP3Kα-KD-GFP) in protoplasts, which were collected 0, 15 and 30 minutes after flg22 treatment. **(A, B)** Endogenous MAPK activation of the samples was detected by antibody raised against phosphorylated MAP kinase p44/p42. AvrPto and SpvC (a *Salmonella* effector) served as a negative control and a positive control, respectively, to suppress MAPK activation by constitutively active SlMEK2 or SlMAP3Kα. Ponceau S staining is shown as a loading control. These results are representative of at least two independent repeats.

As shown in Figure 3-6, ectopic expression in tomato protoplasts of a constitutively active SlMEK2 (SlMEK2-DD), or SlMAP3Kα kinase domain (SlMAP3Kα-KD) resulted in the activation of SlMPK1/3 in the absence of flg22. These results indicate that SlMEK2 and SlMAP3Kα act upstream of SlMPK1/3 and are possibly involved in flg22-dependent MAPK

activation whereas the constitutively active SlMEK1 (SlMEK1-DD) and the kinase domain of SlMAP3Kε (SlMAP3Kε-KD) failed to do so and even have a negative impact on the flg22-triggered activation of SlMPK1/3. The expression of SlMEK2-DD and SlMAP3Kα-KD bypassed AvrPto and SFI5-SFI7 suppression of SlMPK1/3 activation by flg22 but did not override the suppressing effect of SpvC, an effector from *Salmonella typhimurium*, that was shown to act in a trans-kingdom manner and to inactivate AtMPK6/3, most likely by causing their irreversible dephosphorylation (Mazurkiewicz et al., 2008; Neumann et al., 2014) (Figure 3-7). The conclusion from these experiments is that SFI5-SFI7 block the flg22-induced signaling pathway very early, probably at the level or upstream of MAPKKK activation.

3.1.5. SFI7 interferes with PCD triggered by INF1 but not by Cf-4/Avr4

As stated in 3.1.4, it has been demonstrated in *Solanaceae* that MAPK cascades play an important role in the control of cell death activated by the MAMP INF1 or occurring during ETI, for example, upon recognition of the *Cladosporium fulvum* effectors Avr4/9 by the tomato Cf-4/9 resistance proteins (del Pozo et al., 2004; Takahashi et al., 2007; Melech-Bonfil and Sessa, 2010). Therefore, and in collaboration with H. Mc Lellan, JHI Dundee, UK, SFI5-SFI7 were expressed transiently in *N. benthamiana* leaves and their effect on these two PCD responses was examined.

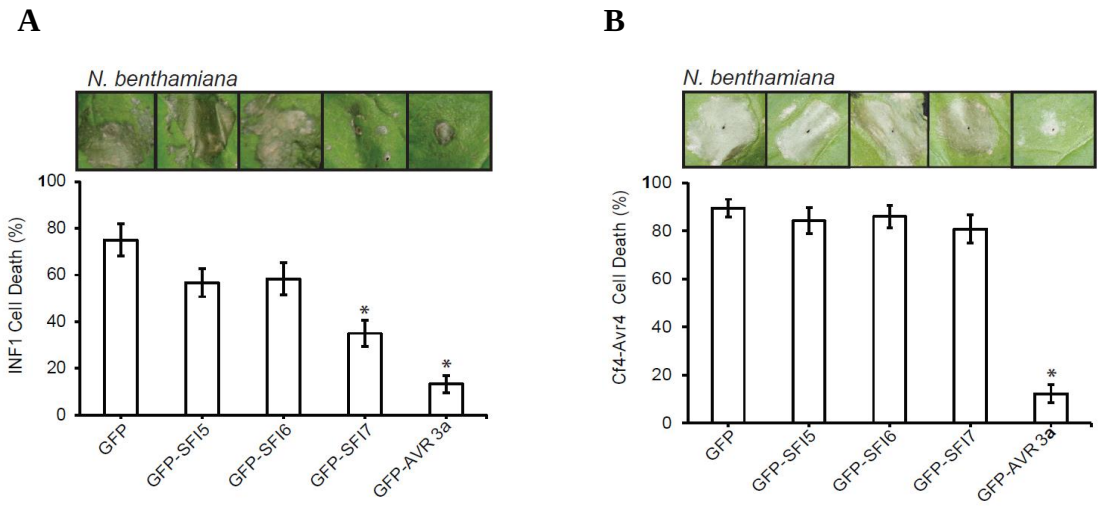

Figure 3-8. Effect of GFP-fused SFI5, SFI6 and SFI7 on INF1-mediated PCD as well as Avr4/Cf4-triggered HR responses in *N.benthamiana*.

(A) Percentage of infiltrated sites with confluent cell death at 7 days post-agro-infiltration, following co-expression of each GFP-fused effectors and INF1. **(B)** Percentage of infiltrated sites with confluent cell death at 7 days post-agro-infiltration, following co-expression of each GFP-effectors with *C. fulvum* effector Avr4 and tomato resistance protein Cf-4. Results in **(A)** and **(B)**, shown as mean values ± SEM, are representative of five

independent experiments, each using 18 inoculation sites. Statistical significance (*, p-value < 0.01) compared to the empty control (GFP) is determined by one-way ANOVA.

Compared to the PiRXLR effector AVR3a, which was identified as a suppressor of PCD promoted by INF1 or by the interaction between Cf-4 and Avr4 (Bos et al., 2006; Bos et al., 2009; Gilroy et al., 2011), GFP-SFI5 and GFP-SFI6 had no effect (Figure 3-8). Only GFP-SFI7 was able to significantly inhibit INF1-mediated cell death, although not as strong as AVR3a, and it had also no effect on Cf-4/Avr4-triggered cell death (Figure 3-8). These observations indicate that SFI5 and SFI6 do not impair MAPK signaling leading to INF1 or Cf-4/Avr4-dependent PCD in *N. benthamiana* whereas SFI7 possesses a broader suppressive effect by affecting INF1 but not Cf-4/Avr4-mediated PCD.

3.1.6. SFI1-8 effectors display different sub-cellular localization patterns

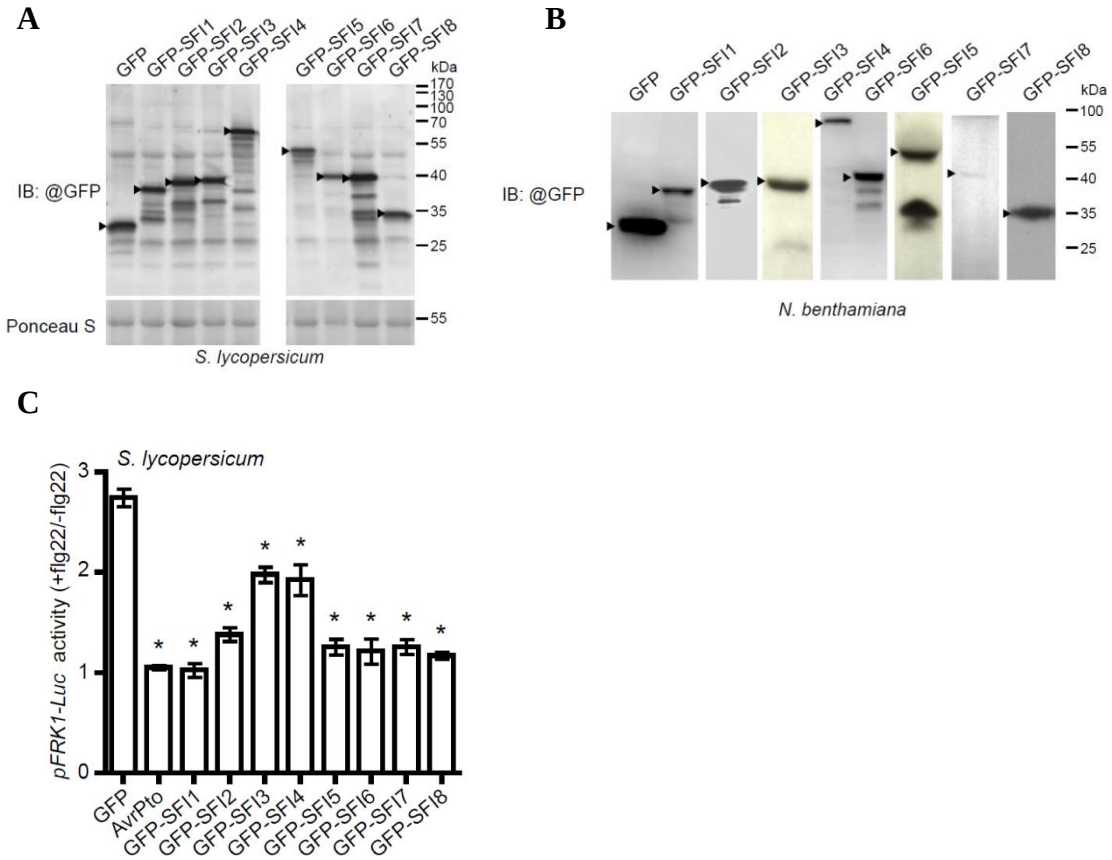

Figure 3-9. Expression profile and *pFRK1-Luc* reporter gene assay for GFP-tagged SFI effectors in protoplasts.

(A, B) Protein accumulation of SFI effectors N-terminally fused with GFP in *S. lycopersicum* protoplasts **(A)** and *N. benthamiana* leaves **(B)**. Total protein extracted from 12 hours post-transfected protoplasts or 48 hours post-agro-infiltrated leaves was used for immunoblot assay with anti-GFP antibody. The corresponding GFP-

fused SFI proteins with expected molecular sizes are pointed out with an arrow. Partial protein degradation was observed in some samples. Ponceau S staining was given as a loading control. At least two biological replicates were conducted and one representative result is presented. **(C)** Effect of GFP-fused SFI effectors on suppressing *FRK1* promoter activity in *S. lycopersicum* protoplasts. Mesophyll protoplasts were transformed and the luciferase activity were measured as described in Figure 3-2 and Figure 3-3. Mean values ± SEM of four independent experiments were given. *, p-value < 0.05 by one-way ANOVA followed by Dunnett's multiple comparison test.

Preliminary results about the functional characterization of SFI1-8 provide evidence that they target different steps of flg22 signaling, from the very early events upon FLS2 activation till more downstream responses associated with transcriptional reprogramming and the up-regulation of immunity-associated genes. To uncover more details about the action mode of SFI1-8 inside plant cells, we investigated their subcellular localization by expressing GFP fused effectors transiently in tomato protoplasts and in *N. benthamiana* leaves.

Immunodetection experiments confirmed the expression and stability of GFP-tagged SFI effectors (Figure 3-9 A, B) and the *pFRK1-Luc* assay in protoplasts showed that GFP-SFI1-8 retain the suppression activity (Figure 3-9 C). Sub-cellular localization analysis revealed that GFP-SFI1, GFP-SFI2 and GFP-SFI8/Avrblb2 strongly accumulate in the nucleus though they display distinct sub-nuclear distribution patterns (Figure 3-10 A, B). Localization studies in *N. benthamiana* further supported the observations made in protoplasts and allowed higher image resolution. It revealed that GFP-SFI1 was enriched in the nucleolus and GFP-SFI2 appeared to display several types of sub-nuclear localization, ranging from excluded of the nucleolus to even nucleus/nucleolus distribution and occasionally to punctuated structures (Figure 3-10 B). A significant proportion of GFP-SFI8/AVRblb2 is localized in the cytoplasm, whereas GFP-SFI1 and GFP-SFI2 are nearly exclusively localized in the nucleus/nucleolus (Figure 3-10 A). The nuclear localization of SFI1, SFI2 and SFI8/AVRblb2 is in accordance with their suppressing function on the expression of MTI-associated genes downstream of MAP kinase activation and could be explained by manipulation of components of the transcriptional or post-transcriptional machinery. GFP-SFI3 and GFP-SFI4 showed nuclear-cytoplasmic localization with GFP-SFI3 forming a ring surrounding the nucleolus (Figure 3-10 A, B). GFP-SFI5, GFP-SFI6 and GFP-SFI7 had different extent of cytoplasmic distribution and accumulation at the plasma membrane (Figure 3-10 A), which is in line with their suppressing effect on the earliest components involved in MAMP perception and signal transduction.

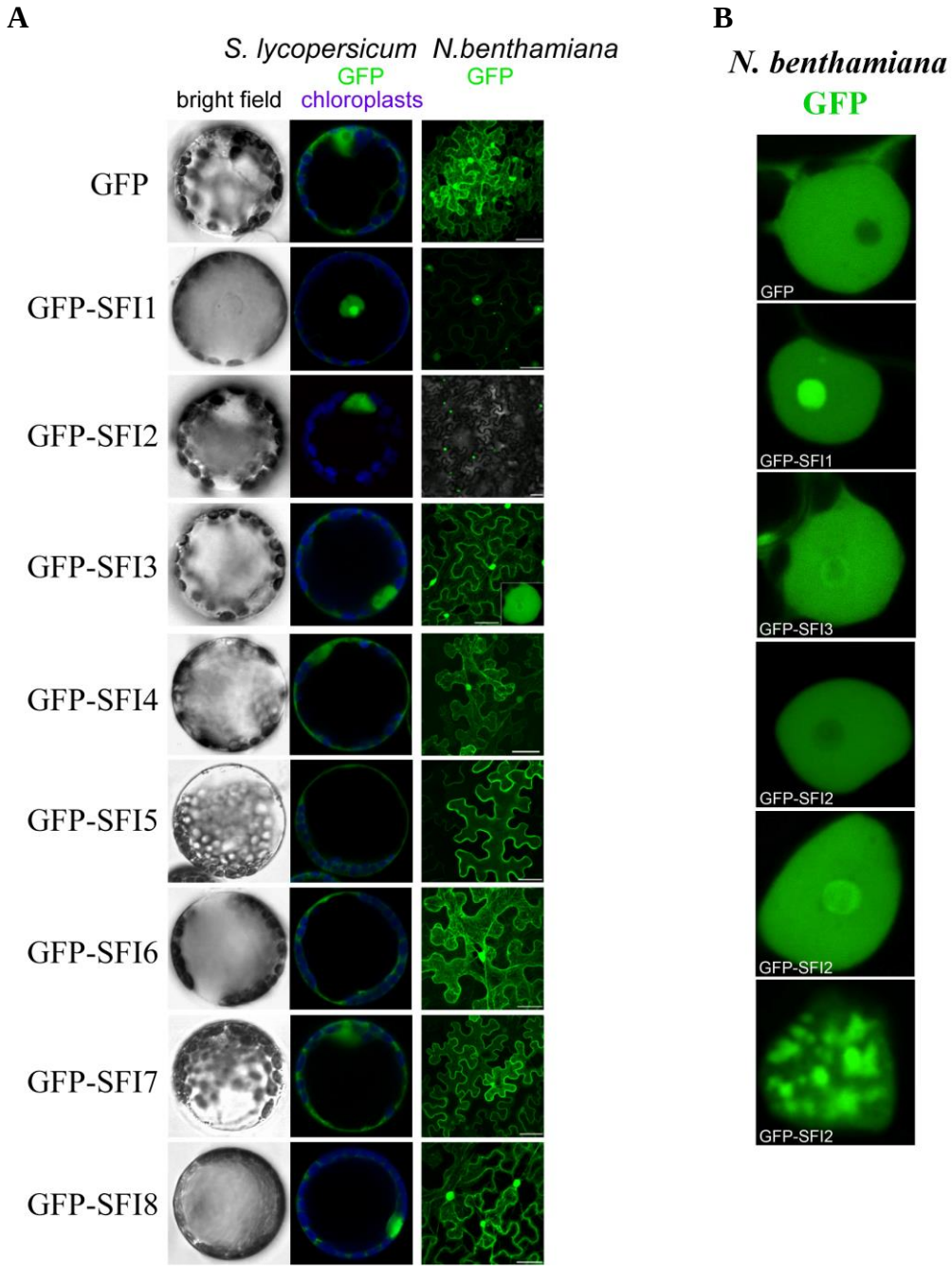

Figure 3-10. Subcellular distribution of GFP-SFI effectors in *S. lycopersicum* protoplasts and in *N. benthamiana* leaves.

(A) Mesophyll protoplasts and *N.benthamiana* leaves transiently expressing *p35S-GFP-effector* were observed using confocal laser scanning microscope after 12 hours and 48 hours transformation, respectively. The image shows representative optical sections of bright field and merged fluorescence of GFP (green) and chloroplast (blue) in protoplasts, as well as GFP fluorescence in *N.benthamiana* leaves. **(B)** Sub-nuclear distribution of SFI1, SFI2 and SFI3 in *N.benthamiana* leaves. Confocal imaging of GFP or N-terminally GFP-SFI effectors in the nucleus of *N.benthamiana* was observed using confocal laser scanning microscope after 48 hours transformation.

3.1.7. SFI effectors contribute to *P. infestans* virulence

RXLR effectors have been shown to be major contributors to oomycete pathogenicity. Therefore, we tested in collaboration with H. McLellan (JHI, Dundee, UK) whether SFI1-8 enhance the growth of *P. infestans* on *N. benthamiana*. We transiently expressed SFI1-8 in *N. benthamiana* leaves via Agrobacterium infiltration and after 24 hours, we proceeded to inoculation with a suspension of *P. infestans* zoospores (1 x 10^5 / ml). *P. infestans* development including lesion size and disease symptoms was evaluated at 7^{th} day post-inoculation. Ectopic expression of SFI2 caused cell death, disturbing the measure of disease development and therefore, we could not make a conclusion about its role in virulence.

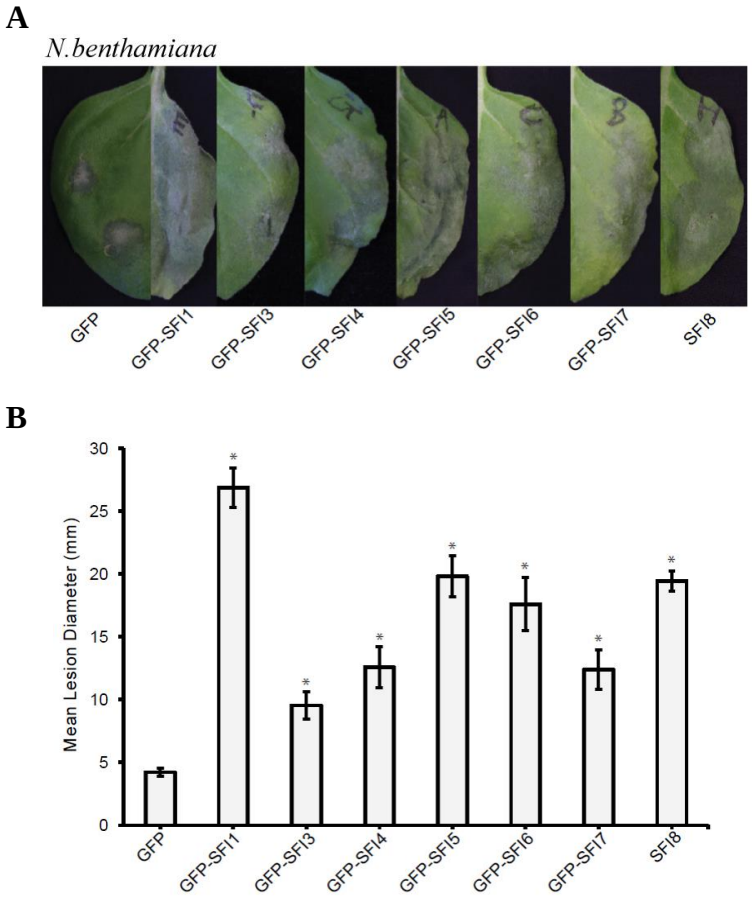

Figure 3-11. Expression of SFI effectors in *N.benthamiana* promote the growth of *P. infestans*.

(A, B) N-terminally GFP-tagged SFI1-SFI7 and non-tagged SFI8 were transiently expressed via agro-infiltration in one half of a *N.benthamiana* leaf and GFP control in the other half. After 24 hours, leaves were inoculated with *P. infestans*. **(A)** Typical disease development symptoms and **(B)** mean lesion diameter were measured 7 days after inoculation. Results are mean values ± SEM from three biological replicates, each of which used 24 leaves for inoculation per construct. Significant difference (*, p-value < 0.01) in lesion size compared to empty vector control was determined by one-way ANOVA.

The other 7 PiRXLR effectors (SFI1 and SFI3-SFI8) enhanced all the susceptibility of *N. benthamiana* to *P. infestans* (Figure 3-11 A and B). We measured a two- to five- fold increase in disease lesion size (p-value < 0.01) compared to the GFP control. The most potent PiRXLR effector was GFP-SFI1, which caused a 5-fold increase of the average lesion size (~25 mm) vs GFP control (~ 5 mm). The nucleus/nucleolus localization of SFI1 coupled to its function as inhibitor of flg22-induced MTI genes in both tomato and Arabidopsis downstream of MAPK activation prompted us to look further at the association of SFI1 nuclear localization with its virulence activity.

3.1.8. The nuclear localization is important for the function of SFI1

Based on the preliminary data gained from the analysis of SFI1, we assumed that the nuclear localization is required for the inhibition of MTI responses. To test this hypothesis, a myristoylation site, aiming to re-direct SFI1 at the plasma membrane, was introduced at the N-terminus of GFP-SFI1. The resulting construct (myr-GFP-SFI1) was transformed into Arabidopsis protoplasts and agro-infiltrated in *N. benthamiana* for further analysis.

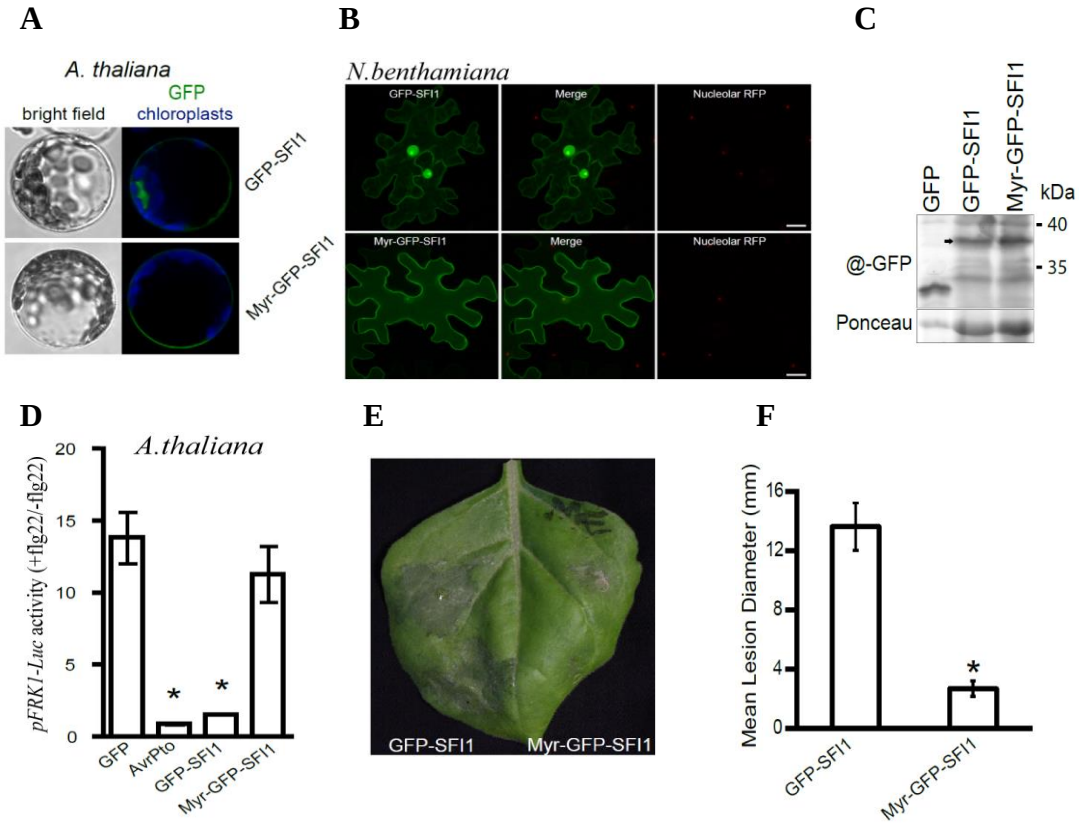

Figure 3-12. The nuclear accumulation of SFI1 is critical for inhibiting flg22-triggered *pFRK1-Luc* expression and promoting growth of *P. infestans*.

(A, B) Sub-cellular localization of GFP-SFI1 or myr-GFP-SFI1 expressed in *A.thaliana* protoplasts **(A)** or *N.benthamiana* leaves **(B)**. **(A)** Representative optical sections of bright field and merged fluorescence of GFP

(green) and chloroplast (blue) in protoplasts were shown. **(B)** Confocal imaging of *N. benthamiana* cells expressing GFP-SFI1 or myr-GFP-SFI1 (left panels, in green) with the nucleolar marker RFP-fibrillarin (right panels, in red); the merged images are shown in the central panels. **(C)** Stable and intact protein expression of GFP-SFI1 and myr-GFP-SFI1 in planta was detected by immunoassay using anti-GFP antibody. The band corresponding to the expected protein size is shown by an arrow. **(D)** *pFRK1-Luc* reporter gene activity in *A.thaliana* protoplasts expressing GFP-SFI1 or myr-GFP-SFI1, as well as GFP or AvrPto. Mean values ± SEM were given from four independent replicates. Significant differences (*, p-value < 0.05) in luciferase activity relative to GFP control were determined by one-way ANOVA followed by Dunnett's multiple comparison test. **(E, F)** Effect of GFP-SFI1 and myr-GFP-SFI1 on *P. infestans* virulence. Via Agrobacterium-mediated transfection, GFP-SFI1 and myr-GFP-SFI1 were respectively expressed in one half of a *N.benthamiana* leaf one day before inoculation with *P. infestans*. **(E)** Typical disease development symptoms and **(F)** mean lesion diameter were measured on 7 days post-inoculated leaves. Results are mean values ± SEM from three biological replicates. Significant difference (*, p-value < 0.01) was determined by one-way ANOVA.

Subcellular localization showed that the myristoylation site prevented nuclear accumulation of SFI1 and myr-GFP-SFI1 was indeed targeted to the plasma membrane in both Arabidopsis protoplasts and *N. benthamiana* leaves (Figure 3-12 A, B). The expression of of myr-GFP-SFI1 was confirmed by immunoblot (Figure 3-12 C). Notably, myr-GFP-SFI1 failed to repress induction of *pFRK1-Luc* activity by flg22 (Figure 3-12 D) and lost the ability to enhance *P. infestans* growth on *N. benthamiana*, compared to GFP-SFI1 (Figure 3-12 E, F), confirming further that the nucleus/nucleolus localization of SFI1 is critical for its ability to subvert MAMP-induced immune responses.

Table 3-1 summarizes the results obtained in the first part of our work. Altogether, we have shown that a subset of PiRXLR effectors suppresses flg22-induced early immune responses in tomato and/or Arabidopsis. Some of them (SFI1, SFI2 and SFI8) are functional in a broad range of plants including natural host (tomato and *N. benthamiana*) and non-host (Arabidopsis) plant species of *P. infestans*. Other effectors (SFI5-SFI7) are efficient only in host plants or as shown for effectors PITG_00821, PITG_05750, PITG_16737 and PITG_21388, only active in the non-host Arabidopsis. Plasma membrane localization is correlated with the suppression of immune signaling upstream of the activation of the MAP kinase cascade whereas nuclear localization affects immune signaling downstream of MAP kinase activation by interfering with the expression of immunity-associated genes. Importantly, we have shown that MTI suppression is an important factor in the strategy employed by *P. infestans* to colonize host plants.

Table 3-1. Summary of PiRXLR effectors with MTI-suppressing activity

PiRXLR	Flg22-induced					Sub-cellular Localization	*P.infestans* growth
	pFRK1-Luc activity		MAMP gene expression	MAP Kinase activation			
	S. lycopersium	*A. thaliana*	*A. thaliana*	*S. lycopersicum*	*A. thaliana*	*N. benthamiana*	*N. benthamiana*
SFI1						nucleus/nucleolus	
SFI2						nucleus/nucleolus	n.d.
SFI3						nucleus/nucleolus	
SFI4						cytoplasm/nucleus	
SFI5						PM	
SFI6						cytoplasm/PM	
SFI7						cytoplasm/PM	
SFI8						cytoplasm/nucleus	
PITG_00821				n.d	n.d.	n.d.	n.d.
PITG_05750				n.d	n.d.	n.d.	n.d.
PITG_16737				n.d	n.d.	n.d.	n.d.
PITG_21388				n.d	n.d.	n.d.	n.d.

Suppression | No Suppression | Enhanced | n.d. not determined

3.2. Functional characterization of SFI5

The screen of *P. infestans* RXLR effectors disturbing the earliest signaling events of MTI leaded to the identification of SFI1-SFI8. These effectors were shown to be relevant for host adaptation. With the objective to understand how MTI-suppressing PiRXLR effectors manipulate the host immune network, we searched in several publicly available protein databases for the presence of functional domains within SFI1-SFI8 and we performed immunoprecipitation assays followed by mass spectrometry (MS) analysis with tomato and Arabidopsis protoplasts to identify potential host targets with presumed or demonstrated function in regulating immunity. SFI1 was initially ranked as our top candidate (see 3.1.8) but because of the absence of any functional domain and the lack of any putative interactor from the IP assay, we decided to prioritize SFI5 for a detailed functional characterization. SFI5 showed tomato-specific suppression of flg22-induced post-translational MAP kinase activation, which may be related to its plasma membrane localization.

In the second part of this thesis, we have tried to bring some new insights about the mechanism of action of SFI5 in modulating plant immune responses. The objectives were (i) to explore the structure-function relationships of identified SFI5/target pairs, and (ii) to determine the biochemical consequences of these relationships for MTI signalling. It is postulated that effectors directly or indirectly interact with host proteins, and that the structure-function relationship of the effector-target interaction determines complexity and specificity of plant-pathogen relationships.

3.2.1. *In silico* prediction of CaM interaction with SFI5

SFI5 is a 241-amino acid protein bearing the typical signature of RXLR effectors with the presence of a N-terminal signal peptide for secretion in the extracellular space, followed by a sequence (Ala^{28} to Arg^{62}) containing the RXLR motif necessary for translocation into the host cytosol and a predicted C-terminal effector domain of 178 amino acid residues (Phe^{63} to Arg^{241}) (Figure 3-13). Bioinformatics analysis run on the Calmodulin Target Database (http://calcium.uhnres.utoronto.ca/ctdb/ctdb/home.html) (Yap et al., 2000) revealed the presence of a putative calmodulin (CaM)-binding site, located at the C-terminal end of SFI5 between Pro^{222} and Leu^{239} (Figure 3-13 B). CaMs function as calcium sensors in eukaryotes and after conformational change induced by Ca^{2+} binding to EF-hand motifs, interact and regulate the function of diverse target proteins (McCormack et al., 2005). They are conserved in plant species and important for various biological processes, including the plant immune responses (Snedden and Fromm, 2001; Hoeflich and Ikura, 2002; Cheval et al., 2013; Poovaiah et al., 2013). So far, there are very few reports describing an interaction between CaMs and effectors from pathogenic microorganisms (Wolff et al., 1980; Nakahara et al., 2012; Guo et al., 2016). Thus, it is interesting to confirm and find out about the relationship between CaM interaction and SFI5 function.

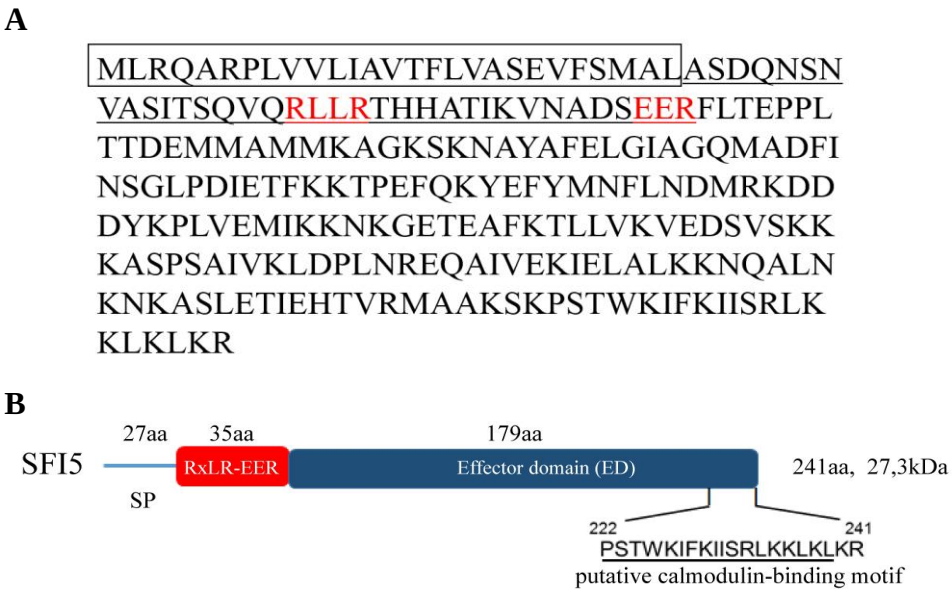

Figure 3-13. Schematic illustration of SFI5.

(A) The amino acid sequence of SFI5 protein. The predicted signal peptide is boxed; The RXLR-EER motif is underlined. **(B)** Schematic representation of SFI5 showing the predicted amino acid (aa) length of the signal peptide (SP), the RXLR-EER motif for translocation into the host and the effector domain (ED). Numbers

indicate positions of amino acid residues beginning from the N terminus. The putative calmodulin-binding motif is underlined.

3.2.2. SFI5 interacts *in vitro* with CaM in a Ca^{2+} -dependent manner

With the help of N. Wagener, a post-doc within the Dept. of Plant Biochemistry at the ZMBP, we monitored the interaction between SFI5 and CaM by performing *in vitro* interaction assays. The Arabidopsis CaM1/4, fused to glutathione S-transferase (GST-AtCaM1/4), and SFI5, fused to maltose-binding protein (MBP-SFI5), were expressed in *E. coli* and subsequently purified from bacterial extracts by affinity chromatography using GSH agarose and amylose resin, respectively. GST-AtCaM1/4 and MBP-SFI5 were mixed together in a buffer containing calcium or the calcium chelator EDTA.

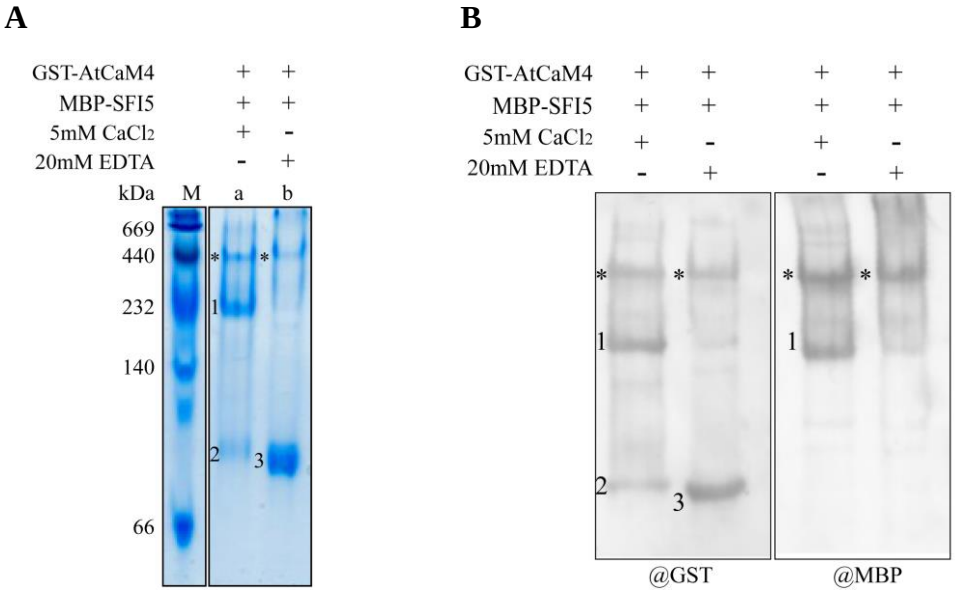

Figure 3-14. *In vitro* Ca^{2+}-dependent interaction between SFI5 and AtCaM1/4.

(A) Blue Native (BN) gel analysis of the SFI5 interaction with AtCaM1/4. 25 µg of recombinant MBP-SFI5 was incubated with 25 µg GST-AtCaM1/4 in the presence of 5mM $CaCl_2$ (a) or 20mM EDTA (b) at 4 °C for 1 hour. Samples were separated by BN-PAGE and stained with Coomassie Brilliant Blue. **(B)** Immunoblots of the BN gel described in **(A)**. Immunodetection of GST-AtCaM1/4 and MBP-SFI5 was performed by using an anti-GST antibody (left panel) or anti-MBP antibody (right panel), respectively. MBP-SFI5 and GST-holoAtCaM4 complex (1), free GST-holoAtCaM4 (2) and free GST-apoAtCaM4 (3). Unspecific band (Asterisks). These results are representative of three replicates.

After blue native (BN) gel electrophoresis, we detected in the sample with Ca^{2+} a band of approximately 220 kDa that would fit the molecular mass of a heterodimeric complex between MBP-SFI5 and GST-AtCaM4 (Figure 3-14 A). This band was nearly absent in presence of EDTA and, instead of, a higher amount of Ca^{2+}-free AtCAM4 accumulated (Figure 3-14 A). It also appeared that in the absence of Ca^{2+} and CaM, MBP-SFI5 tends to aggregate and becomes insoluble, illustrated by the absence of a band corresponding to MBP-SFI5 on BN-PAGE. The presence of both GST-AtCaM1/4 and MBP-SFI5 in the 220 kD complex was verified by performing immunodetection assays (Figure 3-14 B). These results indicate that SFI5 and AtCaM4 interact *in vitro* in a Ca^{2+}-dependent manner.

3.2.3. SFI5 interacts *in vivo* with both Arabidopsis and tomato CaMs

In order to confirm the results of the *in vitro* interaction between SFI5 and AtCaM4 and to identify additional potential host targets or interactors of SFI5, we perormed immunoprecipitation assays followed by liquid chromatography – tandem mass spectrometry (LC-MS/MS) analysis with tomato protoplasts expressing an N-terminal HA-tagged SFI5 (HA-SFI5). In this experiment, we identified a number of candidate proteins associated with SFI5, which did not appear in protoplasts expressing HA-SFI1 or empty vector control (Appendix table 6-3). Homologs of AtCAM1/4 and AtCaM2/3/5 were among the best candidates, providing additional evidence that CaM associates with SFI5 *in planta.*

In Arabidopsis, there are seven distinct *CaM* genes encoding four protein isoforms sharing 97 to 99 % amino acid identity between each other. *AtCaM1* and *AtCaM4* encode the same isoform, a second isoform is encoded by *AtCaM2*, *AtCaM3* and *AtCaM5*. *AtCaM6* and *AtCaM7* encode for a third and fourth isoform, respectively (McCormack et al., 2005). A tomato genome-wide analysis identified six *CaM* genes, which also encode four isoforms: SlCaM1, SlCaM2, SlCaM3/4/5 and SlCaM6, which share 91 %-99 % amino acid sequence identity between each other (Zhao et al., 2013). Phylogenetic analysis showed that the CaMs from Arabidopsis and tomato appear very high sequence identity. SlCaM1-SlCaM5 exhibit 98% or 99% sequence identity to the canonical AtCaM3, while the most distantly related SlCaM6 still shares 91% amino acid sequence identity with AtCaM3 (Figure 3-15 A).

In the next step, we decided to perform pair-wise interaction studies between SFI5 and different Arabidopsis and tomato CaMs in order to define the interaction specificities. In addition to AtCaM1/4 and AtCaM2/3/5, we were able to clone from a tomato cDNA library three CaM genes corresponding to SlCaM1, SlCaM3/4/5 and SlCaM6. The association of

HA-CaMs with GFP-SFI5 was tested in pull-down experiments in tomato protoplasts. This experiment showed that SFI5 interacts with every CaM without apparent specificity (Figure 3-15 B).

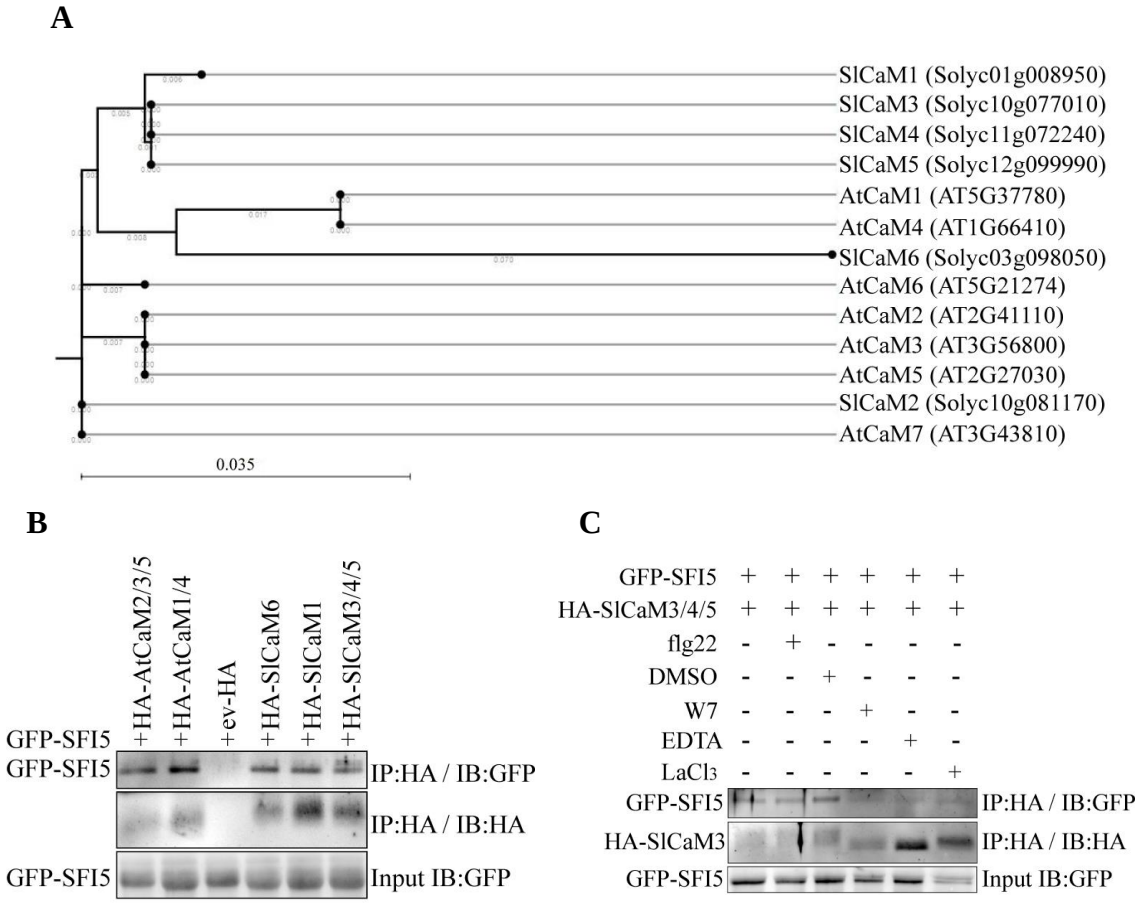

Figure 3-15. SFI5 interacts with Arabidopsis and tomato CaMs *in vivo.*

(A) Phylogenetic tree on amino acid similarity of CaM proteins from *S. lycopersicum* and *A. thaliana*. The full-length protein sequences of each member were aligned and the tree was built using ClustalW method of CLC Main Workbench 7 program. The accession numbers for these CaMs are indicated in the brackets. **(B)** Co-immunoprecipitation analysis of transiently expressed GFP-SFI5 and HA-At/SlCaMs in tomato protoplasts. Extracted proteins (input) were subjected to immunoprecipitation (IP) with anti-HA affinity matrix followed by immunobloting (IB) with anti-GFP antibodies to detect the tomato calmodulins and anti-HA antibodies to detect SFI5. **(C)** Interaction analysis of SFI5 with SlCaM3/4/5 by different treatments. Protoplast samples were treated with 500 nM flg22, 0.75 % DMSO (mock), 250 nM W7 (stock solution: 33 mM W7 dissolved in 99.5 % DMSO) or 1mM LaCl3 before the protoplasts were harvested for the IP. For EDTA treatment, total proteins were extracted with IP buffer containing 20mM EDTA.

In vitro interaction studies have shown that the interaction between SFI5 and CaM is Ca^{2+}-dependent. The increase of cytosolic Ca^{2+} is among the earliest response to MAMP

perception. Therefore, we tested if the association between CaM and SFI5 might increase or occur in a MAMP-dependent manner. Immunoprecipitation assays with HA-SlCaM3/4/5 and GFP-SFI5 before and after flg22 treatment clearly showed that the association is independent and not modulated by flg22 (Figure 3-15 C). A pharmacological approach using the conventional CaM antagonist N-(6-aminohexyl)-5-chloro-1-naphthalene-sulphonamide (W7), interfered significantly with the interaction between HA-SlCaM3/4/5 and GFP-SFI5. The requirement of Ca^{2+} for the interaction between SFI5 and CaMs *in planta* was tested by adding the Ca^{2+} channel blocker LaCl3 or EDTA (upon protein extraction and prior immunoprecipitation). In both cases, the ability of GFP-SFI5 to associate with HA-SlCaM3/4/5 was dramatically reduced, demonstrating the absolute necessity of Ca^{2+} for the SFI5-CaM complex formation.

3.2.4. The C-terminal amphipathic helix of SFI5 is critical for CaM-binding

Although the Calmodulin Target Database search predicted a CaM-binding site spaning the C-terminus of SFI5, the amino acid sequence in this region does not contain a canonical CaM-binding motif, according to a Calmodulation meta-analysis (http://cam.umassmed.edu) (Mruk et al., 2014). A helical wheel projection of the 18-amino acid stretch (Pro^{222} to Leu^{239}) encompassing the putative CaM binding site showed that it exhibits a basic amphipathic structure with one side enriched in positively charged residues (Lys^{226}, Lys^{229}, Arg^{233}, Lys^{236}) and the opposite side rich in hydrophobic residues (Try^{225}, Ile^{227}, Phe^{228}, Ile^{231}), which in turns, is typical for a CaM recognition and binding site (Figure 3-16 A).

To further identify the molecular determinants involved in binding of SFI5 to CaM, a synthetic peptide corresponding to the region from Ser^{223} to Arg^{241} (peptide1) was synthetized and used in BN gel mobility shift assay with recombinant GST-AtCaM4 and in presence of Ca^{2+}. As shown in Figure 3-16 C, the peptide1-GST-AtCaM4 complex appears as a higher molecular mass band than free GST-AtCaM4, indicating that the last 19aa at the C-terminus of SFI5 are sufficient for physical interaction with CaM.

In many identified CaM interacting proteins, the modification of the amphipathic property or net charge of the CaM-binding domain has been demonstrated to have a negative impact on their ability to bind CaMs (Herring, 1991; Fitzsimons et al., 1992; Kim et al., 2002; Moon et al., 2005; Katou et al., 2007; Wang et al., 2009). To characterize the key amino acid residues for CaM-binding, a series of truncated or mutated derivatives of peptide 1 were synthesized and tested for their CaM-binding properties in the mobility shift assay (Figure 3-16 B, C). The

removal of the last two amino acid residues (Lys^{240}-Arg^{241}) in peptide 2 decreases the net charge at pH 7 from +8 to +6 without affecting binding to CaM, suggesting that these two residues are not important for the association with CaM.

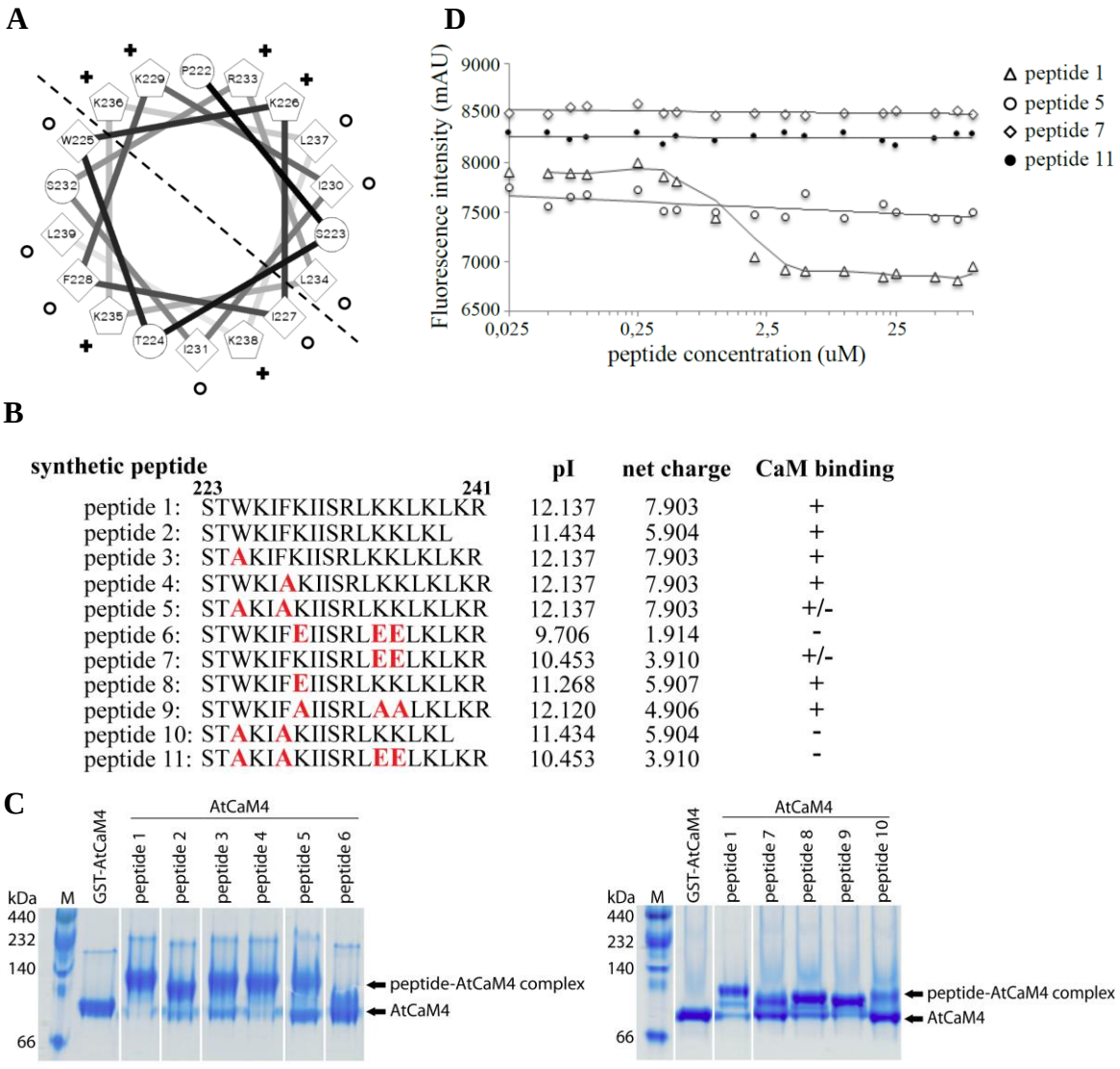

synthetic peptide (223–241)		pI	net charge	CaM binding
peptide 1:	STWKIFKIISRLKKLKLKR	12.137	7.903	+
peptide 2:	STWKIFKIISRLKKLKL	11.434	5.904	+
peptide 3:	ST**A**KIFKIISRLKKLKLKR	12.137	7.903	+
peptide 4:	STWKI**A**KIISRLKKLKLKR	12.137	7.903	+
peptide 5:	ST**A**KI**A**KIISRLKKLKLKR	12.137	7.903	+/-
peptide 6:	STWKIF**E**IISRL**EE**LKLKR	9.706	1.914	-
peptide 7:	STWKIFKIISRL**EE**LKLKR	10.453	3.910	+/-
peptide 8:	STWKIF**E**IISRLKKLKLKR	11.268	5.907	+
peptide 9:	STWKIF**A**IISRL**AA**LKLKR	12.120	4.906	+
peptide 10:	ST**A**KI**A**KIISRLKKLKL	11.434	5.904	-
peptide 11:	ST**A**KI**A**KIISRL**EE**LKLKR	10.453	3.910	-

Figure 3-16. The C-terminal α-helix of SFI5 binds to CaM *in vitro*.

(A) Helical wheel projection of the predicted 18-amino acid CaM-binding region of SFI5 (Pro222 to Leu239). Hydrophobic and potentially positively charged residues are marked with **O** and **✚**, respectively. The dashed line divides the amphipathic helix into the hydrophobic side and hydrophilic side. Numbers refer to amino acid positions in SFI5 protein. **(B, C, D)** A series of synthetic peptides derived from the CaM-binding region of SFI5 were tested for their ability to bind CaM. Peptide 1 represents the last 19aa at the C-terminus of SFI5. Peptides 2-11 are truncated or mutated versions of peptide 1, in which the substituted amino acids are presented in red bold. The pI and net charge (at pH7.0) of each peptide were calculated by Editseq (Lasergene v.8; DNASTAR). **(C)** Gel mobility shift assay. Purified GST-AtCaM4 (50 μM) was incubated with different peptides (133 μM), respectively, in the presence of 5 mM CaCl2. Samples were separated by BN-PAGE followed by Coomasssie

Briliant Blue staining. Arrows indicates the position of bands representing free GST-AtCaM4 and peptide-GST-AtCaM4 complex. **(D)** ANS fluorescence competition assay. GST-AtCaM4 (1 µM), ANS (100 µM) in the buffer with 20mM Tris-HCl pH 7.5, 100 mM NaCl, 1 mM $CaCl_2$ were incubated with increasing concentration of the indicated peptides and kinetic changes of fluorescence was monitored at an excitation wavelength of 360nm (λ_{ex}) and an emission wavelength of 460nm (λ_{em}). Data points represent the mean values ± SEM of three technical replicates from three independent assays.

The replacement of both hydrophobic residues, Trp^{225} and Phe^{228}, by Ala significantly reduced the ability of peptide 5 to bind CaM with an equimolar ratio of peptide 5/GST-AtCaM4 complex and unbound GST-AtCaM4. The C-terminal helix contains several lysine residues and some of them were predicted by computer modeling to be important for direct interaction with CaM. The replacement of Lys^{229}, Lys^{235} and Lys^{236} by Glu caused a drastic change in the net charge of peptide 6 from +8 to + 2 and the interaction with GST-AtCaM4 was nearly abolished. Interestingly, replacement of the lysine residues by alanine (peptide 9), did not affect the binding affinity to CaM, suggesting that the net charge of the helix is a crucial factor for CaM binding. Further analysis has shown that Lys^{229} seems to be dispensable for CaM binding (peptide 8), the most important residues apparently being Lys^{235} and Lys^{236} (peptide 7).

To underpin the importance of the two hydrophobic residues (Trp^{225} and Phe^{228}) and the two basic residues (Lys^{235} and Lys^{236}) for the binding with CaM, we carried out competition assays between a selection of mutated peptides and 1-Anilinonaphthalene-8-sulfonate (ANS), a compound highly affine to CaM and fluorescent upon binding. The kinetics of ANS fluorescence change was monitored in the presence of increasing concentration of different peptides. As shown in Figure 3-16 D, the fluorescence curve rapidly declined with increasing concentration of peptide 1 (IC50 = 1 µM), indicating that competition occurred between ANS and the peptide for binding to CaM. By contrast, ANS fluorescence decreased smoothly or remained unchanged with increasing amounts of peptide 5, peptide 7 and peptide 11 (a quadruple mutant of Trp^{225}, Phe^{228}, Lys^{235} and Lys^{236}).

We used the information gained from the *in vitro* binding studies to perform interaction analysis between GFP-SFI5 and SlCaM3/4/5 in tomato protoplasts. We generated a series of N-terminal or C-terminal deletion constructs of SFI5 and employed site-directed mutagenesis to replace the four key residues identified above to further validate their role in the interaction between SFI5 and CaM *in vivo*. Upon co-immunoprecipitation and subsequent western blot analysis, an interaction could be detected for all the N-terminal deletion mutants of SFI5

including the shortest truncated protein version corresponding to the last 63 amino acids (178-241 aa - Figure 3-17 A).

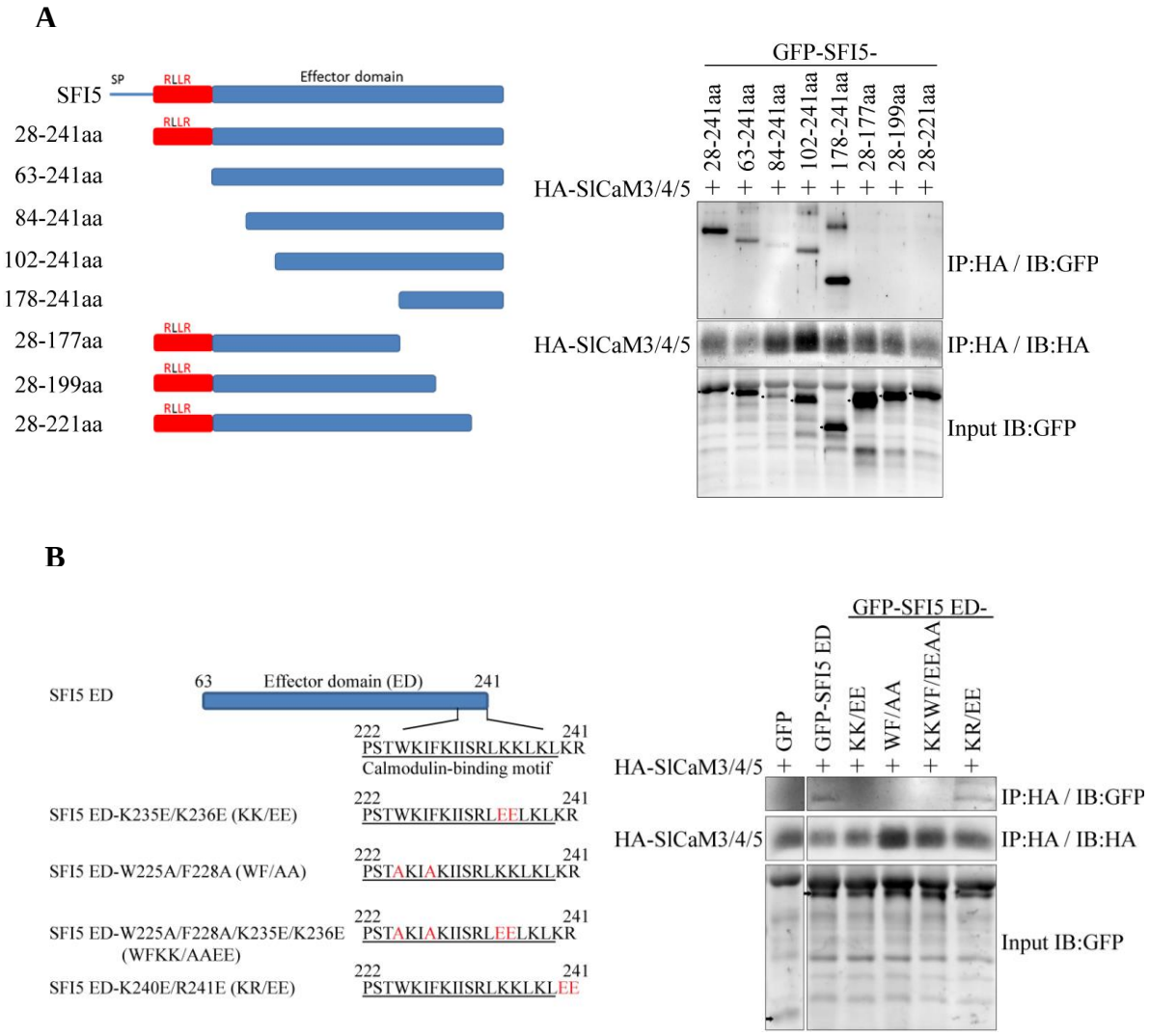

Figure 3-17. The C-terminal amphipathic helix is necessary and sufficient for SFI5/CaM interaction *in vivo*.

(A) Schematic diagrams of SFI5 deletion mutants (left panel). Numbers indicate positions of amino acid (aa) residues based on the full-length protein sequence. Co-immunoprecipitation of SFI5 deletion mutants with SlCaM3/4/5 (right panel). *S.lycopersicum* protoplasts transiently co-expressing GFP-fused SFI5 deletion variants and HA-fused SlCaM3/4/5 were co-immunoprecipitated using anti-HA antibody. Bands corresponding to the GFP-tagged SFI5-deletion mutants are indicated by arrows. (**B**) Schematic diagrams of site-directed mutant constructs of SFI5 effector domain (ED) (left panel). Numbers indicate the amino acid positions based on the full-length protein sequence. KK/EE, WF/AA, WFKK/AAEE and KR/EE correspond to amino acid exchanges of Lys^{235} and Lys^{236} with Glu, Trp^{225} and Phe^{228} with Ala, Lys^{235} and Lys^{236} with Glu and Trp^{225} and Phe^{228} with Ala, and Lys^{240} and Arg^{241} with Glu, respectively. Mutations are indicated in red bolt letters. Co-immunoprecipitation of SFI5 ED-point mutants with SlCaM3/4/5 (right panel). *S.lycopersicum* protoplasts co-expressing GFP-tagged SFI5 ED-point mutants and HA-tagged SlCaM3/4/5 were co-immunoprecipitated by anti-HA antibody. Bands corresponding to GFP or GFP-tagged SFI5 ED point mutants are indicated by arrows.

By contrast, none of the three C-terminal deletion variants, including the one lacking only the amphipathic helix of 19 amino acids (28-221 aa), was able to associate with HA-SlCaM3/4/5 (Figure 3-17 A). We did also not observe an interaction with the SFI5 variants carrying mutations for the two hydrophobic (Trp^{225}Ala / Phe^{228}Ala - WF/AA) or basic (Lys^{235}Glu / Lys^{236}Glu – KK/EE) residues or the quadruple (Trp^{225}Ala / Phe^{228}Ala / Lys^{235}Glu / Lys^{236}Glu - WFKK/AAEE) mutant (Figure 3-17 B). As expected, a SFI5 protein, in which the last two amino acids (Lys^{240} and Arg^{241}) were replaced by glutamic acid (KR/EE), did not affect CaM binding (Figure 3-17 B).

According to the results from the *in vitro* and *in vivo* interaction assays, we concluded that SFI5 has a unique CaM binding site formed by a 17-aa core region (Ser^{223} to Leu^{239}) having an α-helical folding and amphipathic properties, in which the two hydrophobic residues (Trp^{225} and Phe^{228}) and the two basic residues (Lys^{235} and Lys^{236}) fill a critical role in binding with CaMs.

3.2.5. The CaM-binding motif is necessary for the plasma membrane localization of SFI5

As mentioned in 3.1.6, GFP-SFI5 is distributed mainly at the plasma membrane and, to a lesser extent, within the cytoplasm in tomato protoplasts. To determine whether the CaM binding site might be relevant for the intracellular localization of SFI5, we performed co-localization studies with selected N-terminal or C-terminal deletion variants or amino acid point mutants of SFI5 and the bacterial effector AvrPto, which has been shown to associate with the plasma membrane through the presence of a N-terminal myristoylation site (Shan et al., 2000; He et al., 2006). Laser scanning confocal microscopy imaging showed that the three N-terminal deletion mutants of SFI5 fused to GFP (GFP-SFI5 28-241aa, GFP-SFI5 63-241aa and GFP-SFI5 84-241aa) and AvrPto-RFP co-localize at the plasma membrane as illustrated by a large overlap of the GFP and RFP fluorescence signal (Figure 3-18), indicating that the N-terminal region of SFI5 is not required for the localization at the plasma membrane. By contrast, the distribution pattern of the two C-terminal deletion variants (GFP-SFI5 28-199 aa and GFP-SFI5 28-221aa) and the quadruple point mutant (GFP-SFI5 ED-WFKK/AAEE) changed, with a shift in the fluorescent peaks and only partial overlapping (Figure 3-18), implying a re-localization of SFI5 into the cytosol and indicating that the plasma membrane association of SFI5 is dependent on the C-terminal CaM-binding motif.

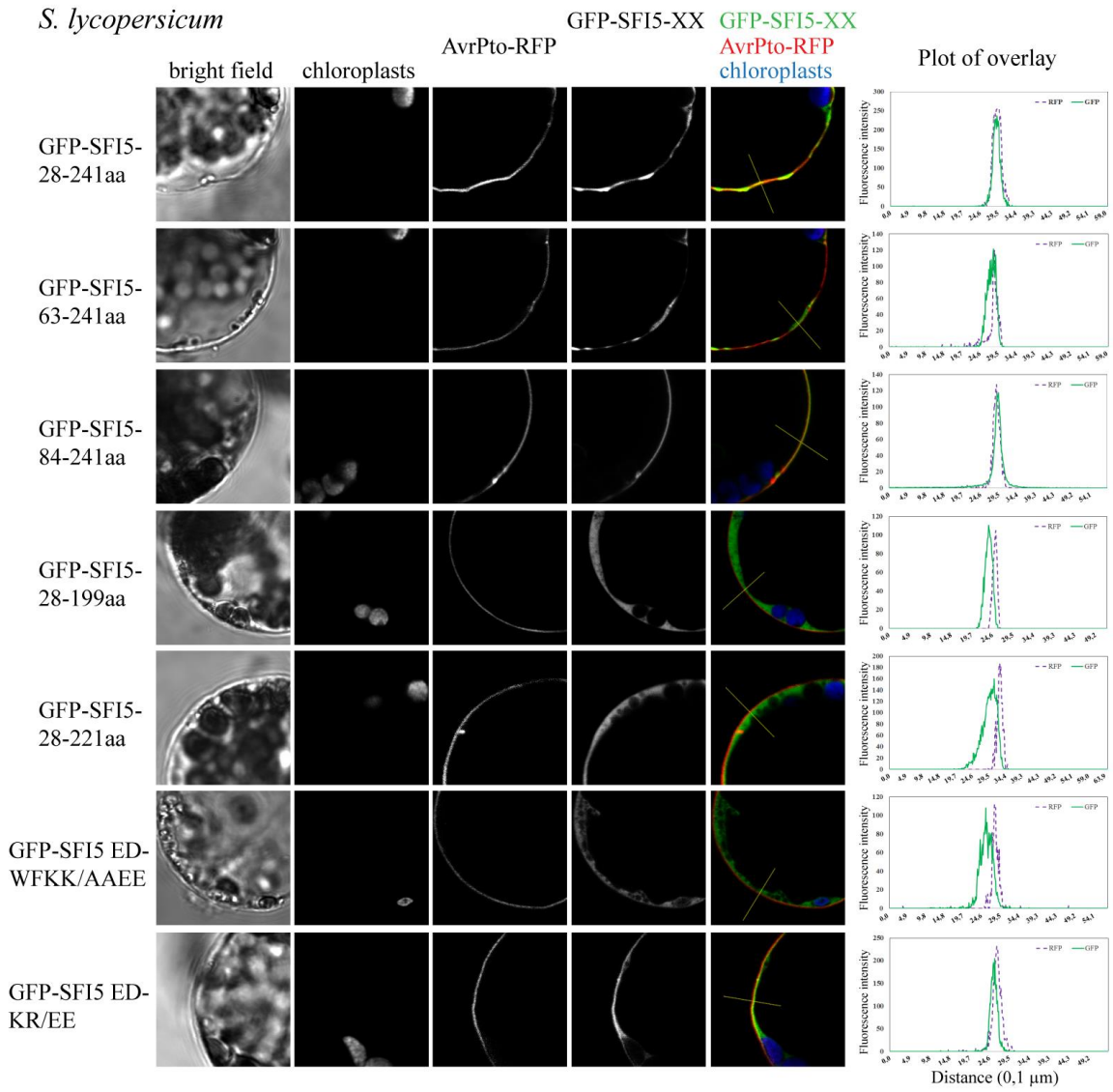

Figure 3-18. The CaM binding motif of SFI5 is required for plasma membrane localization.

S. lycopersicum protoplasts co-expressing N-terminally GFP-tagged SFI5 deletion or point mutant variants and C-terminally RFP-tagged AvrPto were monitored using confocal microscopy. Confocal images were taken 12 hours after transfection and show optical sections of bright field, chloroplast, RFP and GFP fluorescence as indicated. Merged fluorescence images between GFP (green), RFP (red) and chloroplast (blue) fluorescence were created and ImageJ software was used to analyze signal intensity of GFP and RFP fluorescence along the indicated distance (yellow line) from intracellular to extracellular in the overlay picture.

3.2.6. Both C-terminal CaM-binding motif and N-terminal region are required for the full function of SFI5

To examine the relationship between CaM binding and the suppression of early MAMP-induced immune responses, we performed a detailed structure-function analysis of SFI5 in tomato protoplasts. The set of SFI5 deletion and site-point mutation variants with a N-

terminal HA fusion were transiently expressed in tomato protoplasts (Figure 3-19 A) and tested in an array of bio-assays to measure early immune responses triggered by flg22. Some of the read-outs have already been described in 3.1.2.1 and 3.1.3.

First, we measured the impact of truncated and mutated SFI5 proteins on the activity of the *pFRK1-Luc* reporter gene upon flg22 treatment. As shown in Figure 3-19 B, the expression of the three C-terminal deletion variants (HA-SFI5 28-177 aa, HA-SFI5 28-199 aa or HA-SFI5 28-221 aa) did not block flg22-induced Luc activity in comparison to protoplasts expressing SFI5 without its native signal peptide (HA-SFI5 28-241aa) or AvrPto. Point mutations in the CaM-binding region (HA-SFI5 ED-KK/EE, HA-SFI5 ED-WF/AA or HA-SFI5 ED-WFKK/AAEE) also reduced the ability of SFI5 to block flg22-triggered reporter gene activation, although the effect was less severe than with the deletion mutants. The HA-SFI5 ED-KR/EE mutant was as active as the positive controls (Figure 3-19 B).

Interestingly, we also found the abolition of the suppression of the flg22-mediated reporter gene activation in tomato protoplasts expressing N-terminal deletion constructs of SFI5 (HA-SFI5 84-241aa, HA-SFI5 102-241aa or HA-SFI5 178-241aa), excepted for the SFI5 variant lacking the RXLR motif (HA-SFI5 63-241aa) which retained full suppressing activity (Figure 3-19 B). Altogether, these results indicate that the C-terminal CaM-binding helix and a domain spanning approximate 20 aa residues (Phe^{63}- Lys^{84}), located after the RXLR motif, are equally important for SFI5 function in the host cell.

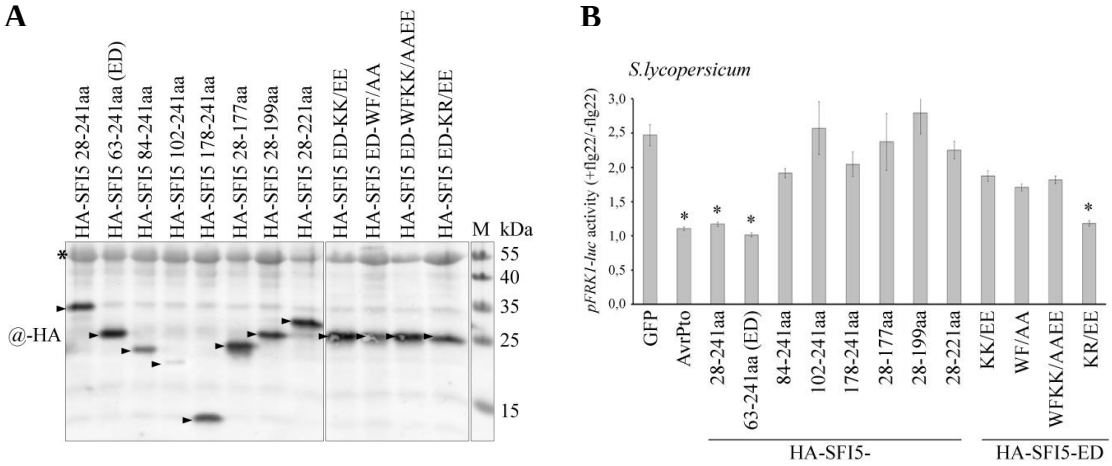

Figure 3-19. Suppression of flg22-triggered *FRK1* promoter activity by HA-SFI5 deletion and point mutants.

(A) Immunoblot analysis of HA-tagged SFI5 deletion mutants and site-directed mutants transiently expressed in *S. lycopersicum* protoplasts. The corresponding HA-tagged SFI5 protein variants with expected molecular sizes are pointed out with an arrow. Non-specific Rubisco band is pointed out with an asterisk and served as a loading control. **(B)** *S. lycopersicum* protoplasts co-expressing a mutated HA-SFI5 variant with the two reporter genes

pFRK1-Luc and *pUBQ10-GUS* were treated with or without flg22 (+/-flg22) and the *Luc* reporter activity was measured. GFP and AvrPto served respectively as a negative and positive control for repressing *pFRK1-Luc* activation by flg22. The promoter activity was presented by calculating the ratio of flg22-induced luciferase activity relative to the untreated sample, which was normalized to the internal GUS activities (*pFRK1-Luc* activity +flg22/−flg22). Each data set represents the mean ± SEM from four independent experiments, for each of which three technical replicates were carried out. *, p-value < 0.05 by one-way ANOVA followed by Dunnett's multiple comparison test.

Our previous studies have shown that SFI5 blocks the flg22-dependent post-translational activation of SlMPK1 and SlMPK3 in tomato protoplasts. Therefore, we hypothesized that structural deletions or mutations in the N- and C-terminal part may impair the MAP kinase suppressing activity of SFI5. Immunodetection with the p44/p42 antibody was used to monitor flg22-dependent endogenous SlMPK1 and SlMPK3 activation in tomato protoplasts. This assay showed that the suppression of the activation of immunity-associated MAP kinase requires the same structural determinants with the same specificity as described above in the case of the suppression of *pFRK1-Luc* induction (Figure 3-20 A).

During flg22-elicitated MTI signaling, it is thought that ROS production occurs in parallel or independently of the MAPK cascade activation and that Ca^{2+} influx acts upstream of these two signaling branches (Grant et al., 2000; Choi et al., 2009; Jeworutzki et al., 2010; Galletti et al., 2011; Segonzac et al., 2011; Xu et al., 2014). CaM serves predominantly as a Ca^{2+} sensor and is possibly involved in the regulation of Ca^{2+} channels and ROS production (Harding et al., 1997; Yang and Poovaiah, 2002a; Hua et al., 2003). In order to find out whether SFI5 has influence on the ROS burst and Ca^{2+} influx triggered by flg22, we have developed new assays in tomato protoplasts.

The oxidative burst in tomato protoplasts expressing the collection of SFI deletion and point mutants was measured using a modified luminol-based detection method, initially established in Arabidopsis leaves (see material & methods). Despite a great variation in the relative amount of ROS generated from experiment to experiment, this assay revealed strong parallels with the results of the *pFRK1-Luc* and MAP kinase assays and validate the conclusion about the crucial role of both the N-terminal and C-terminal domain for the suppressing activity of SFI5 (Figure 3-20 B). Notably, the HA-SFI5 mutant carrying a substitution for the two hydrophobic residues (HA-SFI5 ED-WF/AA) retained the ability to repress ROS production under the defined experimental conditions (Figure 3-20 B). It implies that SFI5 needs the CaM-binding activity to inhibit flg22-induced oxidative burst and that the two basic lysine

residues may play a more critical role in the binding to CaM than the two hydrophobic amino acids.

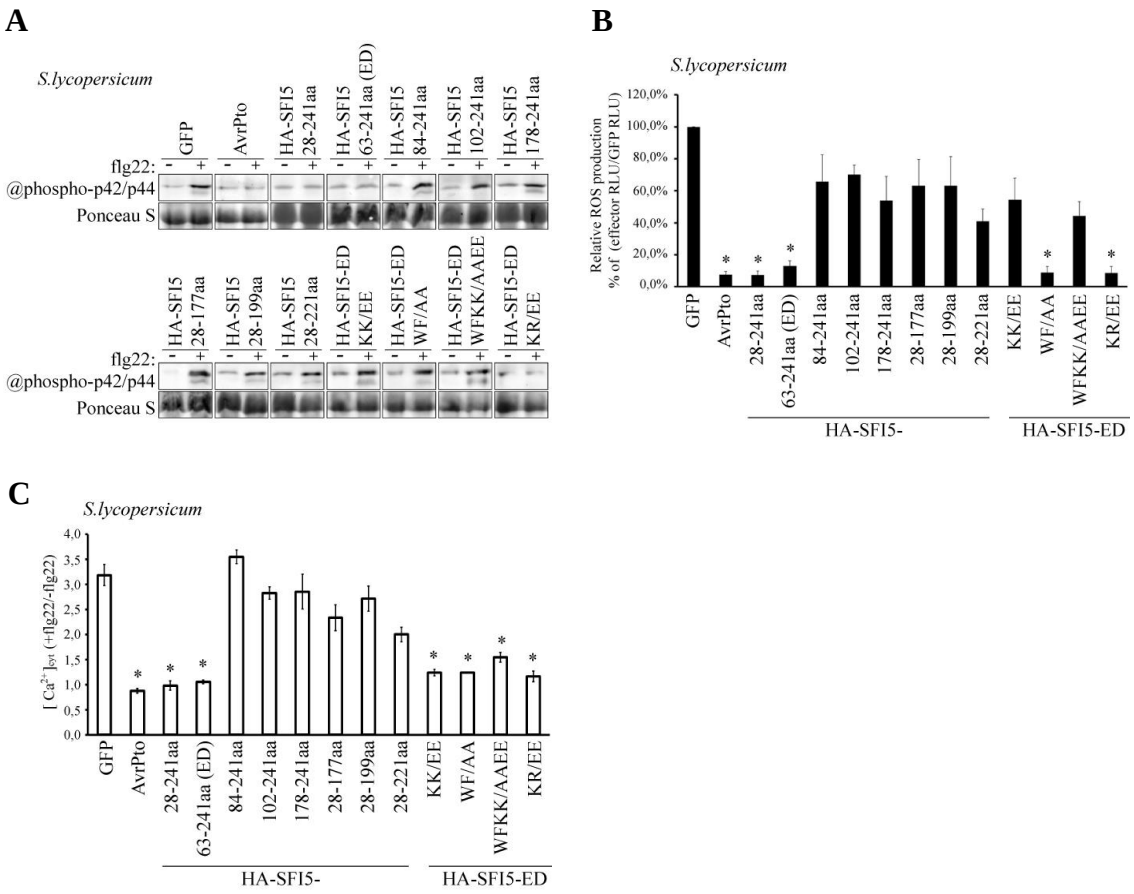

Figure 3-20. Suppression of flg22-triggered MAP kinase, ROS and Ca^{2+} burst by HA-SFI5 deletion and point mutants.

(A) *S. lycopersicum* protoplasts expressing mutated HA-SFI5 variants were collected 20 minutes after flg22 treatment (+) or without flg22 treatment (-), and the phosphorylated MAP kinases were detected by immunobloting with the antibody raised against phosphorylated MAP kinase p44/p42. Ponceau S staining is shown as a loading control. **(B)** The oxidative burst in *S. lycopersicum* protoplasts expressing mutated HA-SFI5 variants was represented in percentage of the total photon counts measured between 6-20 minutes after flg22 treatment of the GFP control, set to 100 %. **(C)** flg22-triggered Ca^{2+} burst was measured in tomato protoplasts co-expressing mutated HA-SFI5 variants, Ca^{2+}-sensitive Aqueorin and GUS. For each data set, cytosolic Ca^{2+} level was assessed by calculating the sum of photon counts 5-15 minutes with or without flg22 treatment (+/-flg22) and the ratio was normalized to the internal GUS activities ($[Ca^{2+}]$cyt (+flg22/-flg22)). GFP and AvrPto served respectively as negative and positive control for suppression of MAPK activation, ROS and Ca^{2+} burst by flg22. The result in (B) is representative of at least three independent experiments. Data in (C) and (D) represent the mean ± SEM from four independent experiments, for each of which three technical replicates were carried out. *, p-value < 0.05 by one-way ANOVA followed by Dunnett's multiple comparison test.

Ca^{2+} is crucial for SFI5 binding to CaM but also for MAMP-mediated intracellular signaling and activation of immune responses. The binding of flg22 to its receptor leads to a rapid increase in the concentration of cytosolic Ca^{2+} but obviously, this increase is not required for the association of SFI5 with CaM (Figure 3-15 C). In order to investigate the effect of SFI5 on the flg22-mediated Ca^{2+} burst in tomato protoplasts, the aequorin luminescence-based technology provides a mean to accurately measure the change of cytosolic Ca^{2+} level (Knight et al., 1991; Knight et al., 1993). The two SFI5 variants containing an intact effector domain (HA-SFI5 28-241aa and HA-SFI5 63-241aa) consistently suppressed the Ca^{2+} burst compared to the GFP control, while the other N- and C-terminal deletion mutants failed to do so (Figure 3-20 C). Unexpectedly, all the site-point mutants that are deficient in interaction with CaM were not significantly affected in their capability to subvert the Ca^{2+} burst, although HA-SFI5 ED-WFKK/AAEE was less severe (Figure 3-20 C). A possible explanation for this observation is that CaM binding is not required for the suppression of the Ca^{2+} burst and that the C-terminal domain is involved in binding with other proteins than CaM to block Ca^{2+} signaling.

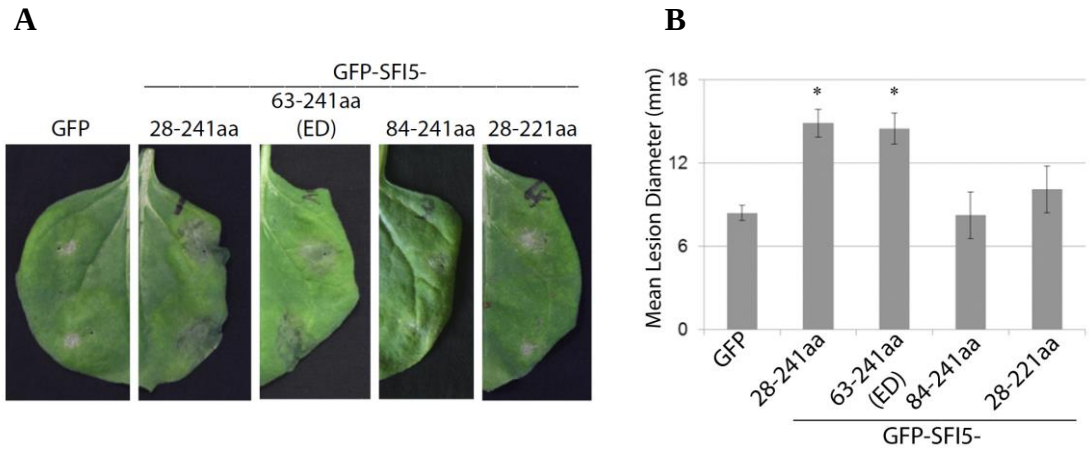

Figure 3-21. N-terminal and CaM-binding domain deletion in SFI5 abolish growth of *P. infestans* in *N. benthamiana*.

N-terminal or C-terminal deletion variants of SFI5 and empty vector (GFP) were transiently expressed via agro-infiltration in one half of a *N. benthamiana* leaf, respectively. After 24h, the infiltrated leaves were inoculated with *P. infestans*. Typical disease development symptoms **(A)** and mean lesion diameter **(B)** were measured on 7 days post-inoculation. Results are mean values ± SEM from three biological replicates, each of which used 24 leaves for inoculation per construct Significant difference (*, p-value < 0.01) in lesion size compared to empty vector control was determined by one-way ANOVA.

We have shown in 3.1.7 that the suppression of early events of MTI signaling by SFI5 contributes to the virulence of *P. infestans*. In order to determine the role of the N-terminal

and CaM binding domains for the virulence function of SFI5, we further tested, in collaboration with H. McLellan, JHI Dundee, UK, two GFP-SFI5 variants with a N-terminal deletion (GFP-SFI5 63-241 aa and GFP-SFI5 84-241 aa) and one with a C-terminal deletion (GFP-SFI5 28-221 aa) in patho-assays conducted with *P. infestans* in *N. benthamiana*. Transient expression of GFP-SFI5 84-241aa or 28-221 aa did not improve the susceptibility to *P. infestans* since we observed similar values of lesion size (~ 9 mm) than with the GFP control (Figure 3-21). GFP-SFI5 63-241 aa promoted *P. infestans* growth to the same level than GFP-SFI5 28-241 aa (~ 15 mm) which was used as a positive control (Chapter 3.1.7.) (Figure 3-21). These results indicate that there is a correlation between CaM binding, suppression of early MTI signaling and virulence function of SFI5. In addition, another domain of unknown function, located at the N-terminal part of SFI5 is equally required for the activity of SFI5.

3.2.7. A predicted ATP/GTP-binding motif at the N-terminal of SFI5 is also important for suppression of MTI signaling

Structure-function analysis have shown that, in addition of the C-terminal CaM binding domain, another domain within SFI5 that comprises the amino acid residues between Phe^{63} and Lys^{84} is essential for the suppression of the flg22-dependent immune responses and for supporting pathogen's growth on the host. Based on an online analysis tool used for motif scanning (http://myhits.isb-sib.ch/cgi-bin/motif_scan), a predicted ATP/GTP-binding site motif (P-loop) was found in this region and its significance was examined by replacement of the conserved lysine residue at position 82 with alanine (SFI5 ED-K82A). We also included in this analysis a mutant in which a predicted phosphorylated threonine residue at position 70, outside the P-loop motif, was replaced by alanine (SFI5 ED-T70A) (Figure 3-22 A).

Subcellular localization studies and pull-down assays showed that these two mutations did not affect the PM localization and interaction with SlCaM3/4/5 of SFI5 (Figure 3-22 B and C). However, the Lys^{82} residue revealed to be crucial for the inhibition of *pFRK1-Luc* and MAPK activation, ROS burst and Ca^{2+} influx triggered by flg22, while the SFI5 ED-T70A mutant acted similar to the SFI5 ED control (Figure 3-23, A, B, C and D). These results suggest that SFI5 may be an ATP/GTP-binding protein and that an intact P-loop motif is essential for its function.

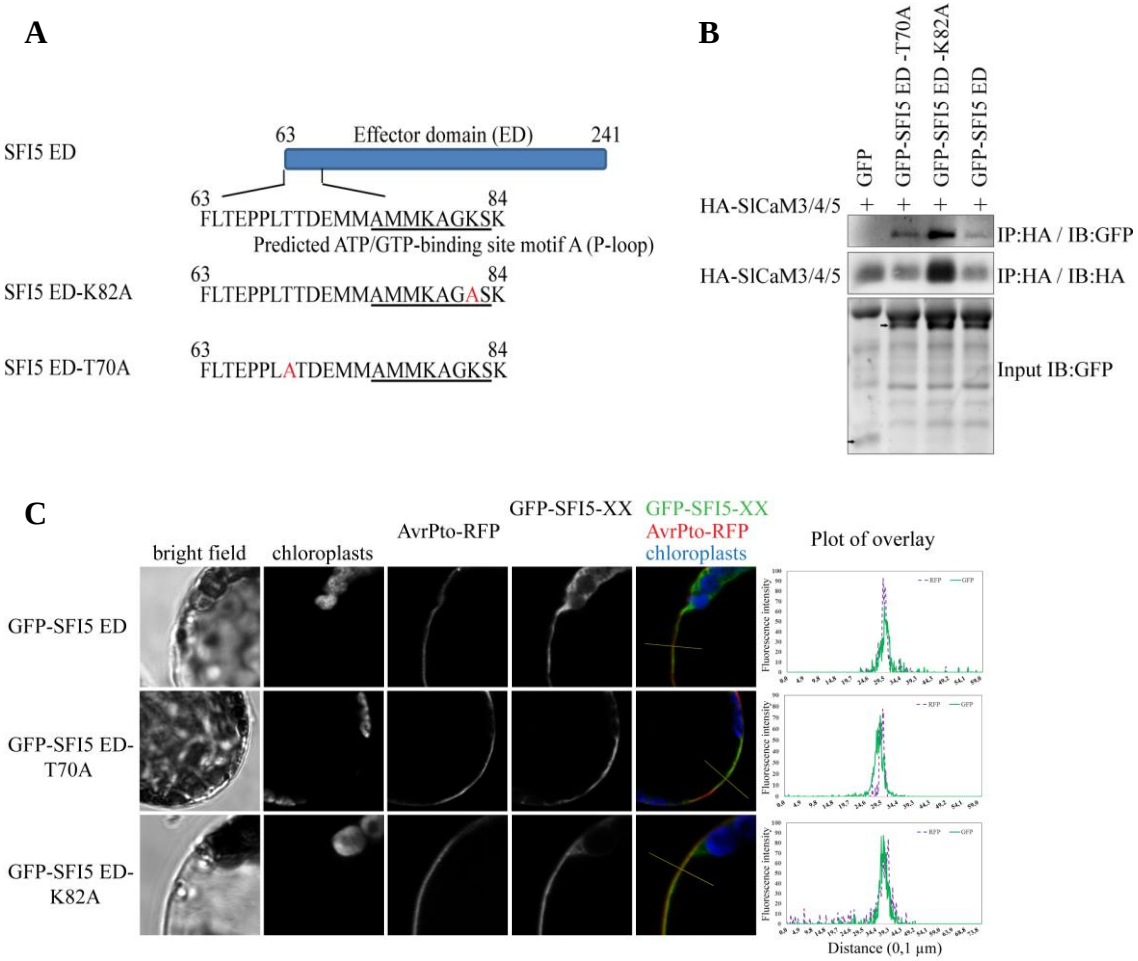

Figure 3-22. The predicted N-terminal ATP/GTP-binding motif of SFI5 is not critical for CaM binding and PM localization.

(A) A schematic view of SFI5 effector domain (SFI5 ED) highlighting the predicted ATP/GTP-binding site motif. Numbers indicate positions of the amino acid residues in the sequence of the full-length protein. Site-directed mutagenesis of the putative ATP/GTP-binding site motif was performed by replacing the conserved lysine residue at position 82 with alanine, (SFI5 ED K82A). The putative phosphorylation site at Thr70 was also mutated through replacement with Ala. **(B)** *S. lycopersicum* protoplasts co-expressing mutated GFP-SFI5 ED variants and HA-SlCaM3/4/5 were co-immunoprecipitated using anti-HA antibody coupled to agarose beads and immunodetection was performed using anti-HA or anti-GFP antibodies. Signals corresponding to GFP or GFP fusion proteins are indicated by arrows. **(C)** *S.lycopersicum* protoplasts co-expressing GFP-tagged SFI5 ED, SFI5 ED-T70A or SFI5 ED-K82A and C-terminally RFP-tagged AvrPto (AvrPto-GFP) were monitored using confocal microscopy. Confocal images were taken 12 hours after transfection and show optical sections of bright-field, chloroplast, RFP and GFP fluorescence as indicated. Merged fluorescence images between GFP (green), RFP (red) and chloroplast (blue) fluorescence were created and ImageJ software was used to analyze signal intensity of GFP and RFP fluorescence along the indicated distance (yellow line) from intracellular to extracellular in the overlay picture.

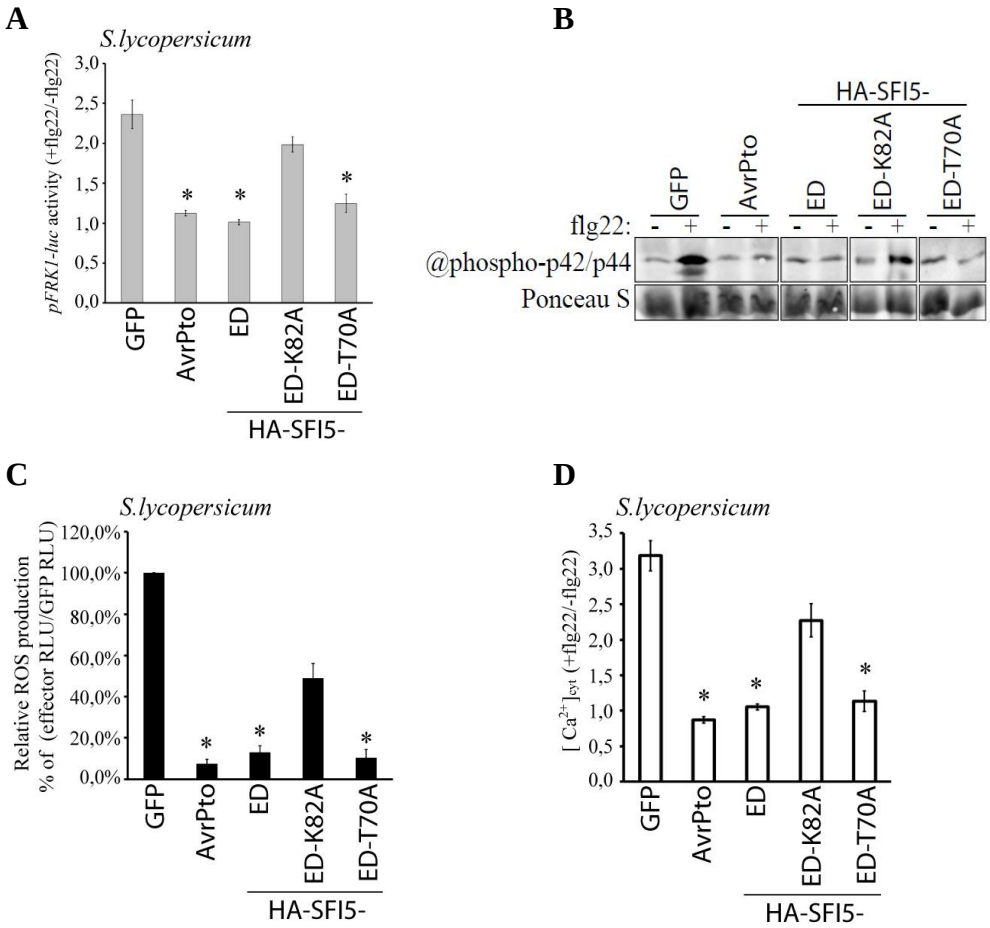

Figure 3-23. The predicted N-terminal ATP/GTP-binding motif of SFI5 is required for the inhibition of early flg22-induced immune responses *in S. lycopersicum* protoplasts.

(A) Reporter gene assay in protoplasts co-expressing the point mutant variants of SFI5 (GFP-SFI5 ED-K80A and GFP-SFI5 ED-T70A) with the two reporter constructs *pFRK1-Luc* and *pUBQ10-GUS*. The luciferase activity from samples treated with flg22 for 3 hours was compared to the untreated samples and the internal GUS activities were used for normalization. **(B)** Endogenous MAPK activation assay for the point mutant variants of SFI5 (GFP-SFI5 ED-K80A and GFP-SFI5 ED-T70A). Protoplasts were collected 20 minutes after flg22 treatment (+) or without flg22 treatment (-). Total proteins were immunoblotted and activated MAP kinases were detected using the p42/p44 antibody. Ponceau S staining served as a loading control. The result is representative of three independent experiments. **(C)** Oxidative burst assay in protoplasts expressing WT and mutated HA-SFI5 ED variants. The graph shows percentage relative to the total photon counts measured between 6-20 minutes after flg22 treatment of the GFP control, set to 100%. **(D)** flg22-triggered Ca^{2+} burst was measured in tomato protoplasts co-expressing WT or mutated HA-SFI5 ED variants, Ca^{2+}-sensitive aqueorin and GUS. For each data set, cytosolic Ca^{2+} level was assessed by calculating the sum of photon counts 5-15 minutes with or without flg22 treatment (+/-flg22) and the ratio was normalized to the internal GUS activities ($[Ca^{2+}]$cyt (+flg22/-flg22)). GFP and AvrPto served respectively as negative and positive control for suppression of MAPK and *pFRK1-Luc* activation, ROS and Ca^{2+} burst by flg22. Data in **(A), (C)** and (**D**) represent the mean ± SEM from four independent experiments, for each of which three technical replicates were carried out. *, p-value < 0.05 by one-way ANOVA followed by Dunnett's multiple comparison test.

3.2.8. Does SFI5 inhibit CaM function?

Since the CaM binding is correlated with the MTI-suppressing ability of SFI5 and based on the knowledge that CaMs play important roles in plant immune responses, a direct action mode by which SFI5 interferes with the function of the CaMs is conceivable. Alternatively, it is also possible that CaM is not the operative target of SFI5 but the interaction serves to activate SFI5 and confers the ability to target components that are critical for MTI. .

To address the hypothesis whether CaMs are inhibited by SFI5, we measured whether tomato protoplasts overexpressing SlCaM3/4/5 were capable to override the MTI-suppressing effect of SFI5. We first verified that the overexpression of GFP-SlCaM3/4/5 alone had no effect on the flg22-triggered ROS burst and MAPK activation (Figure 3-24 A and B). The co-expression of GFP-SlCaM3/4/5 and HA-SFI5 28-241 also did not alleviate the suppression of flg22-induced ROS production and MAPK activation, which was identical to protoplasts expressing HA-SFI5 28-241aa alone (Figure 3-24 A and B). Western blot analysis indicated that GFP-SlCaM3/4/5 expression is not influenced by SFI5 and a degradation of CaM as consequence of SFI5 action is very unlikely to occur (Figure 3-24 C). This result suggests that SFI5 does not interfere with the function of CaM in positively regulating MTI.

To build up more evidence that would support the assumption that SFI5 binding to CaM does not inhibit directly MTI signaling, we performed competition experiments in tomato protoplasts by co-expressing an active (HA-SFI5 28-241 aa) and an inactive (HA-SFI5 178-241 aa) SFI5 variant, both having been shown to associate with CaM (Figure 3-17 A, Figure 3-19 B). Dose-response analyses by increasing the HA-SFI5 178-241 aa / HA-SFI5 28-241 aa ratio showed that a 10:1 ratio was sufficient to antagonize the suppressing effect on *pFRK1-Luc* activity of the active SFI5 variant, in contrast to the control experiment with a GFP / HA-SFI5 28-241 aa ratio of 10:1 (Figure 3-24 D). These results suggest that the inactive CaM-binding variant, SFI5 178-241aa, competes with the active SFI5 28-241 aa for the interaction with CaM, but that this interaction does not block the function of CaM, which again, is another indirect proof that SFI5 is not an inhibitor of CaM but needs to associate with CaM to become able to suppress MTI signaling.

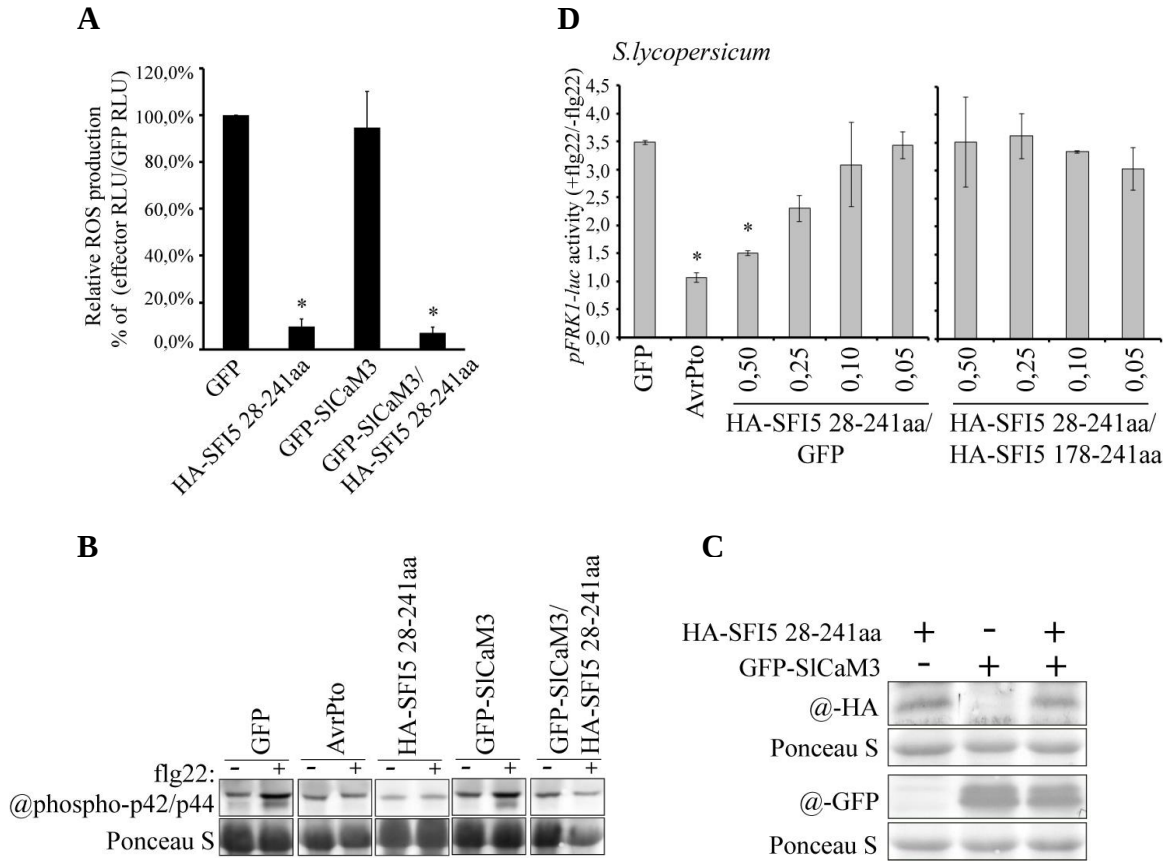

Figure 3-24. Overexpression of SlCaM3/4/5 did not alter SFI5 activities on suppressing flg22-triggered immune responses in *S.lycopersicum*.

(A) ROS burst was measured in *S.lycopersicum* protoplasts single-transfected with HA-SFI5 28-241aa or GFP-SlCaM3/4/5, or co-transfected with GFP-SlCaM3/4/5 and HA-SFI5 28-241aa. The graph shows relative ROS production represented in percentage of the total photon counts measured between 6-20 minutes after flg22 treatment of the GFP control, set to 100 %. **(B)** MAPK activation was detected in *S. lycopersicum* protoplasts expressing HA-SFI5 28-241aa or GFP-SlCaM3/4/5, or co-expressing GFP-SlCaM3/4/5 and HA-SFI5 28-241aa. Protoplast samples were collected 20 minutes after flg22 treatment (+) or without flg22 treatment (-). Total extracted proteins were immunoblotted and activated MAP kinases were detected using the p42/p44 antibody. Ponceau S staining served as a loading control. This result is representative of three independent experiments. **(C)** Immunoblot analysis of single-expression of HA-SFI5 28-241aa or GFP-SlCaM3/4/5 as well as co-expression of them in *S.lycopersicum* protoplasts. Ponceau S staining served as a loading control. **(D)** Reporter gene assay in *S. lycopersicum* protoplasts transformed with increasing amount 0,05-0,50 µg/100 µl protoplasts) of the plasmid construct expressing HA-SFI5 28-241aa together with 5 µg/100 µl protoplasts of the construct expressing GFP or HA-SFI5 178-241aa and the two reporter constructs *pFRK1-Luc* and *pUBQ10-GUS.* The promoter activity was presented by calculating the ratio of flg22-induced luciferase activity relative to the untreated sample, which was normalized to the internal GUS activities (*pFRK1-Luc* activity +flg22/−flg22). GFP and AvrPto served respectively as negative and positive control for suppression of ROS burst as well as MAPK and *pFRK1-Luc* activation by flg22. The mean values ± SEM in **(A)** and **(D)** were obtained from at least three independent experiments, for each of which three technical replicates were carried out. *, p-value < 0.05 by one-way ANOVA followed by Dunnett's multiple comparison test.

4. Discussion

Phytopthora spp form a group of pathogens that are adapted to cause disease in many crop plants. An important criterium for host colonization is the ability of the pathogen to turn down MAMP-triggered immunity (MTI), which is the most common and durable form of resistance in nature, characterized by a high genetic stability. The improvement of our fundamental knowledge about the biology of the pathogen requires better characterization of the molecular determinants and biochemical mechanisms of effector-triggered susceptibility with the objective to understand how these virulence factors function individually and in a system and to decipher at long-term the evolutionary forces that are shaping plant-Phytophthora interaction in terms of host adaptation and host specificity.

The availability of genome sequences for different *Phytophthora spp* is a first step toward addressing these questions. RXLR effectors form the largest family of secreted proteins with proven virulence function. It is in this context that we have chosen to investigate the effect of RXLR effectors from *P. infestans* (PiRXLR), the causal agent of potato and tomato late blight, on the earliest stages of MTI signaling. As an experimental tool, we established a tomato protoplast transient expression system and diverse bio-assays that measure immunity-associated responses in order to be able to perform a functional screen in a medium/high-throughput manner. 8 out of 33 PiRXLR effectors were identified as suppressors of the early immune responses induced by flg22. Among them, three effectors (SFI5, SFI6 and SFI7) with different degrees of plasma membrane association appear to block MAMP signaling at or upstream of MAPKKK activation. Two of them (SFI5 and SFI7) did not affect the programmed-cell death (PCD)-related MAPK signal transduction associated with effector-triggered immunity (ETI). The other five effectors act downstream of the MAPK cascades, three of them (SFI1, SFI2 and SFI8/AVRblb2) also subverting flg22-induced MAMP marker gene expression in the non-host plant Arabidopsis. These results demonstrate that *P. infestans* employs multiple effectors, which act redundantly on interrupting different steps of early MTI signal transduction. In a more detailed study, one of these effectors, SFI5, is shown to interact at its C-termini with host calmodulin (CaM) in a Ca^{2+}-dependent manner. The CaM-binding site has been proved to be important for plasma membrane (PM) localization, suppression of MAMP-mediated signaling and full virulence function of SFI5. Additionally, we have also identified a putative ATP/GTP-binding motif at the N-terminus that is required for MTI suppression and virulence activity of SFI5 but not for the PM localization.

Data generated in this study will be further discussed in order to integrate them into the

current knowledge of plant-microbe interactions and for a better understanding of the relevance of the MTI suppressing RXLR effectors complement of *P. infestans* in host colonization.

4.1. Advantages/disadvantages in using the protoplast system to study flg22-induced early immune responses

It is complicated and time-consuming to characterize the > 500 predicted PiRXLR effectors by reverse and forward genetic methods. Therefore, the development of medium/high throughput approaches to explore their function in plants is very important. The tomato protoplast system allows to study up to 24 effectors/day making a large screen feasible in a reasonable amount of time. Another advantage of using a method based on DNA-transformation of protoplasts is that it is a microorganism-free effector delivery system without any risk of interference on MTI signaling due to the presence of an undesired source of effectors and MAMPs. Although this assay is relatively convenient, it also suffers from some drawbacks. For instance, the ectopic expression of effectors might cause mis-localization inside host cells and overcome certain steps of maturation or post-translational modifications occurring through haustorial delivery and necessary for proper function and targeting of the RXLR effector (Fabro et al., 2011). Other major drawbacks of the protoplast system are the limitations to study late-induced defense responses, cell wall-associated responses such as callose deposition or organ-specific responses. Nevertheless, it is not far-reaching to conclude that early events of MTI are qualitatively conserved between protoplasts and plants and therefore, it justifies our choice to select this approach to perform the functional screen with the PiRXLR effectors.

The use of flg22 as the MAMP to induce MTI signaling in our protoplast assays might be drawn into question since *Phytophthora spp* do not have flagellin. This choice was dictated by the optic to perform a comparative analysis with PiRXLR effectors on a pathway that is highly conserved in both host (tomato) and non-host (Arabidopsis) plants of *P. infestans*, thus our aim was to investigate the effectors' ability to suppress a generic defense pathway and not the role of the FLS2 receptor in defense to oomycetes. The principle of bacterial effector-detector vector (EDV) systems, now being widely employed to study the impact of fungal and oomycete effectors in various pathosystems on late phenotype such as callose deposition, is based upon the effectors' abilities to suppress generic pathways triggered by bacterial MAMPs (Sohn et al., 2007; Fabro et al., 2011). To date, only few MAMPs derived from oomycetes have been characterized, all of them with limited plant recognition specificities.

Pep13, the antigenic peptide motif of *Phytophthora spp* transglutaminase, induces immune responses in potato and parsley but is not active in other plant species that have been tested yet (Brunner et al., 2002; Halim et al., 2004). Elicitins, including INF1 used in this work, are a group of elicitors that are sensed in *Nicotianae* and to some extent in wild Solanum species but not in cultivated tomato or potato species or Arabidopsis (Vleeshouwers et al., 2006). The recently identified nlp20 peptide from the Necrosis and Ethylene-inducing like Proteins (NLPs), widely distributed among oomycetes, is only recognized by Arabidopsis and related *Brassicacea* species (Bohm et al., 2014; Oome et al., 2014). The receptors of nlp20 and elicitins, AtNLP23 (Albert et al., 2015) and StELR (Du et al., 2015) , respectively, belong to the LRR-RLP type and differ structurally from the LRR-RLK class of receptors, comprising FLS2, through the absence of intracellular kinase domain and recruitment of the LRR-RLK adaptor SOBIR1, in addition of BAK1, for proper signal transduction (Gust and Felix, 2014). Accordingly, it is anticipated that the protoplast system could be employed for dissecting other MAMP-inducible signal transduction pathways, triggered by different classes of cell surface-located receptors. Experiments in tomato protoplasts exposed to chitin or xylanase from *T. reesei* have shown that SFI5 also attenuates the induction of a Ca^{2+} burst and MAPK activation, triggered by their cognate receptors, presumably a LysM-RLK or LysM-RLP in the case of chitin and LRR-RLP (SlEix2) for the xylanase, whereas AvrPto only blocked xylanase but not chitin signaling (data not shown). By identifying and characterizing potential PiRXLR effectors that affect other MAMP signaling pathways we have the possibility to uncover novel MTI-related components. This apsect would be beneficial and facilitate the study of the interaction between solanaceous plants and *Phytophthora spp*.

In parallel to studying the relation of PiRXLR effectors with MTI, it is also imaginable to exploit the protoplast system for the identification of novel sources of resistance (R) genes. *Phytophthora* pest management has become a severe problem in that R-mediated host resistance is rapidly overturned because of the high genetic diversity and high genome plasticity of *Phytophthora spp*. The European plant breeding industry is currently undergoing a transition that will make pathogen effector biology an essential component of the decision-making process during the breeding of disease resistance in food crops. The identification of PiRXLR effectors that are recognized during ETI (so-called AVR proteins), and uncovering the genetic variation that exists in these AVR proteins in natural *P. infestans* populations, offers the prospect for significant advances in plant breeding. Effector recognition by R proteins often culminates in a local PCD. Because PCD is readily detectable, PiRXLR effectors can be used as extremely efficient molecular markers to identify novel resistance

genes in protoplasts made from germplasm collections. Therefore, effector-based screening can replace pathogen screens that can be extremely time-consuming. In this perspective, we have performed preliminary experiments in protoplasts generated from tomato cultivars harboring the R protein Pto and transiently expressing AvrPto and observed a remarkable increase of cell death rate, resulting from ETI (data not shown). This result suggests that the protoplast system is fully operational, suitable to measure cell death as a read-out, and can be applied to screen for ETI-inducing PiRXLR effectors.

4.2. Defining the repertoire and function of MTI-suppressing PiRXLR effectors in host adaptation (and specificity)

It is generally admitted that the success of infection depends on the capability of the pathogen to produce a sufficient number of effectors to efficiently damp down the activation of MTI. Several groups have performed large-scale functional screens to identify oomycete effectors that block late responses to MAMPs. For instance, Fabro et al., (2011) used the EDV system to find out that 39 out of 64 RXLR effectors from *Hyaloperonospora arabidopsidis* promote *P. syringae* growth when transiently expressed in Arabidopsis, the natural host of *H. arabidopsidis*. The expression of a large majority of these 39 HaRXLR effectors was correlated with an increased suppression of callose deposition at the cell wall, a hallmark of late MTI responses (Fabro et al., 2011). In another work using the Agrobacterium-based transient expression system, more than half of 169 RXLR effectors form *Phytophthora sojae* were able to block the programmed cell death induced by the pro-apoptotic mouse protein BAX in *N. benthamiana* (Wang et al., 2011). 23 out of a selection of 43 PsRXLR effectors suppressing BAX-induced cell death were also able to suppress INF1-triggered cell death (Wang et al., 2011). In an identical approach, 2 out of 32 PiRXLR effectors emerged as suppressors of INF1-mediated cell death in *N. benthamiana* (Oh et al., 2014). It was assumed that effectors from oomycetes, and thus the pathogen themselves, are able to block signal transduction pathways, as do bacteria, at the level of MAP kinase activation and initial transcriptional changes. But our work, with the identification of approximate 25 % of PiRXLR effector candidates impairing early MTI responses in tomato protoplasts, is the first formal demonstration that this is indeed the case and is an essential platform for future analysis of these effectors to see whether they act on the same host proteins and in the same way as bacterial type III effectors.

One of our principal goals consisted of identifying and ascribing functions to PiRXLR effector proteins that interfere with early plant defense responses upon MAMP sensing.

Interestingly, SFI5 and SFI8/AVRblb2 but not AVR3a or PITG_14736/PexRD8 were among the effectors suppressing flg22-induced *pFRK1-Luc* activation. This is apparently in contrast with the results obtained from the screen for suppression of cell death mediated by INF1 in *N. benthamiana,* in which AVR3a and PITG_14736/PexRD8 but not SFI5 or SFI8/AVRblb2 acted as a suppressor (Figure 3-8 A) (Bos et al., 2006; Bos et al., 2009; Oh et al., 2009). One possible explanation would be that AVR3a and PITG_14736/PexRD8 specifically target the signaling cascade leading to INF1-mediated cell death or hit components located downstream of early MAMP signal transduction, like the targeting of the host ubiquitin proteasome system by AVR3a (Bos et al., 2010). The opposite may be true for SFI5 and SFI8/AVRblb2. Currently, we cannot test these hypotheses for several reasons: 1) INF1 promotes cell death in *N. benthamiana* but not in Arabidopsis or tomato; 2) flg22 treatment does not induce cell death in Arabidopsis or tomato protoplasts) there is no known MAMP that induces an HR-like cell death in Arabidopsis protoplasts. Moreover, SFI7 suppresses flg22/FLS2-mediated signal transduction and attenuates INF1-mediated PCD, but not Cf-4-mediated PCD, whereas AVR3a attenuates both INF1-mediated and Cf-4-mediated PCD. Evidence is thus emerging of PiRXLR effectors with overlapping functions at the phenotypic level, that are likely mediated by distinct modes of action at the mechanistic level.

SFI8, a member of the AVRblb2 family, appears as a suppressor of early MTI responses in our screen, which might provide a novel insight into the function of AVRblb2 and AVRblb2-related effectors. In previous studies, AVRblb2 was identified as an avirulence factor recognized by resistance protein Rpi-blb2 and demonstrated to interfere with plant immunity by preventing secretion of C14, a defense-related apoplastic protease (Oh et al., 2009; Bozkurt et al., 2011). The AVRblb2 family was found to be highly variable and the amino acid at position 69 is critical for the avirulence function (Oh et al., 2009). SFI8 carrying a phenylalanine at position 69 is predicted to evade activation of Rpi-blb2 but putative avirulent variants of the AVRblb2 family with an isoleucine or alanine residue at position 69 also repressed flg22-elicted reporter gene activation in tomato protoplasts (data not shown), suggesting that the interference with MAMP signal transduction might be a common virulence function of the AVRblb2 family. It would be interesting to check if all these AVRblb2 variants possess the ability to perturb C14 trafficking and whether C14 and other papain-like cystein proteases are involved in MAMP signaling. Nevertheless, subcellular localization studies revealed that SFI8 mainly accumulates in the cytosol and the nucleus (Figure 3-10), which differs from AVRblb2, exclusively distributed at the host plasma membrane (Bozkurt et al., 2011). This apparent discrepancy implies that members of the

AVRblb2 family may display distinct or multiple cellular activity, which sustains a recent idea that the polymorphism within the AVRblb2 family helps *P. infestants* to infect diverse solanaceous plants (Oliva et al., 2015).

The main achievement with the protoplast system was the identification of PiRXLR effectors that suppress early MTI signalling involving ROS production, activation of MAP kinase cascades and transcriptional re-programming of genes associated with immunity. However, the protoplast system does not permit to assess the importance of PiRXLR effectors in the adaptation of *P. infestans* to its host. The ectopic expression of 7/8 MTI-suppressing SFI effectors in *N. benthamiana* promoted the growth of *P. infestans* during infection. These results suggest a strong correlation between the MTI-suppressing potential of PiRXLR effectors and successful disease development. The protoplast system revealed that about 1/4 of the PiRXLR effectors interfere with early events of the signal transduction cascade initiated by flg22. Nevertheless, and as stated previously with AVR3a and PITG_14736/PexRD8, more effectors that contribute to pathogenicity might emerge as MTI suppressors by affecting late MAMP-induced responses or alternative signaling branches. Recently, several PiRXLR effectors figuring in our list of tested candidates have been demonstrated to contribute to *P. infestans* growth, but none of them showed MTI-suppressing activity in our assay (PITG_03192/PexRD28 (McLellan et al., 2013), PITG_04089/PexRD41 (Wang et al., 2015) and PITG_04314/PexRD24 (Boevink et al., 2016)). Ultimately, gene gain- and loss-of function experiments in *P. infestans* would further confirm the importance of the SFI1-8 effectors in host adaptation. Because of the technical difficulty to realize these experiments, genetic manipulation of *P. infestans* could be performed in tight collaboration with the lab of P. Birch at JHI in Dundee, UK. Stable silencing of SFI1-8, either individually or multiple, could be achieved using RNAi-mediated post-transcriptional gene silencing or a CRISPR/Cas-based genome editing method, recently adapted to *Phytophthora sojae* (Personal communication B. Tyler, Oregon State University, USA) and tested for virulence on solanaceous host plant species (tomato, potato and *N. benthamiana*). In a complementary gain-of-function approach, individual effectors or combinations of SFI1-8 could be expressed in a heterologous *Phytophthora spp.* genetic background to see whether they increase the virulence of these transgenic strains. However, it should be noticed that the SFI effectors studied here display functional redundancy on inhibiting early flg22/FLS2 signaling events and therefore, they may have a limited impact on pathogen virulence. Nevertheless, silencing experiments with some PiRXLR effectors, such as AVR3a (Bos et al., 2010) and PITG_03192/PexRD28 (McLellan et al., 2013) resulted in compromised pathogenicity of *P.*

infestans, indicating that the function of several effectors is not redundant and indispensible for full virulence.

In summary, we have demonstrated that the effector repertoire of *P. infestans* contains a comparatively high degree of redundancy in suppressing different steps of early MTI signal transduction and defense gene activation (Figure 4-1). A question that needs to be addressed in the future is why such functional redundancy is necessary or has been selected for and why *Phytophthora spp*, in contrast to phytopathogenic bacteria, have evolved such large repertoire of RXLR effectors to confound the host immune system.

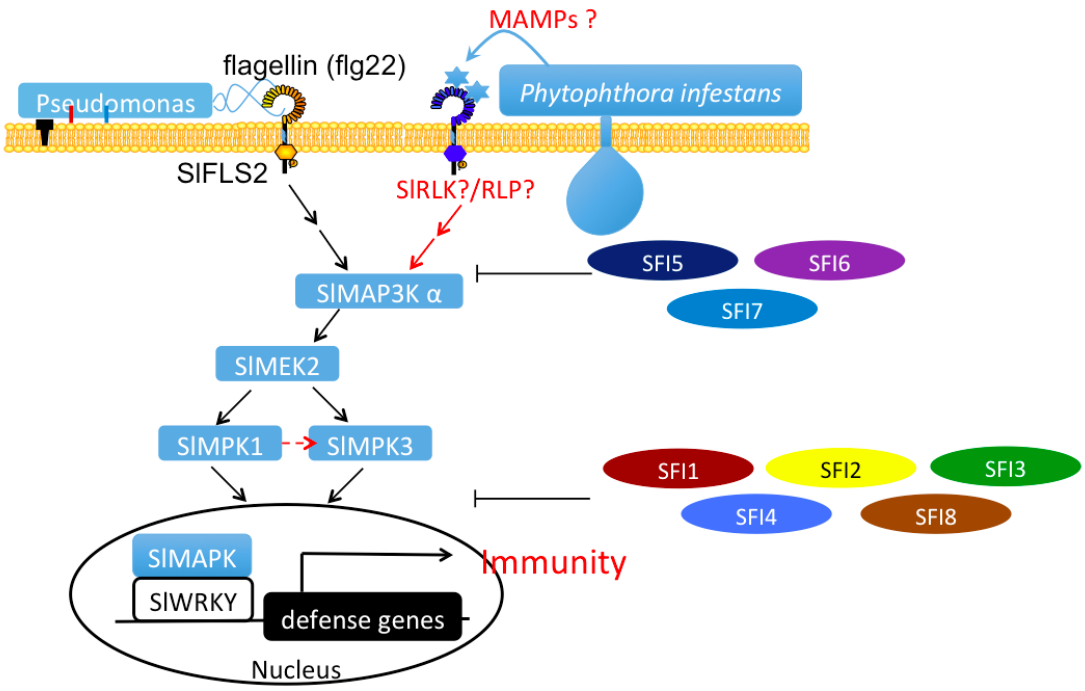

Figure 4-1. SFI1-8 effectors act at different steps to suppress early MTI signaling in tomato cells.

MTI signal transduction and interfering SFI effectors (in colored boxes) are depicted. See main text for additional details. Abbreviations used in the figure: MAMPs, microbe-associated molecular pattens; SlFLS2, *Solanum lycopersicum* FLS2; SlRLK?/RLP?, unknown *Solanum lycopersicum* MAMP receptor-like kinase or receptor-like protein; SlMAP3Kα, *Solanum lycopersicum* MAP kinase kinase kinase α; SlMEK2, *Solanum lycopersicum* MEK2; SlMPK1, *Solanum lycopersicum* MAP kinase 1; SlMPK3, *Solanum lycopersicum* MAP kinase 3; SlWRKY, *Solanum lycopersicum* WRKY transcriptional factors.

4.3. MTI-suppressing PiRXLR effectors in non-adapted plant species

It is proposed that most effectors implicated in manipulation of host immunity are under strong positive selection and co-evolved with their targets during host-pathogen interaction

(Kamoun, 2007; Win et al., 2007), while in non-host plants, effectors fail to efficiently interfere with MTI because they are not able to interact and to manipulate components of the signaling pathway. Accordingly, P. Schulze-Lefert and R. Panstruga recently provided a molecular evolutionary concept that connects non-host resistance and pathogen host range (Schulze-Lefert and Panstruga, 2011). The concept predicts that MTI prevails in non-host plant species that are distantly related to the plant host species of a given pathogen (Figure 4-2). So far, there are very little experimental evidence supporting or confirming this concept. Our results, to some extent, support the hypothesis that failure to suppress MTI is likely to contribute to non-host resistance to *P. infestans* in Arabidopsis. Only SFI1, SFI2 and SFI8/AVRblb2 but not SFI3-SFI7 function in Arabidopsis. This result is in line with a comparative assay showing that only 13 out of 39 HaRXLR identified as enhancers for *P. syringae* growth in Arabidopsis promoted bacterial disease development in turnip (*Brassica rapa*), which is closely related to Arabidopsis but a non-host of *H. arabidopsidis* (Fabro et al., 2011). The authors did not provide molecular evidence for the influence of these RXLR effectors on MTI but again, it is very likely that failure to block MTI plays a significant role in the non-adaptation of *P. syringae* to turnip.

More recently, Antonovics et al. (2013) preferred to use the term of non-evolved resistance, suggesting that failure of infection on a non-host plant may be the result of an incidental by-product of ongoing pathogen evolution by specialization on its operative host (Antonovics et al., 2013). In concordance with this theory, Dong et al. (2014) recently reported the biochemical specialization of two orthologous protease inhibitors from *P. infestans* and *P. mirabilis* that target only the cognate proteases of their respective hosts, tomato and *M. jalapa*. PiEPIC1 from *P. infestans* was able to inhibit activity of the defense-related protease (RCR3) from tomato and potato, while PmEPIC1, the *P. mirabilis* homologue of PiEPIC1, specially suppresses RCR3-like protease (MRP2) activity in *M. jalapa*. In both cases, the absence of inhibition by protease inhibitors originated from non-adapted *Phytophthora* species was related to single amino acid polymorphisms (Dong et al., 2014). Although, the authors did not show whether the interaction between the protease and its inhibitor was important for host adaptation and specificity, this study provides a molecular fundament to the non-evolved resistance hypothesis. In a similar way, we could imagine that the failure of SFI5-SFI7 to block MAPK activation by flg22 in Arabidopsis is caused by a lack of interaction with components of MTI signaling. In the case of SFI5, the interaction with CaM has proven to be insufficient to explain the absence of effect on MAP kinase activation since SFI5 interacts with CaMs from both tomato and Arabidopsis. As part of existing studies in the P. Birch and

our groups, a screen of a potato - *P. infestans* interaction Yeast-two-Hybrid library and the co-immunoprecipitation assays in tomato protoplasts revealed additional candidate host targets for SFI5 with presumed or demonstrated function in regulating immunity. Notably, two membrane-located kinase domain-containing proteins including a MAPKKKK and the malectin-like LRR-RLK IOS1 were identified. The interaction with IOS1 is of special interest, because this protein has been identified recently as a susceptibility factor in Arabidopsis to *H. arabidopsidis* by H. Keller from the "Interactions Plantes-Oomycètes" team at INRA Sophia Antipolis, France (Hok et al., 2011; Hok et al., 2014). Future work will consist to verify and confirm these interactions in tomato vs Arabidopsis, to explore the structure-function relationships of the effector/target pairs, to determine the biochemical consequences of these relationships for the host cells and eventually to provide an explanation for the hypothesized lack of interaction in the non-host plant.

Host jumps are considered to be major drivers of oomycete diversity and may become necessary for pathogen survival in response to biotope changes, for instance by culture rotation, when natural host populations in the pathogen's habitat are replaced by non-host plant species (Raffaele and Kamoun, 2012). By performing a comparative analysis in tomato and Arabidopsis, we found that the biological activity of some PiRXLR effectors e.g SF1, SFI2 and SFI8/AVRblb2 is not necessarily restricted to the source host of *P. infestans*, but is extended to plant species that are not natural hosts of the pathogen. Functional characterization of two homologous RXLR effectors from *H. arabidopsidis* and *P. sojae* also revealed that both were able to affect immune responses in soybean, *N. benthamiana* and Arabidopsis (Anderson et al., 2012). These results corroborate our conclusion that a core set of RXLR effectors is probably targeting proteins that are ubiquitous in all plant species and likely key players in regulating immunity. Accordingly, Mukhtar et al. and more recently, Weßling et al., postulated that an overlapping subset of host proteins, so-called hubs, are targeted by oomycete (*H. arabidopsidis*), bacterial, (*P. syringae*) and fungal (*Golovinomyces orontii*) effectors that have arisen independently through convergent evolution (Mukhtar et al., 2011; Wessling et al., 2014). Our attempt to identify protein interactors of SFI1, SFI2 and SFI8/AVRblb2 by performing IP experiments in Arabidopsis protoplasts failed to yield candidates of interest (data not shown). However, the nuclear localization of these effectors and the demonstrated correlation between localization and suppression of flg22-induced *pFRK1-Luc* activity in the case of SFI1, suggests that these effectors might directly interact with host plant DNA. Pathogenic bacteria of the genus *Xanthomonas* produce transcription activation-like (TAL) effectors that bind with a high specificity to promoters of host genes in

order to re-programme host cellular functions (Boch et al., 2009; Bogdanove et al., 2010).

In an effort to investigate the general contribution of SFI1, SFI2 and SFI8/AVRblb2 to Arabidopsis susceptibility, we tried to deliver them *in planta* utilizing the bacterial EDV system that has proven to work for RXLR effectors (Sohn et al., 2007; Fabro et al., 2011). However, the bacterial growth was not significantly enhanced in Arabidopsis Col-0 inoculated with *P. syringae* expressing the SFI effectors individually. The same tendency was observed with SFI effectors expressed in the less virulent *P. syringae* ΔCEL or ΔAvrPto / ΔAvrPtoB mutant strains (data not shown). One possible explanation would be that the tested SFI effectors and the T3 effectors in these *P. syringae* strains are playing redundant roles in dampening plant immunity, resulting in unobvious improvement in pathogenicity. Thus, the molecular basis of this manifestly broad-range activity requires further investigation.

To our surprise, we discovered that a set of 4 PiRXLR effectors, which has no impact on reporter gene activation in tomato, prevents flg22-triggered *pFRK1-Luc* expression in the non-host Arabidopsis (Figure 3-3). It is tempting to speculate that these RXLR effectors are preparing the terrain for *P. infestans* to adapt to a novel host. However, none of these effectors is capable of inhibiting flg22-induced MAP kinase activation or up-regulation of *FRK1* expression (Figure 3-4). Currently we cannot explain the reason of the suppression of reporter gene activation in Arabidopsis protoplasts but it becomes obvious that additional experiments should be designed to determine which and to what degree MAMP-activated post-transcriptional or translational processes are affected by these effectors. Given that in total 8 PiRXLR effectors were active in Arabidopsis protoplasts, the number may be sufficient to block early flg22-induced responses in Arabidopsis and therefore, we cannot state for now that PiRXLR effectors are more effective in suppressing MTI in tomato plants than in Arabidopsis. A systematic analysis of the whole repertoire of PiRXLR effectors on MTI signaling in both tomato and Arabidopsis including testing individual or combination of effectors and validation of the data generated in protoplasts by functional analysis *in planta* would be necessary to better understand how the expansion of host range is possible in *P. infestans.*

The molecular evolutionary concept also predicts that ETI becomes increasingly important in closely related non-host plant species and even critical, as we learned from ETI studies in the case of host-resistance. Interestingly, 7 HaRXLR effectors that promoted *P. syringae* growth in Arabidopsis had an opposite effect in turnip suggesting that they had activated ETI (Fabro et al., 2011). Recently, Agrobacterium-mediated transient expression of 54 *P. infestans* RXLR

effectors in different pepper cultivars has shown that multiple *R* gene-dependent recognition events could be the major determinant of the non-host resistance against *P. infestans* in pepper, a close relative of potato and tomato (Lee et al., 2014). None of the 8 SFI effectors in our study significantly promoted cell death in Arabidopsis protoplasts. A detailed analysis of the results obtained in the *pFRK1-Luc* assay indicates that only one PiRXLR effector (PITG_18670) among the 33 that we have tested stimulated reporter gene activation significantly above the empty vector control (Figure 3-3). One possible explanation would be that PITG_18670 targets a component of early flg22-induced signaling that is guarded by an R protein resulting in a much stronger activation of p*FRK1-Luc* as a consequence of the activation of the ETI pathway. Such a scenario is supported by the guarding of MPK4, which is activated upon flg22 treatment, by the R protein SUMM2 (Zhang et al., 2012). Further work is needed to determine the relative contributions of ETI versus failure to suppress MTI in Arabidopsis but also in non-host plants among the *Solanaceae*, such as pepper.

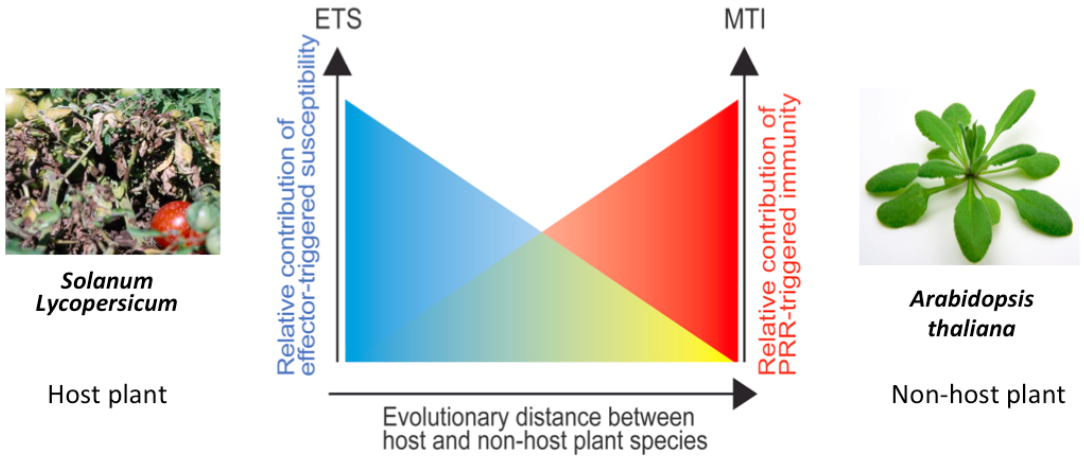

Figure 4-2. Relative contribution of MTI to non-host resistance.

The chart adapted from Schulze-Lefert and Panstruga (2011) illustrates the supposed relation between ETS (blue) and MTI (red) to non-host resistance against *P. infestans* as a function of the evolutionary distance of the authentic host plant species (*S. lycopersicum*) of that pathogen to an assumed non-host species (*A. thaliana*). This model is based on two assumptions: (i) the proportion of pathogen effectors that fail to 'find' corresponding targets raises with increasing divergence time between host and non-host, and (ii) the co-evolutionary arms race in host-adapted interactions 'depletes' the capacity of phylogenetically distant non-hosts to recognize effectors of host-adapted pathogens.

4.4. SFI5 is a member of a larger family of RXLR effectors

According to our work, SFI5 (PITG_13628/PexRD27) is a host-specific effector blocking

MAPK activation upon flg22 treatment in tomato, but not in Arabidopsis. The interaction with host CaM is necessary for the SFI5 localization at the plasma membrane as well as the MTI-suppressing effect and *P. infestans* growth promotion.

Originally, SFI5 is identified as a member of RXLR effector family 6 in *P. infestans* (Haas et al., 2009; Cooke et al., 2012) comprising 18 different RXLR effector-encoding genes (Figure 4-3). Another member of this family, PITG_11384/PexRD2 was recently reported to interact with the kinase domain of MAP3Kε *in planta* (King et al., 2014). This interaction blocked specifically PCD induced by several but not all Avr-R pairs tested and did not interfere with INF1-mediated cell death in *N. benthamiana*. In our study, SFI5 also did not suppress INF1-induced cell death and although we did not test multiple Avr/R combinations, it did not interfere with AVR4-Cf-4 triggered PCD (Figure 3-8). Structural analysis revealed that SFI5 did not possess the core α-helical fold, called "WY-domain", which is characteristic of PexRD2 and hypothesized to serve as an interaction module with kinases (Boutemy et al., 2011). On the other hand, we did not observe an interaction between PexRD2 and CaM although the effector is predicted to contain a CaM-binding motif (data not shown).

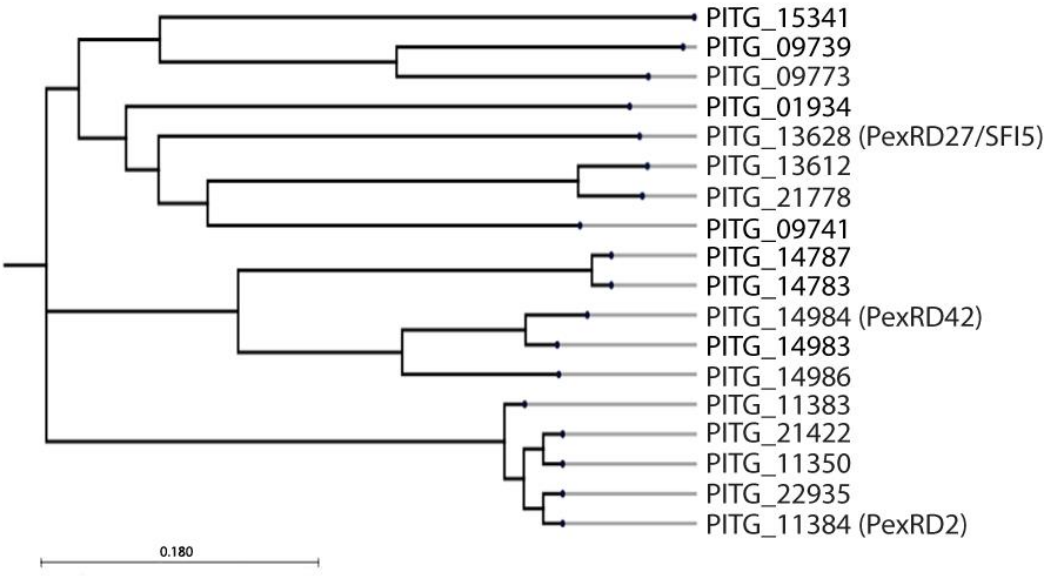

Figure 4-3. A neighbor-joining tree of RXLRfam6 members from *P. infestans*.

The maximum-likelihood relationship was constructed based on the full-length protein sequences of these effectors using CLC Main Workbench 7.

Altogether, these results indicate that structurally related RXLR effectors have evolved

different functions and different target specificities to affect different branches of the immune system. Based on BLASTP analysis within NCBI database (http://blast.ncbi.nlm.nih.gov/Blast.cgi?PAGE=Proteins), homologs of SFI5 and PexRD2, sharing 30% - 59% protein sequence identity, are present in the genome of *P. parasitica, P. ramorum* and *P. sojae* pointing toward a conservation of their function across *Phytophthora spp*. However, the fast evolution of this family suggests the presence of paralogs suppressing MAMP and/or effector-mediated signal transduction by a different mechanism than SFI5 or PexRD2. A comparative analysis of the MTI and ETI-suppressing specificities of all the members of RXLRfam6 offers a very good opportunity to explore evolutionary aspects at the molecular level of effector/target specialization.

4.5. The molecular basis of SFI5-CaM interaction

Structure-function analysis accurately delimited the domain and residues of SFI5 that were involved in CaM binding. Similar to CaM-binding motifs in other proteins, the 18 aa-region of SFI5 binding to CaM forms an amphipathic α-helix wheel with the segregation of basic and hydrophobic residues on opposite sides (O'Neil and DeGrado, 1990; Meador et al., 1992; Crivici and Ikura, 1995). However, the CaM-binding sites are extremely variable in their amino acid sequence and length and several classes have been categorized based on the spacing between hydrophobic anchor residues (Rhoads and Friedberg, 1997). Generally, IQ ([FILV]Qxxx[RK]Gxxx[RK]xx[FILVWY]) and IQ-like motif ([FILV]Qxxx[RK]xxxxxxxx) are characterized as Ca^{2+}-independent CaM-binding motifs, while Ca^{2+}-dependent CaM-binding motifs include 1-8-14 ([FILVW] xxxxxx [FAILVW] xxxxx [FILVW]), 1-5-8-14 ([FILVW] xxx [FAILVW] xx [FAILVW] xxxxx [FILVW]) and 1-5-10 ([FILVW] xxx [FAILVW] xxxx [FILVW]) motifs (Rhoads and Friedberg, 1997; Mruk et al., 2014). Moreover, several recent reports have revealed that CaM can bind to atypical motifs in which the spacing between the hydrophobic anchors is either further apart (16 or 17 amino acids) or closer together (6 amino acids) than the classical Ca^{2+}/CaM-binding motifs, or helicity of which is likely not a strict requirement (Maximciuc et al., 2006; Ataman et al., 2007; Juranic et al., 2010; Kumar et al., 2013).

The CaM-binding site of SFI5 appears to be non-canonical due to the absence/weak similarity to any known CaM-binding domain and rather be characterized as a 1-X-4 or 1-4-X motif. The two hydrophobic residues (Trp^{225} and Phe^{228}) are critical anchor residues but another hydrophobic residues at the same side of the α-helix wheel (Ile^{227}, Ile^{231} or Leu^{239}) might also be important for the interaction with CaM. It is worth noting that mutation of the Trp^{225} and

Phe^{228} residues did not dramatically affect the suppression of flg22-triggered oxidative burst (Figure 3-20 B SFI5-ED WF/AA). Although the ANS fluorescence competition assay and binding studies with synthetic peptides *in vitro* rather suggest the abrogation of interaction with CaM (Figure 3-16 C, D), it is possible that replacement of the two strong hydrophobic amino acids with a weak hydrophobic residue (alanine) compromised, but did not completely abrogate CaM-binding activity of SFI5 *in vivo*. Dose-response assays with SFI5 and SFI5 variants would help to correlate in a more quantitative way CaM binding with the impact on the biological response and underpin unambiguously the importance of CaM binding for the MTI-suppressing activity of SFI5. Alternatively, to rule out any binding of a Trp^{225}/Phe^{228} mutant, we could convert these two hydrophobic residues into hydrophilic arginine or lysine residues as suggested elsewhere (Kim et al., 2002; Yamakawa et al., 2004; Yoo et al., 2005; Katou et al., 2007; Wang et al., 2009).

The molecular determinants of CaM that are engaged in the interaction with SFI5 are unknown. CaMs and CaMs-like (CMLs) form a remarkable and highly conserved Ca^{2+} sensor protein family, which is present in all eukaryotes. The 3D structure of CaM has the hallmark of a dumbbell shape with four EF-hand Ca^{2+}-binding motifs organized in pairs and embedded in two globular domains separated by a long flexible helix. After Ca^{2+} binding, CaM undergoes conformational changes that exposes its hydrophobic surfaces and subsequently interacts with a large array of proteins that are implicated in many cellular processes (Bouche et al., 2005; McCormack et al., 2005). Therefore, it would be interesting to solve the crystal structure of SFI5 in complex with CaM, which could possibly provide new insights on the structural variability of CaM/CaM-binding protein interactions and on the action mode of SFI5 *in planta*.

4.6. CaMs regulate multiple biological functions in plants

Plant dispose of a large repertoire of CaMs and and CMLs, and because of their redundancy and the variabilty of interacting proteins, it is difficult to define the exact functions of each CaM or CML. Therefore, loss-of-function experiments by knocking down individual CaMs or CMLs sparely revealed their function. *Atcam3* knock-out mutants showed clearly reduced tolerance and survival ability to high temperature (45°C), indicating that AtCaM3 plays a key role in heat shock signal transduction (Zhang et al., 2009). Recently, AtCML10 was demonstrated to positively regulate oxidative and osmotic stresses through binding to a protein phosphomannomutase (PMM), an enzyme engaged in the biosynthesis of ascorbic acid (Cho et al., 2016). Large scale protein-protein interaction screens combined with the

availability of genome and transcriptome resources revealed considerable amout of putative CaM/CML-binding proteins, with implication in the regulation of plant immunity, several of them having been documented to act as transcriptional regulators of plant resistance (Yang and Poovaiah, 2003; Ranty et al., 2006; Cheval et al., 2013; Poovaiah et al., 2013). For instance, one member of the CaM-binding transcription activator (CAMTA) family in Arabidopsis, AtCAMTA3 (also designated as AtSR1), was shown to suppress the expression of genes of the salicylic acid (SA) biosynthetic pathway thereby repressing SA-dependent plant defense against bacteria and fungi (Galon et al., 2008; Du et al., 2009). On the contrary, AtCAMTA3 has a positive effect in plant resistance to herbivore attack/wounding by modulating the biosynthesis of jasmonates (JA) (Qiu et al., 2012). In addition, AtCAMTA3 can directly bind to the promoter regions of *Non-race-specific Disease Resistance 1* (*NDR1*) and *Ethylene Insensitive 3* (*EIN3*) to regulate plant defense and ethylene-induced senescence (Nie et al., 2012). Another plant-specific CaM-binding transcription factor, calmodulin binding protein 60g (CBP60g), contributes to MAMP-induced SA accumulation and plant defense against bacterial infection by promoting the expression of *Isochorismate Synthase 1* (*ICS1*) encoding a key enzyme in SA production (Wang et al., 2009; Zhang et al., 2010b). Both AtCAMTA3 and CBP60g have several homologs with Ca^{2+}/CaM-binding activity in plants, but if and how they have effects on plant defense responses remains to be uncovered (Reddy et al., 2002; Yang and Poovaiah, 2002c). Although there are also several reported CaM-interacting TFs, such as TGA3, WRKY7 and WRKY11, playing either positive or negative roles in plant resistance, the functional significance of CaM binding in modulating these proteins is still unknown (Reddy et al., 2011). Moreover, a PM-resident protein, Mildew resistance Locus O (MLO), which does not function as a TF, requires Ca^{2+}/CaM association to repress the defense against powdery mildew in barley (Kim et al., 2002).

Although CaMs and CMLs fulfill an important role in plant immune signaling, there are few publications reporting an interaction with microbial effectors. A tobacco CML, termed rgs-CaM, was found to interact and to destabilize viral RNA silencing suppressors (RSSs), thereby having a positive contribution to host RNAi-based defense against virus infection (Nakahara et al., 2012). However, rgs-CaM being itself an endogenous RSS, it has been recently shown that the RSS βC1 protein encoded by the DNA satellite of tomato yellow leaf curl china virus induces the expression of rgs-CaM to repress the expression of *RNA-dependent RNA polymerase 6* (*RDR6*), which plays a key role in antiviral RNA silencing pathway (Li et al., 2014a). Although a direct interaction between βC1 and rgs-CaM remains to be shown, these data suggest that viruses have also evolved CaM/CML-dependent effectors

that manipulate cellular regulators of RNA silencing to counteract plant antiviral defenses. In bacteria, the *Bacillus anthracis* Anthrax edema factor toxin and *Bordetella pertussis* toxin display both CaM-dependent adenylate cyclase activity leading to increased cellular concentrations of cAMP (Wolff et al., 1980; Leppla, 1982). Very recently, a T3 effector from *P. syringae*, HopE1, was discovered to interact with CaM and this interaction was required for further association with host microtubule-associated protein 65 (MAP65). Upon association, MAP65 dissociates from the microtubule network which is thought to cause suppression of MAMP-induced Pathogensesis-Related protein secretion and enhanced susceptibility to bacterial infection (Guo et al., 2016). To date, it is unclear how HopE1 manipulates MAP65, but a conclusion of the authors was that CaM serves as a factor to activate HopE1 function in host cells, which is the same interpretation we have about the biological meaning of the interaction between SFI5 and CaM. Given that SFI5 does not display specificity in binding distinct CaMs from tomato and Arabidopsis, it is possible that SFI5 association with CaM promotes the interaction with other plant (CaM-binding?) components. In this respect, the identification of potential targets included in SFI5-CaM complexes might provide new findings on the action mode of SFI5.

4.7. Site of action of SFI5 in the host cell

The subcellular localization studies in tomato protoplasts with SFI5 and SFI5 variants with C-terminal deletions or point mutations indicate that the CaM binding motif, and thus CaM binding, is required for the localization of SFI5 at the plasma membrane.

In general, CaMs are distributed in the cytoplasm but they have been found to have multiple subcellular localizations, also depending on the nature of the CaM-binding protein. For example, AtCaM7 has been demonstrated to act as a transcriptional regulator of light-inducible genes, e.g. *Chlorophyll a/b-binding protein 1* (*CAB1)* and *Long Hypocotyl 5* (*HY5*), and physically associates with the transcription factor HY5 in the plant nucleus (Kushwaha et al., 2008; Abbas et al., 2014). Moreover, AtCaM7 was recently shown to interact and to co-localize with ATP-binding cassette (ABC) transporter PENETRATION 3 (PEN3) at the plama membrane-cytoplasm interface and affect PEN3-mediated nonhost resistance (Campe et al., 2016). The PM-resident PSK receptor, PSKR1, binds to all CaM isoforms, a step that is necessary for the activation of the PSK-promoted growth signaling pathway (Hartmann et al., 2014).

Several hypotheses can be formulated about the role of CaM in SFI5 PM localisation.

Bioinformatics do not predict the presence of a transmembrane or membrane-anchoring domain in the sequence of SFI5 and therefore, it is possible that upon CaM binding and activation, SFI5 interacts with operative targets that are localized at the PM. We have tried first to perform co-localization studies with SFI5 and SlCaM3 using bimolecular fluorescence complementation (BiFC) in *N. benthamiana*, but a high background, due to the possible interaction of CaM with cYFP or nYFP, prevented us to draw any conclusion (data not shown). *In vivo* Förster Resonance Energy Transfer-Fluorescence Lifetime Imaging Microscopy (FRET-FLIM) would provide an alternative approach to study the interaction between SFI5 and CaM and even give information about the dynamic of their coupling. This method has been successfully applied to study the spatio-temporal interaction dynamics of barley MLO with its activator, CaM. It revealed an increasing number of MLO/CaM complex in the vicinity of the penetration sites coincident with successful pathogen entry into host cells (Bhat et al., 2005).

In addition, we do not know whether the CaM-bound form of SFI5 is required for MTI-suppressing activity or whether CaM can dissociate from SFI5 upon activation and conformational change. This hypothesis emerged with the observation that a weak proportion of SFI5 localizes in the cytoplasm, which may reflect different mode of actions of SFI5 and interactions with different targets in the host cell. To further determine the role of CaM-mediated PM-localization for the SFI5 MTI-suppressing activity, a PM anchor myristoylation site could be introduced into SFI5 and SFI5 variants deficient in CaM-binding and the resulting proteins could be tested for their MTI-suppressing activity. Such an approach has been successfully used in our work to re-locate SFI1 from the nucleus to the plasma membrane and to demonstrate that SFI1 must enter the nucleus to suppress MTI (Figure 3-12)

An interesting question is the order of the sequence for the activation of SFI5 or, in other words, what is the correlation between CaM binding, nucleotide binding and biochemical function. The fact that SFI5 ED-K82A was still localized at the PM and associated with CaM (Figure 3-22 B, C) suggests that nucleotide binding occurs after CaM binding and even that CaM binding is prerequisite for the nucleotide binding. It would explain why deletion of the N-terminal domain encompassing the putative ATP/GTP binding site resulted in inactive SFI5 variants while keeping associated with CaM.

4.8. Molecular mechanisms underlying SFI5 MTI-suppressing activity

Our work revealed that, in the presence of SFI5, the flg22-induced Ca^{2+} burst, ROS

production and MAP kinase activation were dramatically suppressed in tomato protoplasts, suggesting that SFI5 interferes at an very early step of MTI signaling (Figure 3-20). Although we have confirmed that CaM-binding and the presence of a putative ATP/GTP binding site are required for full function of SFI5, it is still unclear how SFI5 interferes with MTI signaling.

The Ca^{2+} influx is one of the first event occurring after PRR activation and has been demonstrated to be necessary for the downstream MAMP-induced ROS production, MAPK activation, as well as defense gene expression (Jeworutzki et al., 2010; Segonzac et al., 2011). How the Ca^{2+} signal is decoded and integrated to allow a concerted cellular response is largely unknown. It has been shown that cyclic nucleotide gated channels (CNGCs) and Ca^{2+}-ATPases (ACAs) pumps involved in Ca^{2+} transport can be either inactivated or activated by binding of CaM, indicating that it is a key factor in the modulation of cytosolic Ca^{2+} oscillations (Hua et al., 2003; Kaplan et al., 2007; Giacometti et al., 2012). A conserved IQ motif for Ca^{2+}/CaM binding is present at the C-terminus of CNGC20, which is strongly up-regulated in response to salt stress (Kugler et al., 2009; Fischer et al., 2013). A more recent study revealed that CNGC17 is able to interact with BAK1 as well as H^{+}-ATPases AHA1 and AHA2, forming a functional complex with the phytosulfokine (PSK) receptor PSKR1 to mediate the PSK signaling (Ladwig et al., 2015). It is conceivable that Ca^{2+}/CaM-regulated CNGC members might be implicated in MAMP-induced RLK/BAK1 or RLP/BAK1 signaling and that this step is targeted by SFI5. It is also conceivable that SFI5 through its association with CaM has a pleitropic effect and affects simultaneously different steps of MAMP-dependent signaling cascade. Ca^{2+}/CaM seems to have both positive and negative effects on the regulation of H_2O_2 levels in plants. It was shown that the H_2O_2 level is down-regulated by the Ca^{2+}/CaM-activated plant catalase (Yang and Poovaiah, 2002a). On the other hand, the generation of H_2O_2 in tobacco is strongly enhanced by the activation of Ca^{2+}/CaM-dependent NAD kinases, likely through the increase of NADP for the NADPH-Oxidase (Harding et al., 1997). The NADPH-oxidase AtRBOHD, which is activated in response to flg22, has been identified as a substrate of AtCPK5, a calmodulin-like Ca^{2+} binding domain-containing protein kinase (Dubiella et al., 2013). Similarly, StCPK5 positively regulates the function of RBOHB in basal resistance in *Solanacea* species (Kobayashi et al., 2007). In addition, CaM was also reported to regulate MAPK signaling as Ca^{2+}/CaM binding is either observed in some MAP kinase phosphatases, such as NtMKP1 and OsMKP1, or required for full activation of Arabidopsis MPK8, which are components engaged in the wound signaling pathway (Yamakawa et al., 2004; Katou et al., 2007; Takahashi et al., 2011).

One possible mechanism of MTI-signaling suppression is that SFI5 directly targets and inhibits the function of CaM or CMLs that consists to regulate the activity of downstream CaM- and CML-binding proteins (like the CNGCs and RBOHs), which have a positive role on MTI. However, the gain-of-function experiment with the overexpression of SlCaM3/4/5 did not titrate out the SFI5-mediated MTI suppressing effect with no recovery, even partial, of the ROS production and MAP kinase activation by flg22 (Figure 3-24 A, B). In our experimental conditions, SFI5 interacts with all CaM isoforms in protoplasts but, under natural conditions of infection, a certain level of interaction specificity may exist and we cannot rule out that some CaMs, eventually those that are more specifically involved in MAMP signaling, are more affine to SFI5 and would eventually attenuate the MTI-suppression by SFI5 when overexpressed in protoplasts. To test further the hypothesis of SFI5 antagonizing CaM activity, we performed competition assays in which we co-expressed SFI5 with an inactive N-terminal deletion mutant of SFI5 that is still able to interact with CaM. This assay led to a reduction of the inhibition of the flg22-dependent *pFRK1-Luc* induction, which can be interpreted as a competition between inactive and active SFI5 forms to bind to CaM and an indirect proof that SFI5 does not inhibit CaM function. These results further support our proposition that CaM is not the operative target of SFI5 but that SFI5 utilizes plant CaMs as positive regulators of its effector activity after translocation into the host cell.

During the structure-function analysis with deletion and mutated constructs of SFI5, we found that a 21 amino acid residues stretch (from Phe^{63} to Ser^{83}) was critical for the MTI-suppressing activity and virulence function of SFI5 (Figure 3-19, 3-20, 3-21). Bioinformatic analysis and motif scanning revealed an ATP/GTP-binding site (A^{76}MMKAGKS^{83} - Figure 3-22 A) within this stretch, which is similar to the Walker A motif [AG]XXXXGK[ST], also called P-loop, that has been found in a wide variety of ATP- or GTP-binding proteins from eukaryotic and prokaryotic organisms (Higgins et al., 1986; Saraste et al., 1990; Higgins, 1992). Mutations of the conserved GK[ST] residues in the P-loop result in inactive proteins that have lost the ability to bind ATP or GTP (van der Wolk et al., 1993; Sandkvist et al., 1995; Deyrup et al., 1998; Doublet et al., 1999; Nishiwaki et al., 2000). Similarly, substitution of lys^{82} by alanine leaded to a SFI5 mutant that was no longer capable of subverting the early MTI immune responses (Figure 3-23). Based on our data (CaM interaction, putative ATP/GTP binding site, putative phosphorylation sites) our primary assumption was that SFI5 does eventually display a Ca^{2+}/CaM-dependent protein kinase (CCaMK) activity *in planta* that is targeting and probably inactivating components involved in early MAMP signaling. CCaMK plays an essential role in symbiotic interactions between plants and arbuscular

mycorrhiza fungi through sensing the nuclear Ca^{2+} spiking (Miller et al., 2013). CCaMK is also involved in response to pathogens and was proposed to cope with stress triggered by penetration of the fungus *Colletotrichium trifolii* (Genre et al., 2009). To assess this hypothesis, we performed an *in vitro* kinase assay with immunoprecipitated material from HA-SFI5-expressing tomato protoplasts, but we measured neither phosphorylation of the MBP substrate nor detected autophosphorylation of SFI5 (data not shown). Future work will consist to carry out molecular and biochemical studies in order to demonstrate, both *in vitro* and *in vivo*, the ATP and/or GTP binding properties of SFI5. This work will hopefully lead to generate new hypotheses about the biochemical function of SFI5 and possible plant interacting partners or substrates.

In order to improve the understanding of the molecular mechanisms underlying the function of SFI5 *in planta*, we have tried to generate stable transgenic tomato lines expressing SFI5 constitutively or using an estradiol-inducible promoter. Although, we could amplify by PCR the genomic fragment corresponding to *SFI5* in primary transformants and detected SFI5 protein when transiently expressed in *N. benthamiana*, we failed to detect the expression of the RXLR effector in tomato plants (data not shown). It is possible that transcriptional or post-transcriptional gene silencing is responsible for the lack of SFI5 expression or that SFI5 possesses toxic features when overexpressed in tomato, leading to fast degradation by the proteasome. Another and more elegant explanation would be that, in the absence of stimuli and increase of cytosolic Ca^{2+} level, SFI5 does not bind to CaM and becomes unstable. It would be in relation with the *in vitro* binding experiments that have shown that, in the absence of CaM, SFI5 has tendency to form aggregates. The protoplast and the Agrobacterium-based approaches might be less problematic for SFI5 expression because they cause a certain level of stress that could be correlated with higher steady-state levels of Ca^{2+}. We need to test this hypothesis and see whether activation of MTI signaling in tomato transformants will permit the detection of SFI5 protein. Infiltration experiments with the *P. syringae* hrc- or hrp- strains, unable to secrete T3 effectors and to grow on tomato, would be very helpful. The advantage for *P. infestans* to produce an effector that is functional only in the early stage of infection, when the suppression of MTI signaling is of key importance, would be to avoid complication during later stages of the infection, when SFI5 activity might interfere with cellular processes that could be detrimental to the pathogen. A similar hijacking strategy of immune signaling has been evolved by Agrobacterium to transfer its T-DNA into the nucleus of the host cell using the activation of the transcription factor VIP1 by MPK3 after pathogen recognition (Djamei et al., 2007).

The finding of a physical association of SFI5 with different CaM isoforms firstly revealed the direct link between an oomycete plant pathogen effector with components of Ca^{2+}/CaM signaling in plants. Our current model predicts that SFI5 activation in host cells requires a two-step process. The first step is the association with CaM, in a Ca^{2+}-dependent manner, at the C-terminal Pro^{222}-Leu^{239} α-helix, triggering a conformational change of SFI5. The second step is the hypothetical binding of ATP/GTP at Lys^{82}, which is crucial for a yet undiscovered enzymatic activity of SFI5, to affect MAMP signal transduction pathway by manipulating one or several unknown membrane-associated proteins, likely pattern recognition receptors and/or signaling components (figure 4-4). Further molecular and biochemical studies are needed to dissect the specific mode of action of SFI5 in host cells and to unravel the molecular basis of the non-functionality of SFI5 in non-host plants.

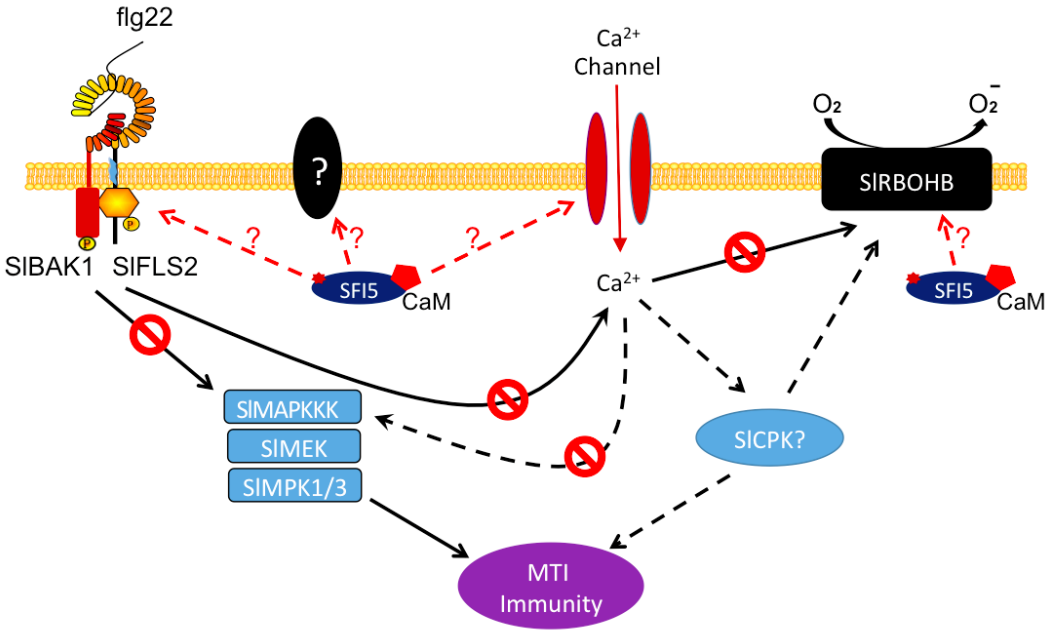

Figure 4-4. Schematic mode of action of *P. infestans* RXLR effector SFI5 in tomato.

Both N-terminal predicted ATP/GTP-binding motif (P-loop) and C-terminal CaM-binding motif are required for full activation of SFI5 after delivery into the host cell. Active SFI5 inhibits MAMP-induced early MTI responses by targeting one or several unknown PM-associated components involved in MTI, most likely pattern recognition receptor complexes i.e. SlFLS2/SlBAK1 and/or ion channels or NADPH oxidase (SlRBOHB). Solid line: demonstrated function, dashed line: hypothetical function. Abbreviations used in the figure: Sl, *Solanum lycopersicum*; BAK1, BRI1 associated receptor kinase 1; FLS2, receptor kinase Flagellin-Sensing 2; CaM, calmodulin; RBOHB, respiratory burst oxidase homolog B; MAPKKK, mitogen-activated protein kinase kinase kinases; MEK, mitogen-activated protein kinase kinases; MPK1/3, mitogen-activated protein kinase 1 and 3; CPK, calcium-dependent protein kinase; MTI, MAMP-triggered immunity.

4.9. Conclusion

Our understanding about RXLR effectors targeting mechanisms is beginning to emerge although it is fragmentary compared with the information gained form studies with effectors from phytopathogenic bacteria. An important question for understanding infection biology is which processes are targeted to dampen plant resistance. Thus, unravelling the mode of action of these effectors and understanding the effector-target biology will certainly continue to represent an important aspect of research activities among the scientific community working on plant-oomycete interactions. Although RXLR effector repertoires are diverse among *Phytophthora* species and even among strains of the same species, they share several properties suggesting that they operate in a repertoire as components of a system. A comparative functional study of effectors originated from different *Phytophthora* spp. in host and non-host plant species will permit to investigate pathogen speciation, host adaptation and the phenomenon of non-host resistance at the molecular level and it offers insights into the plasticity of oomycete genomes, increasing our knowledge on the evolutionary conservation or diversification of RXLR effectors, driven by host-imposed positive selection. A better understanding of the molecular basis of the striking differences in host spectrum between different *Phytophthora spp.* under natural conditions will be instrumental to rationalize and to model pathogen co-evolution with hosts that are either closely (host range expansion) or distantly (host jump) related to the present hosts.

5. Reference

Abbas, N., Maurya, J.P., Senapati, D., Gangappa, S.N., and Chattopadhyay, S. (2014). Arabidopsis CAM7 and HY5 physically interact and directly bind to the HY5 promoter to regulate its expression and thereby promote photomorphogenesis. Plant Cell **26,** 1036-1052.

Abramovitch, R.B., Anderson, J.C., and Martin, G.B. (2006). Bacterial elicitation and evasion of plant innate immunity. Nat Rev Mol Cell Biol **7,** 601-611.

Ahuja, I., Kissen, R., and Bones, A.M. (2012). Phytoalexins in defense against pathogens. Trends Plant Sci **17,** 73-90.

Albert, I., Böhm, H., Albert, M., Feiler, C.E., Imkampe, J., Wallmeroth, N., Brancato, C., Raaymakers, T.M., Oome, S., and Zhang, H. (2015). An RLP23–SOBIR1–BAK1 complex mediates NLP-triggered immunity. Nature Plants **1,** 15140.

Alfano, J.R., and Collmer, A. (2004). Type III secretion system effector proteins: double agents in bacterial disease and plant defense. Annu Rev Phytopathol **42,** 385-414.

Altenbach, D., and Robatzek, S. (2007). Pattern recognition receptors: from the cell surface to intracellular dynamics. Mol Plant Microbe Interact **20,** 1031-1039.

Anderson, R.G., Deb, D., Fedkenheuer, K., and McDowell, J.M. (2015). Recent Progress in RXLR Effector Research. Mol Plant Microbe Interact **28,** 1063-1072.

Anderson, R.G., Casady, M.S., Fee, R.A., Vaughan, M.M., Deb, D., Fedkenheuer, K., Huffaker, A., Schmelz, E.A., Tyler, B.M., and McDowell, J.M. (2012). Homologous RXLR effectors from *Hyaloperonospora arabidopsidis* and *Phytophthora sojae* suppress immunity in distantly related plants. Plant J **72,** 882-893.

Antonovics, J., Boots, M., Ebert, D., Koskella, B., Poss, M., and Sadd, B.M. (2013). The origin of specificity by means of natural selection: evolved and nonhost resistance in host-pathogen interactions. Evolution **67,** 1-9.

Apel, K., and Hirt, H. (2004). Reactive oxygen species: metabolism, oxidative stress, and signal transduction. Annu Rev Plant Biol **55,** 373-399.

Arndt, C., Koristka, S., Bartsch, H., and Bachmann, M. (2012). Native polyacrylamide gels. Methods Mol Biol **869,** 49-53.

Asai, S., Ohta, K., and Yoshioka, H. (2008). MAPK signaling regulates nitric oxide and NADPH oxidase-dependent oxidative bursts in *Nicotiana benthamiana*. Plant Cell **20,** 1390-1406.

Asai, T., Tena, G., Plotnikova, J., Willmann, M.R., Chiu, W.L., Gomez-Gomez, L., Boller, T., Ausubel, F.M., and Sheen, J. (2002). MAP kinase signalling cascade in Arabidopsis innate immunity. Nature **415,** 977-983.

Aslam, S.N., Erbs, G., Morrissey, K.L., Newman, M.A., Chinchilla, D., Boller, T., Molinaro, A., Jackson, R.W., and Cooper, R.M. (2009). Microbe-associated molecular pattern (MAMP) signatures, synergy, size and charge: influences on perception or mobility and host defence responses. Mol Plant Pathol **10,** 375-387.

Ataman, Z.A., Gakhar, L., Sorensen, B.R., Hell, J.W., and Shea, M.A. (2007). The NMDA receptor NR1 C1 region bound to calmodulin: structural insights into functional differences between homologous domains. Structure **15,** 1603-1617.

Ausubel, F.M. (2005). Are innate immune signaling pathways in plants and animals conserved? Nat Immunol **6,** 973-979.

Bar, M., Sharfman, M., and Avni, A. (2011). LeEix1 functions as a decoy receptor to attenuate LeEix2 signaling. Plant Signal Behav **6,** 455-457.

Benedetti, M., Pontiggia, D., Raggi, S., Cheng, Z., Scaloni, F., Ferrari, S., Ausubel, F.M., Cervone, F., and De Lorenzo, G. (2015). Plant immunity triggered by engineered in vivo release of oligogalacturonides, damage-associated molecular patterns. Proc Natl Acad Sci U S A **112,** 5533-5538.

Bethke, G., Unthan, T., Uhrig, J.F., Poschl, Y., Gust, A.A., Scheel, D., and Lee, J. (2009). Flg22 regulates the release of an ethylene response factor substrate from MAP kinase 6 in *Arabidopsis thaliana* via ethylene signaling. Proc Natl Acad Sci U S A **106,** 8067-8072.

Bethke, G., Pecher, P., Eschen-Lippold, L., Tsuda, K., Katagiri, F., Glazebrook, J., Scheel, D., and Lee, J. (2012). Activation of the Arabidopsis thaliana mitogen-activated protein kinase

MPK11 by the flagellin-derived elicitor peptide, flg22. Mol Plant Microbe Interact **25,** 471-480.

Bhat, R.A., Miklis, M., Schmelzer, E., Schulze-Lefert, P., and Panstruga, R. (2005). Recruitment and interaction dynamics of plant penetration resistance components in a plasma membrane microdomain. Proc Natl Acad Sci U S A **102,** 3135-3140.

Bi, D., Cheng, Y.T., Li, X., and Zhang, Y. (2010). Activation of plant immune responses by a gain-of-function mutation in an atypical receptor-like kinase. Plant Physiol **153,** 1771-1779.

Bigeard, J., Colcombet, J., and Hirt, H. (2015). Signaling mechanisms in pattern-triggered immunity (PTI). Mol Plant **8,** 521-539.

Block, A., and Alfano, J.R. (2011). Plant targets for Pseudomonas syringae type III effectors: virulence targets or guarded decoys? Curr Opin Microbiol **14,** 39-46.

Boch, J., Bonas, U., and Lahaye, T. (2014). TAL effectors--pathogen strategies and plant resistance engineering. New Phytol **204,** 823-832.

Boch, J., Scholze, H., Schornack, S., Landgraf, A., Hahn, S., Kay, S., Lahaye, T., Nickstadt, A., and Bonas, U. (2009). Breaking the code of DNA binding specificity of TAL-type III effectors. Science **326,** 1509-1512.

Boevink, P.C., Wang, X., McLellan, H., He, Q., Naqvi, S., Armstrong, M.R., Zhang, W., Hein, I., Gilroy, E.M., Tian, Z., and Birch, P.R. (2016). A *Phytophthora infestans* RXLR effector targets plant PP1c isoforms that promote late blight disease. Nat Commun **7,** 10311.

Bogdanove, A.J., Schornack, S., and Lahaye, T. (2010). TAL effectors: finding plant genes for disease and defense. Curr Opin Plant Biol **13,** 394-401.

Bohm, H., Albert, I., Oome, S., Raaymakers, T.M., Van den Ackerveken, G., and Nurnberger, T. (2014). A conserved peptide pattern from a widespread microbial virulence factor triggers pattern-induced immunity in Arabidopsis. PLoS Pathog **10,** e1004491.

Boller, T., and Felix, G. (2009). A renaissance of elicitors: perception of microbe-associated molecular patterns and danger signals by pattern-recognition receptors. Annu Rev Plant Biol **60,** 379-406.

Boller, T., and He, S.Y. (2009). Innate immunity in plants: an arms race between pattern recognition receptors in plants and effectors in microbial pathogens. Science **324,** 742-744.

Bolton, M.D., van Esse, H.P., Vossen, J.H., de Jonge, R., Stergiopoulos, I., Stulemeijer, I.J., van den Berg, G.C., Borras-Hidalgo, O., Dekker, H.L., de Koster, C.G., de Wit, P.J., Joosten, M.H., and Thomma, B.P. (2008). The novel Cladosporium fulvum lysin motif effector Ecp6 is a virulence factor with orthologues in other fungal species. Mol Microbiol **69,** 119-136.

Bos, J.I., Chaparro-Garcia, A., Quesada-Ocampo, L.M., McSpadden Gardener, B.B., and Kamoun, S. (2009). Distinct amino acids of the *Phytophthora infestans* effector AVR3a condition activation of R3a hypersensitivity and suppression of cell death. Mol Plant Microbe Interact **22,** 269-281.

Bos, J.I., Kanneganti, T.D., Young, C., Cakir, C., Huitema, E., Win, J., Armstrong, M.R., Birch, P.R., and Kamoun, S. (2006). The C-terminal half of *Phytophthora infestans* RXLR effector AVR3a is sufficient to trigger R3a-mediated hypersensitivity and suppress INF1-induced cell death in Nicotiana benthamiana. Plant J **48,** 165-176.

Bos, J.I., Armstrong, M.R., Gilroy, E.M., Boevink, P.C., Hein, I., Taylor, R.M., Zhendong, T., Engelhardt, S., Vetukuri, R.R., Harrower, B., Dixelius, C., Bryan, G., Sadanandom, A., Whisson, S.C., Kamoun, S., and Birch, P.R. (2010). *Phytophthora infestans* effector AVR3a is essential for virulence and manipulates plant immunity by stabilizing host E3 ligase CMPG1. Proc Natl Acad Sci U S A **107,** 9909-9914.

Bouche, N., Yellin, A., Snedden, W.A., and Fromm, H. (2005). Plant-specific calmodulin-binding proteins. Annu Rev Plant Biol **56,** 435-466.

Boudsocq, M., and Sheen, J. (2013). CDPKs in immune and stress signaling. Trends Plant Sci **18,** 30-40.

Boudsocq, M., Willmann, M.R., McCormack, M., Lee, H., Shan, L., He, P., Bush, J., Cheng, S.H., and Sheen, J. (2010). Differential innate immune signalling via Ca(2+) sensor protein kinases. Nature **464,** 418-422.

Boutemy, L.S., King, S.R., Win, J., Hughes, R.K., Clarke, T.A., Blumenschein, T.M., Kamoun, S., and Banfield, M.J. (2011). Structures of Phytophthora RXLR effector proteins: a conserved but adaptable fold underpins functional diversity. J Biol Chem **286,** 35834-35842.

Bouwmeester, K., de Sain, M., Weide, R., Gouget, A., Klamer, S., Canut, H., and Govers, F. (2011). The lectin receptor kinase LecRK-I.9 is a novel *Phytophthora* resistance component and a potential host target for a RXLR effector. PLoS Pathog **7,** e1001327.

Bozkurt, T.O., Schornack, S., Banfield, M.J., and Kamoun, S. (2012). Oomycetes, effectors, and all that jazz. Curr Opin Plant Biol **15,** 483-492.

Bozkurt, T.O., Schornack, S., Win, J., Shindo, T., Ilyas, M., Oliva, R., Cano, L.M., Jones, A.M., Huitema, E., van der Hoorn, R.A., and Kamoun, S. (2011). *Phytophthora infestans* effector AVRblb2 prevents secretion of a plant immune protease at the haustorial interface. Proc Natl Acad Sci U S A **108,** 20832-20837.

Brunner, F., Rosahl, S., Lee, J., Rudd, J.J., Geiler, C., Kauppinen, S., Rasmussen, G., Scheel, D., and Nurnberger, T. (2002). Pep-13, a plant defense-inducing pathogen-associated pattern from *Phytophthora* transglutaminases. EMBO J **21,** 6681-6688.

Brutus, A., Sicilia, F., Macone, A., Cervone, F., and De Lorenzo, G. (2010). A domain swap approach reveals a role of the plant wall-associated kinase 1 (WAK1) as a receptor of oligogalacturonides. Proc Natl Acad Sci U S A **107,** 9452-9457.

Buscaill, P., and Rivas, S. (2014). Transcriptional control of plant defence responses. Curr Opin Plant Biol **20,** 35-46.

Caillaud, M.C., Asai, S., Rallapalli, G., Piquerez, S., Fabro, G., and Jones, J.D. (2013). A downy mildew effector attenuates salicylic acid-triggered immunity in Arabidopsis by interacting with the host mediator complex. PLoS Biol **11,** e1001732.

Campe, R., Langenbach, C., Leissing, F., Popescu, G.V., Popescu, S.C., Goellner, K., Beckers, G.J., and Conrath, U. (2016). ABC transporter PEN3/PDR8/ABCG36 interacts with calmodulin that, like PEN3, is required for Arabidopsis nonhost resistance. New Phytol **209,** 294-306.

Canonne, J., Marino, D., Jauneau, A., Pouzet, C., Briere, C., Roby, D., and Rivas, S. (2011). The *Xanthomonas* type III effector XopD targets the Arabidopsis transcription factor MYB30 to suppress plant defense. Plant Cell **23,** 3498-3511.

Cao, Y., Liang, Y., Tanaka, K., Nguyen, C.T., Jedrzejczak, R.P., Joachimiak, A., and Stacey, G. (2014). The kinase LYK5 is a major chitin receptor in Arabidopsis and forms a chitin-induced complex with related kinase CERK1. Elife **3,** e03766.

Caten, C., and Jinks, J. (1968). Spontaneous variability of single isolates of *Phytophthora infestans*. I. Cultural variation. Canadian Journal of Botany **46,** 329-348.

Chang, Y.H., Yan, H.Z., and Liou, R.F. (2015). A novel elicitor protein from *Phytophthora parasitica* induces plant basal immunity and systemic acquired resistance. Molecular plant pathology **16,** 123-136.

Chaparro-Garcia, A., Schwizer, S., Sklenar, J., Yoshida, K., Bos, J.I., Schornack, S., Jones, A.M., Bozkurt, T.O., and Kamoun, S. (2014). *Phytophthora infestans* RXLR-WY effector AVR3a associates with a Dynamin-Related Protein involved in endocytosis of a plant pattern recognition receptor. bioRxiv**,** 012963.

Chen, L.Q., Hou, B.H., Lalonde, S., Takanaga, H., Hartung, M.L., Qu, X.Q., Guo, W.J., Kim, J.G., Underwood, W., Chaudhuri, B., Chermak, D., Antony, G., White, F.F., Somerville, S.C., Mudgett, M.B., and Frommer, W.B. (2010). Sugar transporters for intercellular exchange and nutrition of pathogens. Nature **468,** 527-532.

Cheng, W., Munkvold, K., Gao, H., Mathieu, J., Schwizer, S., Wang, S., Yan, Y., Wang, J., Martin, G., and Chai, J. (2011). The AvrPtoB-BAK1 complex reveals two structurally similar kinase-interacting domains in a single type III effector. Cell Host Microbe **10,** 616-626.

Cheong, J.J., Birberg, W., Fugedi, P., Pilotti, A., Garegg, P.J., Hong, N., Ogawa, T., and Hahn, M.G. (1991). Structure-activity relationships of oligo-beta-glucoside elicitors of phytoalexin accumulation in soybean. Plant Cell **3,** 127-136.

Cheval, C., Aldon, D., Galaud, J.P., and Ranty, B. (2013). Calcium/calmodulin-mediated regulation of plant immunity. Biochim Biophys Acta **1833,** 1766-1771.

Chinchilla, D., Bauer, Z., Regenass, M., Boller, T., and Felix, G. (2006). The Arabidopsis receptor kinase FLS2 binds flg22 and determines the specificity of flagellin perception. Plant Cell **18,** 465-476.

Chinchilla, D., Zipfel, C., Robatzek, S., Kemmerling, B., Nurnberger, T., Jones, J.D., Felix, G., and Boller, T. (2007). A flagellin-induced complex of the receptor FLS2 and BAK1 initiates plant defence. Nature **448,** 497-500.

Chisholm, S.T., Coaker, G., Day, B., and Staskawicz, B.J. (2006). Host-microbe interactions: shaping the evolution of the plant immune response. Cell **124,** 803-814.

Cho, K.M., Nguyen, H.T., Kim, S.Y., Shin, J.S., Cho, D.H., Hong, S.B., Shin, J.S., and Ok, S.H. (2016). CML10, a variant of calmodulin, modulates ascorbic acid synthesis. New Phytol **209,** 664-678.

Choi, H.W., Lee, D.H., and Hwang, B.K. (2009). The pepper calmodulin gene CaCaM1 is involved in reactive oxygen species and nitric oxide generation required for cell death and the defense response. Mol Plant Microbe Interact **22,** 1389-1400.

Choi, J., Tanaka, K., Cao, Y., Qi, Y., Qiu, J., Liang, Y., Lee, S.Y., and Stacey, G. (2014). Identification of a plant receptor for extracellular ATP. Science **343,** 290-294.

Collier, S.M., and Moffett, P. (2009). NB-LRRs work a "bait and switch" on pathogens. Trends Plant Sci **14,** 521-529.

Cooke, D.E., Cano, L.M., Raffaele, S., Bain, R.A., Cooke, L.R., Etherington, G.J., Deahl, K.L., Farrer, R.A., Gilroy, E.M., Goss, E.M., Grunwald, N.J., Hein, I., MacLean, D., McNicol, J.W., Randall, E., Oliva, R.F., Pel, M.A., Shaw, D.S., Squires, J.N., Taylor, M.C., Vleeshouwers, V.G., Birch, P.R., Lees, A.K., and Kamoun, S. (2012). Genome analyses of an aggressive and invasive lineage of the Irish potato famine pathogen. PLoS Pathog **8,** e1002940.

Crivici, A., and Ikura, M. (1995). Molecular and structural basis of target recognition by calmodulin. Annual review of biophysics and biomolecular structure **24,** 85-116.

Cui, H., Wang, Y., Xue, L., Chu, J., Yan, C., Fu, J., Chen, M., Innes, R.W., and Zhou, J.M. (2010). *Pseudomonas syringae* effector protein AvrB perturbs Arabidopsis hormone signaling by activating MAP kinase 4. Cell Host Microbe **7,** 164-175.

Cunnac, S., Lindeberg, M., and Collmer, A. (2009). *Pseudomonas syringae* type III secretion system effectors: repertoires in search of functions. Curr Opin Microbiol **12,** 53-60.

Dagdas, Y.F., Belhaj, K., Maqbool, A., Chaparro-Garcia, A., Pandey, P., Petre, B., Tabassum, N., Cruz-Mireles, N., Hughes, R.K., Sklenar, J., Win, J., Menke, F., Findlay, K., Banfield, M.J., Kamoun, S., and Bozkurt, T.O. (2016). An effector of the Irish potato famine pathogen antagonizes a host autophagy cargo receptor. Elife **5**.

Daudi, A., Cheng, Z., O'Brien, J.A., Mammarella, N., Khan, S., Ausubel, F.M., and Bolwell, G.P. (2012). The apoplastic oxidative burst peroxidase in Arabidopsis is a major component of pattern-triggered immunity. Plant Cell **24,** 275-287.

de Jonge, R., and Thomma, B.P. (2009). Fungal LysM effectors: extinguishers of host immunity? Trends Microbiol **17,** 151-157.

de Jonge, R., van Esse, H.P., Kombrink, A., Shinya, T., Desaki, Y., Bours, R., van der Krol, S., Shibuya, N., Joosten, M.H., and Thomma, B.P. (2010). Conserved fungal LysM effector Ecp6 prevents chitin-triggered immunity in plants. Science **329,** 953-955.

DeFalco, T.A., Bender, K.W., and Snedden, W.A. (2010). Breaking the code: Ca2+ sensors in plant signalling. Biochem J **425,** 27-40.

del Pozo, O., Pedley, K.F., and Martin, G.B. (2004). MAPKKKalpha is a positive regulator of cell death associated with both plant immunity and disease. EMBO J **23,** 3072-3082.

Denoux, C., Galletti, R., Mammarella, N., Gopalan, S., Werck, D., De Lorenzo, G., Ferrari, S., Ausubel, F.M., and Dewdney, J. (2008). Activation of defense response pathways by OGs and Flg22 elicitors in Arabidopsis seedlings. Mol Plant **1,** 423-445.

Desikan, R., Hancock, J.T., Bright, J., Harrison, J., Weir, I., Hooley, R., and Neill, S.J. (2005). A role for ETR1 in hydrogen peroxide signaling in stomatal guard cells. Plant Physiol **137,** 831-834.

Deslandes, L., and Rivas, S. (2012). Catch me if you can: bacterial effectors and plant targets. Trends Plant Sci **17,** 644-655.

Deyrup, A.T., Krishnan, S., Cockburn, B.N., and Schwartz, N.B. (1998). Deletion and site-directed mutagenesis of the ATP-binding motif (P-loop) in the bifunctional murine ATP-sulfurylase/adenosine 5'-phosphosulfate kinase enzyme. J Biol Chem **273,** 9450-9456.

Djamei, A., Pitzschke, A., Nakagami, H., Rajh, I., and Hirt, H. (2007). Trojan horse strategy in *Agrobacterium transformation*: abusing MAPK defense signaling. Science **318,** 453-456.

Doehlemann, G., Requena, N., Schaefer, P., Brunner, F., O'Connell, R., and Parker, J.E. (2014). Reprogramming of plant cells by filamentous plant-colonizing microbes. New Phytol **204,** 803-814.

Doehlemann, G., van der Linde, K., Assmann, D., Schwammbach, D., Hof, A., Mohanty, A., Jackson, D., and Kahmann, R. (2009). Pep1, a secreted effector protein of *Ustilago maydis*, is required for successful invasion of plant cells. PLoS Pathog **5,** e1000290.

Dong, S., Yin, W., Kong, G., Yang, X., Qutob, D., Chen, Q., Kale, S.D., Sui, Y., Zhang, Z., Dou, D., Zheng, X., Gijzen, M., Tyler, B.M., and Wang, Y. (2011). *Phytophthora sojae* avirulence effector Avr3b is a secreted NADH and ADP-ribose pyrophosphorylase that modulates plant immunity. PLoS Pathog **7,** e1002353.

Dong, S., Stam, R., Cano, L.M., Song, J., Sklenar, J., Yoshida, K., Bozkurt, T.O., Oliva, R., Liu, Z., Tian, M., Win, J., Banfield, M.J., Jones, A.M., van der Hoorn, R.A., and Kamoun, S. (2014). Effector specialization in a lineage of the Irish potato famine pathogen. Science **343,** 552-555.

Dou, D., Kale, S.D., Wang, X., Jiang, R.H., Bruce, N.A., Arredondo, F.D., Zhang, X., and Tyler, B.M. (2008). RXLR-mediated entry of *Phytophthora sojae* effector Avr1b into soybean cells does not require pathogen-encoded machinery. Plant Cell **20,** 1930-1947.

Doublet, P., Vincent, C., Grangeasse, C., Cozzone, A.J., and Duclos, B. (1999). On the binding of ATP to the autophosphorylating protein, Ptk, of the bacterium *Acinetobacter johnsonii*. FEBS Lett **445,** 137-143.

Du, J., Verzaux, E., Chaparro-Garcia, A., Bijsterbosch, G., Keizer, L.P., Zhou, J., Liebrand, T.W., Xie, C., Govers, F., and Robatzek, S. (2015). Elicitin recognition confers enhanced resistance to *Phytophthora infestans* in potato. Nature Plants **1**.

Du, L., Ali, G.S., Simons, K.A., Hou, J., Yang, T., Reddy, A.S., and Poovaiah, B.W. (2009). Ca(2+)/calmodulin regulates salicylic-acid-mediated plant immunity. Nature **457,** 1154-1158.

Dubiella, U., Seybold, H., Durian, G., Komander, E., Lassig, R., Witte, C.P., Schulze, W.X., and Romeis, T. (2013). Calcium-dependent protein kinase/NADPH oxidase activation circuit is required for rapid defense signal propagation. Proc Natl Acad Sci U S A **110,** 8744-8749.

Dunning, F.M., Sun, W., Jansen, K.L., Helft, L., and Bent, A.F. (2007). Identification and mutational analysis of Arabidopsis FLS2 leucine-rich repeat domain residues that contribute to flagellin perception. Plant Cell **19,** 3297-3313.

Ebrahim, S., Usha, K., and Singh, B. (2011). Pathogenesis related (PR) proteins in plant defense mechanism. Sci Against Microb Pathog **2,** 1043-1054.

Ellis, J.G., Rafiqi, M., Gan, P., Chakrabarti, A., and Dodds, P.N. (2009). Recent progress in discovery and functional analysis of effector proteins of fungal and oomycete plant pathogens. Curr Opin Plant Biol **12,** 399-405.

Fabro, G., Steinbrenner, J., Coates, M., Ishaque, N., Baxter, L., Studholme, D.J., Korner, E., Allen, R.L., Piquerez, S.J., Rougon-Cardoso, A., Greenshields, D., Lei, R., Badel, J.L., Caillaud, M.C., Sohn, K.H., Van den Ackerveken, G., Parker, J.E., Beynon, J., and Jones, J.D. (2011). Multiple candidate effectors from the oomycete pathogen *Hyaloperonospora arabidopsidis* suppress host plant immunity. PLoS Pathog **7,** e1002348.

Fawke, S., Doumane, M., and Schornack, S. (2015). Oomycete interactions with plants: infection strategies and resistance principles. Microbiol Mol Biol Rev **79,** 263-280.

Felix, G., and Boller, T. (2003). Molecular sensing of bacteria in plants. The highly conserved RNA-binding motif RNP-1 of bacterial cold shock proteins is recognized as an elicitor signal in tobacco. J Biol Chem **278,** 6201-6208.

Felix, G., Duran, J.D., Volko, S., and Boller, T. (1999). Plants have a sensitive perception system for the most conserved domain of bacterial flagellin. Plant J **18,** 265-276.

Felle, H.H., Herrmann, A., Hanstein, S., Huckelhoven, R., and Kogel, K.H. (2004). Apoplastic pH signaling in barley leaves attacked by the powdery mildew fungus *Blumeria graminis f. sp. hordei*. Mol Plant Microbe Interact **17,** 118-123.

Feng, F., and Zhou, J.M. (2012). Plant-bacterial pathogen interactions mediated by type III effectors. Curr Opin Plant Biol **15,** 469-476.

Feng, F., Yang, F., Rong, W., Wu, X., Zhang, J., Chen, S., He, C., and Zhou, J.M. (2012). A *Xanthomonas* uridine 5'-monophosphate transferase inhibits plant immune kinases. Nature **485,** 114-118.

Ferreira, R.B., Monteiro, S., Freitas, R., Santos, C.N., Chen, Z., Batista, L.M., Duarte, J., Borges, A., and Teixeira, A.R. (2007). The role of plant defence proteins in fungal pathogenesis. Mol Plant Pathol **8,** 677-700.

Fischer, C., Kugler, A., Hoth, S., and Dietrich, P. (2013). An IQ domain mediates the interaction with calmodulin in a plant cyclic nucleotide-gated channel. Plant Cell Physiol **54,** 573-584.

Fitzsimons, D.P., Herring, B.P., Stull, J.T., and Gallagher, P.J. (1992). Identification of basic residues involved in activation and calmodulin binding of rabbit smooth muscle myosin light chain kinase. J Biol Chem **267,** 23903-23909.

Fraiture, M., Zheng, X., and Brunner, F. (2014). An Arabidopsis and tomato mesophyll protoplast system for fast identification of early MAMP-triggered immunity-suppressing effectors. Methods Mol Biol **1127,** 213-230.

Fraser, C.M., and Chapple, C. (2011). The phenylpropanoid pathway in Arabidopsis. Arabidopsis Book **9,** e0152.

Frei dit Frey, N., Mbengue, M., Kwaaitaal, M., Nitsch, L., Altenbach, D., Haweker, H., Lozano-Duran, R., Njo, M.F., Beeckman, T., Huettel, B., Borst, J.W., Panstruga, R., and Robatzek, S. (2012). Plasma membrane calcium ATPases are important components of receptor-mediated signaling in plant immune responses and development. Plant Physiol **159,** 798-809.

Fritz-Laylin, L.K., Krishnamurthy, N., Tor, M., Sjolander, K.V., and Jones, J.D. (2005). Phylogenomic analysis of the receptor-like proteins of rice and Arabidopsis. Plant Physiol **138,** 611-623.

Furman-Matarasso, N., Cohen, E., Du, Q., Chejanovsky, N., Hanania, U., and Avni, A. (1999). A point mutation in the ethylene-inducing xylanase elicitor inhibits the beta-1-4-endoxylanase activity but not the elicitation activity. Plant Physiol **121,** 345-351.

Galletti, R., Ferrari, S., and De Lorenzo, G. (2011). Arabidopsis MPK3 and MPK6 play different roles in basal and oligogalacturonide- or flagellin-induced resistance against *Botrytis cinerea*. Plant Physiol **157,** 804-814.

Galon, Y., Nave, R., Boyce, J.M., Nachmias, D., Knight, M.R., and Fromm, H. (2008). Calmodulin-binding transcription activator (CAMTA) 3 mediates biotic defense responses in Arabidopsis. FEBS Lett **582,** 943-948.

Gao, M., Liu, J., Bi, D., Zhang, Z., Cheng, F., Chen, S., and Zhang, Y. (2008). MEKK1, MKK1/MKK2 and MPK4 function together in a mitogen-activated protein kinase cascade to regulate innate immunity in plants. Cell Res **18,** 1190-1198.

Gao, X., Chen, X., Lin, W., Chen, S., Lu, D., Niu, Y., Li, L., Cheng, C., McCormack, M., Sheen, J., Shan, L., and He, P. (2013). Bifurcation of Arabidopsis NLR immune signaling via Ca(2)(+)-dependent protein kinases. PLoS Pathog **9,** e1003127.

Gaulin, E., Drame, N., Lafitte, C., Torto-Alalibo, T., Martinez, Y., Ameline-Torregrosa, C., Khatib, M., Mazarguil, H., Villalba-Mateos, F., Kamoun, S., Mazars, C., Dumas, B., Bottin, A., Esquerre-Tugaye, M.T., and Rickauer, M. (2006). Cellulose binding domains of a Phytophthora cell wall protein are novel pathogen-associated molecular patterns. Plant Cell **18,** 1766-1777.

Genre, A., Ortu, G., Bertoldo, C., Martino, E., and Bonfante, P. (2009). Biotic and abiotic stimulation of root epidermal cells reveals common and specific responses to arbuscular mycorrhizal fungi. Plant Physiol **149,** 1424-1434.

Giacometti, S., Marrano, C.A., Bonza, M.C., Luoni, L., Limonta, M., and De Michelis, M.I. (2012). Phosphorylation of serine residues in the N-terminus modulates the activity of ACA8, a plasma membrane Ca2+-ATPase of Arabidopsis thaliana. J Exp Bot **63,** 1215-1224.

Gilroy, E.M., Taylor, R.M., Hein, I., Boevink, P., Sadanandom, A., and Birch, P.R. (2011). CMPG1-dependent cell death follows perception of diverse pathogen elicitors at the host plasma membrane and is suppressed by *Phytophthora infestans* RXLR effector AVR3a. New Phytol **190,** 653-666.

Gimenez-Ibanez, S., Hann, D.R., Ntoukakis, V., Petutschnig, E., Lipka, V., and Rathjen, J.P. (2009). AvrPtoB targets the LysM receptor kinase CERK1 to promote bacterial virulence on plants. Curr Biol **19,** 423-429.

Giraldo, M.C., and Valent, B. (2013). Filamentous plant pathogen effectors in action. Nat Rev Microbiol **11,** 800-814.

Glazebrook, J. (2005). Contrasting mechanisms of defense against biotrophic and necrotrophic pathogens. Annu Rev Phytopathol **43,** 205-227.

Gohre, V., and Robatzek, S. (2008). Breaking the barriers: microbial effector molecules subvert plant immunity. Annu Rev Phytopathol **46,** 189-215.

Gohre, V., Spallek, T., Haweker, H., Mersmann, S., Mentzel, T., Boller, T., de Torres, M., Mansfield, J.W., and Robatzek, S. (2008). Plant pattern-recognition receptor FLS2 is directed for degradation by the bacterial ubiquitin ligase AvrPtoB. Curr Biol **18,** 1824-1832.

Gomez-Gomez, L., and Boller, T. (2000). FLS2: an LRR receptor-like kinase involved in the perception of the bacterial elicitor flagellin in Arabidopsis. Mol Cell **5,** 1003-1011.

Grant, J.J., and Loake, G.J. (2000). Role of reactive oxygen intermediates and cognate redox signaling in disease resistance. Plant Physiol **124,** 21-29.

Grant, M., Brown, I., Adams, S., Knight, M., Ainslie, A., and Mansfield, J. (2000). The RPM1 plant disease resistance gene facilitates a rapid and sustained increase in cytosolic calcium that is necessary for the oxidative burst and hypersensitive cell death. Plant J **23,** 441-450.

Grouffaud, S., van West, P., Avrova, A.O., Birch, P.R., and Whisson, S.C. (2008). *Plasmodium falciparum* and *Hyaloperonospora parasitic*a effector translocation motifs are functional in *Phytophthora infestans*. Microbiology **154,** 3743-3751.

Guo, M., Kim, P., Li, G., Elowsky, C.G., and Alfano, J.R. (2016). A Bacterial Effector Co-opts Calmodulin to Target the Plant Microtubule Network. Cell Host Microbe **19,** 67-78.

Gupta, R., and Luan, S. (2003). Redox control of protein tyrosine phosphatases and mitogen-activated protein kinases in plants. Plant Physiol **132,** 1149-1152.

Gust, A.A., and Felix, G. (2014). Receptor like proteins associate with SOBIR1-type of adaptors to form bimolecular receptor kinases. Curr Opin Plant Biol **21,** 104-111.

Gust, A.A., Biswas, R., Lenz, H.D., Rauhut, T., Ranf, S., Kemmerling, B., Gotz, F., Glawischnig, E., Lee, J., Felix, G., and Nurnberger, T. (2007). Bacteria-derived peptidoglycans constitute pathogen-associated molecular patterns triggering innate immunity in Arabidopsis. J Biol Chem **282,** 32338-32348.

Haas, B.J., Kamoun, S., Zody, M.C., Jiang, R.H., Handsaker, R.E., Cano, L.M., Grabherr, M., Kodira, C.D., Raffaele, S., Torto-Alalibo, T., Bozkurt, T.O., Ah-Fong, A.M., Alvarado, L., Anderson, V.L., Armstrong, M.R., Avrova, A., Baxter, L., Beynon, J., Boevink, P.C., Bollmann, S.R., Bos, J.I., Bulone, V., Cai, G., Cakir, C., Carrington, J.C., Chawner, M., Conti, L., Costanzo, S., Ewan, R., Fahlgren, N., Fischbach, M.A., Fugelstad, J., Gilroy, E.M., Gnerre, S., Green, P.J., Grenville-Briggs, L.J., Griffith, J., Grunwald, N.J., Horn, K., Horner, N.R., Hu, C.H., Huitema, E., Jeong, D.H., Jones, A.M., Jones, J.D., Jones, R.W., Karlsson, E.K., Kunjeti, S.G., Lamour, K., Liu, Z., Ma, L., Maclean, D., Chibucos, M.C., McDonald, H., McWalters, J., Meijer, H.J., Morgan, W., Morris, P.F., Munro, C.A., O'Neill, K., Ospina-Giraldo, M., Pinzon, A., Pritchard, L., Ramsahoye, B., Ren, Q., Restrepo, S., Roy, S., Sadanandom, A., Savidor, A., Schornack, S., Schwartz, D.C., Schumann, U.D., Schwessinger, B., Seyer, L., Sharpe, T., Silvar, C., Song, J., Studholme, D.J., Sykes, S., Thines, M., van de Vondervoort, P.J., Phuntumart, V., Wawra, S., Weide, R., Win, J., Young, C., Zhou, S., Fry, W., Meyers, B.C., van West, P., Ristaino, J., Govers, F., Birch, P.R., Whisson, S.C., Judelson, H.S., and Nusbaum, C. (2009). Genome sequence and analysis of the Irish potato famine pathogen *Phytophthora infestans*. Nature **461,** 393-398.

Halim, V.A., Hunger, A., Macioszek, V., Landgraf, P., Nürnberger, T., Scheel, D., and Rosahl, S. (2004). The oligopeptide elicitor Pep-13 induces salicylic acid-dependent and-independent defense reactions in potato. Physiological and molecular plant pathology **64,** 311-318.

Halter, T., Imkampe, J., Mazzotta, S., Wierzba, M., Postel, S., Bucherl, C., Kiefer, C., Stahl, M., Chinchilla, D., Wang, X., Nurnberger, T., Zipfel, C., Clouse, S., Borst, J.W., Boeren, S., de Vries, S.C., Tax, F., and Kemmerling, B. (2014). The leucine-rich repeat receptor kinase BIR2 is a negative regulator of BAK1 in plant immunity. Curr Biol **24,** 134-143.

Hamann, T. (2012). Plant cell wall integrity maintenance as an essential component of biotic stress response mechanisms. Front Plant Sci **3,** 77.

Hann, D.R., and Rathjen, J.P. (2007). Early events in the pathogenicity of *Pseudomonas syringae* on *Nicotiana benthamiana*. Plant J **49,** 607-618.

Harding, S.A., Oh, S.H., and Roberts, D.M. (1997). Transgenic tobacco expressing a foreign calmodulin gene shows an enhanced production of active oxygen species. EMBO J **16,** 1137-1144.

Hartmann, J., Fischer, C., Dietrich, P., and Sauter, M. (2014). Kinase activity and calmodulin binding are essential for growth signaling by the phytosulfokine receptor PSKR1. Plant J **78,** 192-202.

Hauck, P., Thilmony, R., and He, S.Y. (2003). A *Pseudomonas syringae* type III effector suppresses cell wall-based extracellular defense in susceptible Arabidopsis plants. Proc Natl Acad Sci U S A **100,** 8577-8582.

He, P., Shan, L., Lin, N.C., Martin, G.B., Kemmerling, B., Nurnberger, T., and Sheen, J. (2006). Specific bacterial suppressors of MAMP signaling upstream of MAPKKK in Arabidopsis innate immunity. Cell **125,** 563-575.

Hemetsberger, C., Herrberger, C., Zechmann, B., Hillmer, M., and Doehlemann, G. (2012). The *Ustilago maydis* effector Pep1 suppresses plant immunity by inhibition of host peroxidase activity. PLoS Pathog **8,** e1002684.

Herring, B.P. (1991). Basic residues are important for Ca2+/calmodulin binding and activation but not autoinhibition of rabbit skeletal muscle myosin light chain kinase. J Biol Chem **266,** 11838-11841.

Higgins, C.F. (1992). ABC transporters: from microorganisms to man. Annu Rev Cell Biol **8,** 67-113.

Higgins, C.F., Hiles, I.D., Salmond, G.P., Gill, D.R., Downie, J.A., Evans, I.J., Holland, I.B., Gray, L., Buckel, S.D., Bell, A.W., and et al. (1986). A family of related ATP-binding subunits coupled to many distinct biological processes in bacteria. Nature **323,** 448-450.

Hoeflich, K.P., and Ikura, M. (2002). Calmodulin in action: diversity in target recognition and activation mechanisms. Cell **108,** 739-742.

Hok, S., Danchin, E.G., Allasia, V., Panabieres, F., Attard, A., and Keller, H. (2011). An Arabidopsis (malectin-like) leucine-rich repeat receptor-like kinase contributes to downy mildew disease. Plant Cell Environ **34,** 1944-1957.

Hok, S., Allasia, V., Andrio, E., Naessens, E., Ribes, E., Panabieres, F., Attard, A., Ris, N., Clement, M., Barlet, X., Marco, Y., Grill, E., Eichmann, R., Weis, C., Huckelhoven, R., Ammon, A., Ludwig-Muller, J., Voll, L.M., and Keller, H. (2014). The receptor kinase IMPAIRED OOMYCETE SUSCEPTIBILITY1 attenuates abscisic acid responses in Arabidopsis. Plant physiology **166,** 1506-1518.

Hua, B.-G., Mercier, R.W., Zielinski, R.E., and Berkowitz, G.A. (2003). Functional interaction of calmodulin with a plant cyclic nucleotide gated cation channel. Plant Physiology and Biochemistry **41,** 945-954.

Ingle, R.A., Carstens, M., and Denby, K.J. (2006). PAMP recognition and the plant-pathogen arms race. Bioessays **28,** 880-889.

Jehle, A.K., Lipschis, M., Albert, M., Fallahzadeh-Mamaghani, V., Furst, U., Mueller, K., and Felix, G. (2013). The receptor-like protein ReMAX of Arabidopsis detects the microbe-associated molecular pattern eMax from Xanthomonas. Plant Cell **25,** 2330-2340.

Jeworutzki, E., Roelfsema, M.R., Anschutz, U., Krol, E., Elzenga, J.T., Felix, G., Boller, T., Hedrich, R., and Becker, D. (2010). Early signaling through the Arabidopsis pattern recognition receptors FLS2 and EFR involves Ca^{2+}-associated opening of plasma membrane anion channels. Plant J **62,** 367-378.

Jiang, R.H., Tripathy, S., Govers, F., and Tyler, B.M. (2008). RXLR effector reservoir in two *Phytophthora* species is dominated by a single rapidly evolving superfamily with more than 700 members. Proc Natl Acad Sci U S A **105,** 4874-4879.

Jones, J.D., and Dangl, J.L. (2006). The plant immune system. Nature **444,** 323-329.

Judelson, H.S., and Blanco, F.A. (2005). The spores of Phytophthora: weapons of the plant destroyer. Nat Rev Microbiol **3,** 47-58.

Juranic, N., Atanasova, E., Filoteo, A.G., Macura, S., Prendergast, F.G., Penniston, J.T., and Strehler, E.E. (2010). Calmodulin wraps around its binding domain in the plasma membrane Ca^{2+} pump anchored by a novel 18-1 motif. J Biol Chem **285,** 4015-4024.

Kadota, Y., Shirasu, K., and Zipfel, C. (2015). Regulation of the NADPH Oxidase RBOHD During Plant Immunity. Plant Cell Physiol.

Kadota, Y., Sklenar, J., Derbyshire, P., Stransfeld, L., Asai, S., Ntoukakis, V., Jones, J.D., Shirasu, K., Menke, F., Jones, A., and Zipfel, C. (2014). Direct regulation of the NADPH oxidase RBOHD by the PRR-associated kinase BIK1 during plant immunity. Mol Cell **54,** 43-55.

Kaku, H., Nishizawa, Y., Ishii-Minami, N., Akimoto-Tomiyama, C., Dohmae, N., Takio, K., Minami, E., and Shibuya, N. (2006). Plant cells recognize chitin fragments for defense signaling through a plasma membrane receptor. Proc Natl Acad Sci U S A **103,** 11086-11091.

Kamoun, S. (2007). Groovy times: filamentous pathogen effectors revealed. Curr Opin Plant Biol **10,** 358-365.

Kamper, J., Kahmann, R., Bolker, M., Ma, L.J., Brefort, T., Saville, B.J., Banuett, F., Kronstad, J.W., Gold, S.E., Muller, O., Perlin, M.H., Wosten, H.A., de Vries, R., Ruiz-Herrera, J., Reynaga-Pena, C.G., Snetselaar, K., McCann, M., Perez-Martin, J., Feldbrugge, M., Basse, C.W., Steinberg, G., Ibeas, J.I., Holloman, W., Guzman, P., Farman, M., Stajich, J.E., Sentandreu, R., Gonzalez-Prieto, J.M., Kennell, J.C., Molina, L., Schirawski, J., Mendoza-Mendoza, A., Greilinger, D., Munch, K., Rossel, N., Scherer, M., Vranes, M., Ladendorf, O., Vincon, V., Fuchs, U., Sandrock, B., Meng, S., Ho, E.C., Cahill, M.J., Boyce, K.J., Klose, J., Klosterman, S.J., Deelstra, H.J., Ortiz-Castellanos, L., Li, W., Sanchez-Alonso, P., Schreier, P.H., Hauser-Hahn, I., Vaupel, M., Koopmann, E., Friedrich, G., Voss, H., Schluter, T., Margolis, J., Platt, D., Swimmer, C., Gnirke, A., Chen, F., Vysotskaia, V., Mannhaupt, G., Guldener, U., Munsterkotter, M., Haase, D., Oesterheld, M., Mewes, H.W., Mauceli, E.W., DeCaprio, D., Wade, C.M., Butler, J., Young, S., Jaffe, D.B., Calvo, S., Nusbaum, C., Galagan, J., and Birren, B.W. (2006). Insights from the genome of the biotrophic fungal plant pathogen Ustilago maydis. Nature **444,** 97-101.

Kaplan, B., Sherman, T., and Fromm, H. (2007). Cyclic nucleotide-gated channels in plants. FEBS letters **581,** 2237-2246.

Karimi, M., Inze, D., and Depicker, A. (2002). GATEWAY vectors for Agrobacterium-mediated plant transformation. Trends Plant Sci **7,** 193-195.

Kaschani, F., Shabab, M., Bozkurt, T., Shindo, T., Schornack, S., Gu, C., Ilyas, M., Win, J., Kamoun, S., and van der Hoorn, R.A. (2010). An effector-targeted protease contributes to defense against *Phytophthora infestans* and is under diversifying selection in natural hosts. Plant Physiol **154,** 1794-1804.

Katou, S., Kuroda, K., Seo, S., Yanagawa, Y., Tsuge, T., Yamazaki, M., Miyao, A., Hirochika, H., and Ohashi, Y. (2007). A calmodulin-binding mitogen-activated protein kinase phosphatase is induced by wounding and regulates the activities of stress-related mitogen-activated protein kinases in rice. Plant Cell Physiol **48,** 332-344.

Kazan, K., and Lyons, R. (2014). Intervention of Phytohormone Pathways by Pathogen Effectors. Plant Cell **26,** 2285-2309.

Kemen, E., and Jones, J.D. (2012). Obligate biotroph parasitism: can we link genomes to lifestyles? Trends Plant Sci **17,** 448-457.

Kim, J.G., Taylor, K.W., Hotson, A., Keegan, M., Schmelz, E.A., and Mudgett, M.B. (2008). XopD SUMO protease affects host transcription, promotes pathogen growth, and delays symptom development in *Xanthomonas*-infected tomato leaves. Plant Cell **20,** 1915-1929.

Kim, M.C., Panstruga, R., Elliott, C., Muller, J., Devoto, A., Yoon, H.W., Park, H.C., Cho, M.J., and Schulze-Lefert, P. (2002). Calmodulin interacts with MLO protein to regulate defence against mildew in barley. Nature **416,** 447-451.

King, S.R., McLellan, H., Boevink, P.C., Armstrong, M.R., Bukharova, T., Sukarta, O., Win, J., Kamoun, S., Birch, P.R., and Banfield, M.J. (2014). *Phytophthora infestans* RXLR effector PexRD2 interacts with host MAPKKK epsilon to suppress plant immune signaling. Plant Cell **26,** 1345-1359.

Klarzynski, O., Plesse, B., Joubert, J.M., Yvin, J.C., Kopp, M., Kloareg, B., and Fritig, B. (2000). Linear beta-1,3 glucans are elicitors of defense responses in tobacco. Plant Physiol **124,** 1027-1038.

Knight, M.R., Campbell, A.K., Smith, S.M., and Trewavas, A.J. (1991). Transgenic plant aequorin reports the effects of touch and cold-shock and elicitors on cytoplasmic calcium. Nature **352,** 524-526.

Knight, M.R., Read, N.D., Campbell, A.K., and Trewavas, A.J. (1993). Imaging calcium dynamics in living plants using semi-synthetic recombinant aequorins. J Cell Biol **121,** 83-90.

Kobayashi, M., Ohura, I., Kawakita, K., Yokota, N., Fujiwara, M., Shimamoto, K., Doke, N., and Yoshioka, H. (2007). Calcium-dependent protein kinases regulate the production of reactive oxygen species by potato NADPH oxidase. Plant Cell **19,** 1065-1080.

Koeck, M., Hardham, A.R., and Dodds, P.N. (2011). The role of effectors of biotrophic and hemibiotrophic fungi in infection. Cell Microbiol **13,** 1849-1857.

Kong, G., Zhao, Y., Jing, M., Huang, J., Yang, J., Xia, Y., Kong, L., Ye, W., Xiong, Q., Qiao, Y., Dong, S., Ma, W., and Wang, Y. (2015). The Activation of Phytophthora Effector Avr3b by Plant Cyclophilin is Required for the Nudix Hydrolase Activity of Avr3b. PLoS Pathog **11,** e1005139.

Kouzai, Y., Nakajima, K., Hayafune, M., Ozawa, K., Kaku, H., Shibuya, N., Minami, E., and Nishizawa, Y. (2014). CEBiP is the major chitin oligomer-binding protein in rice and plays a main role in the perception of chitin oligomers. Plant Mol Biol **84,** 519-528.

Krol, E., Mentzel, T., Chinchilla, D., Boller, T., Felix, G., Kemmerling, B., Postel, S., Arents, M., Jeworutzki, E., Al-Rasheid, K.A., Becker, D., and Hedrich, R. (2010). Perception of the Arabidopsis danger signal peptide 1 involves the pattern recognition receptor AtPEPR1 and its close homologue AtPEPR2. J Biol Chem **285,** 13471-13479.

Kudla, J., Batistic, O., and Hashimoto, K. (2010). Calcium signals: the lead currency of plant information processing. Plant Cell **22,** 541-563.

Kugler, A., Kohler, B., Palme, K., Wolff, P., and Dietrich, P. (2009). Salt-dependent regulation of a CNG channel subfamily in Arabidopsis. BMC Plant Biol **9,** 140.

Kumar, V., Chichili, V.P., Zhong, L., Tang, X., Velazquez-Campoy, A., Sheu, F.S., Seetharaman, J., Gerges, N.Z., and Sivaraman, J. (2013). Structural basis for the interaction of unstructured neuron specific substrates neuromodulin and neurogranin with Calmodulin. Sci Rep **3,** 1392.

Kunze, G., Zipfel, C., Robatzek, S., Niehaus, K., Boller, T., and Felix, G. (2004). The N terminus of bacterial elongation factor Tu elicits innate immunity in Arabidopsis plants. Plant Cell **16,** 3496-3507.

Kushwaha, R., Singh, A., and Chattopadhyay, S. (2008). Calmodulin7 plays an important role as transcriptional regulator in Arabidopsis seedling development. Plant Cell **20,** 1747-1759.

Ladwig, F., Dahlke, R.I., Stuhrwohldt, N., Hartmann, J., Harter, K., and Sauter, M. (2015). Phytosulfokine Regulates Growth in Arabidopsis through a Response Module at the Plasma Membrane That Includes CYCLIC NUCLEOTIDE-GATED CHANNEL17, H+-ATPase, and BAK1. Plant Cell **27,** 1718-1729.

Laemmli, U.K. (1970). Cleavage of structural proteins during the assembly of the head of bacteriophage T4. Nature **227,** 680-685.

Le Roux, C., Huet, G., Jauneau, A., Camborde, L., Tremousaygue, D., Kraut, A., Zhou, B., Levaillant, M., Adachi, H., Yoshioka, H., Raffaele, S., Berthome, R., Coute, Y., Parker, J.E., and Deslandes, L. (2015). A receptor pair with an integrated decoy converts pathogen disabling of transcription factors to immunity. Cell **161,** 1074-1088.

Lee, H.A., Kim, S.Y., Oh, S.K., Yeom, S.I., Kim, S.B., Kim, M.S., Kamoun, S., and Choi, D. (2014). Multiple recognition of RXLR effectors is associated with nonhost resistance of pepper against *Phytophthora infestans*. New Phytol **203,** 926-938.

Lee, J., Eschen-Lippold, L., Lassowskat, I., Bottcher, C., and Scheel, D. (2015). Cellular reprogramming through mitogen-activated protein kinases. Front Plant Sci **6,** 940.

Lehtonen, M.T., Akita, M., Frank, W., Reski, R., and Valkonen, J.P. (2012). Involvement of a class III peroxidase and the mitochondrial protein TSPO in oxidative burst upon treatment of moss plants with a fungal elicitor. Mol Plant Microbe Interact **25,** 363-371.

Leppla, S.H. (1982). Anthrax toxin edema factor: a bacterial adenylate cyclase that increases cyclic AMP concentrations of eukaryotic cells. Proc Natl Acad Sci U S A **79,** 3162-3166.

Lewis, L.A., Polanski, K., de Torres-Zabala, M., Jayaraman, S., Bowden, L., Moore, J., Penfold, C.A., Jenkins, D.J., Hill, C., Baxter, L., Kulasekaran, S., Truman, W., Littlejohn, G., Prusinska, J., Mead, A., Steinbrenner, J., Hickman, R., Rand, D., Wild, D.L., Ott, S., Buchanan-Wollaston, V., Smirnoff, N., Beynon, J., Denby, K., and Grant, M. (2015). Transcriptional Dynamics Driving MAMP-Triggered Immunity and Pathogen Effector-Mediated Immunosuppression in Arabidopsis Leaves Following Infection with *Pseudomonas syringae pv tomato* DC3000. Plant Cell **27,** 3038-3064.

Li, F., Huang, C., Li, Z., and Zhou, X. (2014a). Suppression of RNA silencing by a plant DNA virus satellite requires a host calmodulin-like protein to repress RDR6 expression. PLoS Pathog **10,** e1003921.

Li, L., Li, M., Yu, L., Zhou, Z., Liang, X., Liu, Z., Cai, G., Gao, L., Zhang, X., Wang, Y., Chen, S., and Zhou, J.M. (2014b). The FLS2-associated kinase BIK1 directly phosphorylates the NADPH oxidase RbohD to control plant immunity. Cell Host Microbe **15,** 329-338.

Li, X., Lin, H., Zhang, W., Zou, Y., Zhang, J., Tang, X., and Zhou, J.M. (2005). Flagellin induces innate immunity in nonhost interactions that is suppressed by *Pseudomonas syringae* effectors. Proc Natl Acad Sci U S A **102,** 12990-12995.

Libault, M., Wan, J., Czechowski, T., Udvardi, M., and Stacey, G. (2007). Identification of 118 Arabidopsis transcription factor and 30 ubiquitin-ligase genes responding to chitin, a plant-defense elicitor. Mol Plant Microbe Interact **20,** 900-911.

Liebrand, T.W., van den Burg, H.A., and Joosten, M.H. (2014). Two for all: receptor-associated kinases SOBIR1 and BAK1. Trends Plant Sci **19,** 123-132.

Liu, T., Liu, Z., Song, C., Hu, Y., Han, Z., She, J., Fan, F., Wang, J., Jin, C., Chang, J., Zhou, J.M., and Chai, J. (2012). Chitin-induced dimerization activates a plant immune receptor. Science **336,** 1160-1164.

Liu, W., Liu, J., Triplett, L., Leach, J.E., and Wang, G.L. (2014). Novel insights into rice innate immunity against bacterial and fungal pathogens. Annu Rev Phytopathol **52,** 213-241.

Lo Presti, L., Lanver, D., Schweizer, G., Tanaka, S., Liang, L., Tollot, M., Zuccaro, A., Reissmann, S., and Kahmann, R. (2015). Fungal effectors and plant susceptibility. Annu Rev Plant Biol **66,** 513-545.

Ma, W., Smigel, A., Tsai, Y.C., Braam, J., and Berkowitz, G.A. (2008). Innate immunity signaling: cytosolic Ca^{2+} elevation is linked to downstream nitric oxide generation through the action of calmodulin or a calmodulin-like protein. Plant Physiol **148,** 818-828.

Ma, Z., Song, T., Zhu, L., Ye, W., Wang, Y., Shao, Y., Dong, S., Zhang, Z., Dou, D., Zheng, X., Tyler, B.M., and Wang, Y. (2015). A *Phytophthora sojae* Glycoside Hydrolase 12 Protein Is a Major Virulence Factor during Soybean Infection and Is Recognized as a PAMP. Plant Cell **27,** 2057-2072.

Macho, A.P., and Zipfel, C. (2014). Plant PRRs and the activation of innate immune signaling. Mol Cell **54,** 263-272.

Manzoor, H., Kelloniemi, J., Chiltz, A., Wendehenne, D., Pugin, A., Poinssot, B., and Garcia-Brugger, A. (2013). Involvement of the glutamate receptor AtGLR3.3 in plant defense signaling and resistance to *Hyaloperonospora arabidopsidis*. Plant J **76,** 466-480.

Mao, G., Meng, X., Liu, Y., Zheng, Z., Chen, Z., and Zhang, S. (2011). Phosphorylation of a WRKY transcription factor by two pathogen-responsive MAPKs drives phytoalexin biosynthesis in Arabidopsis. Plant Cell **23,** 1639-1653.

Maximciuc, A.A., Putkey, J.A., Shamoo, Y., and Mackenzie, K.R. (2006). Complex of calmodulin with a ryanodine receptor target reveals a novel, flexible binding mode. Structure **14,** 1547-1556.

Mazurkiewicz, P., Thomas, J., Thompson, J.A., Liu, M., Arbibe, L., Sansonetti, P., and Holden, D.W. (2008). SpvC is a *Salmonella* effector with phosphothreonine lyase activity on host mitogen-activated protein kinases. Mol Microbiol **67,** 1371-1383.

McCormack, E., Tsai, Y.C., and Braam, J. (2005). Handling calcium signaling: Arabidopsis CaMs and CMLs. Trends Plant Sci **10,** 383-389.

McLellan, H., Boevink, P.C., Armstrong, M.R., Pritchard, L., Gomez, S., Morales, J., Whisson, S.C., Beynon, J.L., and Birch, P.R. (2013). An RxLR effector from Phytophthora infestans

prevents re-localisation of two plant NAC transcription factors from the endoplasmic reticulum to the nucleus. PLoS Pathog **9,** e1003670.

Meador, W.E., Means, A.R., and Quiocho, F.A. (1992). Target enzyme recognition by calmodulin: 2.4 A structure of a calmodulin-peptide complex. Science **257,** 1251-1255.

Medzhitov, R., and Janeway, C.A., Jr. (1997). Innate immunity: the virtues of a nonclonal system of recognition. Cell **91,** 295-298.

Melech-Bonfil, S., and Sessa, G. (2010). Tomato MAPKKKepsilon is a positive regulator of cell-death signaling networks associated with plant immunity. Plant J **64,** 379-391.

Melech-Bonfil, S., and Sessa, G. (2011). The SlMKK2 and SlMPK2 genes play a role in tomato disease resistance to *Xanthomonas campestris pv. vesicatoria*. Plant Signal Behav **6,** 154-156.

Melotto, M., Underwood, W., and He, S.Y. (2008). Role of stomata in plant innate immunity and foliar bacterial diseases. Annu Rev Phytopathol **46,** 101-122.

Melotto, M., Underwood, W., Koczan, J., Nomura, K., and He, S.Y. (2006). Plant stomata function in innate immunity against bacterial invasion. Cell **126,** 969-980.

Meng, X., and Zhang, S. (2013). MAPK cascades in plant disease resistance signaling. Annu Rev Phytopathol **51,** 245-266.

Mentlak, T.A., Kombrink, A., Shinya, T., Ryder, L.S., Otomo, I., Saitoh, H., Terauchi, R., Nishizawa, Y., Shibuya, N., Thomma, B.P., and Talbot, N.J. (2012). Effector-mediated suppression of chitin-triggered immunity by *Magnaporthe oryzae* is necessary for rice blast disease. Plant Cell **24,** 322-335.

Meyers, B.C., Kozik, A., Griego, A., Kuang, H., and Michelmore, R.W. (2003). Genome-wide analysis of NBS-LRR-encoding genes in Arabidopsis. Plant Cell **15,** 809-834.

Miller, J.B., Pratap, A., Miyahara, A., Zhou, L., Bornemann, S., Morris, R.J., and Oldroyd, G.E. (2013). Calcium/Calmodulin-dependent protein kinase is negatively and positively regulated by calcium, providing a mechanism for decoding calcium responses during symbiosis signaling. Plant Cell **25,** 5053-5066.

Miya, A., Albert, P., Shinya, T., Desaki, Y., Ichimura, K., Shirasu, K., Narusaka, Y., Kawakami, N., Kaku, H., and Shibuya, N. (2007). CERK1, a LysM receptor kinase, is essential for chitin elicitor signaling in Arabidopsis. Proc Natl Acad Sci U S A **104,** 19613-19618.

Moon, B.C., Choi, M.S., Kang, Y.H., Kim, M.C., Cheong, M.S., Park, C.Y., Yoo, J.H., Koo, S.C., Lee, S.M., Lim, C.O., Cho, M.J., and Chung, W.S. (2005). Arabidopsis ubiquitin-specific protease 6 (AtUBP6) interacts with calmodulin. FEBS Lett **579,** 3885-3890.

Mruk, K., Farley, B.M., Ritacco, A.W., and Kobertz, W.R. (2014). Calmodulation meta-analysis: predicting calmodulin binding via canonical motif clustering. J Gen Physiol **144,** 105-114.

Mueller, A.N., Ziemann, S., Treitschke, S., Assmann, D., and Doehlemann, G. (2013). Compatibility in the *Ustilago maydis*-maize interaction requires inhibition of host cysteine proteases by the fungal effector Pit2. PLoS Pathog **9,** e1003177.

Mukhtar, M.S., Carvunis, A.R., Dreze, M., Epple, P., Steinbrenner, J., Moore, J., Tasan, M., Galli, M., Hao, T., Nishimura, M.T., Pevzner, S.J., Donovan, S.E., Ghamsari, L., Santhanam, B., Romero, V., Poulin, M.M., Gebreab, F., Gutierrez, B.J., Tam, S., Monachello, D., Boxem, M., Harbort, C.J., McDonald, N., Gai, L., Chen, H., He, Y., European Union Effectoromics, C., Vandenhaute, J., Roth, F.P., Hill, D.E., Ecker, J.R., Vidal, M., Beynon, J., Braun, P., and Dangl, J.L. (2011). Independently evolved virulence effectors converge onto hubs in a plant immune system network. Science **333,** 596-601.

Naito, K., Taguchi, F., Suzuki, T., Inagaki, Y., Toyoda, K., Shiraishi, T., and Ichinose, Y. (2008). Amino acid sequence of bacterial microbe-associated molecular pattern flg22 is required for virulence. Mol Plant Microbe Interact **21,** 1165-1174.

Nakahara, K.S., Masuta, C., Yamada, S., Shimura, H., Kashihara, Y., Wada, T.S., Meguro, A., Goto, K., Tadamura, K., Sueda, K., Sekiguchi, T., Shao, J., Itchoda, N., Matsumura, T., Igarashi, M., Ito, K., Carthew, R.W., and Uyeda, I. (2012). Tobacco calmodulin-like protein provides secondary defense by binding to and directing degradation of virus RNA silencing suppressors. Proc Natl Acad Sci U S A **109,** 10113-10118.

Narvaez-Vasquez, J., and Ryan, C.A. (2004). The cellular localization of prosystemin: a functional role for phloem parenchyma in systemic wound signaling. Planta **218,** 360-369.

Navarro, L., Zipfel, C., Rowland, O., Keller, I., Robatzek, S., Boller, T., and Jones, J.D. (2004). The transcriptional innate immune response to flg22. Interplay and overlap with Avr gene-dependent defense responses and bacterial pathogenesis. Plant Physiol **135,** 1113-1128.

Neumann, C., Fraiture, M., Hernandez-Reyes, C., Akum, F.N., Virlogeux-Payant, I., Chen, Y., Pateyron, S., Colcombet, J., Kogel, K.H., Hirt, H., Brunner, F., and Schikora, A. (2014). The *Salmonella* effector protein SpvC, a phosphothreonine lyase is functional in plant cells. Front Microbiol **5,** 548.

Newman, M.A., Daniels, M.J., and Dow, J.M. (1995). Lipopolysaccharide from *Xanthomonas campestris* induces defense-related gene expression in *Brassica campestris*. Mol Plant Microbe Interact **8,** 778-780.

Newman, M.A., Sundelin, T., Nielsen, J.T., and Erbs, G. (2013). MAMP (microbe-associated molecular pattern) triggered immunity in plants. Front Plant Sci **4,** 139.

Nguyen, H.P., Chakravarthy, S., Velasquez, A.C., McLane, H.L., Zeng, L., Nakayashiki, H., Park, D.H., Collmer, A., and Martin, G.B. (2010). Methods to study PAMP-triggered immunity using tomato and *Nicotiana benthamiana*. Mol Plant Microbe Interact **23,** 991-999.

Nicaise, V., Roux, M., and Zipfel, C. (2009). Recent advances in PAMP-triggered immunity against bacteria: pattern recognition receptors watch over and raise the alarm. Plant Physiol **150,** 1638-1647.

Nie, H., Zhao, C., Wu, G., Wu, Y., Chen, Y., and Tang, D. (2012). SR1, a calmodulin-binding transcription factor, modulates plant defense and ethylene-induced senescence by directly regulating NDR1 and EIN3. Plant Physiol **158,** 1847-1859.

Niepmann, M., and Zheng, J. (2006). Discontinuous native protein gel electrophoresis. Electrophoresis **27,** 3949-3951.

Nishiwaki, T., Iwasaki, H., Ishiura, M., and Kondo, T. (2000). Nucleotide binding and autophosphorylation of the clock protein KaiC as a circadian timing process of cyanobacteria. Proc Natl Acad Sci U S A **97,** 495-499.

Noirot, E., Der, C., Lherminier, J., Robert, F., Moricova, P., Kieu, K., Leborgne-Castel, N., Simon-Plas, F., and Bouhidel, K. (2014). Dynamic changes in the subcellular distribution of the tobacco ROS-producing enzyme RBOHD in response to the oomycete elicitor cryptogein. J Exp Bot **65,** 5011-5022.

Nomura, H., Komori, T., Uemura, S., Kanda, Y., Shimotani, K., Nakai, K., Furuichi, T., Takebayashi, K., Sugimoto, T., Sano, S., Suwastika, I.N., Fukusaki, E., Yoshioka, H., Nakahira, Y., and Shiina, T. (2012). Chloroplast-mediated activation of plant immune signalling in Arabidopsis. Nat Commun **3,** 926.

Nuhse, T.S., Peck, S.C., Hirt, H., and Boller, T. (2000). Microbial elicitors induce activation and dual phosphorylation of the Arabidopsis thaliana MAPK 6. J Biol Chem **275,** 7521-7526.

Nuhse, T.S., Bottrill, A.R., Jones, A.M., and Peck, S.C. (2007). Quantitative phosphoproteomic analysis of plasma membrane proteins reveals regulatory mechanisms of plant innate immune responses. Plant J **51,** 931-940.

Nurnberger, T., and Brunner, F. (2002). Innate immunity in plants and animals: emerging parallels between the recognition of general elicitors and pathogen-associated molecular patterns. Curr Opin Plant Biol **5,** 318-324.

O'Brien, J.A., Daudi, A., Finch, P., Butt, V.S., Whitelegge, J.P., Souda, P., Ausubel, F.M., and Bolwell, G.P. (2012). A peroxidase-dependent apoplastic oxidative burst in cultured Arabidopsis cells functions in MAMP-elicited defense. Plant Physiol **158,** 2013-2027.

O'Connell, R.J., and Panstruga, R. (2006). Tete a tete inside a plant cell: establishing compatibility between plants and biotrophic fungi and oomycetes. New Phytol **171,** 699-718.

O'Neil, K.T., and DeGrado, W.F. (1990). How calmodulin binds its targets: sequence independent recognition of amphiphilic α-helices. Trends in biochemical sciences **15,** 59-64.

Oh, S.K., Kwon, S.Y., and Choi, D. (2014). Rpi-blb2-Mediated Hypersensitive Cell Death Caused by *Phytophthora infestans* AVRblb2 Requires SGT1, but not EDS1, NDR1, Salicylic Acid-, Jasmonic Acid-, or Ethylene-Mediated Signaling. Plant Pathol J **30,** 254-260.

Oh, S.K., Young, C., Lee, M., Oliva, R., Bozkurt, T.O., Cano, L.M., Win, J., Bos, J.I., Liu, H.Y., van Damme, M., Morgan, W., Choi, D., Van der Vossen, E.A., Vleeshouwers, V.G., and Kamoun, S. (2009). In planta expression screens of Phytophthora infestans RXLR effectors

reveal diverse phenotypes, including activation of the *Solanum bulbocastanum* disease resistance protein Rpi-blb2. Plant Cell **21,** 2928-2947.

Oliva, R.F., Cano, L., Raffaele, S., Win, J., Bozkurt, T.O., Belhaj, K., Oh, S., Thines, M., and Kamoun, S. (2015). A recent expansion of the RXLR effector gene Avrblb2 is maintained in global populations of *Phytophthora infestans* indicating different contributions to virulence. Mol Plant Microbe Interact.

Oome, S., Raaymakers, T.M., Cabral, A., Samwel, S., Bohm, H., Albert, I., Nurnberger, T., and Van den Ackerveken, G. (2014). Nep1-like proteins from three kingdoms of life act as a microbe-associated molecular pattern in Arabidopsis. Proc Natl Acad Sci U S A **111,** 16955-16960.

Panstruga, R., and Dodds, P.N. (2009). Terrific protein traffic: the mystery of effector protein delivery by filamentous plant pathogens. Science **324,** 748-750.

Park, C.H., Chen, S., Shirsekar, G., Zhou, B., Khang, C.H., Songkumarn, P., Afzal, A.J., Ning, Y., Wang, R., Bellizzi, M., Valent, B., and Wang, G.L. (2012). The *Magnaporthe oryzae* effector AvrPiz-t targets the RING E3 ubiquitin ligase APIP6 to suppress pathogen-associated molecular pattern-triggered immunity in rice. Plant Cell **24,** 4748-4762.

Pedley, K.F., and Martin, G.B. (2004). Identification of MAPKs and their possible MAPK kinase activators involved in the Pto-mediated defense response of tomato. J Biol Chem **279,** 49229-49235.

Petre, B., and Kamoun, S. (2014). How do filamentous pathogens deliver effector proteins into plant cells? PLoS Biol **12,** e1001801.

Petutschnig, E.K., Jones, A.M., Serazetdinova, L., Lipka, U., and Lipka, V. (2010). The lysin motif receptor-like kinase (LysM-RLK) CERK1 is a major chitin-binding protein in Arabidopsis thaliana and subject to chitin-induced phosphorylation. J Biol Chem **285,** 28902-28911.

Pieterse, C.M., Leon-Reyes, A., Van der Ent, S., and Van Wees, S.C. (2009). Networking by small-molecule hormones in plant immunity. Nat Chem Biol **5,** 308-316.

Pitzschke, A., Schikora, A., and Hirt, H. (2009a). MAPK cascade signalling networks in plant defence. Curr Opin Plant Biol **12,** 421-426.

Pitzschke, A., Djamei, A., Bitton, F., and Hirt, H. (2009b). A major role of the MEKK1-MKK1/2-MPK4 pathway in ROS signalling. Mol Plant **2,** 120-137.

Pogany, M., von Rad, U., Grun, S., Dongo, A., Pintye, A., Simoneau, P., Bahnweg, G., Kiss, L., Barna, B., and Durner, J. (2009). Dual roles of reactive oxygen species and NADPH oxidase RBOHD in an Arabidopsis-Alternaria pathosystem. Plant Physiol **151,** 1459-1475.

Poovaiah, B.W., Du, L., Wang, H., and Yang, T. (2013). Recent advances in calcium/calmodulin-mediated signaling with an emphasis on plant-microbe interactions. Plant Physiol **163,** 531-542.

Qi, Z., Verma, R., Gehring, C., Yamaguchi, Y., Zhao, Y., Ryan, C.A., and Berkowitz, G.A. (2010). Ca2+ signaling by plant Arabidopsis thaliana Pep peptides depends on AtPepR1, a receptor with guanylyl cyclase activity, and cGMP-activated Ca2+ channels. Proc Natl Acad Sci U S A **107,** 21193-21198.

Qiao, Y., Shi, J., Zhai, Y., Hou, Y., and Ma, W. (2015). Phytophthora effector targets a novel component of small RNA pathway in plants to promote infection. Proc Natl Acad Sci U S A **112,** 5850-5855.

Qiao, Y., Liu, L., Xiong, Q., Flores, C., Wong, J., Shi, J., Wang, X., Liu, X., Xiang, Q., Jiang, S., Zhang, F., Wang, Y., Judelson, H.S., Chen, X., and Ma, W. (2013). Oomycete pathogens encode RNA silencing suppressors. Nat Genet **45,** 330-333.

Qiu, J.L., Zhou, L., Yun, B.W., Nielsen, H.B., Fiil, B.K., Petersen, K., Mackinlay, J., Loake, G.J., Mundy, J., and Morris, P.C. (2008a). Arabidopsis mitogen-activated protein kinase kinases MKK1 and MKK2 have overlapping functions in defense signaling mediated by MEKK1, MPK4, and MKS1. Plant Physiol **148,** 212-222.

Qiu, J.L., Fiil, B.K., Petersen, K., Nielsen, H.B., Botanga, C.J., Thorgrimsen, S., Palma, K., Suarez-Rodriguez, M.C., Sandbech-Clausen, S., Lichota, J., Brodersen, P., Grasser, K.D., Mattsson, O., Glazebrook, J., Mundy, J., and Petersen, M. (2008b). Arabidopsis MAP kinase 4 regulates gene expression through transcription factor release in the nucleus. EMBO J **27,** 2214-2221.

Qutob, D., Kemmerling, B., Brunner, F., Kufner, I., Engelhardt, S., Gust, A.A., Luberacki, B., Seitz, H.U., Stahl, D., Rauhut, T., Glawischnig, E., Schween, G., Lacombe, B., Watanabe, N., Lam, E., Schlichting, R., Scheel, D., Nau, K., Dodt, G., Hubert, D., Gijzen, M., and Nurnberger, T. (2006). Phytotoxicity and innate immune responses induced by Nep1-like proteins. Plant Cell **18,** 3721-3744.

Raffaele, S., and Kamoun, S. (2012). Genome evolution in filamentous plant pathogens: why bigger can be better. Nat Rev Microbiol **10,** 417-430.

Ranf, S., Eschen-Lippold, L., Pecher, P., Lee, J., and Scheel, D. (2011). Interplay between calcium signalling and early signalling elements during defence responses to microbe- or damage-associated molecular patterns. Plant J **68,** 100-113.

Ranf, S., Grimmer, J., Poschl, Y., Pecher, P., Chinchilla, D., Scheel, D., and Lee, J. (2012). Defense-related calcium signaling mutants uncovered via a quantitative high-throughput screen in Arabidopsis thaliana. Mol Plant **5,** 115-130.

Ranf, S., Gisch, N., Schaffer, M., Illig, T., Westphal, L., Knirel, Y.A., Sanchez-Carballo, P.M., Zahringer, U., Huckelhoven, R., Lee, J., and Scheel, D. (2015). A lectin S-domain receptor kinase mediates lipopolysaccharide sensing in Arabidopsis thaliana. Nat Immunol **16,** 426-433.

Ranty, B., Aldon, D., and Galaud, J.P. (2006). Plant calmodulins and calmodulin-related proteins: multifaceted relays to decode calcium signals. Plant Signal Behav **1,** 96-104.

Rasmussen, M.W., Roux, M., Petersen, M., and Mundy, J. (2012). MAP Kinase Cascades in Arabidopsis Innate Immunity. Front Plant Sci **3,** 169.

Reddy, A.S., Ali, G.S., Celesnik, H., and Day, I.S. (2011). Coping with stresses: roles of calcium- and calcium/calmodulin-regulated gene expression. Plant Cell **23,** 2010-2032.

Reddy, V.S., Ali, G.S., and Reddy, A.S. (2002). Genes encoding calmodulin-binding proteins in the Arabidopsis genome. J Biol Chem **277,** 9840-9852.

Ren, D., Yang, H., and Zhang, S. (2002). Cell death mediated by MAPK is associated with hydrogen peroxide production in Arabidopsis. J Biol Chem **277,** 559-565.

Rhoads, A.R., and Friedberg, F. (1997). Sequence motifs for calmodulin recognition. FASEB J **11,** 331-340.

Robatzek, S., Bittel, P., Chinchilla, D., Kochner, P., Felix, G., Shiu, S.H., and Boller, T. (2007). Molecular identification and characterization of the tomato flagellin receptor LeFLS2, an orthologue of Arabidopsis FLS2 exhibiting characteristically different perception specificities. Plant Mol Biol **64,** 539-547.

Robert-Seilaniantz, A., Grant, M., and Jones, J.D. (2011). Hormone crosstalk in plant disease and defense: more than just jasmonate-salicylate antagonism. Annu Rev Phytopathol **49,** 317-343.

Ron, M., and Avni, A. (2004). The receptor for the fungal elicitor ethylene-inducing xylanase is a member of a resistance-like gene family in tomato. Plant Cell **16,** 1604-1615.

Rose, J.K., Ham, K.S., Darvill, A.G., and Albersheim, P. (2002). Molecular cloning and characterization of glucanase inhibitor proteins: coevolution of a counterdefense mechanism by plant pathogens. Plant Cell **14,** 1329-1345.

Ryan, C.A., and Pearce, G. (2003). Systemins: a functionally defined family of peptide signals that regulate defensive genes in Solanaceae species. Proc Natl Acad Sci U S A **100 Suppl 2,** 14577-14580.

Sagi, M., and Fluhr, R. (2006). Production of reactive oxygen species by plant NADPH oxidases. Plant Physiol **141,** 336-340.

Sakano, K. (2001). Metabolic regulation of pH in plant cells: role of cytoplasmic pH in defense reaction and secondary metabolism. Int Rev Cytol **206,** 1-44.

Sanchez-Vallet, A., Saleem-Batcha, R., Kombrink, A., Hansen, G., Valkenburg, D.J., Thomma, B.P., and Mesters, J.R. (2013). Fungal effector Ecp6 outcompetes host immune receptor for chitin binding through intrachain LysM dimerization. Elife **2,** e00790.

Sandkvist, M., Bagdasarian, M., Howard, S.P., and DiRita, V.J. (1995). Interaction between the autokinase EpsE and EpsL in the cytoplasmic membrane is required for extracellular secretion in Vibrio cholerae. EMBO J **14,** 1664-1673.

Sang, S., Li, X., Gao, R., You, Z., Lu, B., Liu, P., Ma, Q., and Dong, H. (2012). Apoplastic and cytoplasmic location of harpin protein Hpa1Xoo plays different roles in H_2O_2 generation and pathogen resistance in Arabidopsis. Plant Mol Biol **79,** 375-391.

Saraste, M., Sibbald, P.R., and Wittinghofer, A. (1990). The P-loop--a common motif in ATP- and GTP-binding proteins. Trends Biochem Sci **15,** 430-434.

Sarris, P.F., Duxbury, Z., Huh, S.U., Ma, Y., Segonzac, C., Sklenar, J., Derbyshire, P., Cevik, V., Rallapalli, G., Saucet, S.B., Wirthmueller, L., Menke, F.L., Sohn, K.H., and Jones, J.D. (2015). A Plant Immune Receptor Detects Pathogen Effectors that Target WRKY Transcription Factors. Cell **161,** 1089-1100.

Schirawski, J., Mannhaupt, G., Munch, K., Brefort, T., Schipper, K., Doehlemann, G., Di Stasio, M., Rossel, N., Mendoza-Mendoza, A., Pester, D., Muller, O., Winterberg, B., Meyer, E., Ghareeb, H., Wollenberg, T., Munsterkotter, M., Wong, P., Walter, M., Stukenbrock, E., Guldener, U., and Kahmann, R. (2010). Pathogenicity determinants in smut fungi revealed by genome comparison. Science **330,** 1546-1548.

Schulze-Lefert, P., and Panstruga, R. (2011). A molecular evolutionary concept connecting nonhost resistance, pathogen host range, and pathogen speciation. Trends Plant Sci **16,** 117-125.

Segonzac, C., Feike, D., Gimenez-Ibanez, S., Hann, D.R., Zipfel, C., and Rathjen, J.P. (2011). Hierarchy and roles of pathogen-associated molecular pattern-induced responses in *Nicotiana benthamiana*. Plant Physiol **156,** 687-699.

Seybold, H., Trempel, F., Ranf, S., Scheel, D., Romeis, T., and Lee, J. (2014). Ca^{2+} signalling in plant immune response: from pattern recognition receptors to Ca^{2+} decoding mechanisms. New Phytologist **204,** 782-790.

Shabab, M., Shindo, T., Gu, C., Kaschani, F., Pansuriya, T., Chintha, R., Harzen, A., Colby, T., Kamoun, S., and van der Hoorn, R.A. (2008). Fungal effector protein AVR2 targets diversifying defense-related cys proteases of tomato. Plant Cell **20,** 1169-1183.

Shan, L., Thara, V.K., Martin, G.B., Zhou, J.M., and Tang, X. (2000). The pseudomonas AvrPto protein is differentially recognized by tomato and tobacco and is localized to the plant plasma membrane. Plant Cell **12,** 2323-2338.

Shan, L., He, P., Li, J., Heese, A., Peck, S.C., Nurnberger, T., Martin, G.B., and Sheen, J. (2008). Bacterial effectors target the common signaling partner BAK1 to disrupt multiple MAMP receptor-signaling complexes and impede plant immunity. Cell Host Microbe **4,** 17-27.

Shimizu, T., Nakano, T., Takamizawa, D., Desaki, Y., Ishii-Minami, N., Nishizawa, Y., Minami, E., Okada, K., Yamane, H., Kaku, H., and Shibuya, N. (2010). Two LysM receptor molecules, CEBiP and OsCERK1, cooperatively regulate chitin elicitor signaling in rice. Plant J **64,** 204-214.

Shinya, T., Motoyama, N., Ikeda, A., Wada, M., Kamiya, K., Hayafune, M., Kaku, H., and Shibuya, N. (2012). Functional characterization of CEBiP and CERK1 homologs in arabidopsis and rice reveals the presence of different chitin receptor systems in plants. Plant Cell Physiol **53,** 1696-1706.

Shinya, T., Osada, T., Desaki, Y., Hatamoto, M., Yamanaka, Y., Hirano, H., Takai, R., Che, F.S., Kaku, H., and Shibuya, N. (2010). Characterization of receptor proteins using affinity cross-linking with biotinylated ligands. Plant Cell Physiol **51,** 262-270.

Shiu, S.H., and Bleecker, A.B. (2003). Expansion of the receptor-like kinase/Pelle gene family and receptor-like proteins in Arabidopsis. Plant Physiol **132,** 530-543.

Shiu, S.H., Karlowski, W.M., Pan, R., Tzeng, Y.H., Mayer, K.F., and Li, W.H. (2004). Comparative analysis of the receptor-like kinase family in Arabidopsis and rice. Plant Cell **16,** 1220-1234.

Simon-Plas, F., Elmayan, T., and Blein, J.P. (2002). The plasma membrane oxidase NtrbohD is responsible for AOS production in elicited tobacco cells. Plant J **31,** 137-147.

Snedden, W.A., and Fromm, H. (2001). Calmodulin as a versatile calcium signal transducer in plants. New Phytologist **151,** 35-66.

Sohn, K.H., Lei, R., Nemri, A., and Jones, J.D. (2007). The downy mildew effector proteins ATR1 and ATR13 promote disease susceptibility in *Arabidopsis thaliana*. Plant Cell **19,** 4077-4090.

Song, J., Win, J., Tian, M., Schornack, S., Kaschani, F., Ilyas, M., van der Hoorn, R.A., and Kamoun, S. (2009). Apoplastic effectors secreted by two unrelated eukaryotic plant pathogens target the tomato defense protease Rcr3. Proc Natl Acad Sci U S A **106,** 1654-1659.

Spalding, E.P., and Harper, J.F. (2011). The ins and outs of cellular Ca(2+) transport. Curr Opin Plant Biol **14,** 715-720.

Suarez-Rodriguez, M.C., Adams-Phillips, L., Liu, Y., Wang, H., Su, S.H., Jester, P.J., Zhang, S., Bent, A.F., and Krysan, P.J. (2007). MEKK1 is required for flg22-induced MPK4 activation in Arabidopsis plants. Plant Physiol **143,** 661-669.

Sun, W., Cao, Y., Jansen Labby, K., Bittel, P., Boller, T., and Bent, A.F. (2012). Probing the Arabidopsis flagellin receptor: FLS2-FLS2 association and the contributions of specific domains to signaling function. Plant Cell **24,** 1096-1113.

Taguchi, F., Shimizu, R., Nakajima, R., Toyoda, K., Shiraishi, T., and Ichinose, Y. (2003). Differential effects of flagellins from Pseudomonas syringae pv. tabaci, tomato and glycinea on plant defense response. Plant Physiology and Biochemistry **41,** 165-174.

Takahashi, F., Mizoguchi, T., Yoshida, R., Ichimura, K., and Shinozaki, K. (2011). Calmodulin-dependent activation of MAP kinase for ROS homeostasis in Arabidopsis. Mol Cell **41,** 649-660.

Takahashi, Y., Nasir, K.H., Ito, A., Kanzaki, H., Matsumura, H., Saitoh, H., Fujisawa, S., Kamoun, S., and Terauchi, R. (2007). A high-throughput screen of cell-death-inducing factors in *Nicotiana benthamiana* identifies a novel MAPKK that mediates INF1-induced cell death signaling and non-host resistance to *Pseudomonas cichorii*. Plant J **49,** 1030-1040.

Takai, R., Isogai, A., Takayama, S., and Che, F.S. (2008). Analysis of flagellin perception mediated by flg22 receptor OsFLS2 in rice. Mol Plant Microbe Interact **21,** 1635-1642.

Tanaka, K., Choi, J., Cao, Y., and Stacey, G. (2014). Extracellular ATP acts as a damage-associated molecular pattern (DAMP) signal in plants. Front Plant Sci **5,** 446.

Tao, Y., Xie, Z., Chen, W., Glazebrook, J., Chang, H.S., Han, B., Zhu, T., Zou, G., and Katagiri, F. (2003). Quantitative nature of Arabidopsis responses during compatible and incompatible interactions with the bacterial pathogen *Pseudomonas syringae*. Plant Cell **15,** 317-330.

Thaler, J.S., Humphrey, P.T., and Whiteman, N.K. (2012). Evolution of jasmonate and salicylate signal crosstalk. Trends Plant Sci **17,** 260-270.

Thomma, B.P., Nurnberger, T., and Joosten, M.H. (2011). Of PAMPs and effectors: the blurred PTI-ETI dichotomy. Plant Cell **23,** 4-15.

Tian, M., Benedetti, B., and Kamoun, S. (2005). A Second Kazal-like protease inhibitor from Phytophthora infestans inhibits and interacts with the apoplastic pathogenesis-related protease P69B of tomato. Plant Physiol **138,** 1785-1793.

Tian, M., Huitema, E., Da Cunha, L., Torto-Alalibo, T., and Kamoun, S. (2004). A Kazal-like extracellular serine protease inhibitor from *Phytophthora infestans* targets the tomato pathogenesis-related protease P69B. J Biol Chem **279,** 26370-26377.

Torres, M.A., Jones, J.D., and Dangl, J.L. (2006). Reactive oxygen species signaling in response to pathogens. Plant Physiol **141,** 373-378.

Tsuda, K., and Katagiri, F. (2010). Comparing signaling mechanisms engaged in pattern-triggered and effector-triggered immunity. Curr Opin Plant Biol **13,** 459-465.

Tyler, B.M., Tripathy, S., Zhang, X., Dehal, P., Jiang, R.H., Aerts, A., Arredondo, F.D., Baxter, L., Bensasson, D., Beynon, J.L., Chapman, J., Damasceno, C.M., Dorrance, A.E., Dou, D., Dickerman, A.W., Dubchak, I.L., Garbelotto, M., Gijzen, M., Gordon, S.G., Govers, F., Grunwald, N.J., Huang, W., Ivors, K.L., Jones, R.W., Kamoun, S., Krampis, K., Lamour, K.H., Lee, M.K., McDonald, W.H., Medina, M., Meijer, H.J., Nordberg, E.K., Maclean, D.J., Ospina-Giraldo, M.D., Morris, P.F., Phuntumart, V., Putnam, N.H., Rash, S., Rose, J.K., Sakihama, Y., Salamov, A.A., Savidor, A., Scheuring, C.F., Smith, B.M., Sobral, B.W., Terry, A., Torto-Alalibo, T.A., Win, J., Xu, Z., Zhang, H., Grigoriev, I.V., Rokhsar, D.S., and Boore, J.L. (2006). Phytophthora genome sequences uncover evolutionary origins and mechanisms of pathogenesis. Science **313,** 1261-1266.

Ulker, B., and Somssich, I.E. (2004). WRKY transcription factors: from DNA binding towards biological function. Curr Opin Plant Biol **7,** 491-498.

van den Burg, H.A., Harrison, S.J., Joosten, M.H., Vervoort, J., and de Wit, P.J. (2006). *Cladosporium fulvum* Avr4 protects fungal cell walls against hydrolysis by plant chitinases accumulating during infection. Mol Plant Microbe Interact **19,** 1420-1430.

van den Burg, H.A., Spronk, C.A., Boeren, S., Kennedy, M.A., Vissers, J.P., Vuister, G.W., de Wit, P.J., and Vervoort, J. (2004). Binding of the AVR4 elicitor of *Cladosporium fulvum* to chitotriose units is facilitated by positive allosteric protein-protein interactions: the chitin-

binding site of AVR4 represents a novel binding site on the folding scaffold shared between the invertebrate and the plant chitin-binding domain. J Biol Chem **279,** 16786-16796.

van der Hoorn, R.A. (2008). Plant proteases: from phenotypes to molecular mechanisms. Annu Rev Plant Biol **59,** 191-223.

van der Wolk, J., Klose, M., Breukink, E., Demel, R.A., de Kruijff, B., Freudl, R., and Driessen, A.J. (1993). Characterization of a *Bacillus subtilis* SecA mutant protein deficient in translocation ATPase and release from the membrane. Mol Microbiol **8,** 31-42.

van Esse, H.P., Bolton, M.D., Stergiopoulos, I., de Wit, P.J., and Thomma, B.P. (2007). The chitin-binding *Cladosporium fulvum* effector protein Avr4 is a virulence factor. Mol Plant Microbe Interact **20,** 1092-1101.

van Esse, H.P., Van't Klooster, J.W., Bolton, M.D., Yadeta, K.A., van Baarlen, P., Boeren, S., Vervoort, J., de Wit, P.J., and Thomma, B.P. (2008). The *Cladosporium fulvum* virulence protein Avr2 inhibits host proteases required for basal defense. Plant Cell **20,** 1948-1963.

Vandenabeele, S., Van Der Kelen, K., Dat, J., Gadjev, I., Boonefaes, T., Morsa, S., Rottiers, P., Slooten, L., Van Montagu, M., Zabeau, M., Inze, D., and Van Breusegem, F. (2003). A comprehensive analysis of hydrogen peroxide-induced gene expression in tobacco. Proc Natl Acad Sci U S A **100,** 16113-16118.

Vleeshouwers, V.G., Driesprong, J.D., Kamphuis, L.G., Torto-Alalibo, T., Van't Slot, K.A., Govers, F., Visser, R.G., Jacobsen, E., and Kamoun, S. (2006). Agroinfection-based high-throughput screening reveals specific recognition of INF elicitins in Solanum. Mol Plant Pathol **7,** 499-510.

Voigt, C.A. (2014). Callose-mediated resistance to pathogenic intruders in plant defense-related papillae. Front Plant Sci **5,** 168.

Wan, J., Zhang, X.C., Neece, D., Ramonell, K.M., Clough, S., Kim, S.Y., Stacey, M.G., and Stacey, G. (2008). A LysM receptor-like kinase plays a critical role in chitin signaling and fungal resistance in Arabidopsis. Plant Cell **20,** 471-481.

Wang, G., Fiers, M., Ellendorff, U., Wang, Z., de Wit, P.J., Angenent, G.C., and Thomma, B.P. (2010a). The diverse roles of extracellular leucine-rich repeat-containing receptor-like proteins in plants. Critical Reviews in Plant Science **29,** 285-299.

Wang, L., Tsuda, K., Sato, M., Cohen, J.D., Katagiri, F., and Glazebrook, J. (2009). Arabidopsis CaM binding protein CBP60g contributes to MAMP-induced SA accumulation and is involved in disease resistance against Pseudomonas syringae. PLoS Pathog **5,** e1000301.

Wang, Q., Han, C., Ferreira, A.O., Yu, X., Ye, W., Tripathy, S., Kale, S.D., Gu, B., Sheng, Y., Sui, Y., Wang, X., Zhang, Z., Cheng, B., Dong, S., Shan, W., Zheng, X., Dou, D., Tyler, B.M., and Wang, Y. (2011). Transcriptional programming and functional interactions within the Phytophthora sojae RXLR effector repertoire. Plant Cell **23,** 2064-2086.

Wang, X., Boevink, P., McLellan, H., Armstrong, M., Bukharova, T., Qin, Z., and Birch, P.R. (2015). A Host KH RNA-Binding Protein Is a Susceptibility Factor Targeted by an RXLR Effector to Promote Late Blight Disease. Mol Plant **8,** 1385-1395.

Wang, Y., Li, J., Hou, S., Wang, X., Li, Y., Ren, D., Chen, S., Tang, X., and Zhou, J.M. (2010b). A Pseudomonas syringae ADP-ribosyltransferase inhibits Arabidopsis mitogen-activated protein kinase kinases. Plant Cell **22,** 2033-2044.

Wessling, R., Epple, P., Altmann, S., He, Y., Yang, L., Henz, S.R., McDonald, N., Wiley, K., Bader, K.C., Glasser, C., Mukhtar, M.S., Haigis, S., Ghamsari, L., Stephens, A.E., Ecker, J.R., Vidal, M., Jones, J.D., Mayer, K.F., Ver Loren van Themaat, E., Weigel, D., Schulze-Lefert, P., Dangl, J.L., Panstruga, R., and Braun, P. (2014). Convergent targeting of a common host protein-network by pathogen effectors from three kingdoms of life. Cell Host Microbe **16,** 364-375.

Whisson, S.C., Boevink, P.C., Moleleki, L., Avrova, A.O., Morales, J.G., Gilroy, E.M., Armstrong, M.R., Grouffaud, S., van West, P., Chapman, S., Hein, I., Toth, I.K., Pritchard, L., and Birch, P.R. (2007). A translocation signal for delivery of oomycete effector proteins into host plant cells. Nature **450,** 115-118.

White, F.F., Potnis, N., Jones, J.B., and Koebnik, R. (2009). The type III effectors of *Xanthomonas*. Mol Plant Pathol **10,** 749-766.

Willmann, R., Lajunen, H.M., Erbs, G., Newman, M.A., Kolb, D., Tsuda, K., Katagiri, F., Fliegmann, J., Bono, J.J., Cullimore, J.V., Jehle, A.K., Gotz, F., Kulik, A., Molinaro, A.,

Lipka, V., Gust, A.A., and Nurnberger, T. (2011). Arabidopsis lysin-motif proteins LYM1 LYM3 CERK1 mediate bacterial peptidoglycan sensing and immunity to bacterial infection. Proc Natl Acad Sci U S A **108,** 19824-19829.

Win, J., Morgan, W., Bos, J., Krasileva, K.V., Cano, L.M., Chaparro-Garcia, A., Ammar, R., Staskawicz, B.J., and Kamoun, S. (2007). Adaptive evolution has targeted the C-terminal domain of the RXLR effectors of plant pathogenic oomycetes. Plant Cell **19,** 2349-2369.

Wolff, J., Cook, G.H., Goldhammer, A.R., and Berkowitz, S.A. (1980). Calmodulin activates prokaryotic adenylate cyclase. Proc Natl Acad Sci U S A **77,** 3841-3844.

Wong, H.L., Pinontoan, R., Hayashi, K., Tabata, R., Yaeno, T., Hasegawa, K., Kojima, C., Yoshioka, H., Iba, K., Kawasaki, T., and Shimamoto, K. (2007). Regulation of rice NADPH oxidase by binding of Rac GTPase to its N-terminal extension. Plant Cell **19,** 4022-4034.

Xiang, T., Zong, N., Zhang, J., Chen, J., Chen, M., and Zhou, J.M. (2011). BAK1 is not a target of the *Pseudomonas syringae* effector AvrPto. Mol Plant Microbe Interact **24,** 100-107.

Xiang, T., Zong, N., Zou, Y., Wu, Y., Zhang, J., Xing, W., Li, Y., Tang, X., Zhu, L., Chai, J., and Zhou, J.M. (2008). Pseudomonas syringae effector AvrPto blocks innate immunity by targeting receptor kinases. Curr Biol **18,** 74-80.

Xin, X.F., and He, S.Y. (2013). *Pseudomonas syringae pv. tomato* DC3000: a model pathogen for probing disease susceptibility and hormone signaling in plants. Annu Rev Phytopathol **51,** 473-498.

Xu, J., Xie, J., Yan, C., Zou, X., Ren, D., and Zhang, S. (2014). A chemical genetic approach demonstrates that MPK3/MPK6 activation and NADPH oxidase-mediated oxidative burst are two independent signaling events in plant immunity. Plant J **77,** 222-234.

Yamaguchi, Y., Pearce, G., and Ryan, C.A. (2006). The cell surface leucine-rich repeat receptor for AtPep1, an endogenous peptide elicitor in Arabidopsis, is functional in transgenic tobacco cells. Proc Natl Acad Sci U S A **103,** 10104-10109.

Yamakawa, H., Katou, S., Seo, S., Mitsuhara, I., Kamada, H., and Ohashi, Y. (2004). Plant MAPK phosphatase interacts with calmodulins. J Biol Chem **279,** 928-936.

Yang, B., Sugio, A., and White, F.F. (2006). Os8N3 is a host disease-susceptibility gene for bacterial blight of rice. Proc Natl Acad Sci U S A **103,** 10503-10508.

Yang, T., and Poovaiah, B.W. (2002a). Hydrogen peroxide homeostasis: activation of plant catalase by calcium/calmodulin. Proc Natl Acad Sci U S A **99,** 4097-4102.

Yang, T., and Poovaiah, B.W. (2002c). A calmodulin-binding/CGCG box DNA-binding protein family involved in multiple signaling pathways in plants. J Biol Chem **277,** 45049-45058.

Yang, T., and Poovaiah, B.W. (2003). Calcium/calmodulin-mediated signal network in plants. Trends Plant Sci **8,** 505-512.

Yap, K.L., Kim, J., Truong, K., Sherman, M., Yuan, T., and Ikura, M. (2000). Calmodulin target database. J Struct Funct Genomics **1,** 8-14.

Yeats, T.H., and Rose, J.K. (2013). The formation and function of plant cuticles. Plant Physiol **163,** 5-20.

Yoo, J.H., Park, C.Y., Kim, J.C., Heo, W.D., Cheong, M.S., Park, H.C., Kim, M.C., Moon, B.C., Choi, M.S., Kang, Y.H., Lee, J.H., Kim, H.S., Lee, S.M., Yoon, H.W., Lim, C.O., Yun, D.J., Lee, S.Y., Chung, W.S., and Cho, M.J. (2005). Direct interaction of a divergent CaM isoform and the transcription factor, MYB2, enhances salt tolerance in arabidopsis. J Biol Chem **280,** 3697-3706.

Yoo, S.D., Cho, Y.H., and Sheen, J. (2007). Arabidopsis mesophyll protoplasts: a versatile cell system for transient gene expression analysis. Nat Protoc **2,** 1565-1572.

Yu, Q., An, L., and Li, W. (2014). The CBL-CIPK network mediates different signaling pathways in plants. Plant Cell Rep **33,** 203-214.

Zeng, L., Velasquez, A.C., Munkvold, K.R., Zhang, J., and Martin, G.B. (2012). A tomato LysM receptor-like kinase promotes immunity and its kinase activity is inhibited by AvrPtoB. Plant J **69,** 92-103.

Zhang, J., Shao, F., Li, Y., Cui, H., Chen, L., Li, H., Zou, Y., Long, C., Lan, L., Chai, J., Chen, S., Tang, X., and Zhou, J.M. (2007). A Pseudomonas syringae effector inactivates MAPKs to suppress PAMP-induced immunity in plants. Cell Host Microbe **1,** 175-185.

Zhang, J., Li, W., Xiang, T., Liu, Z., Laluk, K., Ding, X., Zou, Y., Gao, M., Zhang, X., Chen, S., Mengiste, T., Zhang, Y., and Zhou, J.M. (2010a). Receptor-like cytoplasmic kinases integrate signaling from multiple plant immune receptors and are targeted by a *Pseudomonas syringae* effector. Cell Host Microbe **7,** 290-301.

Zhang, L., Kars, I., Essenstam, B., Liebrand, T.W., Wagemakers, L., Elberse, J., Tagkalaki, P., Tjoitang, D., van den Ackerveken, G., and van Kan, J.A. (2014). Fungal endopolygalacturonases are recognized as microbe-associated molecular patterns by the arabidopsis receptor-like protein RESPONSIVENESS TO BOTRYTIS POLYGALACTURONASES1. Plant Physiol **164,** 352-364.

Zhang, W., Zhou, R.G., Gao, Y.J., Zheng, S.Z., Xu, P., Zhang, S.Q., and Sun, D.Y. (2009). Molecular and genetic evidence for the key role of AtCaM3 in heat-shock signal transduction in Arabidopsis. Plant Physiol **149,** 1773-1784.

Zhang, W., Fraiture, M., Kolb, D., Loffelhardt, B., Desaki, Y., Boutrot, F.F., Tor, M., Zipfel, C., Gust, A.A., and Brunner, F. (2013). Arabidopsis receptor-like protein30 and receptor-like kinase suppressor of BIR1-1/EVERSHED mediate innate immunity to necrotrophic fungi. Plant Cell **25,** 4227-4241.

Zhang, Y., Xu, S., Ding, P., Wang, D., Cheng, Y.T., He, J., Gao, M., Xu, F., Li, Y., Zhu, Z., Li, X., and Zhang, Y. (2010b). Control of salicylic acid synthesis and systemic acquired resistance by two members of a plant-specific family of transcription factors. Proc Natl Acad Sci U S A **107,** 18220-18225.

Zhang, Z., Wu, Y., Gao, M., Zhang, J., Kong, Q., Liu, Y., Ba, H., Zhou, J., and Zhang, Y. (2012). Disruption of PAMP-induced MAP kinase cascade by a *Pseudomonas syringae* effector activates plant immunity mediated by the NB-LRR protein SUMM2. Cell Host Microbe **11,** 253-263.

Zhao, C., Nie, H., Shen, Q., Zhang, S., Lukowitz, W., and Tang, D. (2014). EDR1 physically interacts with MKK4/MKK5 and negatively regulates a MAP kinase cascade to modulate plant innate immunity. PLoS Genet **10,** e1004389.

Zhao, Y., Liu, W., Xu, Y.P., Cao, J.Y., Braam, J., and Cai, X.Z. (2013). Genome-wide identification and functional analyses of calmodulin genes in *Solanaceous* species. BMC Plant Biol **13,** 70.

Zhou, J., Wu, S., Chen, X., Liu, C., Sheen, J., Shan, L., and He, P. (2014). The *Pseudomonas syringae* effector HopF2 suppresses Arabidopsis immunity by targeting BAK1. Plant J **77,** 235-245.

Zipfel, C., Robatzek, S., Navarro, L., Oakeley, E.J., Jones, J.D., Felix, G., and Boller, T. (2004). Bacterial disease resistance in Arabidopsis through flagellin perception. Nature **428,** 764-767.

Zipfel, C., Kunze, G., Chinchilla, D., Caniard, A., Jones, J.D., Boller, T., and Felix, G. (2006). Perception of the bacterial PAMP EF-Tu by the receptor EFR restricts Agrobacterium-mediated transformation. Cell **125,** 749-760.

6. Appendix

Table 6-1. List of Primers mentioned in this study

Primer name	Sequence (5` - 3`)
For_FRK1_qRT	GATGGCGGACTTCGGGTTATC
Rev_FRK1_qRT	CGAATAGTACTCGGGGTCAAGGTAA
For_WRKY17_qRT	GCCGCTTTCTGGTCTTCCTTACAG
Rev_WRKY17_qRT	CCGTGGATGTGGTGAGCCTTTG
For_4CL_qRT	CCCTGAGACGGAGAGATACGACTTG
Rev_4CL_qRT	TCGGTCATTCCATAACCCTGACCA
For_EF1α_qRT	GCCCATGGTTGTGGAGACCTTC
Rev_EF1α_qRT	CACCTGCGGCAGATAGAGTTTTGAG
For_actin_qRT	AGTGGTCGTACAACCGGTATTGT
Rev_actin_qRT	GAGGAAGAGCATACCCCTCGTA
SlMAP3Kε-KD_attB1	AAAAAGCAGGCTTCACCATGAAATATATGCTTGGAGATGAG
SlMAP3Kε-KD_attB2	AGAAAGCTGGGTCTATCCAAGGATGTGAAAGC
SlMAP3Kα-KD_attB1	AAAAAGCAGGCTTCACCATGAAATGGAAGAAAGGCAGG
SlMAP3Kα-KD_attB2	AGAAAGCTGGGTCAACAAAAGGGTGCTCTAGTAGT
SlMEK2_attB1	AAAAAGCAGGCTTCACCATGCGACCAGCCGCCAAC
SlMEK2_attB2	AGAAAGCTGGGTCAGAAGAGGAGGAAAAATGAGGAG
SlMEK1_attB1	AAAAAGCAGGCTTCACCATGAAGAAAGGATCTTTTG
SlMEK1_attB2	AGAAAGCTGGGTCTAGCTCAGTAAGTGTTGCC
AtCaM1-attB1	AAAAAGCAGGCTTCATGGCGGATCAACTCACT
AtCaM1-attB2	AGAAAGCTGGGTCTCACTTAGCCATCATAATCTTG
AtCaM2-attB1	AAAAAGCAGGCTTCATGGCGGATCAGCTCACAGAC
AtCaM2-attB2	AGAAAGCTGGGTCTCACTTAGCCATCATAACCTTCAC
SlCaM1-attB1	AAAAAGCAGGCTTCATGGCGGATCAGCTCACCGAA
SlCaM1-attB2	AGAAAGCTGGGTCTCACTTAGCCATCATAACCTTGAC
SlCaM3-attB1	AAAAAGCAGGCTTCATGGCGGATCAGCTTACAGATG
SlCaM3-attB2	AGAAAGCTGGGTCTCACTTAGCCATCATGAC
SlCaM6-attB1	AAAAAGCAGGCTTCATGGCAGAGCAGCTGAC
SlCaM6-attB2	AGAAAGCTGGGTCTCACTTGGCAAGCATCAT
SFI5 28aa-attB1	AAAAAGCAGGCTTCACCATGGCCTCCGACCAGAAT

SFI5 63aa-attB1	AAAAAGCAGGCTTCACCATG TTCCTGACAGAACCCCC
SFI5 84aa-attB1	AAAAAGCAGGCTTCACCATGAACAGCGGGCTACCAGAT
SFI5 102aa-attB1	AAAAAGCAGGCTTCACCATGAACAGCGGGCTACCAGAT
SFI5 178aa-attB1	AAAAAGCAGGCTTCACCATGGATCCTTTAAATAGGGAGCAG
SFI5 199aa-attB2	AGAAAGCTGGGTCTTAAGCCTGATTCTTTTTAAGAGCAA
SFI5 221aa-attB2	AGAAAGCTGGGTCTTATTTGGACTTGGCTGCCATA
SFI5 ED-WF/AA-F	AGCACGGCTAAAATCGCTAAAATTATCTCGA
SFI5 ED-WF/AA-R	TTAGCGATTTTAGCCGTGCTTGGTTTGGA
SFI5 ED-KK/EE-F	GGCTTGAGGAGTTAAAGCTAAAACGTTAACACCC
SFI5 ED-KK/EE-R	TTAACTCCTCAAGCCTCGAGATAATTTTAAAGATTTTC
SFI5 ED-KR/EE-F	GCTAGAGGAGTAACACCCAGCTTTCTTGTAC
SFI5 ED-KR/EE-R	TGTTACTCCTCTAGCTTTAATTTTTTAAGCCTCG
attB1-adapter	GGGGACAAGTTTGTACAAAAAAGCAGGCT
attB2-adapter	GGGGACCACTTTGTACAAGAAAGCTGGGT

Table 6-2. List of the PiRXLR effector genes tested in the MTI-suppressor screen in *S. lycopersicum* and *A. thaliana* protoplasts.

Gene identification number, affiliation to an RXLR gene family, nucleotide and protein sequence (without signal peptide) are presented.

Gene ID	**RXLR Family**	**Cloned Nucleotide Sequence**	**Translated Amino Sequence**
PITG_00366	80	>pDonr_00366_1 ATGAACGTGCTACATGTACCGACACAAGT GACGAAATCACACGCGGTCTCGCCAGATG CGCAGTTTGTCGTCGCCATGGGCAGAAGAT CTTTGCGAACGAGTGGCGAAGCTAATGAA GAGAGAACCAGACTGAACACGCTGCTTCT CCTCGACGACGTCACTGAAGCAGAAATGT CATCAATAAAGAAACTAGCTTCGACGTTTG CGAAATTGGAAAATAGGAACGACGGAGCA GCTGACCTATTCAACATGCTACGTCGCCAA GGACATACGAAGGAAAGTGCAAGAAACGC CGGCAACCTATACACCAAATACCTTCAAAA CCCTTCAGCATTTCATACTTAG	>pDonr_00366_1 MNVLHVPTQVTKSHAVSPDAQFVVA MGR**RSLR**TSGEANEERTRLNTLLLLDD VTEAEMSSIKKLASTFAKLENRNDGAA DLFNMLRRQGHTKESARNAGNLYTKY LQNPSAFHT*
PITG_00821 (PexRD21)	108	>pDonr_00821_2 ATGACCCCCGTCATAAAAGAAGCGAACCA GGCCATGCTCGCTAATGGACCACTACCTAG CATCGTCAATACGGAGGGTGGGCGACTTTT GCGTGGCGTCAAGAAGCGTACAGCGGAGA GAGAAGTGCAGGAAGAGAGGATGTCTGGC GCGAAACTCAGCGAAAAGGGGAAACAATT CTTAAAATGGTTTTTTCGTGGCAGCGATAC ACGCGTTAAAGGCAGAAGCTGGAGATAA	>pDonr_00821_2 MTPVIKEANQAMLANGPLPSIVNTEGG **RLLR**GVKKRTAEREVQEERMSGAKLS EKGKQFLKWFFRGSDTRVKGRSWR*
PITG_03192 (PexRD28)	66	>pDonr_03192_16 ATGGAGAGCACCGTCGTCATGAATAACCG GAATTTCGACTCCATCAACGTCCCCATTAG CGATGATATCACAAGTCGCAACCTCAGGG CGAGCGGTGAAGAGAGAGCCTACGCCTTT GTGGACAAGATCAAGAGTCTTTTTAGCAGG CCTGGTATCAGCCAGAAAGTCGAGAGTCT GCAGAAGAATCCCGCCATGGTCAAGAACT TGGAGAAGGCTGCGTTAAGCCAGAAGGGC TCCAGCAAGGTCCGCGACTGGTTCATGCAT ATGTACAACAACAGCTCCAAGAGAGACAA GTTCTTCATTCTCGCGACCCTCGTCATGTTC CCTATCGGCGTATGGGCAGTTGTTACTAAT TATAGGAGGTAG	>pDonr_03192_16 MESTVVMNNRNFDSINVPISDDITS**RN LR**ASGEERAYAFVDKIKSLFSRPGISQK VESLQKNPAMVKNLEKAALSQKGSSK VRDWFMHMYNNSSKRDKFFILATLVM FPIGVWAVVTNYRR*
PITG_04089 (PexRD41)	5	>pDonr_04089_1 ATGGCGCTTCCGAATCCCGACGAAACTCGG CTCTTATCAGACACTTTTACCAAAAGATCC CTTCGGGTCGCAGGCCAAGAAGCTGCCCG GGGCGAAGAGATTGTGAGAGTTACAGCCC AGAGTACTAACAAAATCTTCAAGAGACCG GCGGAAAAAGACATGAGCAAACTGCTTGA AGCGGCTAAGAAGGCGCTGTTGGAGAAAA GGATGGCTGAGCTCTCAAAGGTCATTAAG AAGCCAGCGAAGTAG	>pDonr_04089_1 MALPNPDETRLLSDTFTK**RSLR**VAGQE AARGEEIVRVTAQSTNKIFKRPAEKDM SKLLEAAKKALLEKRMAELSKVIKKPA K*
SFI1/PITG_04097	5	>pDonr_04097_1 ATGTTCCCGAATCCCAAGGAGCCTCAGCTC TTGTCAAAGGCGTCCCCTGACAAAAGATCC CTTCGGGTCGAAGGCCAAGAAGTTGTCCA AGGCGGCACGCTGGACGGGAACGGTGGAG TCTGGAAAGCCATAGCCCATACTACTAATA AGATCGTCAAGAAGCCGGAGATAGACGTT AGCAAACTCATCGACGTGGCCAAGAAGGC AAAAAAGGTGAAGAAGTTGAAAAACTTGA TGAAGCTTAAGAAATCGTCATCGTAG	>pDonr_04097_1 MFPNPKEPQLLSKASPDK**RSLR**VEGQE VVQGGTLDGNGGVWKAIAHTTNKIVK KPEIDVSKLIDVAKKAKKVKKLKNLM KLKKSSS*

SFI2/PITG_04145	17	>pDonr_04145_2 ATGTTCACGAATGCCGATGACTCTCAGCTC TTGTCGAAGGTCTCTCCCGACTTCGCAGCC AACGATATGACCTATACTGTTTCCCGGAAG AGACTTCTTCGAGTCGCAGGCCGGGAAGA TGATGACGCGACGACCGATGAAGAAGATC GAGGTTTTACCAGCATCGTTGATGTCATCA AGAGATCGGATGCCGCCGAAGCACTACAA AAGTTATCGAAAGCCTCCGCCAAAAAAGT GAAAAAGGCCGGCAAAGCTGTCAAAGAAC TGACTGCAAAAGAGAAAGAGGCCTTGAAA GCCCTCTTGGCACTGAAGGACGGCAATTAA	>pDonr_04145_2 MFTNADDSQLLSKVSPDFAANDMTYT VSRK**RLLR**VAGREDDDATTDEEDRGF TSIVDVIKRSDAAEALQKLSKASAKKV KKAGKAVKELTAKEKEALKALLALKD GN*
PITG_04266	RXLRsng248	>pDonr_04266 ATGCGCGTCCAGTACATCGCTCTGGTAGCT GCTATCGCCTATCTCTCGAGTATCGACGGT CTTCAGATCGTCCCATATTCGGCCAAATCC TCATCTCTTCGAGCGCCTGCTGACGCCCGC AACCAACCTTACGTGGAAGGCAAGACAGA CCGGTTCCTGATCAGCGAGTCTAAGACTTA CGAAGCCACCAAGGCTCCGACTGGGTACG TGTTTGATACCCTCCACGATGACGATGATA TGCTATGGAAGGACGAGGATAATGAGTAC GAAGACGAAGACGAAAACTCGTCGTTTGA CAACGACGAGCGTGGTCTTTTTAAGAGGA GGAAAAGAAAGAAGAAGAAAAAGAAACA CAAAGAGACGCTGACGCCAACCCCTGCAC TAAATAGTACGGCGACACCCACACCCACA CCAACTCCAAAGCCTACGCGTGGTGGTCTC CTCGGGTGGATTGATCGTATTAGCGAT	>pDonr_04266 MRVQYIALVAAIAYLSSIDGLQIVPYSA KSSSLRAPADARNQPYVEGKTDRFLIS ESKTYEATKAPTGYVFDTLHDDDDML WKDEDNEYEDEDENSSFDNDERGLFK RRKRKKKKKKHKETLTPTPALNSTATP TPTPTPKPTRGGLLGWIDRISD*
PITG_04314 (PexRD24)	49	>pDonr_04314_1 ATGGTATCGACCGAAGCTAATGGGCAGGT TGCCCTATCTACGAGCAAAGGCCAACTAGC TGGCGAGCGTGCTGAGGAGGAAAACAGCA TCGTCAGGTCCCTCCGCGCAGTCGAGACAA GTGAAGACGAAGAAGAGAGGGATTTGCTT GGGCTTTTTGCCAAGAGCAAGCTGAAGAA GATGATGAAAAGCGAAAGCTTCAAGCTGA AGAGGTTTGGAGAATGGGACGATTTCACA GTGGGTTATATTCGTGAAAAGCTCAAAAAC AAGTATCCGGACCTCCTTTTGAACTACCTA AATGTCTACAAGAAGGCAGGCAATGAGAT CGTTAGACACGCTAACAATCCCAACAAGG TGACTTTCTCGAACAAAGTCCGAGCTCGTA TCTACAAAACCAACTCGTAG	>pDonr_04314_1 MVSTEANGQVALSTSKGQLAGERAEE ENSIV**RSLR**AVETSEDEEERDLLGLFA KSKLKKMMKSESFKLKRFGEWDDFTV GYIREKLKNKYPDLLLNYLNVYKKAG NEIVRHANNPNKVTFSNKVRARIYKTN S*
PITG_04339 (PexRD20)	81	>pDonr_04339_1 ATGACGACGGACGCCCAGCTGAGTGACGC CCGAGCGGTCCGCGCCTCTTTTAATACCAA GCGCGCGCTGCGGTCCCATACTAAGGCGA CTGACCATGGCGAGGAGAGAGCTTACAAG CCCAGTCTCAGTGTCGTCGAGAGCCTCAAC AACTGGATGCAAAGAGCATCGAAGAATAT CTTGCCTGACGACGTTATTTTGGTCATGGC CAGTAAGGCGATGACAAAGAAGACCTCAT CTTCGGACGCTGTCTTCGCGATGCTCCAGC TTGACCAGGGACTAAAGGGAATCCTGAGC AATCCCAACTTGAAACAATTTGCCTACTAT CTCGTATTGACGGAGAAAGCGCCAAGCCA GGCTCTGATCACCAAGTTGATCAGTCAATA CGGAGACGACGTAGTGGCGAAATATCTCTT CGACATCAAGCACAAAGCGATCAACGTGA GCGAGAAACTCAAGGCCGAAGCGAGGTTT TGGCAAGGCGCGCAGTATGTCAAGTGGTTC GATGAAGGGGTAACGCCAGCTCTGGTCCG TCAAAAATACAACGTCCACCCCGAAACGT GGTACAAGAACCCGTACGAGGGCGTGTAC TGGGAATACACTGGCGTGTACGCCAAATTG GCGAGCAAGTCAAATAAACCCCTGCCCGT GGAAGTATAG	>pDonr_04339_1 MTTDAQLSDARAVRASFNTK**RALR**SH TKATDHGEERAYKPSLSVVESLNNWM QRASKNILPDDVILVMASKAMTKKTSS SDAVFAMLQLDQGLKGILSNPNLKQFA YYLVLTEKAPSQALITKLISQYGDDVV AKYLFDIKHKAINVSEKLKAEARFWQ GAQYVKWFDEGVTPALVRQKYNVHP ETWYKNPYEGVYWEYTGVYAKLASK SNKPLPVEV*

PITG_04388	1	>pDonr_04388_2 ATGGAGCAAGCTGCCGCAGCCAAGGAGCT TCGACTAAACTCTTTCGTGCACCGATCATT CGACGCCCATATTCATGCCCAGCGGCTCTT GAGGGATCGTCGCTCCGTCGATGAAGAGA GAGGGCTTCCGACCGTAATTGAGAAAACC AAGACTTTGTTTTCGACGAAGGTGACCGAC AAGACGCTACAGCGCTGGGCAGCCAACAA GAAGTCCCCCCAACACGCTCTGATTCGCTT GGACCTTGACAATGCAGGAAAAGACCTTTT CACAAAAGCTAAATTCGCCGACTGGGTCTC CTTTATGACAAAACGGAATCCGCAGAACG CCGAGGCGGCCATGCTGTCCGCACTGATGA CACGCTATAGCGACGACGTTCTGTCAGGCA TGCTTATAGCAGCAAAGAAGGCTCCTGATA CGAAGACTATTGCCACTAACCTGCAAATCC AGCAGCTTCGGGGGTGGATGAAGAAGGGG AAAACCGCGGACGACGTTTTCAACCTATTT AACCTCAAGGGAAAGGCAACGAGCTTGGA TGATCTCGTCAGTGACGGTCAATTCGCCCC TTGGGTCACCTACGTGACTGCTCTTAACAA AGGAGATCCCAAGAAGACAAACATGATGG TGGTAAAGACGTTGACAACTTACAACAAG AAAACACACAAGGGCGTGTACGATATGCT CAGTGCGTCCAAGAATAAGCAGCTGGCCG CAGACTTGCAAAGAGGACAGTTCGACAAC TGGTTGGCTAACAATGTCCAATTCTACGAT GTTAGTGCCATGGTGGGAGCGAAGGGAAC TCCACGAGGTAGTCCGCAGAGACTGTTCGT GAAGGACTATGTTGCTGCGTACAACAAGA AGCACCAGCTGTAA	>pDonr_04388_2 MEQAAAAKELRLNSFVHRSFDAHIHA Q**RLLR**DRRSVDEERGLPTVIEKTKTLF STKVTDKTLQRWAANKKSPQHALIRL DLDNAGKDLFTKAKFADWVSFMTKR NPQNAEAAMLSALMTRYSDDVLSGML IAAKKAPDTKTIATNLQIQQLRGWMK KGKTADDVFNLFNLKGKATSLDDLVS DGQFAPWVTYVTALNKGDPKKTNMM VVKTLTTYNKKTHKGVYDMLSASKN KQLAADLQRGQFDNWLANNVQFYDV SAMVGAKGTPRGSPQRLFVKDYVAAY NKKHQL*
PITG_05750 (PexRD49)	29	>pDonr_05750_1 ATGCGCTCGGCCACCGAACATGCCCAGCTC ATGGTGTCGCAGTCGGAGCTGGACCAACC CACCCGGTGGAACGTCGCCGACAAACGCT TACTGCGGGCCAACGACGGCACGAATGCT GCCGAGGAAGAACGAGGAATGGCGGACAT TGCAACGAAGATGAAGACGTGGACACAAA GCTTAAAAACTCATGTCGGCAGCTCGAAGC CGTTTCAGATAGCGGCTCAGAAATGGAGA AACACGAAGGTGCAGCGAATGATCAAAAA GGGAATTTCTGATACGGCTTTGTTTGAAAA CAAGGTCACTCCTGACGAATTTTTCAAGGC GCTGAGGCTGAAACCAGGGTTGAAACAAT CGTCTGTTACAAACAACCCTGCTCTGAACA AGTACCGCGCCTACAAGAGCTTTTACGAGT CCAAGATCAAGACTGCTGCTACGTAA	>pDonr_05750_1 MRSATEHAQLMVSQSELDQPTRWNVA DK**RLLR**ANDGTNAAEEERGMADIATK MKTWTQSLKTHVGSSKPFQIAAQKWR NTKVQRMIKKGISDTALFENKVTPDEF FKALRLKPGLKQSSVTNNPALNKYRA YKSFYESKIKTAAT*
SFI3/PITG_06087 (PexRD16)	87	>pDonr_06087_1 ATGGCGGTCGCTGAGACGTCAAATGACAT CAACACGATGAACAACAACCAGGAATTTG CTCGATCTCTGCGCAACACGGAGGAGCGCT CGATTGCGGCAATTCTCGCCGAAGCGGGTG AAGAGGACCGCGCAGCGTGGAGGATCAAT TATCGTGCCTGGTACAAGGCTAAGCTGACG CCGACGCAAGTCAAGACGGTGCTGGGCGT CTCCCAAGCAGAGATGAATAATGTTGCGA AGCAACTCCAGCGACTATACCTCGGCTACT ACTCCTTCTACACGGCGATGGAGAAGAAG AAAGAAGAGAAGAAGAGGCTGGCCACACC TTGA	>pDonr_06087_1 MAVAETSNDINTMNNNQEFA**RSLR**NT EERSIAAILAEAGEEDRAAWRINYRAW YKAKLTPTQVKTVLGVSQAEMNNVA KQLQRLYLGYYSFYTAMEKKKEEKKR LATP*

PITG_06099 (PexRD50)	36	>pDonr_06099_4 ATGTCGGACTCGGAGAAAGCTGCTAAGAT TTCCAACGACCAAGTGCTTTCAGGCCGCCA GTTGATTGACACTGTCGCCAAGGACAACA AGAAGCGCTTGCTGCGAGCCTACAAAGAT GCTGAGGACGACAGCGAAGACTCCAAGAA CGTGAAACCCACCGCTGACTCCAAGCACG CCGACGAATCGGAAGACTCTGAAGACAGC CAGGAGGAGCGGTTCTCGCTCATCCAGAC GTCCAACCAGCCCCGATACTACTGGTGGTT CCAGCATCACATGACTCCTCTCGATGTTCG TCGGGACCTGGAATTGACGGCGGACACGA TCAATCCCATTAAGCGCTCGGTCTACACAG GTTATGTCGACTACTACGAGGACCACTGCT CTTACTACGAAAACCGCAAGGAGGAATTTT GCAAGGCAGAAGACTTTTAG	>pDonr_06099_4 MSDSEKAAKISNDQVLSGRQLIDTVAK DNKK**RLLR**AYKDAEDDSEDSKNVKPT ADSKHADESEDSEDSQEERFSLIQTSNQ PRYYWWFQHHMTPLDVRRDLELTAD TINPIKRSVYTGYVDYYEDHCSYYENR KEEFCKAEDF*
PITG_06308 (Avr3b homolog P.sojae)	23	>pDonr_06308-1 ATGTCGATCTCTTCTTTCTCCGACCCAACA AGCATTGTGAACATCAATCACGATGCTAAC CGTCTGTCTCGTGCGCTAGCTGCTGGTCAG AATCAAACTCAGCGATCTCTTCGTCAGCAT GAAGGTGAAGACAGAGGGGCCATTGACAA GGCGGACGAGGTCGTATCAAAGATGAAAG CGTTAATGGGAACTGCAAAAAACGTTCCG AACAATCTGGCCGCTTTGATCGCGAAAAG GTCAAAAACCGCTGGAGAATTTGTGAGGC GTCCGTTTCTAGTGAGCAAATTATCCAAGA GATACAACATTGCTGACCAATTAAGCTTCT CGACACTGAAGCAATTGGACAAGATCGAC AACATGAGGATCGTGGATATCAAAAATGG TATTAAAGGCAATAAGAAGACCCCAAACG GCATGCGAAGAAAAATCAAGCACTTTGAG GGAATGAAAACGGCTCCTCAAAAGTTTCTA GAATCCCACGTCGGTCGTGACATGCAACGT TATGGAAAGGATGGAAGCCGGTGGCTATC AGCCGGCGTGGTTACGCGGACAACTGATC AAGGCGAGCGTCAGATCTTATTGATATCGA GCTCGAACCCGGCGAGAGGGGACTTTCTG CTTCCTAAGGGAGGCTGGGATAGAGGCGA GAAAATTAAAAAGGCGGCGTTGCGTGAGG TCATGGAAGAAGGAGGAGTATGTCGTGCT CTTTGA	>pDonr_06308-1 MSISSFSDPTSIVNINHDANRLSRALAA GQNQTQ**RSLR**QHEGEDRGAIDKADEV VSKMKALMGTAKNVPNNLAALIAKRS KTAGEFVRRPFLVSKLSKRYNIADQLS FSTLKQLDKIDNMRIVDIKNGIKGNKK TPNGMRRKIKHFEGMKTAPQKFLESH VGRDMQRYGKDGSRWLSAGVVTRTT DQGERQILLISSSNPARGDFLLPKGGW DRGEKIKKAALREVMEEGGVCRAL

PITG_06478	16	>pDonr_06478_2 ATGCAAACACCCCCTGGACAAGCCGACAA GTCGAAGCTGATTGCTCACGATGTTCTCAT GAAGACCACGTCACTGTCAGAAACCACAA TTGCTACTTCATCTAAGCGGTTCTTGAGGC TCTACGACGCAGAAGTCCGAGATACAGTC CGCGGAGATAATGACGTAGACCGCGAGGA GAGAGGAAGCTCGCCGTTGTTATCGAAGG TCGACGATCTGATACACAAAGTATTTAAAT CCAATCCGGAGCAAGCACAAATCAAGGCG TGGATGAAGTCTGGAATGCACCCTCAAAC AATTTTTGATACTTTGCGTCTAGCAAAGAG TACGACAAAACAGAACGATGACCCGAATC TTCTCCTTTGGCTCAAGCTCGTTGCTGCTTT TAGAGCTAAGAATGGTAACCAGGCGTTTTC GGATCTGGATCTTTACTATTTGCTACTGAA GAGAAGCAGTGGCGACGAGCTGAAAATAC TTATTGAGTCTTTTCGGAAGACTGGAGCCT TAAAGGAGCTAGGCAAAAGTATGCAGAAA TCGCTATCTGGTTCGTGGGTGTCAAAAACC TTACAGCACGAAACAGGTCCAAAAATTGTT TACGATACATTACGTCTTCAAGAGGCTGGC ACGAAACTGGTCGATTCGCCAATCTTTCAT CAGTGGCTGGCCTACGCGCAGCAGTATCG GGCGCAGAAGGGGATCCACTGGTTCGGAG ACGACGATATGCTCGACCTGTTTCGAAAAA CCATGCCGGAAAAAGACGTGGTAACGCTT CTGCATTTGCTTCGAAACGTCCCGGGCATG AAAGATCATGGCGATACGATGCAGCGGTT CTTGTTTTTATCGTCTAAAACCAGCCGAAA AATGATGCACGACGTGTGGCTGAACTACG ACGTACCGCCCGAACAAGTTTTCAAGATTT TACGCTTGGTAAAGGTCAATATGGACGCTG TGGATACGAACGCAATGTTTATACATTGGC TTAGGTACGTCAACTTGTACAGGAGCCACA CAAAAAAAAACGTTTTATCCAGCGTACAA ATGGTGCATTTCCTTGCGGACACCAAACCG TTGCGGTCAGAGTGGCAATTTGCCACATTT TTTGAATCGCTCAAGGACGTCCCTGATTTA AAGAGGCTGGCTGAAAACATGCAAACTTA CCTATTCCAAAACTGGCTGCACACGGAGTG GGACCCGAAGGCTGTGTCGAGTATGCTGG CCATTCCTTTTCCTACGAGTGCTGTGTATCT GCCGAAGAACGATCCCATTTACAAGACTTG GGTGGCGTACACCCTTTACTATACAGAGAG GAAGGGCGGGGTGTCGTTGCTGAATAAAG TGAAGACACTGCTCGACAACGACAACCCT ATCGGCGCACTTACCGCAGCTATGAAAGCT CAGTGA	>pDonr_06478_2 MQTPPGQADKSKLIAHDVLMKTTSLSE TTIATSSK**RFLR**LYDAEVRDTVRGDND VDREERGSSPLLSKVDDLIHKVFKSNPE QAQIKAWMKSGMHPQTIFDTLRLAKS TTKQNDDPNLLLWLKLVAAFRAKNGN QAFSDLDLYYLLLKRSSGDELKILIESF RKTGALKELGKSMQKSLSGSWVSKTL QHETGPKIVYDTLRLQEAGTKLVDSPIF HQWLAYAQQYRAQKGIHWFGDDDML DLFRKTMPEKDVVTLLHLLRNVPGMK DHGDTMQRFLFLSSKTSRKMMHDVW LNYDVPPEQVFKILRLVKVNMDAVDT NAMFIHWLRYVNLYRSHTKKNVLSSV QMVHFLADTKPLRSEWQFATFFESLKD VPDLKRLAENMQTYLFQNWLHTEWD PKAVSSMLAIPFPTSAVYLPKNDPIYKT WVAYTLYYTERKGGVSLLNKVKTLLD NDNPIGALTAAMKAQ
PITG_07387 (Avr4)	52	>pDonr_07387_1 ATGGATTCTTTAGCTCGTACCGTCAGCGTT GTTGACAACGTCAAAGTAAAAAGCAGATT TCTGAGGGCTCAAACGGACGAGAAGAACG AAGAGAGAGCAACGATAACGCTTGGAGAC AGGGTTGTTTCCGACAAGGCGGCGACAAA AGATCTGCTACAGCAGCTTCTTGCACTGGG CACGCCACTGGAAAAAGTCCAGAAGCAAT TCCTGAACATACCGCAGATGAAAACATTTG CGGAGTTGAGCAAACACCCGAACTGGAAA GCGCTTGACAAATATGAACGGATGCAGTG GCAGAAGCTAAAGGAGGGCGAAACACTGA CATTTATGCGTCTTGGCGATCGATTATACT CTAAAGAGAAAGCGCAAGAACAGCTCCTT AGGTGGGTTGCGCAGAAAAAACCTGTGGA GAGTGTATATGATGACCTACAAGTGGCAG GCTTTGCACATAATACTGTTGCTGCTCGCC AGAACTGGAGAGCATATATTATGTACGAC AAGTGGTTTACGGCGGCCTCACAAATGCA GAGGAACCCGCAGCAGTATGCCAAGTTCG GCACGGGATATCATTCGGAGCAAAAGACG	>pDonr_07387_1 MDSLARTVSVVDNVKVKS**RFLR**AQTD EKNEERATITLGDRVVSDKAATKDLLQ QLLALGTPLEKVQKQFLNIPQMKTFAE LSKHPNWKALDKYERMQWQKLKEGE TLTFMRLGDRLYSKEKAQEQLLRWVA QKKPVESVYDDLQVAGFAHNTVAARQ NWRAYIMYDKWFTAASQMQRNPQQY AKFGTGYHSEQKTTELFEKWAMEGTH IKSVITTLKLNGKSASEMANNENFPALL KYVKLYLDFKPVRDLNAKSRLQARRPI S

		ACGGAGTTGTTCGAGAAGTGGGCCATGGA GGGAACCCATATAAAAAGTGTCATCACGA CGCTTAAACTCAACGGTAAGTCGGCGTCTG AGATGGCAAATAACGAGAATTTTCCCGCG CTCCTGAAGTATGTCAAGTTGTATCTTGAT TTTAAACCAGTCAGGGACCTTAACGCAAA ATCCCGTCTCCAAGCTAGACGGCCCATATC TTAG	
SFI4/PITG_09585	90	>pDonr_09585_1 ATGGCTGAAGACGAACCTAAGACTCCGGA GTCCACATCTAGCGCGAACCCGCGTGACA ATGACCCCGTTATCCAAGAGATCCGTGGAT TACGGAACTCTGGCATGAAGCTGAACGAC GCCAAGGACTTTAAAGGCGCCATCGCGAA GCTACGTGGGGCTATTACACTGCTACACGA CCGAGTGTTTGGTGAAGGACGTGAGGCCA TCACCGACCCCAGCGACATCTCGCAGGAC GCGGCTCTCTACGCCCAGATCCTCAACGAC TACGGCACGGTACTTATCCGTGCCAAGCAA TACGACGAGGCCATCGAAGTGCTGGAGGA CTCGGTAGCGATGGTAGAGAAGATCTACG GAGACAGCCACCCGTCGCTCGGTCTGTCGC TGCGTAGCTTGGCCGACGCATACATGGCCA AGGAGGAGTACAAGATGGCCATTAAAAAG TACAAAACCCTCCGCAAACATGTCAAAAA GGGCCTGGAAACGACCCACGAAGCGTACA TTGAGGCGTCGTTGAGGATTGCCGAGGGGT ACAAGAAACTGGGCAATACAAAGAAGAAC TTAAAGGTGCTAAAGGACGCCGTGGAGGC TCAAAACGGAGAGATCAATGGCCTGACGA CGGGCATCGCCGAGCTCTACATGGAGCTGT CGACGGCTCACGTGGCTGTGGGCGAGATC GATGACGCTCTGAGAGCCGCGGAGGTTGC AAGTGCGATCTTCCGGCAACGTGACGGCG AGGACACGCTGTCGTTTGCGTTCAGCTTGA ATGCTCTGGCCGGCGTCAAGATGCGCCAG AAGAAGGTGGACGAGGCCATTAAGTTGCT GGAACAGGCCCACAGAATTGCTGTGCAGA TCTACGGCGAGAAGGACCCAATCACTCAA GCTAGCGCAAAGACTCTACGAGAGGTGAA GGAGTACAAACTCGACTTGCAGGCGCAGA AGGACGAGCTGTAG	>pDonr_09585_1 MAEDEPKTPESTSSANPRDNDPVIQEI**R** **GLR**NSGMKLNDAKDFKGAIAKLRGAI TLLHDRVFGEGREAITDPSDISQDAALY AQILNDYGTVLIRAKQYDEAIEVLEDS VAMVEKIYGDSHPSLGLSLRSLADAY MAKEEYKMAIKKYKTLRKHVKKGLET THEAYIEASLRIAEGYKKLGNTKKNLK VLKDAVEAQNGEINGLTTGIAELYMEL STAHVAVGEIDDALRAAEVASAIFRQR DGEDTLSFAFSLNALAGVKMRQKKVD EAIKLLEQAHRIAVQIYGEKDPITQASA KTLREVKEYKLDLQAQKDEL
PITG_12722	4	>pDonr_12722_1 ATGCTACCCATTGCCAAGGAGTCCATCCCT ACCATCAAGAACGAAGCCTCACCTGATAT AGATCGAATAGTAGACGCAGACGGTGGTC GAATGCTGCGTCGTGCCGAGCAACACGCA ACAAACGAAGTGGGGGTCGAAGAAGAAAG ATTCTACACGAAGGCTAAGCAGCTCTTCAA TCAAGCTATTTACGCTGCGAAGGTGAAGGC CAACAGTAACGACGCAGGGTATTTTGCCGC CCAGCTAGCACGTCTAAGGGGGGAGGGCA AGTAA	>pDonr_12722_1 MLPIAKESIPTIKNEASPDIDRIVDADGG **RMLR**RAEQHATNEVGVEEERFYTKAK QLFNQAIYAAKVKANSNDAGYFAAQL ARLRGEGK*

SFI5/PITG_13628 (PexRD27)	6	>pDonr_13628_2 ATGGCCTCCGACCAGAATTCGAACGTTGCA TCGATCACGAGCCAAGTCCAGCGGCTTCTG CGGACTCATCACGCTACCATAAAAGTCAAC GCTGACTCTGAAGAAAGATTCCTGACAGA ACCCCCGCTGACGACGGATGAAATGATGG CGATGATGAAGGCAGGGAAGTCTAAAAAT GCGTACGCTTTCGAGCTGGGTATTGCTGGA CAAATGGCCGATTTCATCAACAGCGGGCTA CCAGATATAGAAACGTTCAAGAAGACTCC GGAGTTCCAGAAGTACGAATTCTACATGA ACTTCTTGAACGATATGCGGAAGGACGAC GATTATAAGCCGTTGGTGGAGATGATCAA GAAGAACAAGGGCGAGACAGAAGCTTTTA AGACTTTGTTGGTGAAGGTCGAGGATAATG TAAGCAAGAAGAAGGCTTCTCCGTCGGCC ATTGTCAAGCTTGATCCTTTAAATAGGGAG CAGGCTATCGTGGAGAAGATCGAGCTTGCT CTTAAAAAGAATCAGGCTTTAAATAAGAA TAAGGCTTCGTTGGAGACGATCGAGCACA CTGTACGTATGGCAGCCAAGTCCAAACCA AGCACGTGGAAAATCTTTAAAATTATCTCG AGGCTTAAAAAATTAAAGCTAAAACGTTA A	>pDonr_13628_2 MASDQNSNVASITSQVQ**RLLR**THHATI KVNADSEERFLTEPPLTTDEMMAMMK AGKSKNAYAFELGIAGQMADFINSGLP DIETFKKTPEFQKYEFYMNFLNDMRKD DDYKPLVEMIKKNKGETEAFKTLLVK VEDNVSKKKASPSAIVKLDPLNREQAI VEKIELALKKNQALNKNKASLETIEHT VRMAAKSKPSTWKIFKIISRLKKLKLK R*
SFI6/PITG_13959	3	>pDonr_13959_1 ATGGATCAGGCCAGTGAGTTGAACGTGGA TGTTCACTCCTCAAATGTTCTCGCTACCGA GGACACGAGATTTCTTCGAAGTCACCAGAT AACGGATGACAAGGTCGAAATTAACGAAC ACGGCGAGGAAGAGAGGATGTCTGGGTCT AATTTGTTCTCTGCACTGAAGCTGGAGAAA ATGGGGCGGGATACATCTTACCGCGATAA GGAGTTCCAGCGTTGGAAAAACTATGGAA ATTCAGTGGGAGATGTTACTCCCCATGTGC CAGTTTCTCTCAAAGAAGCGTACGCAACAT ACTTGCGAATCCGAGAAATGGTTTTGGTCA ACGACTAG	>pDonr_13959_1 MDQASELNVDVHSSNVLATEDT**RFLR** SHQITDDKVEINEHGEEERMSGSNLFS ALKLEKMGRDTSYRDKEFQRWKNYG NSVGDVTPHVPVSLKEAYATYLRIREM VLVND*
PITG_14371 (Avr3a fam, Avr3aEM, PexRD7	58	>pDonr_14371 ATGATCGACCAAACCAAGGTCCTGGTGTAT GGGACGCCAGCTCACTACATACACGATTCA GCCGGCAGAAGACTTCTTCGCAAGAACGA AGAGAATGAAGAAACGTCTGAGGAGCGAG CCCCAAATTTCAATTTGGCGAATCTAAATG AGGAGATGTTTAATGTGGCTGCGTTGACGG AGAGAGCAGATGCCAAAAAGCTAGCGAAA CAGCTTATGGGTAATGATAAGCTGGCGGAT GCTGCATACATGTGGTGGCAGCACAACAG GGTTACGCTAGACCAGATTGACACGTTCCT GAAGCTTGCAAGCCGCAAGACGCAAGGCG CAAAGTACAATCAGATCTACAATAGCTAC ATGATGCACCTGGGGCTCACTGGATATTAG	>pDonr_14371 MIDQTKVLVYGTPAHYIHDSAGR**RLL** **R**KNEENEETSEERAPNFNLANLNEEMF NVAALTERADAKKLAKQLMGNDKLA DAAYMWWQHNRVTLDQIDTFLKLAS RKTQGAKYNQIYNSYMMHLGLTGY*
PITG_14371 (Avr3a fam, Avr3aKI)	58	>pDonr_14371 ATGATCGACCAAACCAAGGTCCTGGTGTAT GGGACGCCAGCTCACTACATACACGATTCA GCCGGCAGAAGACTTCTTCGCAAGAACGA AGAGAATGAAGAAACGTCTGAGGAGCGAG CCCCAAATTTCAATTTGGCGAATCTAAATG AGGAGATGTTTAATGTGGCTGCGTTGACGA AGAGAGCAGATGCCAAAAAGCTAGCGAAA CAGCTTATGGGTAATGATAAGCTGGCGGAT GCTGCATACATTTGGTGGCAGCACAACAG GGTTACGCTAGACCAGATTGACACGTTCCT GAAGCTTGCAAGCCGCAAGACGCAAGGCG CAAAGTACAATCAGATCTACAATAGCTAC ATGATGCACCTGGGGCTCACTGGATATTAG	>pDonr_14371 MIDQTKVLVYGTPAHYIHDSAGR**RLL** **R**KNEENEETSEERAPNFNLANLNEEMF NVAALTKRADAKKLAKQLMGNDKLA DAAYIWWQHNRVTLDQIDTFLKLASR KTQGAKYNQIYNSYMMHLGLTGY*

PITG_14736 (PexRD8)	3	>pDonr_14736_8 ATGGCAGCCGAAGCCTCCGAGCCCATGCC CAATATCGCGAAGTATGCATCACCAGAAG TTTCAGTTCACCTTGGTGCTGAGCGCGAGA AGAGGCTTTTGCGCTTCGACAGCAACGATT ATCGCGACGATGACGATGAAGAGGAAAGG GCGAATGCTGCCAACCTCTTCAACGTCGAC AAGCTAACGGTGTATGTAAACAAAGCCCA GAAGCGAACTGCCAACAATGTGAGTGGAA GCCTCTTGAATTATTTTAAGAGATTGGAAG CATACGGCTACAGCCCTGTCAAACTCGGTA ACAGAATTCCTGACGAGGAGTACGACAAT CTCCGTATGCTGTACCGCAGCTGGTACTAC CACAACAAGTAA	>pDonr_14736_8 MAAEASEPMPNIAKYASPEVSVHLGAE REK**RLLR**FDSNDYRDDDDEEERANAA NLFNVDKLTVYVNKAQKRTANNVSGS LLNYFKRLEAYGYSPVKLGNRIPDEEY DNLRMLYRSWYYHNK*
PITG_14783	6	>pDonr201_14783 ATGCTCGTGAACTCGAACCAAGCTATGCTC TCTTCACCAAATGAGCAGCACCAACGTCAA TTGCGGTCTCACCAGACCCCTGTGGAGGAT CAGGAACCCGATGAGGAGAGGTCTCTATC TAAAGCCGAGATGAAGCGGTTATTTGAAG CGGGGAATTCTTTGGACGATTTTGCTAAGC ACTTAGGCATTGCTGACGATGTTGTACGTG CTCAAAGCTCGAACACCGTTCTCCAGCGGC TCATGCAAACGGACGAGTACATGAAGTAC TCTACGTATCTCAACTTTCTGTCGAAACAA AACAAGAAGAAGAAGCCACCTACTTTCTA CCATTTATAA	>pDonr201_14783 MLVNSNQAMLSSPNEQHQ**RQLR**SHQT PVEDQEPDEERSLSKAEMKRLFEAGNS LDDFAKHLGIADDVVRAQSSNTVLQR LMQTDEYMKYSTYLNFLSKQNKKKKP PTFYHL*
PITG_15287 (PexRD1, Nuk10)	96	>pDonr_15287_1 ATGCTATCTGCCCATCGGGCGCAGATAATG AACGTCGCGACGTCAGATCTCATCTCACCG ATCGAGTCTACAGTCCAAGACGACAACTA CGACAGACAGTTGCGGGGGTTCTACGCTAC AGAAAATACAGACCCTGTTAACAATCAAG ACACTGCGCATGAGGATGGCGAGGAGAGG GTCAATGTCGCCACGGTGCTTGGAAAGGG GGATGAAGCTTGGGACGATGCACTGATGC GCTTGGCCTATCAGCACTGGTTCGACGGAG GCAAAACTAGTGACGGCATGCGATTAATA ATGGACCTTCCAGCGAAAGGTGAAGCACT CCGACACCCGAATTGGGGGAAATACATTA AATACTTAGAGTTCGTTAAGGAGAAAAAG AAGGAGGCTGCAGACGCTGCGGCAGTCGC GGCGCTCAAGCGAAGGCGGACTTACAGGG GATGGTATGTCGACGGGAAAACGGAGAAA GACGTACGCAAGATTTTCGGACTTCCGGCA ACAGGAAAAGCCAAGAACCACCCAAACTG GGCAGATTTTCAGGAATACTTAAACGTCGT CAGAGAATACTCAAAAGTAGTTTTTAAATA A	>pDonr_15287_1 MLSAHRAQIMNVATSDLISPIESTVQD DNYD**RQLR**GFYATENTDPVNNQDTA HEDGEERVNVATVLGKGDEAWDDAL MRLAYQHWFDGGKTSDGMRLIMDLP AKGEALRHPNWGKYIKYLEFVKEKKK EAADAAAVAALKRRRTYRGWYVDGK TEKDVRKIFGLPATGKAKNHPNWADF QEYLNVVREYSKVVFK*
PITG_16240 (PexRD12)	9	>pDonr_16427_1 ATGTTGACCACGACTGTGGCTGACACGGCC CAGACGGCAACCAGCATTCTAACTCCTGTT CTAGCTGGGGAGCCGAACAAACACGTTGC AACGCGATCTTTGAGAACGCATCCGATAG ACGACAGCGACGATGGCGAAGAGCGACTG CTTAATGGTATGACAGATTTTTTCAAGTAC CACGCTGGAAAGATGAGTCCCGAGCAGCT TTACAAGTACTTAAACTTAAAAGGACTTGG TCAAGAAGCCTACAAACACAAGAACTACG CTAGTTACATTAAGAAGTCGAAGAAGTGG TGGAAGAACCAGTAA	>pDonr_16427_1 MLTTTVADTAQTATSILTPVLAGEPNK HVAT**RSLR**THPIDDSDDGEERLLNGMT DFFKYHAGKMSPEQLYKYLNLKGLGQ EAYKHKNYASYIKKSKKWWKNQ*

PITG_16663 (Avr1)	2	>pDonr_16663_2 ATGTTCGACCACGACAAGGTTCCAAGGACT GTTGAACGAGGTGGCGGTGCAAGACAACT GCGCACGGCCACGATGAGCGACGACGAAG CTAGAGTGTCGAAATTGCCGTCGTTTATCG AGTCCTTCGTTAAAAACCGAAAAATCGAGT CTTGGATTCAGAACAAAGTTACTGACGACT TTGTCCTGAGCGAGCTAAAACTCGTGAGAT TGCCCGGAACGAGCCTGGCGGACGACCCA AATTTCAAGCTCTTTCAAAAGTTTAAGATT GGCGGCTGGCTCGAGGAAAAGGCTACTAC AACGAAAGCCTGGGAAAACCTTGGCTTGG ATTCACTCCCATTTGATCAAGTGAGCAAGA TCGACGAGTTCAAGACTTATACGCAGTATG TGACGGTGCTTAACAAGAAGGCAAGCAAA CTCGATATTGATCAGTGGCACGGGCTGTTA AGTGGAGGATCACCTGAGGAATTGATGGC CAAAGCAATGATATTGAGGACTTTGGGCA GAGATGTTCTAGAGCGCAGAGTCATGCTTG GTGGACATGTTGTGGTACCATTTTAA	>pDonr_16663_2 MFDHDKVPRTVERGGGA**RQLR**TATM SDDEARVSKLPSFIESFVKNRKIESWIQ NKVTDDFVLSELKLVRLPGTSLADDPN FKLFQKFKIGGWLEEKATTTKAWENL GLDSLPFDQVSKIDEFKTYTQYVTVLN KKASKLDIDQWHGLLSGGSPEELMAK AMILRTLGRDVLERRVMLGGHVVVPF *
PITG_16737	8	>pDonr_16737_1 ATGACAAGGGAATTGAATATGAGGGCCGC CCCTAGCGATTCAACTCGCGTTGTCGACTA CGCCACGACTGAGAGGCTTCTAAGGGCCC ACAGTAGTGACAAGGAAGAACAAAAAGAA GAAGAGGAAAGGGCAATTTCGATAAATTT TTCAAGCCTGGAGAAAATCTTTAAAAAAGT TACGTCAGCCAAAACTACGGAGCTGCAAG GAATGCTTAAGGCTGACGAGGCCCTTGGG AGTGCTTTCAAGACGCTAAAACTTGGTACA ATGCGGATTGGCAAGGATGGCTCTGTCGAT CCCAAGATGGTGGCAAAATTTCTGTCAAGT CGCAATTTCAAGATTTGGTCCCAGCACGCC GTCAAGATCAACAAAGATGATCCCTATGG CGAGATGCTTAAAGCACTCACAAATGTCTT TGGTGAGAAAAATGTGGCGATGATGATCC TAGTCGGGAACCTGTCCAGAAACTCGCGC GACGTCGCAAAGAAGTTAGAAAAGGCCCA GTTCTACAAGTGGTACTTCGTTGATAAGTA CAAGACAGCAGATGAGGTTTTCACGAACG TGCTGAAAGCTGATCGAAATAGAATTCATG GGTATGGTCGGGAGAAAGAAATTTGGGGA GATTACGCGAAGTACGTCACGACCACAGT GATGAAATATTGA	>pDonr_16737_1 MTRELNMRAAPSDSTRVVDYATTE**RL LR**AHSSDKEEQKEEEERAISINFSSLEKI FKKVTSAKTTELQGMLKADEALGSAF KTLKLGTMRIGKDGSVDPKMVAKFLS SRNFKIWSQHAVKINKDDPYGEMLKA LTNVFGEKNVAMMILVGNLSRNSRDV AKKLEKAQFYKWYFVDKYKTADEVF TNVLKADRNRIHGYGREKEIWGDYAK YVTTTVMKY*
SFI7/PITG_18215	124	>pDonr_18215 ATGACGTACTCGACTTCAAAGGGGGAGAT GAATTTAACCGGAACTGTCGAAAATAACC GCCCGACTCGCTCTCTTCGTGTTGCACCCA GTGGCGGCAATGGTGAAGAAAGATCGTGG TCAACCATTTACGGAATTTCTCGATCGAAG GCGGAGACTGTGAGAGATTGGTTGATGCC CCGGCTTAACCAAGGAATGGACGTACAGG CGCTCGCCAGAGAAATGGGGATTACTTCG AGACAGGCGGCTACGCAGCATCAGAACTG GGACGCTCTCGTGAAGTACCTGAAGATGTA TAATTACGCTGTAAGGGGCGAAAAGATGT CGAAATCGATGGCTGAGAGCGTACTCCTCC ATAACGTCCTGACCGCAAAGAACAATTTCT AA	>pDonr_18215 MTYSTSKGEMNLTGTVENNRPT**RSLR** VAPSGGNGEERSWSTIYGISRSKAETV RDWLMPRLNQGMDVQALAREMGITS RQAATQHQNWDALVKYLKMYNYAV RGEKMSKSMAESVLLHNVLTAKNNF*
PITG_18670	5	>pDonr_18670_1 ATGTTCCCGAATCCCGACGAAACTCGGCTC TTACCAGACACTTTTACCAAAAGATCCCTT CGGGTCGCAGGCCAAGAAGTTGCCCGGGG CGACCGGGGCGAAGAGATTGTGAGAGTTA TAGTCCAGAGTACTAACAAAATCTTCAAGA GACCGGCGGAAAAAGACATGAGCAAACTG	>pDonr_18670_1 MFPNPDETRLLPDTFTK**RSLR**VAGQEV ARGDRGEEIVRVIVQSTNKIFKRPAEKD MSKLIAAAKIAMLEKKMAKLSFVGKK AAK*

		ATTGCAGCGGCTAAGATTGCGATGTTGGAG AAAAAGATGGCTAAGCTCTCATTCGTCGGT AAGAAGGCAGCGAAGTAG	
SFI8/PITG_20303 (AVRblb2 fam)	5	>pDonr_20303 ATGTTCCCAATCCCCGACGAGTCTCGCCCC TTGTCGAAGACATCTCCTGACACTGGGGCC ACAAGATCGCTTCGGGTCGAGGCCCAAGA AGTTATTCAGAGCGGCCGGGGAGACGGAT ATGGTGGGTTCTGGAAAAACGTTTTTCCGA GTACTAACAAGATCATCAAGAAGCCGGAT ATCAAGATAAGCAAACTTATCGCGGCGGC CAAGAAGGCAAAAGCAAAAATGACGAAGT CCTGA	>pDonr_20303 MFPIPDESRPLSKTSPDTGAT**RSLR**VEA QEVIQSGRGDGYGGFWKNVFPSTNKII KKPDIKISKLIAAAKKAKAKMTKS*
PITG_21388 (AVRblb1 fam, ipiO1, PexRD6)	54	>pDonr_IPI01_1 ATGGTTTCATCCAATCTCAACACCGCCGTG AATTACGCTTCCACATCCAAGATTCGCTTT CTGTCGACTGAGTACAACGCCGATGAAAA AAGAAGCTTGCGAGGTGACTACAACAATG AGGTCACAAAAGAGCCCAACACGTCTGAC GAAGAGCGGGCGTTTTCTATCTCAAAGTCT GCGGAATACGTGAAGATGGTACTTTATGG ATTCAAACTTGGATTTTCTCCTCGCACTCA GTCCAAGACGGTGTTGCGATACGAAGATA AACTGTTTACGGCTCTCTATAAATCCGGAG AGACGCCGAGAAGCCTAAGGACCAAGCAT CTCGATAAGGCTTCCGCTAGCGTATTTTTC AACAGATTCAAAAAATGGTACGATAAAAA CGTTGGCCCTAGCTAG	>pDonr_IPI01_1 MVSSNLNTAVNYASTSKIRFLSTEYNA DEK**RSLR**GDYNNEVTKEPNTSDEERA FSISKSAEYVKMVLYGFKLGFSPRTQS KTVLRYEDKLFTALYKSGETPRSLRTK HLDKASASVFFNRFKKWYDKNVGPS*
PITG_21388 (AVRblb1 fam, ipiO4)	54	>pDonr_IPI04_1 ATGGTTTCATCCAATCTCAACACCGCCGGG AATGACGCTTCCACATCCAAGATTCGCTTT CTGTCGACTGAGTACAACGCCGATGAAAA AAGAAGCTTGCGGGGTGACTACAACAATG AGGTCACAAAAGAGCCCAACACGGCTGAC GAAGAGCGGGCGTTTTCTATCTCAAACTCT GTGGAAAAAGTGAAGTTGGGATTGTATGC ATTAAAGATTGCTTTTTCCCCTCGCACTCA GTCCAAGACGGTGTTGCGATACGAAGATA AACTGTTTACGTATCTCCATAAATCCGGAG AGACGCCGGCTAGCTACAAGAACAAGCAT CCCGATAAGGCTTCCGCTGGCGTATTTTTC AACAGATTCAAAAACTGGTACGATAAAAA CGTTGGCCCTAGCTAG	>pDonr_IPI04_1 MVSSNLNTAGNDASTSKIRFLSTEYNA DEK**RSLR**GDYNNEVTKEPNTADEERA FSISNSVEKVKLGLYALKIAFSPRTQSK TVLRYEDKLFTYLHKSGETPASYKNKH PDKASAGVFFNRFKNWYDKNVGPS*

Table 6-3. Potential SFI5-interacting proteins identified by LC-MS/MS analysis.
HA-SFI5-expressing protoplasts of *S.lycopersicium* were immunoprecipitated with anti-HA affinity matrix and the eluted protein was subject to mass spectrum analysis. Protein eluted from protoplasts expressing HA-SFI1 served as a negative control. The table shows the selected proteins that were identified only in the presence of HA-SFI5.

		Experiment (HA-SFI5 28-241aa)		Experiment (HA-SFI1)	
Protein ID	Protein Descriptions	Intensity	# of Peptide	Intensity	# of Peptide
Q8RXB8_SOLLC	N-hydroxycinnamoyl-CoA:tyramine N-hydroxycinnamoyl transferase THT1-3; [Solanum lycopersicum (Tomato) (Lycopersicon esculentum).]	4588200	1	0	0
IPI00938824.1	CAM1 (CALMODULIN 1); calcium ion binding;Calmodulin-1/4	2128200	3	0	0
IPI00548063.1	60S ribosomal protein L5-1;60S ribosomal protein L5-2	1567500	1	0	0
IPI00543640.1	50S ribosomal protein L17, chloroplastic	1428200	1	0	0
IPI00548475.1	60S ribosomal protein L18a-2	1195800	2	0	1
IPI00536958.1	Calmodulin-7;Calmodulin-2/3/5;Calmodulin-6;CAM5 (CALMODULIN 5)	959950	3	0	0
IPI00657454.1	EIF4A1 (EUKARYOTIC TRANSLATION INITIATION FACTOR 4A1); ATP-dependent helicase/ translation initiation	572990	2	0	0
RR8_SOLLC	30S ribosomal protein S8, chloroplastic; [Solanum lycopersicum (Tomato) (Lycopersicon esculentum).]	552660	3	0	0
IPI00526224.1	30S ribosomal protein S18, chloroplastic; [Solanum lycopersicum (Tomato) (Lycopersicon esculentum).]	528660	3	0	0
TL29_SOLLC	Thylakoid lumenal 29 kDa protein, chloroplastic; [Solanum lycopersicum (Tomato) (Lycopersicon esculentum).]	378590	2	0	0
IPI00528531.1	Calmodulin-like protein 8	333140	1	0	0
IPI00529254.2	30S ribosomal protein S14, chloroplastic; [Solanum lycopersicum (Tomato) (Lycopersicon esculentum).]	318030	1	0	0
RR16_SOLLC	30S ribosomal protein S16, chloroplastic; [Solanum lycopersicum (Tomato) (Lycopersicon esculentum).]	298370	1	0	0
IPI00539263.1	Prx B 2-Cys Prx B (2-Cysteine peroxiredoxin B); antioxidant/ peroxiredoxin	221600	1	0	0
IPI00520130.1	ATP synthase alpha chain, mitochondrial, putative;ATP synthase subunit alpha, mitochondrial;ATPase subunit 1	209090	1	0	0
IPI00519748.1	Glutamine synthetase cytosolic isozyme 1-1	177900	1	0	0
O49877_SOLLC	Cysteine protease TDI-65; [Solanum lycopersicum (Tomato) (Lycopersicon esculentum).]	152200	1	0	0
IPI00520128.1	AtRABA1e (Arabidopsis Rab GTPase homolog A1e);Putative GTP-binding protein	140620	1	0	0
IPI00543126.2	Chlorophyll a-b binding protein 7, chloroplastic; [Solanum lycopersicum (Tomato) (Lycopersicon esculentum).]	136110	1	0	0
IPI00539779.3	Putative vacuolar proton ATPase subunit E; [Solanum lycopersicum (Tomato) (Lycopersicon esculentum).]	132260	1	0	0
Q9M7M2_SOLLC	DnaJ-like protein; [Solanum lycopersicum (Tomato) (Lycopersicon esculentum).]	102830	1	0	0
IPI00542662.1	26S protease regulatory subunit 8 homolog A;26S protease regulatory subunit 8 homolog B	63488	1	0	0
IPI00539067.1	Probable UDP-glucose 6-dehydrogenase 2	62907	1	0	0
Q4W5U8_SOLLC	FtsH protease; [Solanum lycopersicum (Tomato) (Lycopersicon esculentum).]	57105	1	0	0
Q9LEG3_SOLLC	Putative alcohol dehydrogenase; [Solanum lycopersicum (Tomato) (Lycopersicon esculentum).]	50268	1	0	0
IPI00526133.1	Proteasome subunit alpha type-5-A	47313	1	0	0
C6K2K9_SOLLC	GDP-mannose 3',5'-epimerase; EC=5.1.3.18; [Solanum lycopersicum (Tomato) (Lycopersicon esculentum).]	41934	2	0	1
A7LI54_SOLLC	Phototropin-2; [Solanum lycopersicum (Tomato) (Lycopersicon esculentum).]	31052	1	0	0
IPI00938787.1	phosphoglucomutase, cytoplasmic, putative / glucose phosphomutase, putative	30334	1	0	0

7. Acknowledgements

As an international student with a dream to enter science, I am lucky to have been offered to join and to enjoy the intellectual and academic atmosphere of the department of plant biochemistry at the center for plant molecular biology of the university of Tübingen. Therefore, my deepest appreciation goes first and foremost to my supervisor, Dr. Frédéric Brunner, for providing me the opportunity to do my PhD at the ZMBP and for his constant support through my research work. His diligence and dedication to science is always an inspiring example for me and motivates me to move further in the field of plant-microbe interactions. Although, I suffered an evident lack in English speaking and writing skills, he was always patient to discuss with me and invested tremendous efforts in improving my thesis.

I would like to thank my thesis committee, Prof. Dr. Georg Felix, Prof. Dr. Thomas Lahaye and Prof. Dr. Claudia Oecking for their valuable advice along this project and and for accepting to evaluate my dissertation.

I would like to convey my sincere gratitude to all the colleagues of our department including the present and past members of our research group for their encouragement and generous help in my life and study. I want to give special thanks to Dr. Malou Fraiture and Dr. Nadine Wagener, who provided me excellent scientific and technical support; to Birgit Löffelhardt, for taking care of the Arabidopsis plants and for the birthday gift she offered me every year; to our greenhouse gardeners, who cultivated the tomato plants for my numerous experiments.

Moreover, it is my pleasure to acknowledge our collaborators, especially Prof. Dr. Paul Birch and his team at the James Hutton Institute / University of Dundee, UK (Dr. Eleanor Gilroy, Dr. Petra Boevink and Dr. Hazel Mc Lellan) for their constructive contribution to my project. I am also sincerely thankful to Prof. Dr. Thorsten Nürnberger, Prof. Dr. Georg Felix, Dr. Andrea Gust for their expert suggestions and stimulating ideas during the discussions we had in frame of my progress reports.

Not least, I owe my warmest thanks to my parents for their endless love and care despite the distance that separates us. Their understanding and encouragements guide me to grow up step by step. Finally to my friends around the world for all the moral support they provided.

8. Curriculum vitae

Name Xiangzi Zheng

Date of birth 30.05.1983

Citizenship P.R.China

Education

06/2010 ~ present PhD student in Tuebingen University, Germany.

09/2005 ~ 06/2008 Master of Science in Fujian Agriculture and Forest University, China

09/2001 ~ 06/2005 Bachelor of Science in Fujian Agriculture and Forest University, China

Research Experience

2001 ~ 2005 B.S. in Bioscience, Fujian Agriculture and Forest University. Thesis: "Cloning of Candidate Disease Resistant Genes for Rice and Establishment of Regeneration system from Mature Embryo of *MingHui 63*", (Advisor: Prof. Zonghua Wang, Prof. Guodong Lu), Fuzhou, China

2005 ~ 2008 M.S. in Biochemistry and Molecular Biology, Fujian Agriculture and Forest University. Thesis: "Biochemical and Molecular Characterization of a Putative Ferulic Acid Esterase in *Magnaporthe grisea*", (Advisor: Prof. Jie Zhou, Prof. Zonghua Wang, Prof. Guodong Lu), Fuzhou, China

2010 ~ 2016 Ph.D study in Plant Biochemistry, Tuebingen University. Thesis: "Identification of MAMP-triggered immunity (MTI)-suppressing RXLR effectors from *Phytophthora infestans* and functional characterization of the calmodulin-binding effector SFI5", (Supervisor: Dr. Brunner Frédéric), Tübingen, Germany.

Publications:

- **Xiangzi Zheng***, Hazel McLellan*, Malou Fraiture, Xiaoyu Liu, Petra Boevink, Eleanor M Gilroy, Ying Chen, Kabindra Kandel, Guido Sessa, Paul R.J.Birch, Frédéric Brunner. Functionally Redundant RXLR Effectors from Phytophthora infestans Act at Different Steps to Suppress Early flg22-Triggered Immunity. Plos Pathogens, 10(4): e1004057 (2014).

- Malou Fraiture, **Xiangzi Zheng**, Frédéric Brunner. An Arabidopsis and Tomato Mesophyll Protoplast System for Fast Identification of Early MAMP-Triggered Immunity-Suppressing Effectors. Methods in molecular biology (Clifton, N.J.), 1127:213-230 (2014)

- Jie Zhou, **Xiang-zi Zheng**, Lan Lan, Chen-zeng Lin, Yu-bing Wu, Xiong-jie Lin, Daniel Ebbole, Guo-dong Lu, Zong-hua Wang. Biochemical and molecular characterization of a putative endoglucanase in Magnaporthe grisea. Curr Genet., 53(4): 217-224 (2008)

- Jie Zhou, Cheng-zeng Lin, **Xiang-zi Zheng**, Xiong-jie Lin, Wei-jian Sang, Shi-hua Wang, Zong-hua Wang, Daniel Ebbole, Guo-dong Lu. Functional analysis of an alpha-1, 2-mannosidase from *Magnaporthe oryzae*. Curr Genet., 55(4):485-96(2009)

- **Xiang-zi Zheng**, Jie Zhou, Chen-zeng Lin, Xiong-jie Lin, Lan Lan, Zong-hua Wang, Guo-dong Lu. Secretion Property and Gene Expression Pattern of a Putative Feruloyl Esterase. The 4th International Rice Blast Conference, G.-L. Wang, B. Valent (eds.), Advances in Genetics, Genomics and Control of Rice Blast Disease, DOI 10.1007/978-1-4020-9500-9 5 (2009)